ABSTRACT

Title of Dissertation: TOWARD A BETTER UNDERSTANDING OF THE CELLULAR, MOLECULAR AND GENETIC BASES OF THE RUGOSE MORPHOLOGY OF *SALMONELLA* TYPHIMURIUM

Yuda Adha Anriany, Doctor of Philosophy, 2005

Dissertation directed by: Professor Sam W. Joseph
Department of Cell Biology and Molecular Genetics

The origin of rugose (wrinkled) colony morphology of *Salmonella* Typhimurium, which is formed only at stationary phase, low temperature, and under low osmolarity, is attributed to the production of an extracellular matrix and is associated with biofilm and pellicle formation, likely for survival strategies. The regulator CsgD is required for the synthesis of both matrix components: curli, encoded by the *csgBAC* operon, and cellulose, encoded by the *bcs* operon. Transcription of *csgD*, in turn, depends upon a number of transcriptional regulators such as σ^S, OmpR and HNS.

Using random mutagenesis, two groups of mutants with altered rugose phenotype were identified. The two mutations in the first group caused retardation of rugosity and

altered *waaG* and *ddhC*, which are required for synthesis of the core and O antigen of lipopolysaccharide synthesis, respectively. Both mutants exhibited lack of motility, decreased levels of curli, and, especially in the *waaG* mutant, increased cellulose production. In media containing high osmolarity, both mutants produced more biofilms. Non-polar gene knockout and complementation performed on the *waaG* further confirmed these phenotypes in this transposon mutant. Thus, alteration in the LPS seemed to influence both curli and cellulose in opposing manners, and appeared to direct cells toward alternative pathways to produce biofilm matrix.

The regulatory mutation in the second group affected *hfq*, and produced only minimal amounts of cellulose and curli protein. This phenotype was confirmed in an *hfq* deletion mutant. Transcriptional fusion between the *csgB* or *csgD* promoter and *lacZ* showed a drastic reduction in activity of both promoters in an *hfq* mutant compared to that in the wt. These were surprising results given the known function of Hfq as a post-transcriptional regulator, including in the regulation of σ^S-encoding gene *rpoS*. However, when the promoter activity was measured in an *rpoS hns* background, where transcription continues under σ^{70}, significant reduction was still shown in the *hfq* mutant. Deletion of the gene that codes for DsrA, a sRNA which, together with Hfq, is required for translation of *rpoS* at low temperatures, had minimal effect in both promoters. These results indicate that Hfq may regulate both promoters independent of σ^S.

TOWARD A BETTER UNDERSTANDING OF THE CELLULAR, MOLECULAR AND GENETIC BASIS OF THE RUGOSE MORPHOLOGY OF *SALMONELLA* TYPHIMURIUM

by

Yuda Adha Anriany

Dissertation submitted to the Faculty of the Graduate School of the
University of Maryland, College Park in partial fulfillment
of the requirements for the degree of
Doctor of Philosophy
2005

Advisory Committee:

Dr. Sam Joseph, Chair
Dr. Douglas Julin
Dr. Suman Mukhophadhyay
Dr. Wenxia Song
Dr. Richard Stewart
Dr. Gisela Storz
Dr. Ronald Weiner

© Copyright by

Yuda Adha Anriany

2005

I dedicate this dissertation to my advisor

Dr. Sam W. Joseph

ACKNOWLEDGEMENTS

I would like to thank my advisor, Dr. Sam Joseph, for his support, guidance, and friendship, and from whom I have learned so much not only about research but also being a researcher and a teacher. Thank you for all the encouragement you have given me and for your confidence in my abilities throughout my graduate studies.

I thank all of my committee members for their suggestions, criticism and encouragement. I am grateful to all of my friends, past and present, in the department for their encouragement and invaluable discussions, especially Liliana Losada, Jamie Bretz, Joshua Hayes, Anand Gupte, Nate Ekborg, Sam Bish, Song Hee Kim, Suchitra Derebail, and Larry Taylor. To Kimberly Wessells and Dr. Patricia Shields, thank you for being there for me. I also would like to thank the undergraduate students in Dr. Joseph's laboratory for their help with my research and for their friendship. For many other friends whose names I cannot list, I thank you all for all your friendship and support.

I would like to thank Dr. Richard Stewart and Dr. Suman Mukhophadhyay who have given me opportunities to learn research in their laboratories. I also extend my thanks to faculty members in the department who have given me advice, suggestions and support during my research. To Dr. Ann Smith, I thank you for introducing me to teaching, which

I know I love doing. I also would like to thank the staff in the graduate office for their assistance.

I would like to thank my parents, Yusuf Syukur and Haidatina, and my family in Indonesia for their constant support and encouragement. I thank my sisters, Yuda Yulisa Restianti and Yuda Auli Purnama Sari, for their invaluable help. To my friend Rahadinia who shares my experience as a parent, thank you for all your help.

Finally, I would like to thank my husband, Gaguk Zakaria, for his love and continuous encouragement and for being there to support me especially at times when things seemed to be going downhill, and to my children, Rahma and Muhamad, who have been waiting patiently for many years for me to finish my graduate studies. The completion of my dissertation would be impossible without all of you.

TABLE OF CONTENTS

SECTION **PAGE**

LIST OF TABLES ..... **xi**

LIST OF FIGURES ..... **xii**

LIST OF ABBREVIATIONS ..... **xv**

CHAPTER 1 - General Introduction **1**

1. Introduction on *Salmonella* **1**

1.1. Genus *Salmonella*- physiology 2

1.2 Taxonomy and Nomenclature 2

1.3. Epidemiology of *Salmonella* 4

2. Emergence of the multiresistant strain DT104 ..... **5**

3. *Salmonella* Genomic Island (SGI) **7**

4. *Salmonella* pathogenesis **9**

4.1. *Salmonella* pathogenesis in bovine infections 11

4.2. Invasion 12

4.3. Inflammatory response 15

5. *Salmonella* in the environment **17**

5.1. Changes in gene expression in response to environment insults 18

5.2. Cell surfaces as the first lines of defense against environmental insults 22

5.3. Survival of *Salmonella* in Viable but Non-Culturable (VBNC) forms .. 25

5.4. Antibiotic resistance as a mechanism of survival 26

6. Overview of Biofilms **28**

6.1. What are the developmental stages of biofilms? 30

6.2. Role of the matrix in biofilm synthesis 33
6.3.The concept of multicellularity of biofilms 34
6.4. Survival advantages of biofilms 35

7. Rugose colony morphology 38

8. Colonial variations in other organisms 39

9. Rugose (rdar) phenotype in *Salmonella* 41
9.1. The regulation of curli production 43
9.2. Regulation of cellulose production 47
9.3. The regulation of *csgD*, the central regulator for rugose formation 50
9.4. The two-component signal transduction systems in rugose formation .. 54

10. Regulation of *rpoS* 58

11. Overview of Hfq 60
11.1. Binding of Hfq to mRNA 61
11.2. Regulation of sRNA by Hfq 63
11.3. Proposed mechanism of Hfq regulation 64

12. Overview of DsrA 65

13. Commentary 66

14. Overview of the dissertation 67

CHAPTER 2 - Characterization of the Rugose Phenotype and Its Function in *Salmonella enterica* Serovar Typhimurium DT104 71

1. Abstract 71

2. Introduction 72

3. Materials and Methods 73
3.1. Strains, media, and growth conditions 73
3.2. Scanning Electron Microscopy (SEM) 75
3.3. Transmission electron microscopy (TEM) 75
3.4. LPS profiles 76
3.5. Biofilms 77
3.6. Susceptibility to osmotic, acidic, and oxidative stress 77

3.7. Macrophage invasion assay 78

4. Results 80

4.1. Rugose and smooth colonies 80

4.2. SEM 82

4.3. Pellicle examination 82

4.4. Transmission electron microscopy 83

4.5. Biofilms 84

4.6. Resistance to acid and oxidative stress. 84

4.7. Macrophage invasion assay 84

5. Discussion 85

CHAPTER 3 – The Effect of Mutations in *ddhC* and *waaG* of *Salmonella enterica* Serovar Typhimurium on Rugose Colony Morphology, Biofilm Formation, and Cellulose Production 99

1. Abstract 99

2. Introduction 100

3. Materials and Methods 106

3.1. Strains 106

3.2. Media and growth conditions 106

3.3. Random mutagenesis and screening for Tn mutants with altered rugose phenotype 107

3.4. RATE analysis of the Tn mutants 108

3.5. BLAST analysis 108

3.6. Deletion of *waaG, csgA,* and *bcsA* and complementation of *waaG* 108

3.7. RT-PCR 109

3.8. LPS profiling 110

3.9. Novobiocin susceptibility 110

3.10. Electron microscopy 111

3.11. Isolation of curli protein 111

3.12. SDS-PAGE and Western blotting 112

3.13. Biofilm assays and microscopic observations 112

3.14. Motility assay 113

3.15. Cellulose Assay 114

4. Results 115

4.1. Random mutagenesis 115

4.2. Phenotypic characterization of *waaG* and *ddhC* mutants 117

4.3. Matrix production 118

4.4. Curli production 119

4.5. Calcofluor binding 119

4.6. Direct knock-out of *waaG* resulted in phenotypes similar to the transposon insertion mutants 120

4.7. Both mutants are biofilm formers 122

4.8. Motility and swarming 124

4.9. Cellulose production 125

5. Discussion 126

5.1. LPS alteration and its effect on the rugose phenotype 126

5.2. Effect on curli production by *ddhC* and *waaG* mutations 128

5.3. The effect of LPS alteration on cellulose overproduction 130

5.4. Effect of LPS mutations on biofilm production 131

5.5. Could cellulose overproduction involve the RcsC/B system? 135

6. Conclusion 138

CHAPTER 4 - Involvement of the RNA-Binding Protein Hfq in the Regulation of *csgDEF* and *csgBA* Operons for Rugose Expression in *Salmonella* Typhimurium 167

1. Abstract 167

2. Introduction 168

3. Materials and Methods 172

3.2. Media and growth conditions 173

3.3. Assay for catalase production 174

3.4. Random mutagenesis and analysis of Tn insertion site 174

3.5. BLAST analysis 175

3.6. Deletion of *hfq*, *dsrA*, and *csgA* 175

3.7. Complementation 176

3.8. Construction of the *hns rpoS* double mutant 177
3.9. Construction of the *csgB* and *csgD*-promoter fusion plasmid 177
3.10. Miller assay 178
3.11. Electron microscopy 180
3.12. Isolation of curli protein 181
3.13. SDS-PAGE and Western blotting 181

4. Results 182
4.1. The effect of mutation in *hfq* on the multicellular behavior of *S.* Typhimurium 182
4.2. Analysis of Tn insertion 183
4.3. Electron microscopy (Analysis of bacterial morphology) 183
4.4. Similarity of the *hfq* knock-out mutant phenotypes to the transposon mutant 184
4.5. The role of Hfq in regulating *csgB* and *csgD* promoters in wild type background 186
4.6. The role of Hfq in regulating *csgBA* promoter activity in the *rpoS hns* background 190
4.7. The effect of deletion of *dsrA* on expression of P*csgD* and P*csgB* 192
4.8. P*csgB* and P*csgD* were differently regulated at 37°C in *rpoS hns* background 194
4.9. Congo red and calcofluor binding characteristics of the mutants 194
4.10. Production of curli protein by wt and *hfq* mutant in the wt and *rpoS hns* double mutant backgrounds 196

5. Discussion 197
5.1. Rugose and its importance 197
5.2. *hfq* mutation eliminates multicellular behaviors 197
5.3. The role of Hfq in the regulation of *csgDEFG* and *csgBA* operons and the use of *rpoS hns* double mutants 198
5.4. Limitations of the current approach and alternative methods 199
5.5. Possible roles of Hfq on rugose matrix production 200
5.6. The involvement of DsrA on *csgB* Promoter 202
5.7. Temperature regulation of *csgBA* is eliminated in *rpoS hns* background 204

6. Conclusions 204

CHAPTER 5 - Concluding Remarks and Future Directions 227

1. Rugose colony phenotype and its significance..... 227

2. Further studies on biofilms 229

3. The new players: cellulose and c-di-GMP 234

4. Is sRNA the next regulator? 235

5. What are the implications of improved knowledge of c-di-GMP, Hfq and/or sRNA involvement? 237

APPENDICES 239

Appendix A- Experimental Protocols 239

Appendix A.1-Preparation of Electrocompetent Cells and Electroporation 239

Appendix A.2-One-Step Gene Knock-out..... 242

Appendix A.3-Preparation of Chemically Competent Cells and Transformation by Heat Shock 245

Appendix A.4-Western blotting of the curli proteins 248

Appendix A.5-Biofilm Assay 256

Appendix B - Determination of total cell density and the number of attached cells to complement the crystal violet assay to measure early adherence.. 259

Appendix C - List of Strains Used in This Study 262

Appendix D - Sequence of the DNA Regions used for promoter–*lacZ* fusion in pQF50Cm..... 268

Appendix E - Miller Assay Procedure and Calculations 269

Appendix F - More data on the Miller assay on P*csgB* activity of *dsrA* mutant in wt and *rpoS hns* background 273

REFERENCES 275

CURRICULUM VITAE..... 300

LIST OF TABLES

Table 1. The macrophage invasion assay of Rugose- (Rv) and smooth- (Stv) colony forming strains of STDT104 91
Table 2. Strains and plasmids used in this study 141
Table 3. Primers used in this study 142
Table 4. MICs for *S.* Typhimurium DT104 and LT2 and their derivatives when exposed to novobiocin 144
Table 5. Biofilm formation by *S.* Typhimurium 145
Table 6. Strains used in this study and their relevant characteristics 206
Table 7. Plasmids used in this study and their relevant characteristics 207
Table 8. Primers used in this study 208
Table 9. Strains used in this study as listed by strain numbers 262

LIST OF FIGURES

CHAPTER 1

Figure 1. Schematic diagram illustrating the currently known regulatory networks controlling the expression of curli and cellulose, two components required for the production of rugose matrix. 69

CHAPTER 2

Figure 2. Morphology of rugose (Rv/25) and smooth (Rv/37) colonies of *S. enterica* serovar Typhimurium DT104. 92

Figure 3. Progression of rugose formation at day 2 through day 4 at 25°C on TSA. 93

Figure 4. Pellicle formation in Rv/25 was absent in Stv. 94

Figure 5. Scanning electron micrograph of pellicle cells. 95

Figure 6. Transmission electron micrographs of cells from the pellicle and from broth under the pellicle. 96

Figure 7. Formation of biofilm matrix on the inner surface of glass flasks. 97

Figure 8. Survival of *S. enterica* serovar Typhimurium DT104 cells. 98

CHAPTER 3

Figure 9. Growth of *S.* Typhimurium DT104 Rv and LT2 and their derivatives on LB CR plates at 4 days and 6 days at 25°C. 146

Figure 10. Growth curves of *S.* Typhimurium DT104 Rv, A1-8, and (A1-9) at 28˚C in LB broth. 147

Figure 11. The sites of transposon insertion in strains A1-8 (*ddhC*::Tn5) and A1-9 (*waaG*::Tn5), and deletion in YA155 (Δ*waaG*::kan). 148

Figure 12. The general structure of lipopolysacharide (LPS) in *Salmonella* Typhimurium and the roles of both *ddhC* and *waaG* in LPS synthesis. 149

Figure 13. Scanning electron micrographs (SEM) of cells from intact colonies of *S.* Typhimurium DT104 Rv, and mutants A1-8 and A1-9 grown on LB agar for 4 days at 25°C. 150

Figure 14. Curli production as judged from the major subunit CsgA production by the wt Rv and LT2 and their derivatives..... 152

Figure 15. Growth of the wt *S.* Typhimurium DT104 Rv and LT2 and their derivatives on LB-calcofluor (CF) at 28˚C for 2 days. 153

Figure 16. Expression of *waaG* and *waaP*, a gene adjacent to and immediately downstream of *waaG*, by the wt LT2 and Δ*waaG* mutant YA155 as shown by Reverse-Transcriptase (RT) PCR products..... 154

Figure 17. Growth curves of the wt strain LT2, YA 155 (Δ *waaG*::*kan*) and the complemented strain YA 156 grown in LB at 25˚C or 37˚C. 155

Figure 18. Production of biofilms by the *ddhC*::Tn5 (A1-8) and *waaG*::Tn5 (A1-9) mutants. 157

Figure 19. Size comparison of the cells of wt LT2, the Δ*waaG*::*kan* YA155 and the *waaG*-complemented strain YA156 and the cell aggregation exhibited by YA155 in LG and LGS media 158

Figure 20. Assay for early adherence of the wt strains Rv and LT2 and their derivatives. 160

Figure 21. Motility assay for the wt Rv and LT2 and their derivatives. 161

Figure 22. Cellulose production by the wt Rv and LT2 with their derivatives. 162

Figure 23. Production of nodular structures and adhesive-like matrix in cellulose overproducing strains YA151 and YA155 as shown by SEM. 163

Figure 24. Resulting model of the effect of LPS truncation by *waaG* and *ddhC* mutations on rugose matrix formation. 165

CHAPTER 4

Figure 25. Multicellular phenotypes of *S.* Typhimurium are eliminated in the *hfq* mutant compared to the wt strain. 209

Figure 26. Scanning electron micrographs of the Rv and *hfq*::Tn5 mutant A1-10 210

Figure 27. Matrix and curli production by the wt Rv and their absence in *hfq*::Tn mutant A1-10 as shown by transmission electron microscopy. 211

Figure 28. Growth curves of wt 14028, Δ*hfq* and *hfq* complemented strains. 212

Figure 29. Fusion construct of promoters for *csgD and csgB* and *lacZ* to assay the expression of *csgB* and *csgD* operons. 213

Figure 30. Biofilm production by thw wt strain 14028 and its derivatives and the expression of P*csgB* and P*csgD* in planktonic, biofilm and pellicle cells of the wt 14028 214

Figure 31. P*csgB* activity in wt 14028, Δ*hfq*, Δ*dsrA*, and complemented strains grown under aerobic conditions at 48h using the Miller assay. 216

Figure 32. P*csgD* activity in wt 14028, Δ*hfq*, Δ*dsrA*, and complemented strains grown under microaerophilic conditions using the Miller assay. 217

Figure 33. P*csgB* activity in *rpoS hns* background at 72h (day 3). 218

Figure 34. P*csgD* activity in wt, Δ*dsrA*, and *dsrA* complemented strains in *rpoS hns* background under microaerophilic conditions at 48h. 219

Figure 35. Growth curves of wt, Δ*dsrA* and *dsrA* complemented strains under aerobic conditions. 220

Figure 36. Activities of P*csgB* and P*csgD* in the wt and *rpoS hns* background at 37˚C. 221

Figure 37. Activities of P*csgD* and P*csgB* in the wt, and *hfq, dsrA, rpoS*, and *hns* single mutants and in multiple background combinations. 222

Figure 38. Western blot showing the production of curli protein (CsgA) by the wt, *hfq* mutants, and *hfq* complemented strains in wt or *rpoS hns* backgrounds. 224

Figure 39. Resulting model of Hfq and DsrA involvements in rugose matrix formation. 225

APPENDICES

Figure 40. Initial adherence of *S.* Typhimurium DT104 Rv and LT2 and their mutants to PVC surface. 261

Figure 41. The DNA sequence of the intergenic region between *csgB* and *csgD* 268

Figure 42. Comparison between Miller units and β-galactosidase specific activities. ... 272

Figure 43. P*csgB* activities from *dsrA* mutant in wt and *rpoS hns* background. 274

LIST OF ABBREVIATIONS

AAF	aggregative adherence fimbriae
ACSSuT-R	Ampicillin chloramphenicol streptomycin sulfonamides and tetracycline resistance
Ag43	Antigen 43
Agf	(Thin) aggregative fimbriae
Amp	Ampicillin
ATCC	American type culture collection
ATR	Acid tolerance response
Bdar	Brown dry and rough phenotype
bp	Base pairs
cAMP	Cyclic adenosine monophosphate
c-di-GMP	Cyclic dimeric guanylic acid monophosphate
CAI	*Cholerae* autoinducer
CRP	cAMP receptor protein
CTC	5-cyano-2,3-ditolyl tetrazolium chloride
CF	Calcofluor
CR	Congo red
CSI	Carbon starvation induced
CXC	Cysteine-other amino acid-cysteine motif
DGC	Diguanylate Cyclase
DT	Definitive type
Fur	Ferric uptake regulator
Gal	Galactose
GDP	Guanidine diphosphate
GEF	Guanine exchange factor
Glc	Glucose
GTP	Guanidine triphosphate
CGSC	(*E.*) *coli* genetic stock center
EAEC	Enteroaggregative *E. coli*
ELR	Glutamine-Leucine-Arginine motif
EPS	Extracellular polymeric substance
ES	Extracellular substance
HF-1	Host factor I
HNS	Histone-like nucleoid structuring protein
HRPO	Horse radish peroxidase
IHF	Integration host factor
IL	Interleukin

IR	Intergenic region
Kan	Kanamycin
kD	Kilo Dalton
LB	Luria Bertani
LPS	Lipopolysacharide
MDR	Multiple drug resistance
MIC	Minimal inhibitory concentration
MW	Molecular weight
nt	Nucleotides
NTR	Nitrogen regulation system
OMP	Outer membrane protein
ORF	Open reading frame
PAI	Pathogenicity island
Pap	Pyelonephritis-associated
PCR	Polymerase chain reaction
P*csgB*	*csgB* promoter
P*csgD*	*csgD* promoter
PDEA	Phosphodiesterase A
PEEC	Pathogen elicited epithelial chemokine
PIA	Polysaccharide intercellular adhesion
PMN	Polymorphonuclear
PT	Phage type
Pdar	Pink, dry and rough phenotype
Rdar	Red, dry and rough phenotype
RT	Room temperature
RT-PCR	Reverse transcriptase polymerase chain reaction
Saw	Smooth and white phenotype
SCV	Small coloy variant
SDS	Sodium dodecyl sulfate
SE	*Salmonella* Enteriditis
SEM	Scanning electron microscopy
SGI	*Salmonella* genomic island
SOD	Superoxide dismutase
SPI	*Salmonella* pathogenicity island
SSA	Solid-surface associated
SSR	Starvation stress response
ST DT104	*Salmonella* Typhimurium DT104
Tafi	Thin aggregative fimbriae
TCS	Two-component system
TEM	Transmission electron microscopy
Tet	Tetracyclin

TLR	Toll-like receptor
TNF	Tumor necrosis factor
TSA	Tryptic soy agar
TSB	Tryptic soy broth
TTSS	Type three secretion system
UAS	Upstream activating sequence
UTR	Untranslated region
VBNC	Viable but non-culturable
Vps	*Vibrio* polysaccharide

CHAPTER 1 - General Introduction

1. INTRODUCTION ON *SALMONELLA*

Salmonella was first isolated from cases of swine cholera in 1885 by Dr. Daniel A. Salmon. *Salmonella* Typhimurium isolates were then identified after isolation from human cases of gastroenteritis in an outbreak in Germany in 1888 (236). Despite its early identification, bacteria from this genus continue to be among the major causes of food borne infections in the U. S and worldwide. In 1995, it was estimated that 1.3 billion cases of salmonellosis with 3 million deaths occur every year throughout the world. In the U.S. alone, approximately 1.3 million cases of human non-typhoidal salmonellosis occur per year with about 1000 deaths. A recent estimate compiled from reported cases taken from the active surveillance network (FoodNet) from 1996-1999 indicates that *Salmonella* infections caused 15,000 hospitalizations, over 150,000 visits to the physician, and 400 deaths annually in the U. S. (121). The total patient-related costs associated with salmonelloses were estimated to be approximately $1 billion per year (236). Furthermore, the relative mortality rate one year post infection for patients, having had gastroenteritis infections, is three times greater than the rate for those who had not contracted *Salmonella* infections (104). Thus, there is a serious consequence of food-borne salmonellosis infections on overall morbidity and mortality, making salmonelloses to be an important public health concern and a heavy economic burden.

1.1. Genus *Salmonella*- physiology

Salmonella are gram negative, facultatively anaerobic, approximately 0.7-1.5 x 2.0-5.0 μm in size, and are motile by peritrichous flagella. The bacteria are characterized by black colonies on xylose-lysine-tergitol (XLT-4) agar medium (146) because of the production of H_2S. They ferment glucose with gas production, but are non-lactose fermenting, thus produce an alkaline/acid gas reaction in TSI tubes, and are lysine decarboxylase positive.

Salmonella are usually transmitted by contamination of either water or food without an intermediate host. Some of them are host adapted, for example *S*. Typhi only infects humans. In addition, *S. Choleraesuis* are only found in swine, *S*. Gallinarum and *S*. Pullorum in poultry, *S*. Dublin in calves, but they can also cause diseases in humans, albeit at a very low frequency. Other *Salmonella* that have a wide host range, such as *S*. Typhimurium, are the most common cause of salmonellosis. Infection by *S*. Typhimurium causes gastroenteritis in humans and calves, but typhoid-like symptoms are seen when *S*. Typhimurium infects mice (thus the name Typhi-murium, "typhoid in murine").

1.2 Taxonomy and Nomenclature

There are two species of *Salmonella*: *S. bongori* (formerly subspecies V) with 20 serovars and *S. enterica* (formerly *S*. *Choleraesuis*), which contains approximately 2300 serovars. The *S. enterica* species is further categorized into six subspecies: *S. enterica* subsp *enterica* (I), comprised of approximately 1400 serovars, subsp. *salamae* (II), subsp. *arizonae* (IIIa), subsp. *diarizonae* (IIIb), subsp. *houtenae* (IV) and subsp. *indica* (VI). Only those serovars belonging to *Salmonella subsp. enterica* are found in warm-blooded

animals, while the remaining serovars are either non-pathogenic or only rarely found in cold-blooded animals.

Because of the large number of serovars in the genus the nomenclature for *Salmonella* differs from the commonly used *Genus species* names for other bacteria. The WHO Collaborating Centre for Reference and Research on *Salmonella* implemented designation for *Salmonella* serovars. While the antigenic forms are used for most serovars, those that belong to subspecies *enterica* must include the name of the serovar. Thus for serovar Typhimurium, which belongs to subspecies *enterica*, the complete name is written as *Salmonella enterica* subsp. *enterica* serovar Typhimurium, which sometimes is shortened to *Salmonella enterica* serovar Typhimurium, or just simply *Salmonella* Typhimurium, with the name of the serovar not italicized and the first letter capitalized. The National *Salmonella* Reference Laboratory at the Centers for Disease Control and Prevention, uses similar nomenclature except that "serotype" is used instead of "serovar" (108).

Salmonella are serotyped based on their O (somatic) antigen, Vi (capsular antigen) and H (flagellar) antigen such as formulated in the Kaufmann-White scheme. Diagnosis is usually done with slide agglutination with antisera against O groups A to E4 of the lipopolysacharide (LPS), to which 98% of *Salmonella* isolates belong, while the remainder of the O groups belong to the few serotypes in *S. bongori* species. There are two phases of flagellar (H) antigen in *Salmonella*. Only one phase is usually expressed by a serotype at one time, and it is regulated under phase variation. Only serovars Typhi, Paratyphi, and Dublin are known to produce the Vi capsular antigen, which is encoded in *Salmonella* Pathogenicity Island (SPI)-7 (181). Outer membrane proteins (OMP) antigens

have been discovered to be effective, as well. Using ELISA-based analysis, antibodies against OMP can be detected and compared measurably in acute and convalescent sera (16, 218).

1.3. Epidemiology of *Salmonella*

Three different diseases are manifested in humans from *Salmonella* infections: typhoid fever, septicemia, and enterocolitis (gastroenteritis). *S.*Typhi causes typhoid fever, a disease, in essence, eradicated in the U. S. In 1999, there were approximately 800 cases with 3 deaths reported in the U. S. mostly due to foreign travel to Asia, Africa or South America (153). In developing countries, typhoid and paratyphoid fevers can account for the majority of febrile illnesses of unknown origin admitted to the hospital (6). Septicemia, indicated by the presence of disease with bacteria in the blood, is the least frequently found in humans, and they are usually caused by two host adapted serotypes: *S.* Choleraesuis from swine and *S.* Dublin from cattle. However, enterocolitis, characterized by diarrhea and abdominal pain, is the second most frequent cause of bacterial food-borne disease in the U. S. *Salmonella* enterocolitis is the most common cause of deaths from food-borne illnesses caused by microorganisms in the U. S. *Salmonella* serotype Typhimurium is the most frequent serotype isolated, which totaled approximately 26% of all *Salmonella* isolates reported in 1998 to the CDC (38).

Typhoid fever, which is caused by *S.*Typhi, was the more predominant *Salmonella* infection in the U. S. at the turn of the twentieth century, and was primarily associated with waterborne infections. Throughout the twentieth century, the number of cases of typhoid fever steadily declined, while animal-associated non-typhoidal *Salmonella* increased. In fact, around 1945 there was a crossover with the total number of

cases of non-typhoidal salmonellosis rising above the incidence and prevalence of typhoid fever. Perhaps the best explanation for this phenomenon is derived from casual observations and anecdotal information. The decline in typhoid fever can be attributed to improved sanitation and hygiene, educational efforts, availability of potable water, and better design of toiletry and sewerage as well as the availability of a typhoid vaccine (236). Control measures in animal farms had been introduced as well. On the other hand, as the century progressed, there was increasing demand for processed animal meat leading to larger intensive animal production in smaller facilities. These evolving production practices may have led to persistent contamination by *Salmonella* species and other bacterial pathogens.

Since 1970, the prevalence of nontyphoidal *Salmonella* infection has increased constantly, mostly due to contamination of food from animals. In the early 1980's *S.* Enteritidis phage type (PT) 8 was the most common isolate found in *Salmonella* infections. Later, phage type 4 of *S.* Enteritidis became the most prevalent strain in Europe and Russia in the 1980's and in the U. S. beginning in 1993. More than 500 outbreaks were reported to the CDC between 1985 and 1997 mostly associated with food containing raw or slightly uncooked shell eggs. Recently, the number of infections by *S. enterica* serotype Typhimurium, responsible for about 21-38 % of the total salmonellosis cases in the U.S., has been on the rise (153).

2. EMERGENCE OF THE MULTIRESISTANT STRAIN DT104

The phage type 104 [Definitive Type (DT) 104] strain of *S.* Typhimurium (ST) with resistance to Ampicillin, Chloramphenicol, Streptomycin, Sulfonamides, and

Tetracycline (ACSSuT-R), has recently emerged in the U. S. (18), the U. K. (240), France, Denmark (11) and in Japan (208). Although the overall increase of antimicrobial resistance (mostly to one antibiotic) among *Salmonella* isolates was gradual (16% in 1980 vs 29% in 1990, 37% in 1996) a very dramatic increase was observed in *S.* Typhimurium DT104 (ST DT104) in the U. S. over the past 10 years. The Centers for Disease Control and Prevention has reported that ST DT104 identified from ST isolates increased from 7%, to 28%, to 32% in 1990, 1995 and 1996, respectively. DT104 is now only the second most prevalent strain of *Salmonella* after serotype Enteritidis Phage Type 4 in the United Kingdom (109). Moreover, new strains with resistance to additional antibiotics such as trimethoprim and fluoroquinolones are beginning to emerge after their use in animal feed (239). This observation has a significant impact clinically, since quinolone antibiotics such as ciprofloxacin are used for treatment of salmonellosis in humans including typhoid fever, and in animals such as cattle, pigs and poultry. The emergence of the multi-resistant DT104 strain is partly responsible for increased efforts to reduce bacterial contamination in food nationally and internationally (51)

Based on epidemiologic evidence, DT 104 has been isolated mostly from cattle products, while *S.* Enteritidis is mostly associated with poultry and poultry products. From cattle, the bacteria spread to other animals such as sheep, pigs and turkeys, which in turn become sources of transmission in fresh and processed foods. Therefore, the existence of these bacteria in many branches of the food chain complicate the food contamination control plan (111). In addition, human illness caused by ST DT104 is more difficult to treat (111). In a case-control study, it was reported that infection by this strain resulted in a higher percentage of hospital admissions and mortality (254). Several

outbreaks in Denmark and in the U. S. seemed to confirm this observation, since infections resulted in bloody diarrhea in 32-75% of cases, indicating that ST DT104 is more invasive. Whether or not the DT104 strain is more virulent than its non-DT104 counterpart is still debatable, since another study showed that both are similarly invasive in 1.3% of the cases (111). Furthermore, in vitro studies showed that the DT104 strain is not more invasive than the non-DT104 counterpart, and that SPI-1, the stretch of genes responsible for invasion, is intact in the 400 ST DT104 strains tested (34, 35). More recently, however, it was reported that the DT104 strain is capable of producing a cytotoxin, which is not produced in the non-DT104 strain (267). Thus, additional virulence factors may exist independent of the multi-resistant characteristic of the ST DT104.

3. *SALMONELLA* GENOMIC ISLAND (SGI)

The multiple antibiotic resistance of DT104 is coded in a cluster of genes called the *Salmonella* genomic island 1 (SGI)1 that presumably has been horizontally transferred as a piece of an integron. Conjugation has been suggested as the mode of SGI acquisition, because of the presence of some genes coding for some part of the conjugation process in the island. Experimental evidence showing that SGI1 can be transferred from ST DT104 to *E. coli* by conjugation in the presence of other components required for conjugation in a helper plasmid further supported this hypothesis (61). Integration of the integron in the chromosome of *Salmonella* has resulted in a more stable retention of SGI1, which is unlike those encoded in a plasmid found in the previously prevalent antibiotic resistant strains DT204 and DT193 of *S.* Typhimurium (31, 240).

The SGI1 is 43 kb long, and is located between *thdF* and *int2* genes in the chromosome of *S.* Typhimurium. The G+C content of the SGI was 47% in contrast to 51-53 % in the remainder of the *S.* Typhimurium genome. The SGI1 is considered to be a class I Integron of the In4 group, as characterized by the presence of *intII* for the integrase and *att1* for the attachment site for recombination at the 5' end. Further at the 3' end, there was a presence of *qacE1*, *sul1* and *orf5*, which code for phenotypes for resistance to antiseptics, and antibiotic sulfonamides, and a gene product of unknown function, respectively. The first gene in the SGI1 apparently codes for integrase, and 18 bp direct repeats were identified at both junctions between SGI1 with the chromosome, all indicating that the presence of this island is a result of horizontal gene transfer, similar to the pathogenicity island (SPI) that codes for virulence genes in *Salmonella* (27). There are 44 ORFs in the SGI1, fifteen of them novel gene products with no homology to known proteins. The sequencing of the island revealed a number of genes coding for resistance to antibiotics in the 13 kb long multiple drug resistance (MDR) stretch of DNA at the 3' end of SGI (26). The MDR region includes genes for resistance to ampicillin (*pse-1*), chloramphenicol/florfenicol (*floR*), streptomycin/spectinomycin (*aadA2*), sulfonamides (*sul1*), and tetracycline [*tet*(G)] (27). Some other variations of the MDR region was obtained from some other strains of *S.* Typhimurium with different antibiotic resistance phenotypes, indicating that this region is prone to recombination (27).

Multiple drug resistance (MDR) poses a major problem, since antibiotics are the only treatment available for systemic infections. These types of infections occur in 1.1% of *Salmonella* cases, and are characterized by pathology in the spleen, liver, and bone

marrow, and could even result in long-term carriers (241). Since MDR will reduce the efficacy of antibiotic therapy, alternative strategies are therefore being pursued for the control of salmonellosis. As a foodborne pathogen, *Salmonella* must have the ability to survive environmental stresses during food production, preparation, and storage. Once they reach the host, they must also be able to surmount stresses posed by the host's defenses. In order to survive, *Salmonella* must be capable surviving in the acid environment in the stomach and crossing the physical barrier of the epithelial cells, as well as myriad other stresses. These insults have to be overcome in order for the organism to survive, grow, and divide, sometimes with a final consequence of illness or even death of the host. Thus, our better understanding of the pathogenesis and the survival ability of *Salmonella* in both the host and in the environment external to the host is necessary for the eventual development of alternative therapies and the prevention of outbreaks of salmonellosis. The question is, how do *Salmonella* survive and cause diseases in humans, and how do they survive in the environment?

4. *SALMONELLA* PATHOGENESIS

Salmonella has evolved intricate machinery for virulence by acquiring virulence genes by horizontal transfer via bacteriophage or plasmids. Most of these genes are found in *Salmonella* Pathogenicity Islands (SPI), a stretch of genes, including an area which encodes for mobility genes such as integrase, flanked by direct repeats. The majority of the pathogenicity islands (PAI) in enteric bacteria are inserted at either *selC*, coding for selenocysteine-specific tRNA, or one of the two genes for phenylalanine tRNA *pheU* or *pheV*. These PAIs then undergo mutations which cause them to no longer be transferable.

There are currently 5 SPIs that have been identified and well characterized. SPI-1 codes for the type III secretion system (TTSS)-1, the needle-like projections that function in the transfer of virulence factors into the host. Included in the SPI1 are different parts of the secretion apparatus, effector proteins, chaperone proteins, and gene regulators. SPI-1 additionally functions in the invasion of epithelial cells and apoptosis in the macrophage. SPI-2, required for invasion into monocytes, encodes for the second system of TTSS (TTSS-2). SPI-3 is necessary for invasion and survival in macrophages and in Mg^{2+} limiting conditions in vitro, while SPI-4 functions in invasion of and survival in monocytes. SopB, an effector protein that is translocated by TTSS-1, is present in SPI-5. Additionally, SPI-7 codes for the Vi capsular polysaccharide only in a limited number of *Salmonella* serovars.

After initial studies showed host cell rearrangement upon *Salmonella* infection (235), most virulence factors of *Salmonella* were discovered in vitro using human tissue culture cells. These studies aided in the initial discovery of SPI1 in centisome 63, for molecular interaction of *Salmonella* and the host cells and subsequent translocation of effectors (68, 75, 132). Experiments using polarized cells, where cells form a monolayer, with distinct apical and basolateral surfaces, have confirmed some results shown from the use of unpolarized tissue culture cells, and recently was used to model polymorphonuclear (PMN) recruitment during the inflammatory reactions induced by *Salmonella* (112).

The *in vivo* pathogenesis of *S.* Typhimurium has been extensively studied in the murine animal model, in which *S.* Typhimurium mimics *S.* Typhi. In this model, the mice develop typhoid-fever like symptoms after a long (between 4-8 days) incubation period,

usually in the absence of diarrhea (275). In addition to fever, the symptoms include systemic spread of bacteria, wherein a high number of bacteria are found in Peyer's patches, mesenteric lymph nodes, the liver and the spleen. In the intestine, very little tissue injury is present, and the disease is characterized by a slowly-developing infiltrate containing mostly mononuclear inflammatory cells, similar to that observed in typhoid fever in humans.

In contrast, enterocolitis caused by non-typhoid *Salmonella* has a distinct manifestation in humans. For example, the primary symptom is non-bloody diarrhea, and fever is rare. Infiltrates obtained from patient biopsies are composed primarily of neutrophils. The inflammation found in the patient is also associated with tissue death (necrosis) of the uppermost intestinal mucosa from the terminal ileum to colon, as well as fluid accumulation (275). These same characteristics are not found in the mice typhoid system. Instead, they are actually found in another *in vivo* model system where *S.* Typhimurium, which is a natural bovine pathogen, infects neonatal calves, or when bovine ligated ileal loops are infected experimentally with *S.* Typhimurium.

4.1. *Salmonella* pathogenesis in bovine infections

The first step involves invasion of epithelial cells 15 min after infection of bovine ligated ileal loops with virulent *S.* Typhimurium strain ATCC 14028 (10^9 dose). Both epithelial cells and M cells in the lamina propria of Peyer patches contain the bacteria. One hour after the infection, the cells are located inside mononuclear phagocytes and neutrophils, and the mucosa begins to be permeated with more neutrophils. At 3 h, neutrophil accumulation has induced tissue injury, which is manifested as epithelial detachment, and initiation of fluid accumulation. Thus, fluid accumulation seems to result

from the loss of the permeability barrier in the intestine. At 8 h, a large amount of neutrophils and fluid rich in protein are effused into the intestinal lumen, and between 12 to 48h after infection, diarrhea develops, where fluid moves from the blood and interstitial space to the intestinal lumen. There is also formation of a pseudomembrane.

The virulence genes required for calf infection including TTSS-1 and the effector proteins SipB, SipC, SipD, as well as SipA, AvrA, SptP are all located in SPI-1. The other TTSS-1 effectors are coded in the genome outside of SPI1- including SopA, SopB (SigD), SopD, SopE1, SopE2, SspH1, and SlrP1. SPI-1 also contains other regulators and transcriptional activators. SPI-2 and the *spv* genes in the *Salmonella* virulence plasmid are also required for infection by *S.* Dublin in calves, which is manifested as a more systemic infection (34).

4.2. Invasion

Infection is initiated by invasion, in which the bacteria penetrate the intestinal epithelial monolayer. Most of the existing information about *Salmonella* pathogenesis, lies in the invasion process (74). Invasion is accomplished by the ability of bacteria to transport effector proteins into host cells that induce cytoskeletal arrangement in the host and membrane ruffling of the host cells and eventually uptake of bacterial cells. A series of events lead to invasion. First, activation of genes in SPI-1 allows the expression of genes for the synthesis of the needle complex of the TTSS-1, which is coded by *prgHIJK*, as well as the effector proteins that are transported by the TTSS. The TTSS spans the inner and outer membrane of the bacteria, allowing the secretion of the effector proteins outside of the cells. In the next step, three of these secereted proteins, SipB, SipC, and SipD form a translocation complex across the host cell's membrane, through which the

rest of the effector proteins (SopB, SopE2, SipA, SopD, SopA, AvrA, SptP, SlrP) are translocated. SopB and SopE2 act together to induce the host cell's membrane ruffling. Mutation of both, but not one, prevents invasion. SopE2 functions in similar fashion to the guanine exchange factor (GEF), activating GTPase Cdc42 by promoting the exchange of GDP for GTP, which leads to a series of reactions to rearrange actin filaments. This cytoskeletal rearrangement is transient, since SptP binds the GTP-form of Cdc42 and catalyzes the exchange of GTP for GDP (182). In addition, SipA is known to bind and stabilize actin filaments, resulting in the outward extension of epithelial cells during *S.* Typhimurium infection (276). The remaining effector proteins act to induce an inflammatory response and fluid accumulation (diarrhea). Bacteria remain in the lymphoid tissue of the intestine, and only during septicemia do they spread further into the blood and collateral lymphoid systems to other organs such as the liver and kidney.

Results from studies with mouse macrophages showed that these bacteria are taken up in a process called micropinosis into spacious vacuoles. The vacuoles mature with the modification of surface markers including those from the lysosome, although the vacuoles are distinct from the lysosome (193). This surface modification allows *Salmonella* to avoid the endocytic pathway, in which bacteria are killed in the lysosomes. The vacuoles are then acidified, which, in addition to the low concentration of Mg^{2+}, trigger the PhoP/PhoQ sensor regulatory system. The PhoP/PhoQ activated genes (*pag*), such as those in SPI-2, are activated, while PhoP/PhoQ repressed genes (*prg*) are downregulated. *Salmonella* are then able to multiply.

Salmonella employ more than 40 genes to control invasion in both diarrheal and typhoid diseases, suggesting that the expression of these genes are very tightly regulated

and are expressed only under the proper conditions (3). All of the proteins coded in SPI-1 function during invasion of intestinal epithelial cells. HilA is a major regulator for both the effector proteins and the transport machinery. It acts as a transcriptional regulator for a set of genes in SPI-I including the *sip* (*ssp*) operon, which codes for the effector proteins, and two other operons which code for the secretion apparatus *inv/spa* and *prg*. HilA also positively regulates another transcriptional regulator in SPI-1, InvF, which functions in positively regulating the expression of the effector proteins in SPI-1 as well as SopB that is located in SPI-5. In turn, the expression of *hilA* is dependent on two other regulators in SPI-1: HilC and HilD. Outside the SPI-1, other activators of *hilA* include CpxA, a member of the two-component transduction system CpxR/CpxA, and the two-component system BarA/SirA, the latter of which regulates HilA indirectly through the activation of the *csr* system. It has been suggested that BarA/SirA positively regulates expression of two components of the *csr* system: CsrB and CsrC, two untranslated RNA molecules that function by binding to CsrA, a repressor protein for SPI-1 genes. The binding of these RNA molecules to CsrA reduces the pool of available CsrA, eventually diminishing the repression of SPI-1 genes by CsrA. Thus BarA/SirA activates expression of SPI-I genes indirectly by derepressing CsrA repression (4).

Environmental conditions also regulate the expression of the genes in SPI-1 in a Hil-A dependent manner. Conditions such as microaerophilic (conditions encountered in brush borders), high osmolarity (> 300 mOsm), and acetate concentration between 15- 30 mM, mimicking those in the distal ileum where invasion takes place, promote SPI-1 expression. In contrast, the presence of substances that are usually common in the colon such as propionate and butyrate, or proximal in the small intestine, such as bile, represses

SPI-I genes. Low levels of Mg^{2+} in the macrophage, the site where SPI-2, rather than SPI-1, is expressed, contributes to the repression of the SPI-1 system.

4.3. Inflammatory response

Evidence from in vitro studies has shown that the inflammatory reaction induced by TTSS-1 effector proteins, is likely due to both direct stimulation of pro-inflammatory signaling events in the host cells as well as indirect stimulation through activation of the Toll-like receptors (TLR) post-invasion. Direct activation was considered to be more predominant, because inactivation of one of the genes coding for the effector protein had different effects on invasion and on the ability of the bacteria to induce neutrophil migration (275). An indirect result of invasion in polymorphonuclear neutrophil (PMN) migration was shown during TTSS-1 dependent induction of IL-8, which is a PMN migration chemoattractant in the epithelial cells. Binding of flagellin during *Salmonella* infection to TLR5 of the host cell aided secretion of IL-8 in the basolateral surface through activation of NF-kB (112). Essentially, IL-8 recruited PMN across the endothelium to the lamina propria.

SipA is an example of direct involvement of effector proteins. It interacts with epithelial surfaces activating protein kinase C, which in turn results in the secretion of a chemokine pathogen elicited epithelial chemokine (PEEC). PEEC molecules induce migration of PMN from the lamina propria across epithelial cells into the lumen. Furthermore, SipB can directly activate caspase-1, which results in the activation of pro-inflammatory cytokine IL-1. Further evidence suggests that the other effector proteins, SopA, SopB, SopD and SopE2 can also specifically activate different molecules, which lead to the production of inflammatory mediators.

A search for a gene in *Salmonella* homologous to *V. cholerae ctxAB*, which codes for cholera toxin (responsible for chloride secretion), revealed *stn*, a gene hybridizing with a *ctxAB*-specific probe (41). Although the finding of the gene seemed to suggest a mechanism of fluid secretion similar to that in *V. cholerae*, further analysis on the function of this gene could not confirm this hypothesis. Inoculation of a strain inactivated in *stn* did not impede fluid accumulation in bovine ligated ileal loops. Furthermore, no homology was found between the DNA sequences in *stn* and *ctx* genes, nor was the amino acid sequence in *stn* gene product and cholera toxin homologous. Evidence instead pointed to the inflammatory response, with resulting loss of membrane integrity, as the main cause of fluid loss instead of chloride secretion. This inflammatory response, characterized by the influx of neutrophils, is likely to be the result of activation of specific chemoattractant cytokines (chemokine) in the host cells. Chemokine proteins from the CXC subfamily (those having two cysteine residues flanking another amino acid in the N-terminal), with an ELR amino acid motif upstream of the two cysteine residues, have been implicated in attracting the migration of predominantly neutrophils (211). How this chemokine is activated, and which effector protein(s) is responsible for this activation are yet to be determined.

Knowledge of *Salmonella* pathogenesis also sheds some light on environmental survival, since the cells employ several systems for both mechanisms that are shared during their encounter with stress in both the intestinal tract and the natural environment outside of the hosts.

5. *SALMONELLA* IN THE ENVIRONMENT

Salmonella are found in nature and in the intestinal tracts of many animals, therefore accounting for their ubiquity. They are transmitted to humans via either contaminated meat and vegetables or water. They have been found in a variety of poultry, eggs, and dairy products such as cheese brine (113), and fresh produce such as lettuce, bean sprouts, and raw tomatoes (19). To some degree all have been linked to salmonellosis outbreaks. *Salmonella* are often detected in sewage, freshwater, marine and coastal waters, and groundwater. They can survive for long periods in natural waters, and in various locations in the household environment. For example, *Salmonella* was isolated from biofilms on toilet surfaces in a household of an infected person, which persisted for 4 weeks even after cleaning and disinfectant treatment (12).

The persistence of epidemic strains such as *S.* Typhimurium is of great concern. This serotype, which is found mostly in humans, has also been found in a variety of niches such as estuaries (37), river water (210), the soil (101), animal farm buildings (136), pig production (209), and cow and chicken manure. It has been suggested that the transmission of these bacteria in water is probably facilitated by their spread from nearby animal farms during storm events (14). Some studies have found that *Salmonella* persists as aggregates in biofilms in poultry farm environments such as chicken crates (191). The control of *Salmonella* in chickens is accomplished at multiple levels including vaccination of chicks, antibiotic/chemical treatment of the feed and water, and disinfection and cleaning of the poultry house. Although these measures have lowered the number of *Salmonella* in production facilities compared to the untreated controls, *Salmonella* can still survive. It has been shown that they survive in poultry litter

microcosms for longer than ten weeks (176). Thus their widespread occurrence may contribute to the frequent transmission of this organism from animals to plant products and eventually to humans, giving rise to recurrent outbreaks of *Salmonella* disease. Their ubiquituous character may be attributed to the survival strategies of the organism. Understanding the ability of these bacteria to survive in the environment and in the food chain is therefore crucial to the goal of either controlling or eliminating this organism (110)

5.1. Changes in gene expression in response to environment insults

Salmonella undergoes many environmental fluctuations in its various niches, which necessitates adaptation to a variety of stresses such as starvation, changes in pH and osmolarity, desiccation and limited iron availability. Some of the stresses encountered by cells in external environments are similar to those inside the host, such as starvation in diluted aquatic environment vs macrophage ingestion, and low pH in the environment vs the interior of the stomach and macrophages. Sometimes, multiple stresses must be managed simultaneously (70). In fact, only a few organisms have the survival capability of *Salmonella,* when encountering a broad range of stresses both in the host and in the environment (70).

Salmonella responds to stresses by expressing stress-response genes. Some of these genes are regulated by RpoS (σ^S), an alternative sigma factor of RNA polymerase, which is produced mainly under starvation and at stationary phase, but also under conditions of low pH and temperature. The expression of stress response genes is dependent on the relay of a signal from the cell surface into the cell, such that bacteria can exert a necessary response as conditions dictate; for example, virulence genes are not

usually expressed unless the cells sense that they are inside the host. Many of these responses are accomplished via two-component signal transduction systems (TCS), which are composed of paired regulatory proteins: the sensors and the modulators. Upon receiving a signal from the environment, the sensors self-phosphorylate at a conserved histidine residue, and then phosphate is transferred to the aspartate residue in the modulator, resulting in its activation. Once the modulator is activated, it triggers transcription of its target gene(s) by attaching to its binding site in the promoter region.

One of the most common stresses encountered by cells in the environment is the limited availability of nutrients. Upon limitation of a single nutrient, bacteria activate scavenging systems such as the cAMP-CRP system, the NTR system, or the PHO regulons. However, when an essential nutrient is depleted, bacteria enter stationary phase, where growth ceases. In response to carbon starvation, *Salmonella* modulate a number of cellular processes, which together are termed the starvation-stress response (SSR). The SSR includes transport proteins, carbon catabolic enzymes, protective enzymes, respiratory enzymes, and virulence products. The majority of these genes are regulated positively at the transcriptional level by σ^S. In addition, the cAMP-CRP complex also either up- or down- regulates a number of loci under the SSR system. There are two classes of genes induced by carbon starvation: the *cst* (carbon starvation) genes including *narZ*, *dadA*, *stiC*, and *rpoS*, which are predominantly for long term survival under starvation conditions, and the *pex* genes that are required for general resistance (C-starvation induced [CSI] cross resistance) to low pH (pH3), H_2O_2, antimicrobial polymyxin B, and high temperatures (55°C). The *cst* genes require cAMP/CRP for induction, while the *pex* genes can also be induced under conditions with N or P

limitation (21, 149). It was recently shown that the SSR response was initiated by envelope stress that is triggered by C starvation. This process in turn activates an additional sigma factor, σ^E, which activates transcription of σ^E regulon to mediate CSI cross resistance. The same genes that are activated by C-starvation can also be activated by P-or N-starvation, or environments inside the host such as macrophage or epithelial cells. Resistance to either H_2O_2, high temperature (*stiC*), or acid conditions (*narZ*), could also be induced under C-starvation conditions (223). These findings indicate that some of the starvation responses even provide cross-protection to other environmental stresses.

Under iron-limiting conditions, the bacteria acquire iron by secreting iron-chelators such as enterobactin, the product of *ent* gene cluster, and express the transport system to import the ferric-enterobactin complex. Iron uptake is regulated by Fur protein, a global regulator that regulates expression of other genes.

In addition, *Salmonella* also has evolved a complex acid tolerance response (ATR) mounted against acid stress due to mine drainage, acid rain and weak acid metabolic byproducts in the environment and the low pH environment present inside the phagolysosome. The response to low acid conditions has been shown in vitro, where actively growing *Salmonella* tolerate very low acid environments (pH 3.3) only after a brief adaptation to a milder acid environment (pH 5.8). This system, however, does not confer cross-protection against other stresses such as H_2O_2, or heat shock (69). In addition, the increased ability to survive under low pH conditions is mediated by a prior exposure to short chain fatty acids such as acetate, propionate, and butyrate at neutral pH (8). These fatty acid mediated tolerances to acid conditions require RpoS.

Survival against reactive oxygen species from environmental agents is dealt with by expression of two systems, one which reacts against hydrogen-peroxide, mediated by *oxyR*, and the other which reacts against superoxide species and is regulated by the *soxRS* locus (70). OxyR activates genes in the OxyR regulon, including catalase-hydroperoxidase I, encoded by *katG* and a ferritin-like, DNA binding protein accumulated at stationary phase (Dps) (87, 97). Superoxide dismutases (SOD) detoxify superoxide anion ($O_2\cdot$) by converting it to H_2O_2, which is further converted to H_2O by catalase. Several types of SOD have been characterized, each requiring a metal ion co-factor for activity (53), e.g.- the manganese type (Mn-SOD), coded by *sodA*, the iron type (Fe-SOD), coded by *sodB*, the copper-zinc type (Cu/Zn-SOD), coded by *sodC*, and the recently-identified nickel type (Ni-SOD), coded by *sodN*. Cross protection against H_2O_2 is also conferred by the activity of CuiD protein, which mainly protects the cells from a high concentration of copper ions. CuiD is homologous to YacK, a protein with the same function in *E. coli*. (137).

When *Salmonella* encounter an environment with fluctuating osmolality, they survive by modulating the concentration of compatible internal solutes. Solutes, such as trehalose, are either accumulated inside the cytoplasm when the external osmolality is high, or are released into the environment when there is a decrease in osmolality. Trehalose originates either from the environment or from biosynthesis. A number of components modulate the process, including the biosynthesis of trehalose, transporter proteins, and mechano-sensitive channels. Trehalose also protects cells against heat shock (266).

RpoS is indispensable for the induction of a large number of stress response genes. However, mutation, and consequently inactivation, of *rpoS* is not uncommon. Naturally occurring mutations in *rpoS* have been shown in clinical and environmental strains of *S*. Typhimurium DT104, which eventually affect the invasive abilities of the organism (117). Overall, cells utilize a variety of genetic, structural and physiological mechanisms to respond to stressful conditions.

5.2. Cell surfaces as the first lines of defense against environmental insults

Bacterial cell surfaces, surrounded by a cell envelope, mark the boundary between cells and their environment. Therefore, the cell envelope provides a protective permeability barrier against unwanted materials such as toxins and antimicrobial agents. However, the cell surface is also the site of interaction between cells and the environment. Cell surface properties determine the ability of cells to attach to both biotic and abiotic surfaces, an important attribute that serves to initiate pathogenesis and survival. In addition, the bacterial envelope houses protein sensors, mostly members of the two-component transduction system, which allow the transfer of messages from the outside of cells to the inside, thus stimulating the cells to exert appropriate responses. Cellular appendages, such as flagella, pili, and fimbriae (based in the cell surface) also serve as attachment mechanisms in many instances. Obviously, the cell surface is central to interaction between cells and the environment.

5.2.1. The structure and roles of LPS.

Lipopolysaccharide or LPS, among the many factors that make up the cell surface of gram negative bacteria and influence cell surface properties, is a component that plays a major role in the integrity of the cell's outer membrane. A complete LPS is composed

of three parts: Lipid A, which anchors the LPS to the membrane, the core polysaccharide, which contains a group of polysaccharides, some of which are phosphorylated, and O-antigen polysaccharide chain, which has about 20-30 repeats of sugars. The lipid A portion of the LPS, covering approximately 75% of the bacterial surface, is the predominant molecule (45%) in the external leaflet of the outer membrane (36). The presence of a lipid A hydrocarbon chain results in low fluidity of the outer leaflet. The outer membrane thus has asymmetric distribution, having mainly phospholipids in the inner leaftlet, and mostly LPS in the outer leaftlet. The consequence of this distribution is a protective barrier for hydrophobic substances, because of the presence of limiting amounts of glycerophospholipid in the outer leaflet. Glycerophospholipid bilayers are required for diffusion of hydrophobic substance. LPS also influences the structural integrity of the outer membrane, because it forms hydrophobic bonds and crosslinking among LPS molecules via divalent cations (Mg^{2+}, Ca^{2+}) and acid groups including phosphates, pyrophosphates, and acid sugars (249).

Distinct features of LPS play different roles in survival and pathogenicity. Lipid A, the hydrophobic moiety of LPS, is essential for growth of most gram-negative bacteria and affects the integrity of the outer membrane. Lipid A with additional Kdo residues is the minimal ingredient for the composition of LPS, and when separated from the walls of dead bacterial cells during an infection, stimulates the immune system of the host. This occurs by binding of lipid A to a receptor molecule TLR4 (188), which activates a cascade of signaling processes. This action promotes the production of a number of inflammatory inducing molecules such as TNFα and IL1-β that direct the immune system to clear infectious bacteria. However, in large amounts, lipid A can induce high

fever, increase heart rate and may cause lung and kidney failure, eventually leading to possible septic shock and death, especially in older individuals.

The composition of both lipid A and the core polysaccharide is conserved within a particular bacterial genus, which is important for the stability of the outer membrane. The core polysaccharide contains two parts: the inner and the outer core. They are assembled by sequential addition of the different sugars by glucosyltransferases on the lipid A substrate located in the periplasmic space of the outer membrane (103). All of the genes required for the synthesis of the core polysaccharide are coded in the *waa* operon. In contrast to the smooth strain, which has a complete LPS, truncation of the core oligosaccharide results in deep rough LPS mutants. The deep rough mutants are characterized by a loss of integrity and negative-charge in the outer membrane. Such mutants are more susceptible to hydrophobic antibiotics such as novobiocin, and other antimicrobials such as SDS, indicating that the core polysaccharide has a role in maintaining membrane integrity. Phosphorylation of the core polysaccharide allows cross-linking between LPS molecules by divalent cations, and to other positively charged proteins. Thus, either the loss of heptoses with their phosphorylation sites, or loss of other LPS phosphorylation could result in both structural and compositional changes in the outer membrane. The loss of these heptoses leaves gaps, which are replaced by phospholipids.

In *Salmonella*, only one predominant core oligosaccharide has been identified. It contains heptoses in the inner core and hexoses in the outer membrane. In contrast, *E. coli* has a number of different core oligosaccharides, which are termed K1-K12 and R1-R4. The inner core of *Salmonella* LPS contains three heptoses, HepI, HepII and HepIII,

with HepI at the proximal end. HepI is linked to a P group or PPEtn, Heptose II is phosphorylated, and Heptose III branches from HepII. It is these phosphate groups that allow crosslinking among LPS molecules. The outer core contains GlcI, GalI, and GlcII, with another sugar GalII branched from GlcI and a GlcNac molecule branched from GlcII (103).

Lastly, O-antigen synthesis is coded in the *rfb* operon. O antigen is located in the outermost part and is exposed to host surfaces. It is also antigenic, and in *Salmonella* is used to determine serologically the more than 2000 serotypes within the genus. O antigen affects the sensitivity to several LPS-specific bacteriophages. The O antigens also have a role in protecting bacteria against complement during infection. *Salmonella* with a complete O Ag is smooth, and those lacking O antigen are called rough strains, in contrast to the *deep* rough strains with incomplete core polysaccharide or core phosphorylation.

The LPS, with its unique structure and location, influences the surface of bacterial cells by affecting the overall hydrophobicity and surface charge of the cell. On the other hand, the cell surface is far from being homogeneous, and in response to changes in the environment, can undergo dramatic changes as well.

5.3. Survival of *Salmonella* in Viable but Non-Culturable (VBNC) forms

The ability of *Salmonella* to survive adverse environmental conditions is also attributed to their ability to exist in other forms. After a long period of starvation, *Salmonella* switch to a viable but non-culturable (VBNC) form. Analogous to spore formation in some gram-positive bacteria, VBNC cells have very low metabolic activity. Although they cannot be detected in regular growth media, Live-Bac fluorescence

staining reveals that these cells have intact DNA and cell walls. In addition, a very low respiratory activity was detected using the CTC stain. The cells were found to be more rounded, and some formed filaments which broke up to form individual cells upon resuscitation with heat shock or a shift to rich, optimally osmotic media at 37°C. The VBNC form of ST DT104 has been shown to be more resistant to osmotic and oxidative stresses in vitro (93). The ability to rapidly resuscitate a majority of the VBNC cells to actively growing cells by a brief heating at 65°C, has provided evidence for the viability of these non-culturable cells. Opponents of the VBNC hypothesis maintain that this state could well be due to a few cells out of the total population that survive stressful conditions. The mechanism of VBNC formation is still unclear. In *E. coli*, it was shown that this process involves relaxation of DNA by a decrease in DNA negative supercoiling (caused by DNA gyrase or topoisomerases), since inactivation of the genes coding for these DNA-modifying enzymes increases the proportion of cells that are nonculturable (78). The alternative sigma factor RpoS is required for this process (22, 26). Coutard *et al.* (50) further showed that the VBNC cells of pathogenic strain *V. parahaemolyticus* Vp4 express 16srDNA and *rpoS*, but not the virulence genes *tdh1* and *tdh2*, coding for thermostable direct hemolysin, thus questioning the virulence state of the VBNC cells.

5.4. Antibiotic resistance as a mechanism of survival

To overcome competition with other bacteria and other organisms in natural environments for nutrient acquisition, both prokaryotes and eukaryotes that inhabit the same locale evolve to produce biocides and antibiotics. Antibiotic resistance genes, as well as other virulence factors, are acquired by either mutation of genes in the genome or by horizontal transfer, thus resulting in the emergence of new, more virulent pathogens.

Horizontal transfer can happen by either *conjugation*, which occurs via direct contact mediated by specialized pili; *transduction*, in which the gene is packaged in a bacteriophage and infected to a new host; or *transformation*, where the cells must induce genetic competence to acquire and integrate a piece of DNA. Sometimes, a large piece of DNA containing multiple virulence factors can be transferred as mobile genetic elements. These elements were identified because they were absent in closely related species of bacteria, had a different G/C content compared to the more conserved region of genomes, and were often flanked by direct repeats (106). In *S.* Typhimurium this is exemplified by the SPI (*Salmonella* Pathogenicity Island) (157) and in *S.* Typhimurium DT 104, the SGI (*Salmonella* Genomic Island) (28). In contrast to commonly observed plasmid-encoded genes, the genes in the Genomic Island were shown to have been transferred to the genome, and thus became very stable.

Bacteria have developed different mechanisms to resist antibiotics. Firstly, they acquired the ability to inactivate a drug before it reaches the interior of cells. This action is exemplified by the production and the release of β-lactamase to cleave β-lactam antibiotics. Secondly, there is the alteration of a specific target of the antibiotics. For example, the cells can initiate mutation of DNA gyrase to resist DNA targeting antibiotics. Thirdly, there is a reduction in concentration of antibiotics before they reach the target site. Efflux pumps have evolved in bacteria to export antibiotics from the cells. Additionally, Gram-negative bacteria are protected by the outer membrane, which acts as a barrier to many antibiotics and host defense factors. The structural features of LPS play an important role in protection, which is mainly due to the asymmetric distribution of

lipid components in the outer membrane, where LPS molecules are predominant in the outer leaflet, and phospholipids in the inner leaflet.

Novel resistance to antibiotics is also endowed to the cell in the form of phenotypic switching. For example, when *S. aureus* switches to a smaller, wrinkled form called SCV (small colony variants), they become more resistant to antibiotics and are more capable of forming much more biofilm in comparison to their regular smooth counterparts (141). In. *P. aeruginosa*, a similar SCV colony variant also exhibits greater biofilm-forming ability, and resistance to antibiotics (58). In fact, a large number of studies have shown a strong correlation between biofilm forming ability and antibiotic resistance (73).

6. OVERVIEW OF BIOFILMS

In aquatic environments, *Salmonella*, like many other bacteria, exist not only as single planktonic (swimming) cells, but also are encased in an extracellular polysaccharide matrix forming specialized structures and multicellular communities called biofilms, attached to surfaces (49, 170). Although the biofilm phenomenon has been established only during the past few decades, (possibly due to our use of pure culture and log-phase grown cells in the laboratory) (47), available fossil evidence has revealed that putative early-stage biofilm structures existed as long ago as 3.3 billion years (95). Biofilms have been found in deep-sea hydrothermal environments as well as natural streams. They are formed by both archaeal and bacterial lineages. Thus biofilms have existed in both ancient and modern types of prokaryotes. It has now been proposed

that both planktonic and biofilm forms have evolved concurrently, thereby providing survival advantages to cells under different conditions (227).

Biofilms are sometimes observed either as a ring of growth in the liquid-air interface or as a leathery pellicle floating on the surface of broth media in the laboratory. Biofilms, which can vary in shape, also form in solid-liquid interface attached to a biotic or abiotic surface in submerged conditions. For example, *Pseudomonas* spp form mostly "carpet" like structures instead of pillars, when grown in rich media. "Streamers", biofilm slimes with tail-like structures, are formed only under high shear forces, while a more circular form is produced in the absence of a strong flow (95). Biofilms of different bacteria are very diverse under various environments.

Because of their attachment, biofilms are sometimes referred to as a sessile community compared to their planktonic counterparts. However, it is now widely appreciated that, at the microscopic level, the structure of biofilms is very dynamic. Instead of forming a mere homogenous monolayer, cells in mature biofilms exist as aerial structures that form pillar-like shapes, with hollows in between allowing the flow of liquid. Cell to cell communication takes place, and probably contributes to the formation of mature biofilms. Cells in different parts of the biofilms are heterogeneous in nature. The mushroom-like structures confer a gradient of aerobicity reaching from outside the biofilm to its innermost part. New cells continuously attach to the mature structure, while some cells detach and are dispersed under shear force to start a new biofilm in a new niche elsewhere.

Biofilms have been well studied in several gram-negative bacteria, such as *Pseudomonas spp., E. coli* and *V. cholerae*, as well as gram-positive bacteria, such as

Staphylococcus aureus and *S. epidermidis*. From studies of these and other bacteria, it is known that the structure and physiology of biofilms vary greatly from species to species, and even within the same species as growth conditions are altered. In fact, multiple pathways of biofilm formation by the same bacteria under different conditions have been observed (30). Despite the variation in structure and composition of biofilms among the different genera, biofilms share a few properties, e.g. the formation and the life cycle of biofilms occur similarly in several developmental stages; the requirement for a matrix and a polysaccharide component is common; and they are formed by a congruity of multiple cells (multicellular).

6.1. What are the developmental stages of biofilms?

One of the most studied biofilms is that of the pseudomonads, which have become a model system of biofilm development (170). Most of the developmental studies were performed using submerged biofilms. Although a predominant model has been established, variations exist, because different genera use different mechanisms for attachment and maturation, and the same cells are capable of using several different pathways to form biofilms. Similarly, the differences in environmental conditions may trigger different signals in different genera. Some bacteria form biofilms under starvation conditions while others do so only in the presence of rich nutrients, and yet others only form biofilms in the presence of a specific signal. Some environmental stimuli that promote the formation of biofilms include temperature, osmolarity, pH, iron and oxygen.

In the initial attachment stage of the model system, *P. aeruginosa*, planktonic (free swimming) cells are loosely associated with a surface (244). Type IV pili and motility are required by *P. aeruginosa* at this stage, based on experimental data that

showed cells lacking flagella were defective in the ability to colonize a surface. The capability of a small number of non-flagellated cells to form a few aggregates (probably by random movement to reach the substratum under favorable conditions) suggested that flagella are required to resist the repulsive forces between bacteria and the surface. A transcriptional activator AdnA, which activates flagellar biosynthesis, chemotaxis, and perhaps the O antigen of LPS, seems to influence biofilm formation by directing the cells to use alternative pathways. This explanation is implemented because disruption of one of the genes in the AdnA regulon causes the cells to become non-flagellated, however biofilms continue to be formed (196). Although, in the *Pseudomonas* model, attachment is mediated by expression of a specific cellular appendage, more general and nonspecific cell surface properties, such as hydrophobicity, have been proposed as signals for attachment (177). However, compared to our molecular knowledge of biofilms, relatively little is known about the importance of these physicochemical factors for attachment.

Following the initial attachment stage where cells adhere to the surface, *Pseudomonas* cells are still actively moving using Type IV pili, and within a few hours they form clusters of cells known as microcolonies. This attachment by these microcolonies is still transient, since these clusters can move as a unit or even disperse again to individual cells (170). This stage is then followed by irreversible attachment, where the genes that encode for flagella (*fliC*) are downregulated, and the genes that code for alginate, the polysaccharide components of biofilm matrix (coded by *algD*) are upregulated. Actually, the two genes are regulated simultaneously by AlgT or σ^{22} (268).

At the next stage, the biofilm matures, whereby the microcolonies grow in three dimensions forming aerial structures with pillars and channels. New cells originate from

the growth and multiplication of cells within microcolonies, as well as attachment of incoming cells. Cells in different locations within the biofilm differentiate, forming a community with specialized functions, similar to that in a multicellular structure. In fast moving water, the filamentous "streamers" are formed having a steadfast "head" and moving "tails", while in slow-fluid flow or standing water, the more circular and "mushroom" forms tend to prevail. It has been shown in *P. aeruginosa* that quorum sensing molecules, analogous to pheromones in humans, e.g. LasI, play a positive role in the development of biofilms to form a mature structure (57). Another quorum sensing molecule RhsL, is required at the latter stage of development for maintenance of mature biofilms. Quorum sensing involvement has also been shown in *V. cholerae* biofilm formation, although, in contrast to that shown in *Pseudomonas*, it occurs at low cell density.

The cycle of biofilm development is completed by detachment of cells from the mature structure, either from shear forces in the environment, or from the ability of cells to produce degradative enzymes such as alginate lyase, thus allowing them to spread to other favorable niches and form new biofilm communities. Starvation and the loss of EPS have also been attributed to detachment, by a yet unknown mechanism.

The bacterial community in a biofilm actually is not coordinated in this process, such that at any one time, each stage can be found in different parts of the biofilm, demonstrating the highly dynamic nature of the structure (227). Although there are distinct stages during the development of biofilms, variations do exist in any particular biofilm community.

6.2. Role of the matrix in biofilm synthesis

Although the detailed process of biofilm formation varies greatly, all share a common characteristic, i. e. the production of a matrix. Matrix is defined as any material in the biofilm external to the outer membrane of the cell. The matrix is mostly composed of polysaccharide; however proteins, as well as DNA, have been also documented to be constituents of the matrix (261). In *E. coli*, the presence of type1 fimbriae, curli and colanic acid are required for matrix formation. Cellulose, coded by *bcs* genes, has recently been documented as a matrix constituent in *E. coli* and *Salmonella* spp (221, 279). In gram-positive *Staphylococcus aureus* and *S. epidermidis*, polysaccharide intercellular adhesion (PIA), coded by *ica*, is primarily responsible for attachment. Later, PIA was also found to be produced by gram-negative *E. coli* strain MG1655 and *Yersinia*, and was a requirement for biofilm formation in both bacteria. In the model organism *Pseudomonas* spp., alginate, encoded by *algD*, has been implicated as the main component of biofilms in mucoid strains. In non-mucoid strains, however, two different carbohydrates are produced: Pel, a glucose- rich polysacccharide encoded by *pelA-G* (72) and PSL, a mannose rich polysaccharide coded by *pslA-O* genes (114). The presence and expression of these two operons vary among different strains of *Pseudomonas*. Interestingly, bacteria can express at least two different matrices under different conditions, as was shown in *V. cholerae*, where Vps-containing matrix production was bypassed after addition of Mg2+ to the growth media, and the cells produced a matrix composed of O-antigen polysaccharide (122). In addition, when enteroaggregative *E. coli* (EAEC) cells were grown in media containing glucose and elevated osmolarity, biofilm formation required only aggregative adherence fimbriae (AAFII) but not the type I fimbriae, Ag43 and motility (217). Furthermore, in *E. coli*, only PIA-, and not colanic-

acid-containing, matrix is produced when the carbon regulator *csrA* is mutated. Again this shows that even the most commonly shared characteristic of biofilms among diverse organisms, matrix production, is itself diverse and can be complicated at times.

6.3.The concept of multicellularity of biofilms

The highly structured community that exists in biofilms is proposed to be analogous to the multicellular systems in some bacteria capable of differentiation (such as *Myxococcus xanthus*) or even to eukaryotic systems. Although the term "multicellularity" is sometimes used to describe a structured entity that is comprised of many cells, there is an even greater implication (29). Multicellular behavior in prokaryotes is exemplified by the formation of fruiting bodies in *M. xanthus*, where cells interact by sending signals upon starvation and form aerial structures called fruiting bodies, the site of spore formation (63). Various cells differentiate for the benefit of the whole community such that, in some instances, their specialized functions make it impossible to survive without symbiotic interaction with other distinct differentiated cells. By comparison, biofilm cells do interact and send a number of signals among themselves. Intercellular signaling has been shown to be required for the development of biofilms, and the formation of biofilms that occurs in stages mimics some of the developmental stages of the multicellular structures in *M. xanthus*. However, the niches in biofilms vary greatly and there is a lack of terminal differentiation of cells. It is unknown if cell differentiation is coordinated and could actually benefit the whole biofilm as a system, because cells in these niches can behave independently. Therefore, biofilms fulfill the concept of multicellularity only to some extent, however, the term multicellularity will be used hereafter as a community-based behavior, instead of a strict definition in terms of structure and function.

6.4. Survival advantages of biofilms

Biofilms confer many advantages to cells in the aquatic environment. For example, faced by high shear forces from water, the cells in biofilms are able to maintain stability because of strong adherence by the extracellular matrix. The presence of pillar and mushroom structures allows more efficient diffusion of nutrients both from the environment outside of the biofilms as well as from degradation residues within the biofilms, as compared to open water conditions. At the same time, waste and toxic materials can be exchanged by the flow of liquid through the channels in the system. The matrix also allows cells to be in close proximity, and thereby present conditions where cell-cell interaction becomes possible. This interaction allows genetic exchange to occur, e.g. the acquisition of virulence genes such as those for antimicrobial resistance by horizontal transfer. There is evidence for a higher magnitude of gene transfer in biofilms compared to that in planktonic cells (84). The mechanism of transfer has not been recognized, although structures that behave like F-pili have been suggested (47). Although studies of biofilms in the laboratory are usually done with a single species, in natural environments biofilms are composed of mixed-species of microorganisms, thus allowing possible gene transfer between different genera.

6.4.1. Antibiotic resistance

Biofilm cells seem to be very resistant to antibiotics, apparently due to an inherent resistance phenotype. The persistence of biofilms in medical devices and urinary and vascular catheters, as well as in tissues of patients with bacterial infections such as cystic fibrosis, despite antibiotic treatment, strongly suggest the resistant nature of biofilm cells not only against antibiotics but also the host defense system. Antibiotics readily kill

planktonic cells with 1000x greater efficiency than biofilm cells (169). Physical disruption of biofilms restores the efficiency of antibiotics against biofilm cells similar to that observed for planktonic cells. These observations suggested that EPS matrix may prevent access to cells inside the biofilms. However, the flow of liquid within the biofilm structure allows antibiotic molecules to enter the system (229), suggesting that the presence of matrix is only partially responsible for protecting the cells. Actually the ability of cells in biofilms to adapt is the primary reason that resistance is conferred. The specialization of cells within the biofilm structure results in some cells that are dormant, thus permitting survival of these cells in the presence of antibiotics that require active cell growth for effectiveness. In addition, some cells can acquire new properties such as expression of efflux pumps, alteration of drug targets, as well as the production of antibiotic modifying enzymes that were not present in most other cells in biofilms (170). In the natural ecosystem, biofilms were similarly found to be resistant to antimicrobial agents such as antibacterial peptides. Because of the heterogeneity of biofilm cells, an antibiotic directed against these bacteria must be able to kill cells at all different stages, otherwise, surviving bacteria will re-establish a new community. Thus bacterial resistance in biofilms poses a major health risk.

6.4.2. Metabolism and other environmental stresses

Heterogeneity among cells in biofilms also confers advantages in metabolism, such as shown in biofilm-forming bacteria in the rumen of bovines (125). The diverse state of cells in biofilms creates a very effective system in degradation of potential nutrients such as cellulose. In addition to protection from antimicrobial substances, the extracellular matrix shields the cells from low pH, oxidative stress, and UV exposure, as

well as ingestion by predators such as protozoa in natural waters. The advantages conferred by biofilms go beyond those in natural aquatic environments. Biofilms serve as a reservoir to shed pathogenic bacteria from time to time. Because of their aggregation, biofilms allow the dispersal of bacteria in infective dosages (96). There has been evidence that protection in the biofilm state also increases the survival ability of cells once they infect a host, thus enhancing the persistence of bacteria and extending their presence in the infectious process.

The importance of biofilms in the survival of bacteria has caused them to be an increasingly important subject of investigation during the past half-century. Studies of biofilms in the laboratory involve several different methods (30). For example, laser confocal microscopy allows a three-dimension observation of biofilm structures in cells tagged with fluorescence. The use of crystal violet dye allows visualization of biofilms in flasks, tubes and in microtiter plates. Genes that are involved in the formation of biofilms have been screened using random mutagenesis and selecting for mutants that are no longer able to adhere to the wells of microtiter plates or those that cannot form mature biofilms (172). Production of pellicles, thick leathery material produced on the surface by cells grown in standing culture, is another indication of biofilm forming ability. Lastly, an alternative colony form, called either rugose, rdar or wrinkled morphotype, the focus of this dissertation, has been associated with the formation of biofilms in a number of bacteria.

7. RUGOSE COLONY MORPHOLOGY

The rugose (wrinkled) morphotype was first reported in 1938 when Bruce White observed what seemed to be a phenotypic anomaly in a picturesque colony of *V. cholerae* (263). Subsequent analysis by White showed the presence of slime materials associated with this phenotype, and a role for the phenotype in the survival of *V. cholerae* was proposed. More recent evidence has confirmed White's hypothesis, since it has been shown that the rugose phenotype aids in the survival of *V. cholerae* against chlorine, osmotic, and UV stresses as compared to its smooth counterpart (195, 253, 272). It was suggested that this survival form, in addition to their survival inside protozoa and in the VBNC form, might explain the persistence of *Vibrio cholerae* O1, the cause of the cholera pandemics. Rugose cells were also shown to be more resistant to complement killing and maintained their virulence when administered to human volunteers (115). Thus, the slime or extra polymeric substance (EPS) appeared to be mainly responsible for resistance.

Recent studies have shown that the EPS was actually composed of exopolysaccharide called Vps (*Vibrio* polysaccharide), which is encoded by *vps* (270). Analysis of the rugose morphotype in *V. cholerae* showed that rugose matrix also is associated with the formation of biofilms. A complex regulatory cascade for Vps production has been revealed (271, 277). An autoinducer (a bacterial cell-to cell signaling molecule), acyl homoserine lactone CAI-1 (Cholera autoinducer1) activates LuxO, a response regulator, when present in low amounts. LuxO functions to repress *hapR*, a transcriptional regulator, which negatively regulates *vps*. Therefore at low density, early

in the development of the biofilm, repression by *hapR* is released by activation of LuxO resulting in the synthesis of VPS that promotes attachment of the planktonic cells.

8. COLONIAL VARIATIONS IN OTHER ORGANISMS

Colonial variations occur in a number of microorganisms, and most of them have important implications in allowing the cells to adapt to a specific niche. These variations are usually distinguishable among different strains, probably suggestive of the nature of different matrix components. *E. coli* displays a *frizzy* colony morphology with a rough surface in solid media and forms aggregates in liquid media in the form of flocculates, which settle on the bottom of the media (124). It was found that interaction between outer membrane proteins [called Antigen 43 (Ag43)] among the cells is responsible for the frizzy phenotype and the autoaggregation. In fact, when the gene that encodes Ag43 from *E. coli, flu,* is expressed in other genera (*Pseudomonas fluorescens* and *Klebsiella pneumoniae*), the transformed colonies adopt the frizzy morphotype and the autoaggregation properties. Ag43 also enhances the ability of the cells to form biofilms. In addition, the same strains that exhibit the frizzy colonies could also change to smaller size colonies due to hyperpiliation. Therefore a change from large smooth flat colonies to small, convex, frizzy colonies was due to both Ag 43 and type I pili (100).

A *small*, opaque colony variation (S1) and *small* flat colonies with a granular and irregular surface (S2) were described in *Pseudomonas aeruginosa* strain 57RP as adherent colonies on agar plates after growth in static medium. In general media, such as T-soy agar, the cells revert back to the parental large (L) colonies (58). The S variants form pellicles at the surface of liquid media, and they form biofilms more rapidly than the

L colonies. They were also more susceptible than the parental form when exposed to H_2O_2, thus this colony type does not provide protection against this stress. Studies of the ultrastructure revealed that the S cells were hyperpiliated, therefore similar to colonial variation in *E. coli* K-12, where hyperpiliation resulted in smaller, convex colonial variants (100).

Stable, crenated and corrugated colonies were also reported in the marine bacterium *Hyphomonas* strain MHS-3 when grown on marine agar at 25ºC for two weeks. Similar to rugose colonies of *Vibrio cholerae*, the cells in these colonies also produced capsular exopolysaccharide for attachment to surfaces and for matrix formation in biofilms (187).

In addition, a wrinkled colony variation has been reported in *Salmonella* Enteritidis as a *lacy* phenotype and was shown to be associated with a cell surface matrix composed of flagellin and 35kDa protein components that bound to LPS high molecular weight O-antigen. The SE lacy colonies were induced after 16 h of growth at 42ºC and additional 24 h incubation at 25ºC on brilliant green agar. Prolonged incubation for 72 h resulted in a loss of matrix, which correlated with the loss of O antigen (124).

The baker's yeast *S. cerevisiae* also exhibits colonial growth called mats with elaborated patterns due to cell aggregation on media with 0.3% agar. The mats were associated with the expression of the *flo11* gene, which codes for cell surface glycoprotein required for adhesion. Disruption of the gene abolished the formation of mats and biofilms (194). Therefore the cellular structure that is responsible for the formation of biofilm also appears to play a role in the change of colony morphology.

Colonial variation in *Pseudomonas fluorescencens* from smooth to wrinkled or fuzzy was found only when the cells were incubated in media containing peptone under static conditions, but not shaken, and then subsequently subcultured onto agar plates. This variation was further proposed as being triggered by spatial heterogeneity within the static environment, under which the uncommon morphology has a survival advantage over the common one. Thus, phenotypic switching was proposed as apparently one model of bacterial adaptation in evolution (189).

These examples show that colonial variation can be associated with either the expression of different cellular structures, a change in either the amount or kinetics of biofilm formation, or even greater survival ability. Furthermore, the variations might play a role in survival of the organisms under specific conditions, e.g. inducing the organism to be bottom dwellers, surface growers, or biofilm formers once conditions are favorable. These examples have spurred our interest to examine if the rugose colony variation in *S.* Typhimurium might have a special function as well, and thus may influence their survival ability.

9. RUGOSE (RDAR) PHENOTYPE IN *SALMONELLA*

A rugose phenotype has been shown in *Salmonella* and was referred to as a red, dry and rough (rdar) phenotype because of its appearance on media containing Congo red. This phenotype is exhibited by *S.* Typhimurium (199). *S.* Enteritidis (221), and in some *E. coli* strains (33). The expression of the phenotype only occurs at low temperatures (between 20-30°C) in complex media with low osmolarity (below 0.35 M) (202). Therefore, in contrast to the rugose phenotype of *V. cholerae*, which is expressed

at higher temperature (37°C), rugose in *Salmonella* is thought to aid the cells possibly in the environment outside of the host.

Similar to *V. cholerae*, cell aggregates in the *Salmonella* rdar phenotype are held together by an extracellular matrix. Since the cells in the colony can be lifted as a single piece from the agar plate, rugose colonies have been proposed to be a form of multicellular behavior (202). The morphology has also been associated with the formation of other multicellular structures in liquid media such as pellicles, cell clumping, and biofilms. Similar to cells in biofilms, cells in aggregates (multicellular forms) enjoy improved protection from stress, more efficient food acquisition, and proximity for cell-to-cell communication and gene exchange (201). Therefore, this phenotype has been proposed to have a significant role in survival of cells in the environment. Aggregation may aid in protection from host defenses during infection.

Thin aggregative fimbriae (called curli in *E. coli* or tafi in *S*. Enteriditis) and cellulose are two components of the extracellular matrix, that are associated with the rugose phenotype in *S*. Typhimurium and have been the subject of research in recent years (45, 201, 202, 221, 278). Genes for curli production are coded by the *csg* (formerly *agf)* operon, while genes for cellulose production are coded by *bcs* genes. In addition, White *et al.* (262) showed the presence of a high MW polysaccharide that co-purified with curli proteins. However, the composition and the regulation of this third component have not been well elucidated.

Both curli and cellulose play a role in the tenacious aggregation of rugose colonies. The lack of each of these components resulted in a saw (smooth and white) morphotype on the CR plate, and loss of aggregative ability in the form of either biofilms

on surfaces or pellicles in broth. In contrast, colonies from cells lacking curli appeared pink on a CR plate, [pdar (pink, dry and rough)]. The matrix from these colonies was elastic and with SEM it was shown to be denser than that of the wt strain. The cells formed only partially rugose colonies and exhibited only some form of association (200, 202). Cells lacking cellulose appeared as brownish colonies [bdar (brown, dry and rough)]. These cells were very fragile, and were more susceptible to killing by chlorine. Natural isolates of *S*. Enteriditis showed rdar, bdar or saw morphotype but never pdar (221). In addition some domesticated strains of *E. coli* such as MC4100 did not produce cellulose (278). Therefore the expression and production of these matrix components may vary.

9.1. The regulation of curli production

The aggregative phenotype of cells in the rugose phenotype is mainly due to the expression of curli, small (2nm diameter), proteinaceous, extracellular appendages that are produced by several genera of enterobacteriaceae such as *Escherichia, Salmonella*, *Enterobacter* and *Citrobacter* (46, 82, 173). Distinct from other fimbriae, which are usually straight, these fimbriae appear as twisted, curly aggregates, thus the name curli, or aggregative fimbriae (Agf). Other than serving as a component of bacterial extracellular matrix, this structure enables cells to bind soluble forms of human reticular matrix such as fibronectin, collagen, and laminin. It has a proposed role to aid initial adhesion to surfaces and human tissues such as skin (173). The fimbriae have also been shown to bind to epithelial cells in the small intestine of mice (230). The wide range of surfaces that can be recognized by curli may contribute to adherence and subsequent biofilm formation by *Salmonella* and *E. coli* (10). However, some *E. coli* K-12 laboratory

strains do not express curli, although the genes for curli are present and functional (46, 98, 173). The reason for this different behavior in *E. coli* K-12 strains is not yet fully understood, but possibly involves the impaired expression of *rpoS*, the gene that codes for the sigma factor σ^S required for expression of the *csgBAC* operon (173).

9.1.1 Curli Assembly.

Our knowledge of the mechanism of curli assembly is not fully comprehensive. The machinery for this pathway is coded by the genes in two divergently transcribed *csg* operons: *csgBAC* and *csgDEFG*. Curli synthesis requires the gene products of *csgA* and *csgB,* which code for the major CsgA and minor CsgB subunits of curli, respectively. In addition to the transcriptional regulator CsgD, two putative chaperone proteins CsgE and CsgF, coded by *csgE* and *csgF*, are involved in curli production. The gene *csgG* codes for CsgG, a lipoprotein in the inner leaflet of the outer membrane that helps to serve as a platform for assembly (40). Thus the assembly system is analogous to the well-described type-1 or Pap fimbriae in *E. coli*, in that it requires the nucleator protein (CsgB), and nucleator center (CsgG), as well as a putative chaperone protein (CsgE). However, the mechanisms of assembly between curli and Pap fimbriae seem to be distinct, since the curli subunits CsgA were shown to be capable of self-polymerization on the cell surface, while the Pap pili require chaperone and usher proteins for translocation and polymerization (116). Once translocated outside of the cells by an unknown mechanism, the curli major subunits CsgA self-polymerize on the nucleator CsgB, in what is called the nucleation-precipitation pathway. The levels of CsgA and CsgB are also controlled by the lipoprotein CsgG, without which both subunits are degraded by proteolysis (98, 140).

9.1.2. Physical characteristics of curli protein

Curli proteins (formerly called SEF-17 or *S*. Enteriditis fimbriae 17 kDa, or thin aggregative fimbriae or tafi, or aggregative fimbriae Agf) attach very strongly to cells, making them difficult to separate. They are also very inert in that they cannot be depolymerized by 5M NaOH, or boiling in SDS with β-merchaptoethanol, or 8M urea or deoxycholate, which are usually used to solubilize other fimbriae (46). Only when the proteins were treated with concentrated formic acid (>85%) could they be depolymerized to mostly monomers of 17kDa. Even with this harsh chemical, the degree of depolymerization was variable. Large clumps of protein would not enter the gel during electrophoresis, thus, absolute quantification with the Western blot procedure could be difficult. Sometimes, a dimer, 33kDa in size, could also be seen with the Western Blot procedure (46, 202).

9.1.3. Environmental regulation of curli

Curli proteins, as measured by production of the major subunit CsgA, are expressed only at the stationary phase of growth, at low temperatures (below 30˚C), on solid media with low osmolarity (below 0.35M) (173). Under these conditions, iron deficiency did not influence expression of CsgA. Under similar conditions, but in liquid rich media instead of solid, the wt cells of *S*. Typhimurium 14028 could not produce curli at either exponential phase or after overnight incubation, nor was it produced in minimal media containing glucose under either aerobic or anaerobic conditions. Curli also were not synthesized at 37°C, except when the rich medium was deprived of iron (202). Expression of the CsgA protein appeared to be regulated at the transcriptional level, since the results of transcriptional analysis corresponded to that of the proteins under different

growth conditions. Additionally, the transcriptional patterns of CsgA under different growth conditions also mirrored those of CsgD, studies which had originally provided the initial cues for the role of CsgD as a transcriptional regulator of CsgA expression (202).

9.1.4. Genetic regulation of curli

The strict environmental conditions required for curli production signifies the tight regulation of the *csgBA* operon by a number of regulators. In *E. coli*, a region between –98 to –54 upstream of the *csgBA* transcription start point, upstream AT-rich activating sequence (UAS), is required for activation of the *csgBA* operon (9). It was suggested that the AT-rich region would induce DNA bending, which would promote recognition by RNA polymerase. Binding of CsgD to the region overlapping the –35 box relative to the translational start site is also required for transcription of the *csgBA* operon. The alternative sigma factor σ^S is involved in the regulation of both *csgD* and *csgB* operons. It is encoded by *rpoS*, which is expressed optimally during the stationary phase of growth and during osmotic stress. Lack of expression at the transcriptional level in an *rpoS* mutant indicates that the transcription is dependent on RNA polymerase holoenzyme containing σ^S (E σ^S) (202). It has been shown that direct binding of cytosolic Crl protein to σ^S increased binding specificity of this sigma factor to the *csgB* promoter region, thus stimulating transcription by Eσ^S. This increase in transcription occurs at low temperature because both transcription and stability of Crl are increased under this condition (24), explaining, in part, the temperature dependence of rugose expression.

The expression of curli is regulated by several two-component signal transduction systems (TCS). OmpR/EnvZ responds to high osmolarity by repressing the operon. This response parallels that of CpxA/R TCS, which acts similarly upon either an increase in

osmolarity or curli overexpression (60). Recent studies have shown that the mechanisms of regulation, mainly through CsgD, between these two overlapping systems actually are distinct (118) (see below). The DNA-binding protein H-NS represses σ^{70}-controlled transcription of the operon during growth in the exponential phase, resulting in σ^{S}-dependent regulation. Upon σ^{S} accumulation during stationary phase, this repression is released, and transcription is possible. Thus, in the absence of HNS, promoter activity is no longer dependent on σ^{S}, and is instead regulated by σ^{70} (9, 173). Under this condition, the same promoter site of *csgB* (P*csgB*) as used in the wt strain is active in an *hns rpoS* double mutant background. The double sigma factor recognition is not unique to the *csgBA* promoter, since the promoter for the *hdeA/B* operon is similarly regulated.

9.2. Regulation of cellulose production

Cellulose is a linear chain of glucose molecules in β-1-4 glycosidic linkage. In nature, glucan chains never occur in a single chain, but are synthesized as microfibrils where the chains are interconnected. Both the structure and arrangement contribute to the strength of cellulose. There are two cellulose operons in *Salmonella*: *bcsABZC* and *bcsEFG*. The *bcsABCZ* operon was discovered following the finding of *adrA*, another gene regulated by CsgD, and the subsequent screen for *adrA*-regulated genes (279). The latter was discovered from experiments involving random mutagenesis and screening for loss of calcofluor binding and biofilm formation in *S*. Enteriditis (221).

Cellulose production in bacteria had previously been known only in a few bacterial species such as the acetic acid producing bacteria *Gluconobacter xylinus* (formerly *Acetobacter xylinum*), *Agrobacterium tumefaciens*, *Sarcina ventriculi,* and the plant pathogen *Rhizobium leguminosarum bv. trifolu* (198). Most studies of cellulose

production have been performed in *G. xylinus* and *A. tumefaciens*. The recent finding of cellulose production in enteric bacteria *E. coli*, *Salmonella* spp., and *Klebsiella pneumoniae* and of a set of putative cellulose synthesis genes in *Pseudomonas* demonstrated that the production of this polysaccharide might be more widespread among bacterial genera and species than previously believed.

Sequence comparison has shown that two structural genes were present in the operons of these bacteria: *bcsA* (bacterial cellulose synthesis) also called *acsA* (acetobacter cellulose synthesis), which codes for cellulose synthase, and *bcsB*, which codes for bis-(3'-5') cyclic diguanylic acid (c-di-GMP) binding protein. Cellulase, which is also required for cellulose synthesis, is coded by *bcsZ*, the third gene in the operon of the *Enterobacteriaceae*, but it is located outside of the *bcs* operon in both *A. tumefaciens* and *R. leguminosarum*.

How is cellulose produced? Studies on bacterial cellulose production have been performed most intensively in *A. tumefaciens* and *G. xylinus*. In *G. xylinus*, the cellulose is synthesized from a cellulose-synthesizing complex, which spans both the outer and the inner membranes. The two proteins known to be involved in this process, cellulose synthase and c-di-GMP binding proteins, are located in the cytoplasmic membrane. Approximately 50 cellulose-synthesizing complexes produce cellulose in an actively synthesizing cell. These complexes are located along the longitudinal axis of the cells, with each producing multiple glucan chains, which come together to form larger microfibrils.

BcsA, cellulose synthase, is the catalytic subunit for cellulose biosynthesis lying in close proximity to BcsB, which directs the release of free c-di-GMP, a cofactor for

cellulose synthesis, to BcsA. It has been shown that the c-di-GMP binds reversibly to BcsB and activates the protein. However the mechanism of cellulose production remains unclear, although it is believed that cellulose is synthesized directly from UDP-glucose (151). Binding of the cellulose synthase to UDP-glucose substrate has been demonstrated. In *A. tumefaciens*, a significantly different pathway is used, where the gene products of *celABC* and *celDE* have been shown to connect the UDP-glucose to a lipid carrier for linkage of the glucose molecules to build cellulose without requiring c-di-GMP (198). Once synthesized, the growing chain is secreted probably through a pore, where an unknown accessory protein directs the alignment to form the crystalline structure of the microfibrils.

A pair of enzymes coded by two genes *pdeA* and *dgc* in an operon, coding for Phosphodiesterase A (PDEA) and Diguanylate Cyclase (DGC), respectively, also aid in cellulose synthesis having opposing functions in the control of free c-di-GMP levels in the cells. DGC removes two molecules of PPi from two molecules of GTP, resulting in c-di-GMP. Excess c-di-GMP is modified by PDEA to become inactive pGpG. Both DGC and PDEA are members of the GGDEF family of proteins, which share the GGDEF domain alone or with other domains for signal transduction. Thus, a number of proteins from the GGDEF family take part in cellulose biosynthesis in *G. xylinum*. In *S.* Typhimurium, another protein from the GGDEF family, AdrA, is also required for post-transcriptional regulation of cellulose assembly. By analogy with eukaryotic adenylate cyclase, proteins with this motif are predicted to have nucleotide cyclase activity, thus c-di-GMP probably acts as a general activator of cellulose synthesis in bacteria. However, proteins having this motif are also coded for in the *V. cholerae* genome, where no

nucleotide cyclase activity has been identified. Thus it is unclear if all GGDEF families of proteins have the same functions. Nevertheless, the involvement of AdrA in cellulose biosynthesis in *S*. Typhimurium is a novel finding, whose homology has not been described in *G. xylinus*. In addition, glucose promotes cellulose sythesis in *G. xylinum*, but does not enhance cellulose production in *S.* Typhimurium. This finding suggests that there may be some differences between the two systems of cellulose synthesis in *G. xylinum* and *S*. Typhimurium (198)

The production of cellulose has been implicated in aiding environmental survival of *Salmonella* outside of the host. For example, cellulose deficient stains were shown to be more susceptible to chlorine treatment. However, the virulence of a mutant deficient in cellulose did not seem to be altered in the mouse model system, when compared to the wt strain (221).

9.3. The regulation of *csgD*, the central regulator for rugose formation

Construction of a highly structured form such as the rugose colony requires a process of differentiation, where a group of individual cells are transformed into a matrix-enclosed community. This morphogenesis entails the involvement of a number of regulators, which are able to tune the expression of specific genes as conditions change.

The expression of two main components of the extracellular matrix, curli and cellulose, is regulated by CsgD (also called AgfD), which belongs to the FixJ family of transcriptional regulators (Figure 1). CsgD is coded by *csgD* in the *csgDEFG* operon. Knocking out *csgD* resulted in a complete loss of the rdar phenotype because CsgD is required for the transcription of the two *csg* operons, which code for the machinery for curli synthesis, and *adrA*, whose gene products are required for cellular expression of

cellulose (221, 279). *csgD* deficient colonies become smooth and white (saw), i.e., non-rugose, on Congo red plates, with a resulting lack of all forms of multicellular behavior. CsgD essentially regulates switching between the single-cell (planktonic) and the multicellular state.

CsgD is expressed optimally only at stationary phase at low temperature, low osmolarity, and microaerophilic conditions (6% O_2) (83). However, growth in minimal media allows maximum promoter activity under fully aerobic conditions (20% O_2). The promoter activity is induced by starvation of both nitrogen and phosphate, but not carbon. Quorum sensing did not appear to be involved in promoter induction. At exponential phase, increased activity could be seen, when cells were exposed to 4% ethanol stress. It has been shown also that maximum activity of *csgD* promoter (P*csgD*) could be achieved in rich, liquid media under static microaerophilic conditions, a level similar to that shown with cells grown as colonies on plates (83).

The majority of CsgD regulations take place in the 521 bp intergenic region (IR) (83) between the two divergently transcribed *csgDEFG* and *csgBAC* operons (Figure 1). Alterations in the promoter region, such as insertion of A after position –17, or mutation from G to T at position -44 relative to the transcriptional start site, resulted in semi-constitutive expression of the promoter at both 28 and 37˚C, although both promoters were still sensitive to regulation by other environmental conditions (202).

Extensive regulation is shown by a number of DNA binding proteins involved in the expression of P*csgD*. Phosphorylated OmpR is required to respond to osmolarity. Inactivation of OmpR abolishes the rugose phenotype. In contrast, overexpression of OmpR due to a single point mutation that changes leucine by an arginine residue at

position 43 in the protein allowed non-curli producing *E. coli* K-12 strains to overproduce curli and thus increase biofilm forming ability (251). Control of *csgD* promoter by OmpR is accomplished by binding of this molecule to six different sites in the IR, each with different affinity, although in *E. coli*, the binding is only to one site (118). Binding at one of the sites (D1), centered at -50.5 (or -49.5 in *E. coli*) from the transcriptional start of *csgD*, activates the *csgD* promoter and activates expression of the *csgBAC* operon. However, binding at the D2 site (centered at –70.5) represses the promoter (82). Binding at the other three sites (D3-D6) also represses the promoter in the presence of a high level of OmpR-P, but this repression is relieved by IHF, which binds at the same site (at bp-165 to -199) in response to microaerophilic conditions. Binding of IHF initiates DNA bending, which leads to optimum promoter activity probably by bringing two separate regions of DNA together. IHF binding to another region in the *csgD* ORF (+257 to +287) has also been shown, although the condition under which the IHF binds to this site is still unknown.

More recent findings in *E. coli* showed that sensing of osmolarity depends on a number of regulators over curli production. At high salt concentration CpxR acts as a repressor by binding to sites 1 and 2 between the –35 box and the transcriptional start site to prevent RNA polymerase binding. Binding to sites 3, 4, and 5 overlapping OmpR binding sites may function to modulate gradual expression of *csgD* under conditions where OmpR is present, and binding to a region immediately upstream of *csgBAC* promoter could affect transcription of both *csgDEF* and *csgBAC* operons. In response to high osmolarity, CpxR is upregulated at transcriptional, translational and phosphorylation levels.

In *E. coli*, a different regulation independent of CpxR takes place in the presence of sucrose in the media, where H-NS, a DNA binding protein, which recognizes AT-rich and bent DNA regions, represses *csgD* expression (118). In contrast, sucrose had no effect on *csgD* expression in *S*. Typhimurium (83).

A number of H-NS binding sites have also been demonstrated. Interestingly, while *hns* mutation increases CsgD production in *E. coli* (9, 173), it reduces the production in *S.* Typhimurium 14028 (81). The inactivation of *hns* in *S*. Typhimurium 14028 resulted in mucoid colonies (because of release of repression in genes regulating colanic acid production), with subsequent loss of Congo red binding. The activity of the promoter was reduced to approximately 30% in the *hns*- strain compared to the wt. This was confirmed by the lack of CsgD protein expressed by the *hns* strain. However, the effect of HNS is dependent upon the sites to which these molecules bind (Figure 1). Binding to the intergenic region (at bp 69 to –339) is specific and has a repressing effect, while binding to another region beyond IR (-341 to -685) is probably nonspecific and has an activating effect. The role of HNS is probably beyond transcriptional regulation. HNS may mediate the repression of *csgD* in the presence of high sucrose concentration in *E. coli* (118).

The *csgD* promoter is also regulated by another regulator of the GGDEF family, MlrA (a MerR-like regulator) (33), which shows homology with a mercury resistance stress response regulator. Members of these response regulators have a N-terminal DNA binding domain and a C-terminal receiver domain. However, they have also been shown to interact with RNA polymerase. The mechanism of activation of *csgD* expression by MlrA is still unclear. Sigma factor σ^S is required for the expression of both MlrA and

CsgD, although the promoter sequence of *csgD* is similar to those promoters recognized by σ^{70} (202).

9.4. The two-component signal transduction systems in rugose formation

Central to the ability of the cells to sense environmental changes are the involvement of two-component signal transduction systems (TCS). These systems mediate the transfer of information about changes in environmental conditions from the bacterial surface to its interior, thus allowing the cell to rapidly adapt to changes. A TCS contains a transmitter domain or sensor, which is a histidine kinase that responds to a particular stimulus by self-phosphorylation at a conserved histidine residue. The histidine kinase then transmits the signal by phosphorylation of an aspartate residue in the receiver domain of a response regulator. Once phosphorylated, the response regulator can be activated and binds specifically to the promoter of a gene with an appropriate recognition site, thus activating transcription of that gene to respond to particular stimuli. The sensor is usually bound in the inner membrane and has both periplasmic and cytoplasmic domains, while the response regulator protein is cytosolic with a receiver domain in its N terminus, and DNA binding domain in its C terminus. Sometimes, histidine kinase also has phosphatase activity to ensure that the response regulator will not be active in the absence of stimuli. Otherwise, this activity can be served by a protein having aspartyl-phosphate phosphatase activity, which down-regulates the response regulator (190).

So far, three TCS have been involved in the transfer of osmolarity signals to regulate curli production and rugose expression: CpxA/CpxR, OmpR/EnvZ, and RcsC/B (Figure 1).

The CpxA/R TCS contains the histidine kinase CpxA and response regulator CpxR that respond to stresses in bacterial envelopes, (i.e.- disrupt the transfer of normal proteins through the envelope), such as increase in pH and osmolarity, by alteration of membrane lipid and overproduction of outer membrane protein (OMP) NlpE, and increase in unfolded P pilus proteins (190). Activation of the TCS results in upregulation of DegP, a protease that degrades misassembled proteins, and DsbA, a protein which catalyzes disulfide bond formation, as well as several isomerases. Thus, CpxA/R TCS appears to function by restoring impairments in the envelope region by either increasing protein folding or degrading misfolded proteins. It has been shown that CpxA/R TCS negatively regulates curli production in response to conditions of high osmolarity or curli overproduction when phosphorylated CpxR (CpxR-P) molecules are attached to its binding sites. Both the transcript level of CpxR, and the level of active, phosphorylated CpxR increase at high salt concentration, which is concomitant with the decrease of *csgD* expression. Inactivation of *cpxR* eliminates this repression (118). In effect, inactivation of CpxR increases curli-dependent adherence in *E. coli*, however, inactivation of CpxA decreases adherence, because of the loss of phosphatase activity on CpxR (60). Therefore, CpxA positively regulates *csgBAC* transcription by dephosphorylating CpxR-P, the repressor of transcription.

The OmpR/EnvZ system senses levels of external osmolarity and as a result, regulates the transcription of several genes, including the porin-encoding genes *ompF* and *ompC,* which are oppositely activated under conditions of low and high osmolarity, respectively (183). Binding of OmpR at its specific binding sites is required for transcription of the *csgBAC* operon. Therefore, in the absence of OmpR, curli synthesis is

abolished, which was shown, not only with the usual wt strain expressing wt regulated promoter (rP*csgD*), but also in a strain having a semi-constitutive *csgD* promoter (scP*csgD*) (81, 251). EnvZ has been shown to be involved in transduction of the ethanol stress signal to increase P*csgD* activity in the exponential phase of growth (83). However, inactivation of EnvZ still allows partial expression of the rugose phenotype. It was further shown that EnvZ phosphorylates OmpR more in the exponential than at the stationary phase, suggesting that other proteins may act as a phosphate donor for OmpR during the stationary phase of growth (81).

The RcsC/B TCS includes the membrane- bound proteins RcsC and YojN, and the cytoplasmic transcriptional regulators RcsB and RcsA. The system responds to various signals including either mutations in the *mdoH* gene (involved in the synthesis of membrane-derived oligosaccharides); overproduction of transmembrane DnaJ- DnaK, chaperone proteins (120); osmotic shock; desiccation; or alteration in disulfide bonds by mutations in *dsbA* and *dsbB* (76). Upon receipt of these signals, RcsC, a hybrid sensor kinase protein that contains a transmitter domain and a receiver domain, autophosphorylates at a conserved His residue in the transmitter domain (42). The phosphoryl group is then transferred to Asp in the RcsC receiver domain and then to a His residue in YojN. YojN then phosphorylates RcsB, a cytoplasmic response regulator protein (234). The effect of the RcsB is on two pathways, one where the phosphorylated RcsB binds directly to its target DNA, e.g.- in the regulation of *ftsA, osmC,*and *rprA*, and another where it is dependent on a third protein RcsA (165). RcsA is negatively regulated through degradation by the Lon protease (91) and is produced only under inducing conditions. RcsB/A has been shown to upregulate the *cps* operon for colanic acid

capsular polysaccharide synthesis, and downregulate the *flhDC* operon, which codes for the regulation of the synthesis of flagella as well as for motility and chemotaxis (71). These controls lead to speculation that this system promotes the transition between attachment and development to mature biofilms. A number of other capsular synthesis operons are also upregulated by RcsB, which includes that for production of Vi capsule in *S.* Typhi as well as the *galF* operon, responsible for synthesis of the K-2 capsule in *Klebsiella pneumoniae* (259). A DNA microarray study revealed a number of other genes upregulated by this system (67), including *ugd*, which is required for addition of L-aminoarabinose for modification of lipid A in LPS and has also been implicated in capsule production (164). This study also revealed that activation resulted in reduced expression of *csgD*. More recently, the results of this genomic study were confirmed by transcriptional analysis of *csgD*, which showed that inactivation of *rcsB* resulted in an increase in *csgD* expression compared to the wt under low osmolarity conditions (118). However, the implication of *csgD* repression by RcsB is still unclear. It probably occurs at a later stage of biofilm development when cells encounter niches high in salt content. This reasoning is still speculative, because the natural stimuli of the RcsC/B TCS are still unknown, even though it is known that changes in the cell surface resulting from mutations have been shown to induce RcsC/B TCS (67).

Although the three TCS respond to a single environmental signal, osmolarity, it is possible that each of them may also be activated in the presence of additional cues such as changes in the surface of the cell and the cell envelope. In itself, response to osmolarity illustrates how much energy is invested by the cells in rugose morphotype

production and biofilm formation, suggestive of the importance of these aggregative behaviors.

10. REGULATION OF *rpoS*

The transcription of both *csgD* and *csgBA* promoter requires σ^S, or RpoS which is coded by *rpoS*. Inactivation of *rpoS* abolishes rugose morphology and the expression of σ^S and the curli proteins occur at the same time. RpoS is an alternative sigma factor of RNA polymerase that functions to direct RNA polymerase to specific promoters. This process then activates the transcription of only a subset of genes needed during either the stationary phase of growth, starvation, or other stresses during exponential growth. Therefore this sigma factor replaces the main sigma factor σ^{70}, which is responsible for transcription of most genes in the exponential phase. Both σ^{70} and σ^S have homologous regions in both their DNA sequences and amino acid sequences. The promoter regions of the operon recognized by these sigma factors (regulons) are also very similar. Under various stress conditions, both σ^S and σ^{70} are present in cells, and they seem to recognize similar promoter sequences (138). The specificity of these sigma factors is determined by other regulatory factors such as H-NS, Lrp, CRP, and IHF. Thus, there are regulons that are recognized by both sigma factors, although others are recognized specifically by one sigma factor, but not the other (139).

In order to rapidly turn on the expression of stress response genes of the σ^S regulon and to respond to various environmental stresses, bacterial cells must be able to modulate the level of σ^S upon receiving a specific stress signal. The cells have evolved

multiple levels of regulation for RpoS: transcriptional, translational and post-transcriptional level.

RpoS or σ^S is encoded by *rpoS* (formerly *katE*). The transcription of *rpoS* increases gradually during the exponential phase of growth in rich media under glucose limiting conditions reaching up to 20x its basal level at entry into and during stationary phase, thus the increase in transcription parallels entry into the stationary phase. This control of RpoS production at the cellular level is considered to be slow regulation. cAMP-CRP inhibits *rpoS* transcription, thus the increase in *rpoS* transcription does not occur in minimal media even during entry into stationary phase. PpGpp, which is a signal used by the cells in response to starvation (possibly a decline in cellular amino acid content), is required for transcriptional elongation of *rpoS* transcript. During stress conditions such as either carbon, nitrogen and phosphorus starvation; high osmolarity; low pH; oxidative stress or temperature extremes, translation and protein turnover occurs quickly, resulting in presumed rapid control.

At the translational level, RpoS is regulated by the secondary structure of the RpoS transcript, where the upstream coding region base pair with a translational initiation region prevents access of ribosomes. Upon induction by a stimulus, the base-paired structure may be altered by the action of the RNA-binding protein Hfq, which functions together with small RNA molecules, either DsrA, RprA, or OxyS, resulting in either positive regulation (at either low temperatures or in response to membrane perturbation), or in negative regulation during oxidative stress.

The stability of RpoS proteins also determines the level of σ^S in cells. ClpXP protease specifically functions to degrade excess RpoS proteins (the activity of which is

high at logarithmic phase of growth), resulting in a low level of RpoS at this stage of growth. However activity of the protease declines at stationary phase, thus resulting in higher levels of RpoS without alteration in transcription between the two growth phases. It has been hypothesized that the RpoS also becomes more resistant to ClpX at stationary phase (138).

The role of Hfq as a regulator has been recognized more and more over the past six years since the discovery of its requirement for *rpoS* expression and for its subsequent regulation by small regulatory RNA molecules (sRNA, also called non-coding RNA or ncRNA).

11. OVERVIEW OF HFQ

Hfq (or HF-I) is an RNA binding protein that was first identified for its role in the replication of bacteriophage Qβ in *E. coli* (119). It is coded in a complex operon which includes *amiB, miaA, hfq, hflKC* genes, in which the first two code for RNA modification, and the last one encodes for regulation of FtsH protease. Hfq is a small (11.2 kDa) protein present in abundance in cells with approximately 30, 000 to 60,000 copies per cell, mostly associated with ribosomes (119). The crystal structure of *S. aureus* Hfq showed the protein is similar to the Sm proteins in eukaryotes, the proteins essential for RNA splicing and for the formation of the RNA degradation complexes. However, instead of forming a heptamer like that in eukaryotes, Hfq forms a doughnut-like hexamer.

Cells lacking Hfq exhibit pleiotropic phenotpes (167, 246). They have reduced growth rates, lack of glycogen synthesis, have altered negative supercoiling of reporter

plasmids, increased sensitivity to UV, osmolarity, and starvation, and show cell elongation. These observations indicate that Hfq regulates a number of cellular processes, possibly due, at least in part, to its function in promoting efficient translation of RpoS (246). However, Hfq also regulates genes outside of the *rpoS* regulon (167), that are unaffected by *rpoS* mutation, possibly reflecting the newly recognized role of Hfq as an RNA chaperone in the regulation of many RNA transcripts by a number of sRNA molecules (90, 228).

Hfq has been shown to regulate post-transcriptionally by binding to a number of RNAs, including mRNA and small untranslated regulatory RNAs (sRNA) (228). It acts by binding non-specifically to A/U-rich unstructured regions, usually adjacent to a more structured region of RNA. The effect of this regulation may be either positive (activation) or negative (repression).

11.1. Binding of Hfq to mRNA

In bacteriophage Qβ, Hfq positively regulates phage replication by binding to an A-rich region to melt out the base pairing at the 3'end of the + strand phage, thus allowing synthesis of the minus strand (215). However, other regulation of mRNA by Hfq involves destabilization of transcripts. For example, Hfq increases polyadenylation of mRNA containing Rho-independent transcription terminators by PAPI polymerase by aiding in the recognition of the terminator sequence as a signal for polyadenylation (160). The increase in PAPI activity results in polyadenylation of mRNA tails as observed in *rpsO* mRNA, which codes for the S15 subunit of ribosomal protein in *E. coli*. This polyadenylation consequently subjects the mRNA to degradation by RNase E (127). Negative regulation of Hfq has been shown in *mutS hfq miaA* transcripts, the mechanism

of which is not known. This regulation represents *hfq* autoregulation, since inactivation of *hfq* increases the level of *hfq* transcripts, including those that are transcribed from two promoters of *hfq:* P*miaA* and P1*hfq*HS. In this instance, Hfq appears to act by destabilizing the transcripts (245). In addition, Hfq may stimulate decay of *ompA* mRNA by competing with 30S ribosomes for binding to the *ompA* 5'-UTR, thus abolishing protection by the 30S ribosome on the mRNA against RNaseE degradation (252). Co-immunoprecipitation with *hfq* suggested binding to a number of small mRNA (274) including *hdeA* and *hdeB* mRNA. These mRNA are short, and they code for 110 and 108 nt long transcripts, respectively. However, the significance of Hfq binding to these mRNAs is not yet known.

Very recently, it was established that Hfq also acts as an mRNA chaperone in regulation involving a 90 nt sRNA RyhB in an iron storage and utilization system (79, 148). In this system, the transcription of RyhB is under negative regulation by Fur (Ferric uptake regulator), the latter of which is active under iron sufficient conditions. Thus, the system ensures that under conditions of iron limitation, the synthesis of unneeded iron-containing proteins and iron storage proteins such as FeSOD, and succinate dehydrogenase (encoded *sodB* and *sdhCDAB*, respectively) is terminated (148). The mechanism of *sodB* regulation by Hfq was described because of strong binding to SodB mRNA and not to RyhB sRNA. Binding to *sodB* mRNA results in the modification of the SodB secondary structure, such that the RyhB-complementary sequence becomes free for subsequent recognition and binding by RyhB. Binding of RyhB blocks the translation start codon, resulting in the degradation of both RNA species by RNAseE under conditions where the gene product of *sodB*, Fe superoxide dismutase, is no longer needed

by the cells. Therefore, RyhB acts as antisense RNA and Hfq functions as an mRNA chaperone by its strong binding to the mRNA rather than to the sRNA, although Hfq also binds RyhB (79).

One of the prominent known functions of Hfq is its ability to bind small (regulatory) RNA, which is also called sRNA. Co-immunoprecipitation experiments combined with genomic microarray analyses of bound RNA has identified a number of previously unknown sRNAs that bind *Hfq* with high efficiency, in addition to those already identified (274). Many of these sRNAs are in the range of 80–110 nucleotides, and almost all possess rho-independent terminator sequences, however, their targets still await identification. These observations indicate that the regulatory role of Hfq and sRNA has just begun to be unraveled.

11.2. Regulation of sRNA by Hfq

Recent advances in this area have uncovered the mechanism of sRNA regulation coupled with Hfq. sRNA binds to a specific mRNA target by basepairing (although not perfect complementarity). In most cases, Hfq functions in this mRNA-sRNA interaction mainly as an RNA chaperone to facilitate binding of sRNA with its target mRNA (90). From a structural study, it was shown that RNA was looped around the pore of an *Hfq* hexamer on the top side. The Sm2 motif appeared to be important for this binding. Two mutations of highly conserved residues in this region, Y55A and K56A, disrupt binding of DsrA sRNA. More recently, another RNA binding site on the distal face of the Hfq hexamer has been identified, possibly involved in binding of the polyA stretch of RNA (155). Thus, it was hypothesized that Hfq, sRNA and mRNA may form a stable structure. As a result of this interaction, either sRNA stabilization prevents degradation, or sRNA

assumes a conformation that allows recognition of the target by basepairing. Either positive or negative translational regulation ensues, by either blocking or exposing the ribosomal binding site or the start codon.

11.3. Proposed mechanism of Hfq regulation

Of the 22 sRNAs with known functions, some, such as OxyS, DsrA, RprA, and RyhB, have been studied in some detail in *E. coli* (90). The first three involve post-transcriptional control of *rpoS* mRNA, while RyhB is required for negative regulation under iron limitation as described above.

OxyS RNA is 109 nt long, and is induced by OxyR under oxidative stress by hydrogen peroxide. OxyS controls a number of genes, incuding *rpoS* and *fhlA*. OxyS RNA represses translation of *rpoS* mRNA with a mechanism that is not well known, but requires Hfq. Since OxyS binds Hfq, it was proposed that OxyS may modify the activity of Hfq to repress *rpoS* mRNA translation (273). In contrast, control of OxyS on *fhlA* transcript, encoding a transcriptional activator, has been described. Binding of OxyS to *fhlA* by basepairing occurs at two sites, at the ribosomal binding site and in the coding sequence, thus blocking translation of *fhlA* (5).

RprA, similar to DsrA, basepairs with the complementary sequence in the leader sequence of *rpoS* mRNA. The binding thus releases the ribosomal binding site, which was occluded by the leader sequence, and thus allows translation to occur. However the signal for RprA is different from that in DsrA. RprA is activated by the RcsC/YojN/RcsB two component system; however, the natural stimuli for this system are still unknown. Mutations that result in capsule production also activate the *rprA* promoter. The target of RprA may be multiple, considering that almost 150 genes are activated by

RcsC/YojN/RcsB TCS (67). It is possible that some of these genes may be regulated indirectly by RprA or RprA-regulated RpoS (144).

12. OVERVIEW OF DsrA

At low temperature (20-30°C), the translation of *rpoS* transcript in *E. coli* is promoted by binding of a small, 85 bp untranslated RNA (also called small RNA or sRNA), DsrA, to the leader sequence of *rpoS* mRNA, thus releasing the ribosome binding site normally occluded by the mRNA leader sequence. However, DsrA also acts at the transcriptional level as an anti-silencer of some HNS-repressed genes such as *rcsA*, which codes for the regulator for capsule production (143). Both functions of DsrA require the involvement of Hfq proteins.

DsrA secondary structure contains three stem loop structures with two functions of DsrA assigned to the first two stem loops. Since the first stem loop has some complementary sequence with the *rpoS* mRNA leader sequence, mutation in this region abolishes *rpoS* translational activation (reversed when compensating mutation is introduced in the *rpoS* leader sequence). The second stem loop structure is responsible for the anti-HNS action of DsrA (143).

DsrA also base-pairs with the *hns* mRNA leader sequence, which alters the RNA secondary structure to one that occludes translation initiation. Thus, DsrA acts to inhibit translation of the *hns* transcript. The requirement for DsrA was shown after the loss of DsrA regulation, when the region of basepairing in *hns* mRNA was disrupted by silent mutagenesis. Subsequent complementary mutation in the DsrA returned activity to normal (130). An *hfq* mutant was shown to be defective for *dsrA*-dependent regulation of

both *rpoS* and *hns* (220). In an *hfq* mutant, DsrA is unstable with a half-life of 1 min, compared to the 30 min in the wt, and the transcript is truncated at the 3' end. *Hfq* may act by changing the structure of DsrA RNA or forming an active RNA-RNA complex. Hfq also stabilizes DsrA RNA, protecting it from degradation possibly by competing with RNaseE for the same recognition site.

13. COMMENTARY

Despite our present knowledge of the complex regulation of the rugose morphotype, many questions still remain unanswered. The mechanism of production of both curli and cellulose are only partially known. How are the curli proteins transported outside of the cells? What is the role of AdrA in the synthesis of cellulose? Since the assembly of both of these matrix components occurs on the cell surface, what is the contribution of the cell envelope to the synthesis process? Current knowledge of the transcription of the central regulator *csgD* does not permit us to address completely certain questions, e. g. what is the exact role of RpoS? Binding of RNA polymerase with σ^S to the *csgD* promoter has not been shown (82), although it has been shown at the *csgBA* promoter (24). It is unknown why mutation in the promoter region of *csgD* that upregulates transcription can bypass the requirement of *rpoS* but not OmpR. The function of HNS is still contradictory in different host backgrounds, and the mechanism of MlrA regulation is still elusive. Regulation at levels other than transcription has not been elucidated. Therefore, there is a great likelihood that additional regulators may be playing a part in the entire scheme of regulation. Further studies to answer these questions will

fill knowledge gaps required to fulfill our eventual goal of controlling *Salmonella*. This objective, in part, forms the basis of my dissertation.

14. OVERVIEW OF THE DISSERTATION

The rugose phenotype of the colonies in *Salmonella* species has been observed in our laboratory, in particular *Salmonella* serotype Typhimurium DT 104. It was the initial goal of this study to investigate the physiological factors that affect the formation of the rugose phenotype and to determine the role of this phenotype in the survival of the organisms. Using a spontaneous smooth mutant Stv for comparison, I was able to show that the rugose cells produce an extracellular matrix, and that the rugose phenotype gives protective advantage for the cells against acid and oxidative stresses. This initial study is presented in Chapter 2, which is a modified version of my previously published article (7).

During the course of that study, limited information on the regulation of the rugose (rdar) morphotype and some components of the rugose matrix became available. I, therefore, hypothesized that additional cellular and genetic factors were responsible for this phenotype. The approach I used to identify these factors was random mutation of the wild type *S.* Typhimurium DT104. I further studied two different groups of genes whose mutation resulted in the reduction or loss of rugose phenotype. The first group involved two genes that function in the production of LPS, *ddhC* and *waaG*. The detailed characterization of rugose phenotypes in these partially rugose mutants and the possible role of LPS in rugose formation are featured in Chapter 3.

In chapter 4, I present the data from work involving the effect on rugose expression of the second group, regulatory gene *hfq*, which codes for an RNA binding protein, Hfq. Because of the known function of Hfq as a regulatory protein, I studied its effect on the promoters of the *csgfDEFG* and *csgBA* operons, in which the regulator and the major subunits of curli, respectively, are encoded. Because of the known function of Hfq to regulate RpoS, I further looked at the possible effect of Hfq on the regulation of P*agfB* in a *rpoS hns* double mutant in order to determine if any noticeable effect was independent of RpoS. In addition, because some of the activity of Hfq involves the small regulatory RNA DsrA, the effect of the latter regulator on the transcription of P*agfD* and P*agfB* was also studied. The results showed that, although Hfq is known as a regulator at the post-transcriptional level, it might in fact, regulate the two promoters for curli production at the transcriptional level.

In summary, I have characterized the rugose morphotype in the multiple antibiotic resistant strain, *S.* Typhimurium DT104, and partially defined its potential function. Using different approaches, other determinants of the rugose morphotype were identified and characterized. Realizing that *csgD* controls the switch between the planktonic and the multicellular state of *Salmonella*, our further understanding that Hfq is involved in the regulation of the *csgD* promoter provides us with additional knowledge, which may have potential for controlling the expression of rugose and biofilm formation. This strategy could possibly lead to the development of interventions to reduce the presence of these persistent bacteria, which have long been recognized as, and continue to be, a primary health concern for humans and animals.

Figure 1. Schematic diagram illustrating the currently known regulatory networks controlling the expression of curli and cellulose, two components required for the production of rugose matrix.

The regulation is centered at CsgD, which is regulated by a number of regulators, the majority of which bind to the intergenic region (IR) between the *csgDEFG* and *csgBA* operons. Shown in yellow are the environmental signals influencing *csgD* and *csgB* expressions, and in red are the two component systems (TCS) involved in sensing osmolarity, in green are the genes involved in matrix production. Black arrows show activation, oval arrows (red lines) show repression while green solid lines indicate unknown mechanisms of regulation. Binding sites illustrated are: C for CpxR, D for OmpR, F for IHF, and H for HNS. Numbers after the letter code represent multiple binding sites. Adapted from Gerstel and Romling, 2003 (80).

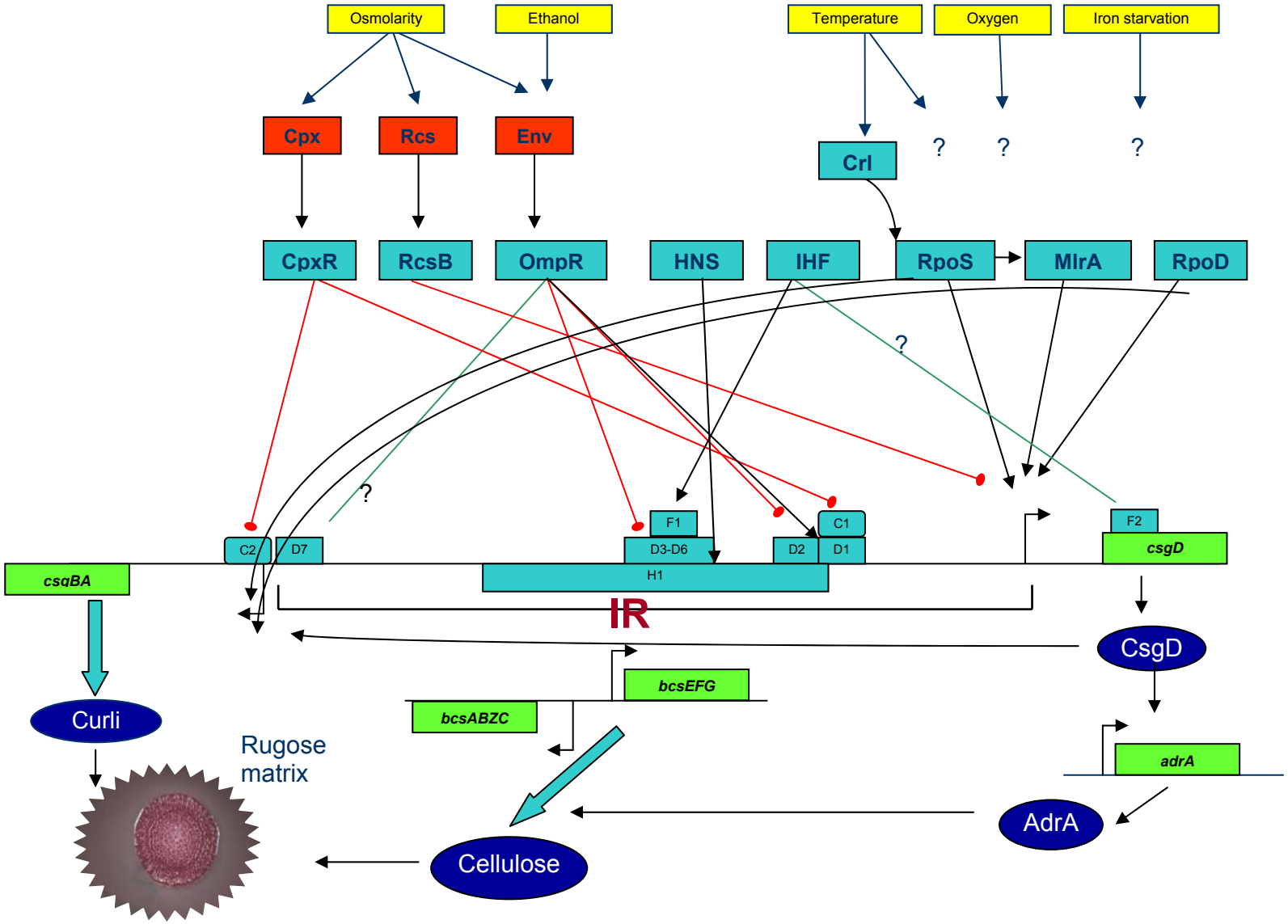
Osmolarity
Ethanol
Temperature
Oxygen
Iron starvation
Cpx
Rcs
Env
Crl
?
?
?
CpxR
RcsB
OmpR
HNS
IHF
RpoS
MlrA
RpoD
?
?
C2
D7
F1
D3-D6
C1
D2
D1
F2
csgD
csgBA
H1
IR
CsgD
bcsEFG
bcsABZC
Curli
Rugose matrix
adrA
AdrA
Cellulose

CHAPTER 2 - Characterization of the Rugose Phenotype and Its Function in *Salmonella enterica* Serovar Typhimurium DT104

(This chapter was published, in part, in AEM 67:4048, 2001)

1. ABSTRACT

Rugosity, such as that observed in *Vibrio cholerae*, confer increased resistance to chlorine, oxidative stress, and complement-mediated killing. In this study a rugose phenotype was identified and defined in *Salmonella enterica* serovar Typhimurium DT104. Induction was shown only on certain media at 25°C after 3 days of incubation. Incubation at 37°C resulted in the appearance of the smooth phenotype. Observation of the ultrastructure of the rugose form and a stable smooth variant (Stv), which was isolated following a series of passages of the rugose cells, revealed extracellular substances (ES) only in cells from the rugose colony. Observation of the extracellular substance by scanning electron microscopy (SEM) was correlated with the appearance of corrugation during development of rugose colony morphology over a 4-day incubation period at 25°C. In addition, the cells also formed a pellicle in liquid broth, which was associated with the appearance of interlacing slime and fibrillar structures, as observed by SEM. The pellicle-forming cells were completely surrounded by capsular material, which bound cationic ferritin, thus indicating the presence of an extracellular anionic component. The rugose cells, in contrast to Stv, showed resistance to low pH, hydrogen peroxide and phagocytosis by macrophages, and an ability to form biofilms. Based on these results and

analogy to the rugose phenotype in *V. cholerae*, a possible role for the rugose phenotype in the survival of *S. enterica* serovar Typhimurium DT104 is proposed.

2. INTRODUCTION

Salmonella enterica serovar Typhimurium is a causative agent of gastrointestinal salmonellosis in humans. The phage type 104 (definitive type 104 [DT104]) strain of *S. enterica* serovar Typhimurium has recently emerged with resistance to ampicillin, chloramphenicol, streptomycin, sulfonamides, and tetracycline in the United States (18) the United Kingdom (240), France, Denmark (11) and Japan (208). This multi-drug resistance has posed a major problem in the treatment of complications resulting from these *Salmonella* infections. Moreover, new strains with resistance to additional antibiotics, such as trimethoprim and fluoroquinolones, are beginning to emerge (161, 239). The Centers for Disease Control and Prevention has reported that DT104 was identified in 32% of the *S. enterica* serovar Typhimurium strains isolated from humans in 1996, an increase from 28% in 1995 and 7% in 1990. DT104 is now only the second most prevalent type of *Salmonella* after serovar Enteritidis phage type 4 in the United Kingdom (109).

During our study on *S. enterica* serovar Typhimurium DT104, we have observed a rugose phenotype, which has also been described for *Vibrio cholerae* after serial passages in alkaline peptone media (115, 163, 263) or in response to starvation (159, 253, 272). This phenotype of *V. cholerae* was defined by corrugated colony morphology, which was associated with the formation of exopolysaccharide (EPS) and cell aggregation. Because there was a question of whether the rugose variant of *V. cholerae*

was virulent, a study was performed and showed that the rugose cells were fully virulent when inoculated into human volunteers and resulted in full-scale diarrheal disease (163). In fact, compared with the smooth variant, rugose cells displayed increased resistance to chlorine, salt, and oxidative stress (195, 253, 272) and had the ability to form biofilms (159, 253, 272), which suggested that this phenotype might be an aid in the survival of *V. cholerae* between outbreaks.

Similarly, the increasing incidence of *S. enterica* serovar Typhimurium in food-borne disease suggested that it may possess an enhanced capacity to survive under adverse conditions. We have observed that this organism assumed the rugose phenotype only on certain media and under particular growth conditions. Here we identify and define the rugose phenotype in *S. enterica* serovar Typhimurium DT104 and show that it appears to enhance survival under unfavorable conditions.

3. MATERIALS AND METHODS

3.1. Strains, media, and growth conditions

3.1.1. Strains and media. *S. enterica* serovar Typhimurium DT104 strain 11601 was routinely cultured on Trypticase soy agar (TSA) (Difco) incubated at 25°C for the formation of rugose colonies (Rv/25) or at 37°C for the formation of smooth colonies (Rv/37). Other agar media, including nutrient agar (NA) (Difco), Luria-Bertani agar (LB), brilliant green agar (BG) (Difco), brain heart infusion agar (BHI) (Difco), xylose lysine tergitol-4 agar (XLT-4) (Difco), and MacConkey's agar (MAC) (Difco) were used to assess the ability of *S. enterica* serovar Typhimurium DT104 to induce the rugose morphotype on agar media other than TSA. Stock cultures were prepared by suspending

individual colonies in 4.0-ml vials containing Trypticase soy broth (TSB) with 15% glycerol added, followed by storage at −80°C. To compare the ability of other *Salmonella* serovars and other *S. enterica* serovar Typhimurium DT104 strains to induce rugose phenotype on TSA, the following strains were used: *S. enterica* serovar Typhimurium DT104 strains 10931, G-10601, G-11704, G-10631, and G-11074 (a kind gift from B. Swaminathan) and *S. enterica* serovar Typhimurium (non-DT104) UMD597, serovar Thompson UMD1317, serovar Senftenberg UMD1408, serovar Enteritidis UMD352, serovar Cowdy UMD1321, serovar Hadar UMD598, and serovar Johannesburg UMD600 (S.W.J. collection).

3.1.2. Growth conditions. Cells were grown in static 10-ml volumes of T soy broth (TSB) or LB Miller base broth (LB) (Difco) in 17- by 150-mm glass test tubes or on TSA for at least 3 days at 25°C to induce pellicle formation or rugose-colony formation, respectively. In order to observe the effect of media volume on pellicle formation by Rv, the strain was inoculated into small size (12x100mm) glass tubes (12 ml capacity) containing 1, 2, 3, 4, 5, or 6 ml of LB media, medium size glass tubes (15x125mm) (20 ml total volume) with 1, 2, 3, 4, 6, 8, or 10 ml of LB media, 50 ml plastic containers with increments of 10 ml of LB media starting with 10 ml and ending with 40 ml, and 100 mL plastic containers (6 cm upper and 5.7 cm lower diameters) with 10-90 ml of media in 20 ml increments. The tubes were incubated at 28˚C for 4 days, and pellicle formation was visually evaluated. To observe Congo red or calcofluor binding, cells were grown in LB broth containing either 40μg/ml Congo red and 20μg/ml Coomassie blue (Sigma) or 40μg/ml calcofluor (Fluorescent brightener 28, Sigma). To induce the development of stable, smooth variants (Stv) at low frequency, serial passage

(>30) of the rugose colonies was performed by sequentially streaking a single rugose colony every 3 days onto a fresh TSA plate at 25°C.

3.1.3. Biochemical and serological testing. Biochemical tests using triple sugar iron agar slants, lysine iron agar, and flagella broth and subsequent serological tests using polyvalent A, group B, and factor 4, 5, and 12 somatic (O) and flagellar (H) *Salmonella* antisera were performed on Rv/25 and Stv. Other biochemical tests using API 20E strips (BioMerieux, Inc.) were also used to confirm the identity of Rv/25 and Stv.

3.2. Scanning Electron Microscopy (SEM)

For scanning electron microscopy (SEM) observation, well-isolated colonies (Rv/25 or Stv) and a broth pellicle (Rv/25), grown on TSA and in TSB, respectively, were processed after growth for at least 4 days at 25°C. Sections of colonies were cut to about 1.0 cm^2, with a 1.0-mm thickness of agar remaining (44). The colonies or pellicles were fixed in 2% glutaraldehyde in phosphate-buffered saline (PBS), pH 7.4, then postfixed with 1% osmium tetroxide, dehydrated with ethanol, critical-point dried, and coated with gold-palladium alloy. Finally, samples were examined with a Hitachi S-4700 SEM (Hitachi Scientific Inst., Gaithersburg, Md.) at 2.7- to 5-kV acceleration.

3.3. Transmission electron microscopy (TEM)

3.3.1. Cationic ferritin staining. Rv/37 and Rv/25 grown in TSB for 7 days at 37 and 25°C, respectively, and the pellicle from Rv/25 grown in TSB for 7 days at 25°C, as well as a TSB cell suspension from colonies of Rv/25 or Rv/37 grown on TSA at 25°C for 4 days, were washed three times with PBS (pH 7.4). After fixation with 2% glutaraldehyde in the same buffer for 1 h at 25°C and overnight at 4°C, the samples were

reacted with 1.0 mg of cationic ferritin (Sigma) per ml for 30 min (115). Cationic ferritin was included at a concentration of 0.25 mg/ml in subsequent washes and during postfixation in 1% osmium tetroxide and in 2% aqueous uranyl acetate. Samples were dehydrated in ethanol, embedded in Spurr resin, sectioned, and observed with a Zeiss EM10 CA (Leo Electron Microscope, Thornwood, N.Y.).

3.3.2. Ruthenium red staining. Rv/25 and Stv grown on TSA for 4 days at 25°C were removed as 2 mm thick, 1.0-cm^2 blocks, fixed with 2% glutaraldehyde in 0.1 M cacodylate buffer (pH 7.2), for 15 to 30 min, transferred to a glass slide, and encased with molten 4% agar. Blocks of 1.0 mm^2 were prepared from the encased colonies. This procedure was used to ensure the integrity of the extracellular substances (ES). The agar blocks were fixed with 0.075% ruthenium red, 75 mM lysine monohydrochloride (Sigma), 2% paraformaldehyde (from a 10% stock solution of methanol-free pure formaldehyde), and 2.5% glutaraldehyde in 0.1 M cacodylate buffer (pH 7.2) for 1 h at room temperature and 18 h at 4°C (66). After a series of washes in the same buffer and postfixation with 1% osmium tetroxide followed by 2% aqueous uranyl acetate, samples were dehydrated with ethanol and embedded in Spurr resin. Thin sections were examined with a Zeiss EM10 CA.

3.4. LPS profiles

Whole-cell lysates were prepared by adding 50.0 μl of lysing buffer (2% sodium dodecyl sulfate [SDS], 4% 2-mercaptoethanol, 10% glycerol, 1 M Tris [pH 6.8], 0.1% bromphenol blue) to a 1.0-ml suspension of a well-isolated colony in TSB. The lysate was then boiled for 10 min and treated with 5 μl of proteinase K (5 mg/ml) at 60°C for 1 h. The lipopolysaccharide (LPS) components were separated using sodium dodecyl

sulfate-polyacrylamide gel electrophoresis and detected by LPS silver staining (105). No LPS differences between Rv/25 and Stv were detected (data not shown).

3.5. Biofilms

S. enterica serovar Typhimurium DT104 strains (Rv/25 and Stv) were grown separately in 500-ml Erlenmeyer flasks containing 25 ml of TSB at 25°C with shaking (50 rpm) in a Psycrotherm controlled environment incubator shaker (New Brunswick Scientific, Edison, NJ). Spent medium was replaced with an equal volume of fresh, sterile TSB every 24 h for a total of 7 days. At day 7, the spent medium was replaced with 20 ml of a 1% crystal violet solution in PBS, and the flasks were incubated for another 5 min at 25°C with shaking (50 rpm) (172). The crystal violet solution was discarded, and the flasks were rinsed with PBS.

3.6. Susceptibility to osmotic, acidic, and oxidative stress

Individual colonies of Rv/25 and Stv approximately 0.5 cm in diameter were taken from TSA incubated at 25°C for 4 days and suspended separately in 10 ml of TSB in 17- by 150-mm glass test tubes. Because the cells in rugose colonies tend to aggregate, glass beads were used to disperse the cells. Therefore, the cell counts included some aggregates as well as cells in the suspension. To assay resistance to oxidative stress, 1.0 ml of the culture, approximately 1×10^7 to 5×10^7 cells in TSB, was mixed with 9.0 ml of prewarmed TSB, and finally hydrogen peroxide was added to a final concentration of 10 mM. To assay resistance to acidic stress, the original 10.0-ml cell suspension was concentrated 20 times. One hundred microliters of this suspension was added to 9.9 ml of TSB to which concentrated HCl was added to a final pH of

3.0 ± 0.05. The reaction mixture was incubated either at 37°C (for the hydrogen peroxide experiment) or at 25°C (for the acid experiment). Aliquots were taken every 10 min for a total of 90 min, were serially diluted in either saline (for the H_2O_2 experiment) or PBS (for the acid experiment) to stop the reaction, and were plated on TSA to determine the viable cell counts. The plates were incubated at 25°C and were observed for up to 5 days to determine whether changes in colony morphology had occurred. The pH remained constant at 3.0 ± 0.05 throughout the acid experiment. Each experiment was repeated at least three times on different days, and corresponding results were obtained.

3.7. Macrophage invasion assay

Mouse macrophage J774 cells were grown in small tissue culture flasks containing 5mL of RPMI 1640 medium supplemented with 10% fetal bovine serum and 1% penicillin and streptomycin at 37˚C in the presence of 5% CO_2. The macrophage cells growing in the flasks were passed every 2-3 days by transferring a drop of J774 cells (a kind gift from Dr. Wenxia Song) into each of several wells containing 1.5 ml of fresh media in a 30-well plate. For the experiments, 2-day old J774 cells from 2 wells were transferred into a 75 cm^2 tissue culture flasks (Corning) containing 20 ml media and incubated at 37˚C for 2-3 days to obtain confluent growth. Cells were treated with 5 ml trypsin-EDTA (0.05% trypsin, 0.53mM EDTA in HBSS [137 mM NaCl, 5.36 mM KCl, 0.20 mM $MgSO_4$, 0.34 mM Na_2HPO_4, 0.44 mM KH_2PO_4, 4.17 mM $NaHCO_3$, 1.26 mM $CaCl_2$, 5.6 mM glucose]) for 30 min to detach the cells from the flasks. A 3.5 ml volume of medium was added to dilute the mixture, and a 0.5 ml aliquot was seeded into each of the wells in a 24-well tissue culture plate (Falcon), each already containing 1 ml RPMI media. The total macrophage cell concentration in the well was approximated by

counting the cells in one of the wells, after trypsin treatment, with a hematocytometer, and concentration was adjusted by further dilution with RPMI media as necessary. The tissue culture plate was incubated in the presence of CO_2 at 37˚C to allow the cells to attach. After overnight incubation (no multiplication of macrophage cells was expected during this 24 h period), the cells were washed three times in PBS buffer at room temperature, after which 900 µl of pre-warmed (at 37°C) PBS buffer (0.137 M NaCl, 2.7 mM KCl, 4.3 mM Na2HPO4, 1.4 mM KH2PO4, pH = 7.4) was added into each well. Then, 100 µl of bacterial cell suspension (from a 1:10 dilution in PBS buffer of either an Rv or Stv colony 0.5 cm in diameter grown in LB agar for 4 days at 25°C in 10 ml sterile dH_2O) containing approximately 10^5 bacteria were added to approximately 10^4 attached macrophage cells per well (multiplicity of infection [MOI] of 10). The mixture was allowed to stand for 25 min at 37˚C to allow phagocytosis of the bacteria by the macrophages and was then followed by 3 washes in cold PBS buffer to stop phagocytosis (time zero). At this point, the time was designated as zero to mark the start of bacterial survival and multiplication inside the macrophage. The macrophage cells were lysed by 3 min incubation in 1 ml of 0.1% TritonX at RT, followed by serial dilution in saline (0.85% NaCl) and plating of the diluted suspension on TSA to calculate the number of live bacterial cells associated with the macrophages. At time zero, the number of bacteria reflects the total number of both attached and internalized bacteria. Lysis after 90 min incubation in 50µg/ml gentamicin at 37°C was done to calculate internalized bacteria only. Alternatively, after 90 min incubation in 50µg/ml of gentamicin at 37°C, the macrophages in the wells were washed and were further incubated in 1 ml of fresh RPMI containing 5 µg/ml of gentamicin at 37°C (to kill bacteria external to the macrophage

cells while allowing internal bacteria to survive and/or multiply) for 22 h. In every experiment, triplicate samples were assayed for each strain, and the experiment was repeated at least two times on different days. A preliminary experiment to compare the effectiveness of bacterial killing by gentamicin by incubating bacterial suspensions in RPMI media containing 50μg/ml of gentamicin at 4°C or 37°C showed that gentamicin lost its effectiveness at either 4°C. Therefore, incubation of macrophages in RPMI-gentamicin solution was performed at 37°C, although this condition still allowed continued phagocytosis by the macrophages, albeit only irrelevant, killed, attached bacterial cells (65).

4. RESULTS

4.1. Rugose and smooth colonies

The temperature-dependent rugose phenotype (Rv/25) was observed when *S. enterica* serovar Typhimurium DT104 was incubated for at least 3 days on TSA at 19 to 28°C (Figure 2A). Even prolonged incubation on TSA at a higher temperature (37°C) showed smooth colonies only (Rv/37) (Figure 2B). Rv/25 colonies were approximately 5 to 10 mm in diameter, raised, and corrugated, had entire edges, which became even more irregular after 7 days of incubation, and had a grayish white pigmentation. Rv/37 colonies were raised with an even appearance and a buttery texture, had entire edges, and were grayish white. The Rv/25 colonies were tenacious, and cells in the rugose colonies aggregated such that the whole colony could be lifted easily with an inoculating loop. The colony remained as an aggregate when suspended, unlike cells from the smooth colonies, which dispersed easily and formed a homogenous suspension in

broth. In contrast to the rugose colonies exhibited by *V. cholerae*, the corrugations of *S. enterica* serovar Typhimurium DT104 rugose colonies were very regular and symmetrical, with a circular pattern in the center of the colonies. Figure 2C shows how the corrugations formed an interlacing pattern, in contrast to the smooth surfaces of Rv/37 colonies (Figure 2D). Spontaneous smooth variants (Stv), which appear to be similar in morphology to Rv/37 and did not turn rugose even after a 3-day incubation period at 25°C, were obtained after repeated passages on TSA. Rv/25 and Stv demonstrated the same reactions typical of *S. enterica* serovar Typhimurium after biochemical and serological tests. Rugose colonies were also formed on NA, LB, and BG but not on BHI, XLT-4, or MAC. Formation of the rugose characteristic on NA, BG, or LB sometimes required more than 3 days of incubation (data not shown).

A few other *Salmonella* serovars and other strains of *S. enterica* serovar Typhimurium DT104 were also tested for their ability to induce rugose formation on TSA. All strains of DT104 tested demonstrated the rugose phenotype, except G-10601, which showed only slight corrugation in the middle of the colony. *Salmonella* serovars Typhimurium non-DT104, Thompson, Senftenberg, and Enteritidis all displayed rugose growth, but serovars Cowdy, Hadar, and Johannesburg remained smooth under the conditions tested.

After initial inoculation of Rv/25 on TSA, the colonies appeared smooth on the first 2 days of incubation at 25°C (Figure 3A), thus resembling Rv/37 and Stv. At day 3, some wrinkles started to appear on the colonies (Figure3B), and the rugose appearance (Rv/25) was fully evident at day 4 (Figure3C), thus demonstrating that observable rugose

formation in *S. enterica* serovar Typhimurium DT104 occurs progressively over a 3- to 4-day period.

4.2. SEM

As shown in Figure 3D, individual Rv/25 cells grown for only 2 days at 25°C appeared to have smooth surfaces, and the cells seemed to be connected to each other by long fibrils that averaged 40 nm. The 3-day-old colonies contained cells that were surrounded by an amorphous extracellular substance (ES), as shown by SEM (Figure3E). In the absence of further analysis, we refer to this material as ES. At 4 days, a large proportion of the cells was encapsulated by ES (Figure3F). Therefore, the presence of ES correlated with the change to wrinkled colony appearance. The cells that were surrounded by the ES seemed to form aggregates, thus providing an indication that the substance may be responsible for the aggregation. The Stv cells showed characteristics similar to those of 2-day-old Rv/25, and no ES was observed (data not shown).

The method of using intact colonies on agar for electron microscopic observation allowed preservation of the cellular surface of the individual cells in the colony. This was an essential method for this purpose, because the ES around the cells could not be detected by SEM when the colonies were suspended in buffer and then washed and centrifuged (data not shown).

4.3. Pellicle examination

The rugose colony morphology seemed to correlate with formation of a surface pellicle by Rv/25 in TSB at 25°C (Figure 4). Conversely, Stv cells showed growth in turbid suspension with only a slight appearance of biofilm on the glass at the surface of

the growth. The pellicles were formed only in small glass tubes with at least 2 ml media, and in medium tubes with at least 3 ml of media, thus requiring at least approximately 16% of the tubes' total volumes for formation to occur. No pellicles were formed in plastic containers with larger diameters (50 or 100 ml capacity). Visual observation of Rv pellicles further showed that the structure bound to both Congo red and calcofluor, while Stv did not seem to form any cell aggregate or a structure that bound these dyes (Figure 4B and Figure 4C). Incubation of Rv/37 cells at 37°C in TSB did not induce pellicle formation. The cells encased in the pellicle were also shown to possess ES (Figure 5) and a more extensive formation of the matrix of the cross-linked fibrils. The ES and fibrillar network resulted in the formation of a very tenacious structure, which seemed to bind the cells together.

4.4. Transmission electron microscopy

Binding of the ES in the pellicle cells from TSB incubated at 25°C to cationic ferritin (Figure 6A) demonstrated that it contained an acidic component(s) (54). Cells sampled from the broth under the pellicle in TSB also showed ferritin binding (Figure 6B), although the ES was not as apparent as that seen in the pellicle cells. In contrast, Rv/37 grown in TSB at 37°C had obvious diminished binding (data not shown). We also observed the slime-like ES present between the cells from the Rv/25 colonies using ruthenium red staining (data not shown), as was shown with *V. cholerae* O1 E1 Tor (272). This ES was preserved only in closely packed rugose colonies during preparation for electron microscopy. Because of the shrinkage and detachment of the hydrated ES during normal electron microscopy preparation, the ES was lost, as reported previously (66). However, the ES in cells from the pellicle was preserved.

4.5. Biofilms

Rv/25 was more capable than Stv of forming biofilms on the inner surfaces of shaken glass flasks when cultured in TSB at 25°C (Figure 7). The biofilms, which retained crystal violet after treatment, were then immediately observable.

4.6. Resistance to acid and oxidative stress.

The cells from Rv/25 were shown to resist exposure to hydrogen peroxide (10 mM) and acid (pH 3) to a much greater extent than Stv (

Figure 8). A 90-min exposure to either condition resulted in a 2-log reduction of rugose cells, whereas all of the Stv cells (approximately 10^7) were killed within the same time frame. After a 50-min exposure to pH 3, a small proportion of the Stv cells turned rugose and thus became more resistant to the acid. This rugose colony morphology developed after 3 days of incubation at 25°C on TSA. At the end of the assay (90-min exposure to acid), all cells that survived eventually formed rugose colonies on TSA. Interestingly, none of the Stv cells converted to the rugose form after 10 to 80 min of exposure to H_2O_2.

4.7. Macrophage invasion assay

The results of the invasion assay showed that there were fewer numbers of Rv cells phagocytosed by the macrophages than Stv since the percentage of intracellular Rv is higher in Stv than in Rv (Table 1). However, the rugose cells could multiply to an extent similar to that of the smooth variant Stv after 22 hours inside the macrophages. Some variations in the number of internalized or surviving Rv or Stv were seen in the results from two separate experiments cells due to the low sensitivity of this assay in

detecting less than 10^2 cells. Nevertheless, a similar trend was shown in both experiments.

5. DISCUSSION

While rugose colonies are observed in both *S. enterica* serovar Typhimurium DT104 and *V. cholerae* serogroups O139, O1 El Tor, and non-O1 strains, there are critical differences in the conditions under which rugosity occurs. First, formation of the rugose colony morphology in *S. enterica* serovar Typhimurium DT104 progresses over 3 to 4 days at room temperature (19 to 30°C) in TSA, while *V. cholerae* formation of rugose colony morphology occurs either after repeated passage of a smooth variant in alkaline peptone at 37°C (2) or under starved conditions at 16°C for 2 to 3 weeks (159, 253, 272). Secondly, with *S. enterica* serovar Typhimurium DT104, under the same growth conditions the phenotype remained constant, while the rugose and smooth variants in *V. cholerae* could revert back to the opposite phenotype at low frequency after 3 to 5 days of incubation in broth (2, 272). Third, unlike *V. cholerae*, the expression of the rugose variant of *S. enterica* serovar Typhimurium DT104 was temperature dependent.

Observation of adequately prepared *S. enterica* serovar Typhimurium DT104 with SEM revealed the presence of extracellular substance (ES) closely associated with the cells in the pellicle and in Rv/25 colonies. Formation of pellicles composed of closely packed cells has also been reported for rugose *V. cholerae* O1 E1 Tor (272). The observation that Rv/25 formed rugose colonies on TSA and pellicles in TSB and that Rv/37 formed neither rugose colonies on TSA nor pellicles in TSB further reinforced the

temperature-dependent nature of the morphogenesis of *S. enterica* serovar Typhimurium DT104. For Stv, neither rugose colonies nor pellicles were observed at either 25 or 37°C. Since pellicles were formed in certain sizes of tubes containing certain amounts of media, the results seem to indicate that pellicle formation may be dependent on oxygen tension. The small amounts of media may have allowed sufficient amounts of oxygen to diffuse into the media, thus preventing pellicle formation. Furthermore, the results seem to suggest that surface tension may be necessary to maintain the cell aggregate on the surface of the media, hence the large surface of the large containers, compared to the smaller surface in the tubes, appeared to lower the tension, thereby inhibiting pellicle formation.

The ES in the pellicle seems to be responsible for the formation of cell aggregates (microcolonies). In contrast, the thinner layer of ES that surrounds the cells under the pellicle does not appear to play a role in aggregation. The ES appears to be composed of an anionic component(s). Whether the ES in the pellicle and that in the rugose colony have the same composition remains to be determined.

Although there are fibrils that seem to connect the cells in smooth colonies, these structures do not seem to provide a very strong support for cell aggregation, since cells in these colonies disperse very easily. These fibrils have been shown in wild-type *S. enterica* serovar Typhimurium during growth in the laboratory, and they are lost during subsequent exposure to epithelial cells and replaced by shorter appendages (85). Morphologically similar types of fibrils in *Myxococcus xanthus* were shown to be composed of equal amounts of protein and carbohydrate and seemed to play a role in communication among bacteria and between bacteria and their host (63). As shown in

Figure 6, the fibrils in *S. enterica* serovar Typhimurium DT104 are stained with ferritin, indicating the presence of an anionic substance. In *Aeromonas veronii* biovar sobria BC88, similar filamentous structures were suggested to be bundle-forming pili, which mediate interactions between bacteria and initial attachment to the intestinal cells (123). However, the diameter of the individual pilus would argue against the fibrils being pili. Because these fibrils appear to connect the bacteria, they might function in signaling for communications among the bacteria rather than for structural purposes, as suggested by Dworkin for *Myxococcus* (63).

Stable, crenated colonies were also observed in the marine bacterium *Hyphomonas* strain MHS-3 when grown on marine agar at 25°C for 2 weeks. Similar to rugose colonies of *V. cholerae*, the cells in these colonies also produced capsular EPS for attachment to surfaces and participated in matrix formation in biofilms. Smooth regions called papillae were shown on the outer edges of the colonies in older plates (187). In addition, a wrinkled colony variation has also been reported for *S. enterica* serovar Enteritidis as a lacy phenotype and was shown to be associated with a cell surface matrix composed of flagellin and 35-kDa protein components that bound to LPS high-molecular-weight O antigen. The serovar Enteritidis lacy colonies were induced after 16 h of growth at 42°C and an additional 24-h incubation at 25°C on BG. Prolonged incubation for 72 h resulted in a loss of matrix from the colonies, which correlates with the loss of O antigen (92). In contrast, we observed that in *S. enterica* serovar Typhimurium DT104, the rugose phenotype was stable in the colonies at 25°C, except that starting around 10 days, additional growth on the outer edge of the colony was smooth and spreading, similar to the papillae of *Hyphomonas* (187). Furthermore, there were no apparent differences in

LPS profiles between the rugose and smooth phenotype in *S. enterica* serovar Typhimurium DT104 (data not shown), similar to the observations made with the rugose form of *V. cholerae* (163, 253, 263). The lack of noticeable differences in the LPS profiles between Rv/25 and Stv as well as the apparent presence of ES further reinforces the notion of rugosity, as opposed to the formation of rough colonies, which results from the expression of truncated LPS (263).

Analogies of rugose phenotypes are found in other bacteria that produce EPSs, such as alginate-expressing *Pseudomonas* spp., which also produce biofilms (25). Similar to these bacteria, *S. enterica* serovar Typhimurium DT104 also formed biofilms in liquid media. Biofilms are known to be composed of mostly EPS with channels for water circulation. This structure enables attachment of the cells for the formation of bacterial communities to obtain nutrients and to provide protection (48). EPS was also shown to promote biofilm formation in rugose *V. cholerae* (253), suggesting that EPS plays an important role in the survival ability of these bacteria in aquatic environments, thus promoting the spread of this pathogenic species.

The occurrence of the phenotypic variation in *S. enterica* serovar Typhimurium DT104 in the natural environment remains hypothetical. However, by analogy with the conclusions drawn for *V. cholerae*, the aggregation of cells by the ES might provide protection for *S. enterica* serovar Typhimurium DT104 cells in the environment. In fact, the results from our susceptibility studies with Rv/25 and Stv showed that the ES in rugose cells appeared to have a unique function, allowing the cells to survive in the presence of acid and hydrogen peroxide and possibly other adverse conditions compared to Stv. In addition, the increasing proportion of surviving Stv cells demonstrating a

phenotypic switch from smooth to rugose in the presence of acid in the later stages of incubation lends further credence to the importance of this phenotype during acid stress (

Figure 8). Typically, these cells did not exhibit the rugose phenotype until 3 days of incubation at 25°C. Although this finding might suggest the possibility of contamination, we discarded this possibility because (i) there was no evidence of rugose colonies in the 0- to 50-min plates after 5 days of incubation at 25°C and (ii) corresponding results were obtained from the three different experiments.

The unique expression of the rugose phenotype that is temperature dependent is intriguing. It is possible that ES may be more beneficial for the cells for survival in the environment outside the host. We speculate that temperature may provide cues for the cells to prevent the formation of ES in a warmer environment such as the human host (131), since this structure might prevent *Salmonella* cells from being phagocytized (Table 1). However, the Rv cells can still multiply inside macrophages. The relatively higher rate of multiplication of Rv compared to Stv cells in the macrophages may reflect the susceptibility of Stv to stresses inside the macrophages, confirming the results from cells exposed to H_2O_2 and acid. Modification of surface polysaccharide expression that affect entry of bacterial cells into the host has been shown with *Haemophilus influenzae* type b capsule (225). The rugose variant of *V. cholerae* can resist complement-mediated killing (115), although the virulence of rugose *V. cholerae* and that of smooth *V. cholerae* are comparable in terms of clinical response when these bacteria are introduced into human volunteers (163). Regardless of these possible functions of rugosity, there are other means for *S. enterica* serovar Typhimurium DT104 to survive, since this organism is also capable of transitioning to the viable-but-nonculturable state (94).

Rugosity is not a unique characteristic of *S. enterica* serovar Typhimurium DT104 11601, since several other DT104 strains and several other serovars of *S. enterica* tested also exhibited this phenotype. Therefore, the rugosity might be a more universal characteristic in *Salmonella*. The rugose state has been observed in O1 and non-O1 groups of *V. cholerae* (2, 115, 159, 163, 253, 272). Regardless of the differences observed between the formation of the rugose phenotype in *S. enterica* serovar Typhimurium DT104 and in *V. cholerae*, we now know that this condition is not exclusive to *V. cholerae*. This phenomenon may be more widespread in other bacteria than heretofore recognized. Hence, knowledge of rugosity may be more important to our understanding of survival of bacteria in their environments than previously appreciated.

Table 1. The macrophage invasion assay of Rugose- (Rv) and smooth- (Stv) colony forming strains of STDT104

Time[a] (hr)	Exp 1[b]		Exp 2[b]		Notes [c]
	Rv/25	Stv	Rv/25	Stv	
	$4.3x10^5$	$8.2x10^5$	$8.0x10^5$	$1.7x10^6$	Total added
0	$2.5x10^3$	$4.8x10^3$	$6.2 x10^3$	$5.0x10^3$	Adherent & intracellular
1.5	$9.0x10^1$	$1.5x10^3$	$1.9x10^2$	$5.8x10^2$	Intracellular[d]
22	$6.1x10^3$	$9.8x10^3$	$7.6x10^2$	$9.6x10^3$	Intracellular, post multiplication
	0.02	0.2	0.02	0.03	%Intracellular [e]

[a] Time 0 was designated after 25 min of phagocytosis period
[b] Invasion assay of J774 cells was performed in PBS buffer at 37°C with an MOI of 10
[c] Indicates explanation of either initial number of bacteria added or the location of calculated bacteria during the assay
[d] Calculated after 1.5 h gentamicin treatment to kill extracellular bacteria
[e] Calculated as (cfu at 1.5h/ cfu of total bacteria added into the wells)

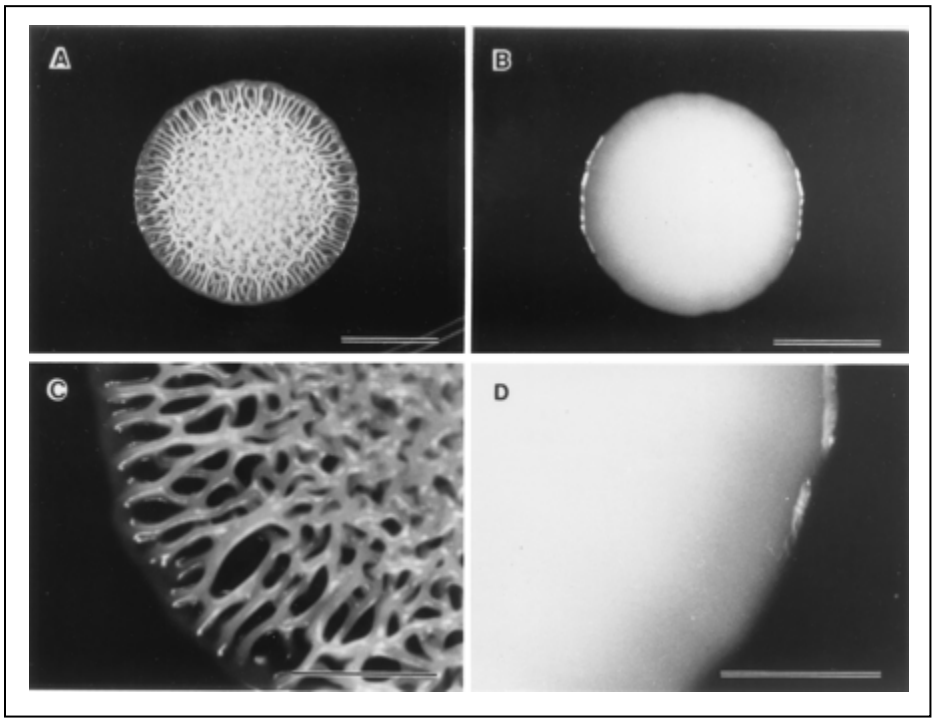

Figure 2. **Morphology of rugose (Rv/25) and smooth (Rv/37) colonies of *S. enterica* serovar Typhimurium DT104.**
Rv cells were grown for 4 days on TSA at 25˚C (Rv/25) (A and C) and at 37°C (Rv/37). Scale bars, 5 mm (A and B) and 2 mm (C and D).

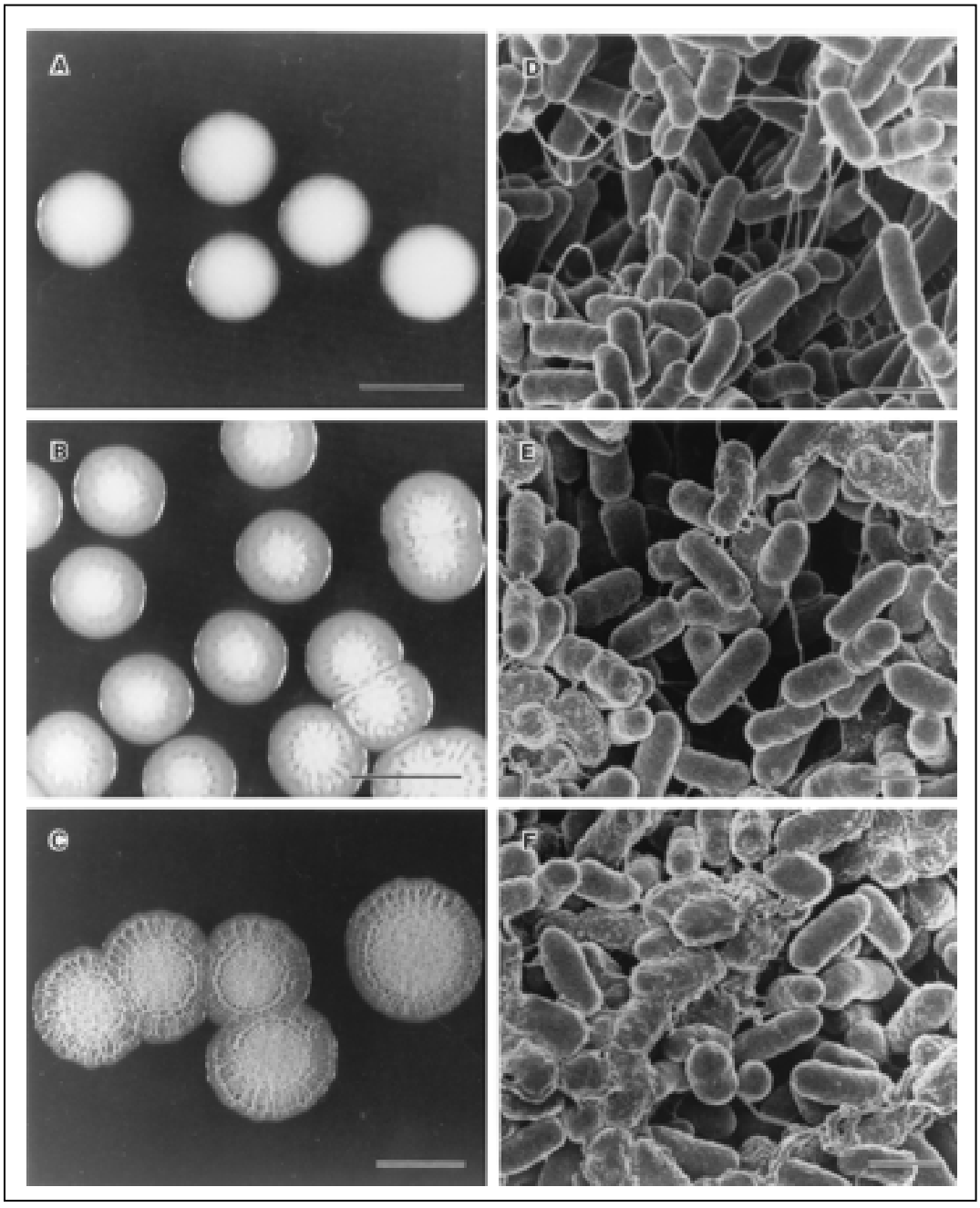

Figure 3. Progression of rugose formation at day 2 through day 4 at 25°C on TSA. Panels A to C show Rv/25 colonies at day 2, 3, and 4, while panels D to F show scanning electron micrographs of cells from the respective colonies. Expression of ES is apparent in cells starting at day 3 when the colonies just became wrinkled. Scale bars, 5 mm (A to C) and 1 μm (D to F).

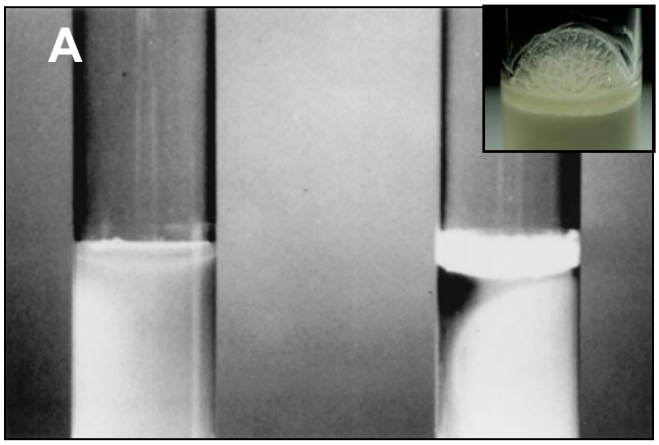

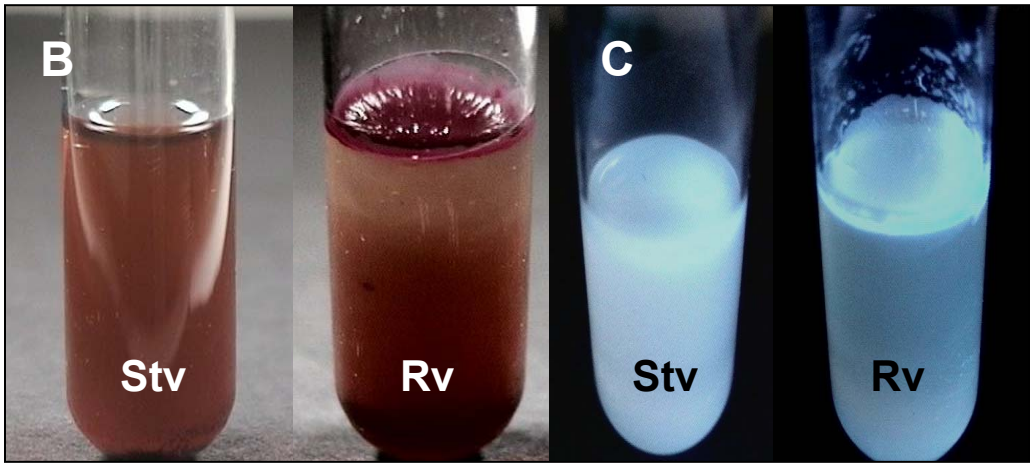

Figure 4. Pellicle formation in Rv/25 was absent in Stv.
(A) Rv (right) but not Stv (left) produced pellicles in TSB after 7 days of incubation at 25°C. Inset shows the wrinkled appearance of the surface of an Rv pellicle. Figures B and C show the binding of Rv pellicles to Congo red (B) and Calcofluor (C), while Stv only produced a turbid suspension with no pellicle. UV light was used to visualize calcofluor binding in (C).

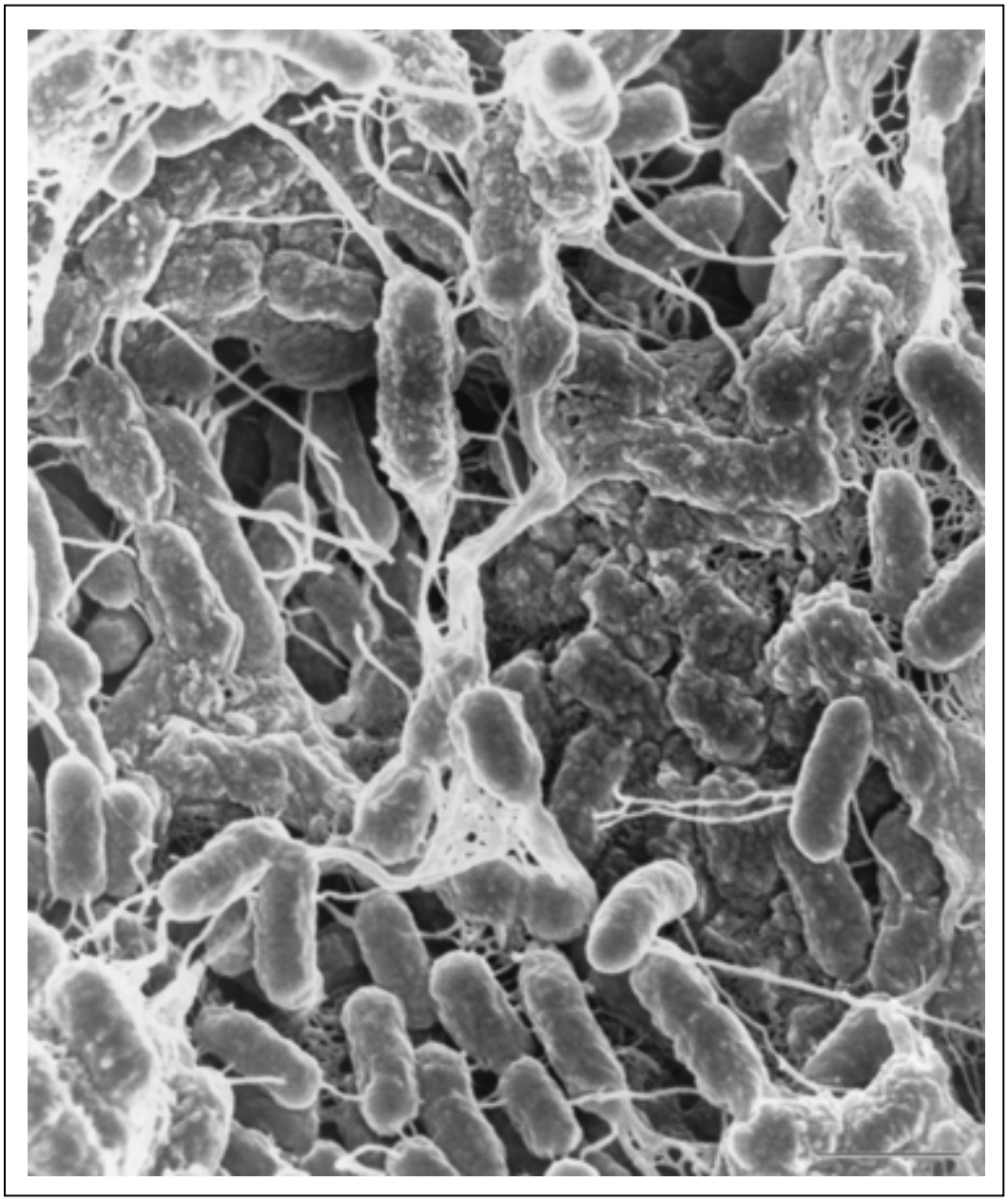

Figure 5. **Scanning electron micrograph of pellicle cells.**

Note the presence of ES in both slime and the fibrillar structure. Scale bar, 1 μm.

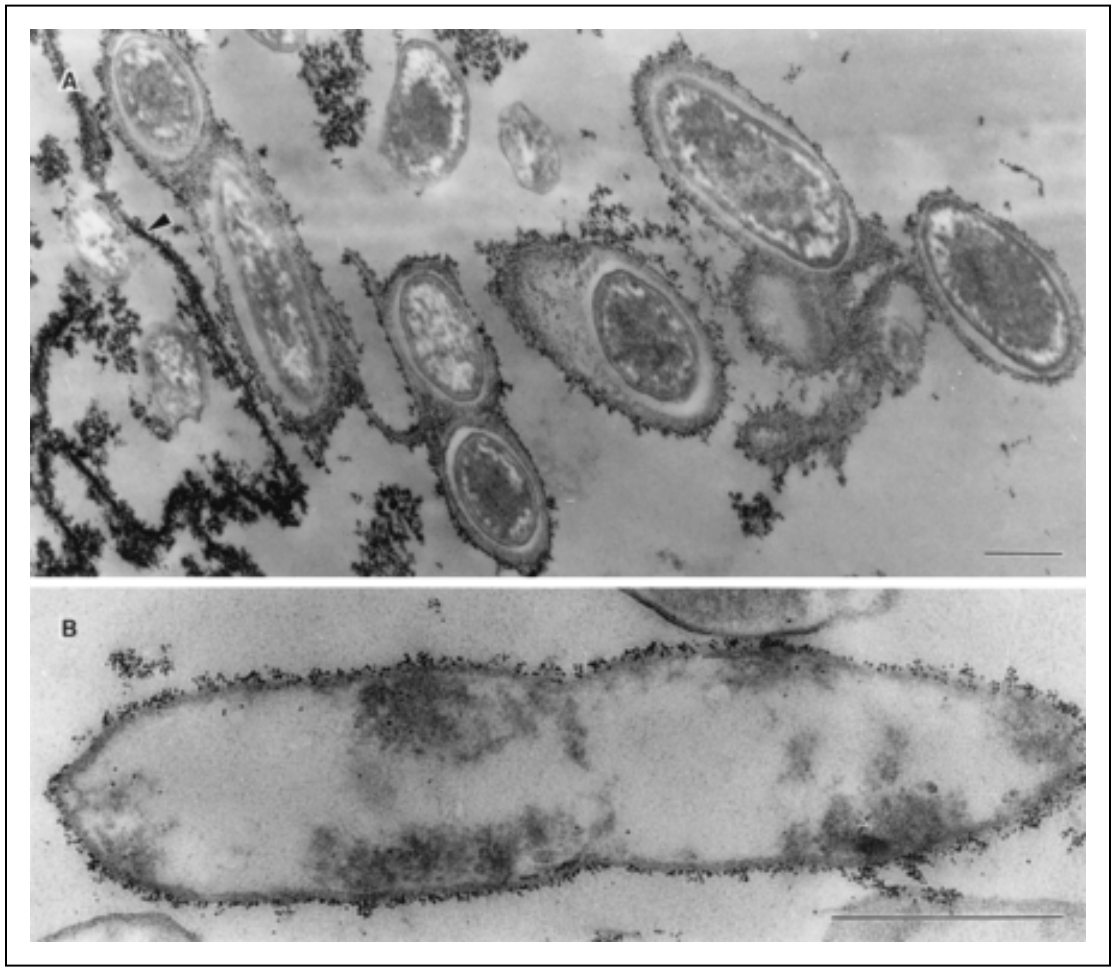

Figure 6. Transmission electron micrographs of cells from the pellicle and from broth under the pellicle.

Cells were grown in TSB for 7 days, and the pellicle cells (A) show the presence of a thick capsular material, while cells from the broth (B) produced a thin layer of Extracellular Substance (ES), both of which bind to cationic ferritin. The fibrillar material that was shown to connect cells in the pellicle was also bound to cationic ferritin (arrow head in panel A). Scale bars, 0.5 μm.

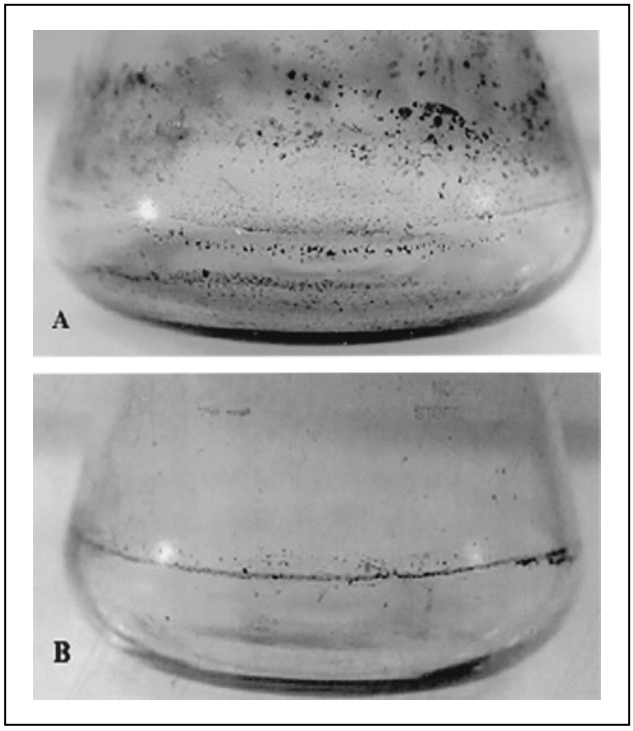

Figure 7. **Formation of biofilm matrix on the inner surface of glass flasks.** The cultures of Rv/25 (A) and Stv (B) in TSB were incubated with shaking (50 rpm) at 25°C for 7 days with the TSB changed every 24 h. The resulting biofilms were stained with crystal violet for immediate observation.

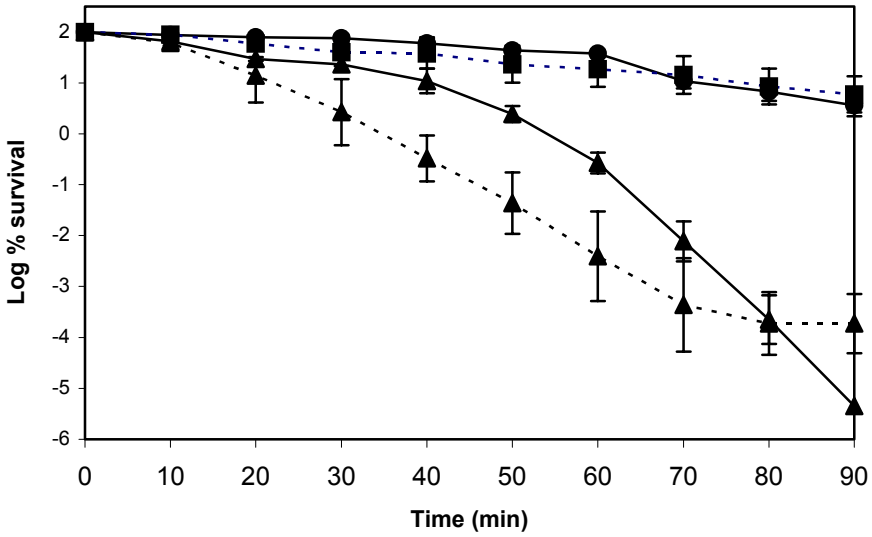

Figure 8. Survival of *S. enterica* serovar Typhimurium DT104 cells.
Survival of cells from 4-day-old colonies of Rv/25 (■) and Stv (▲) suspended in LB broth upon a 90-min exposure to 10 mM hydrogen peroxide at 37°C (–) or pH 3 at 25°C (---) is shown. Each data point represents the mean with standard deviation for three separate experiments.

CHAPTER 3 – The Effect of Mutations in *ddhC* and *waaG* of *Salmonella enterica* Serovar Typhimurium on Rugose Colony Morphology, Biofilm Formation, and Cellulose Production

(This chapter was presented, in part, at the ASM Conference on *Salmonella*: Pathogenesis, Epidemiology, and Vaccine Development, Sardinia, Italy, September 2003)

1. ABSTRACT

The rugose phenotype in *Salmonella* Typhimurium DT104 Rv has been associated with cell aggregation and the ability at low temperature to form biofilms, which assist cells in surviving environmental exposures outside of the host. While screening various factors as mediators of rugose expression, it was observed that two Tn5 insertion mutants of strain Rv exhibited reduced expression of colony rugosity. The transposon insertions were located at *ddhC* (strain A1-8) and *waaG* (strain A1-9), which are involved in the synthesis of O antigen and the core polysaccharide of LPS, respectively. Confirming previous findings, both mutants produced low molecular weight LPS with the *waaG* mutant exhibiting a deep rough phenotype. The reduced rugosity by both mutants was associated with a reduction in pellicle texture. Scanning electron micrographs revealed that the *ddhC* mutant showed reduced amounts of extracellular matrix , while there was relatively more, profuse matrix production in the *waaG* mutant, as compared to the parent strain Rv. Both the *ddhC* and *waaG* mutants appeared to produce decreased levels of curli, as judged by Western blots probed with anti SEF17

(curli) antibodies. Both mutants, surprisingly, were observed to have increased amounts of cellulose relative to Rv. Biofilm formation was also reduced in A1-9 at lower temperatures in rich media, but was absent in A1-8. However, in the presence of glucose and NaCl at either 28°C or 37°C in rich and minimal media, only the mutants formed biofilms, accompanied by the formation of large aggregates of cells. The phenotypes of the *waaG* mutant were further confirmed in a constructed, non-polar deletion mutant of *S.* Typhimurium LT2 with restoration to the wild type phenotypes by complementation. These results highlight some of the contributions of LPS to the production of curli proteins, and cellulose, thereby adding another possible component to the complex regulatory system over multicellular, rugose colony and biofilm formation.

2. INTRODUCTION

Bacteria often exist in natural environments, not only as individual (planktonic) cells, but also as sessile, multicellular forms such as biofilms attached to surfaces. These sessile modes are primarily associated with the ability of these cells to attach to the surface and to each other in aggregates, usually by producing extracellular matrix. Aggregation allows the cells to exist as a community, in which some cells differentiate and assume different roles (258). In addition to cells protected by the extracellular matrix, cells that are transformed to become slow growing or that undergo phenotypic changes make up a community that is highly resistant to antimicrobial agents (49). The cells also benefit from the extracellular matrix through a nutrient absorption process, and the close proximity between cells allows gene exchange for traits necessary for survival. Because

of the highly resistant nature of cells in biofilms, the issue of biofilms has aroused public health concern in medical settings and in food production.

Multicellular behavior can also be manifested as aggregates in colonies, which has been observed with *Salmonella enterica* serovar Typhimurium DT104 strain 11601 Rv cells grown on rich solid media (7). The colonies, which appear rugose (wrinkled), are expressed only at low osmolarity and at low temperature. This morphology is also associated with cell aggregations in liquid culture, i.e. a pellicle in standing culture and biofilms in agitated culture. When compared to a spontaneous smooth mutant Stv, the cells in rugose colonies exhibit resistance to oxidative and acid stresses, thus the phenotype concomitantly confers survival advantages. Therefore, the multicellular forms perhaps are preferred modes of *Salmonella* growth in their natural environments, such as production farms, possibly allowing cells to survive better in the presence of environmental stresses.

In fact, the occurrence of this morphology is widespread among a number of enteric bacteria, such as *E. coli, Enterobacter, and Klebsiella* (278), possibly suggesting that this phenotype is the rule in *Enterobacteriaceae* rather than the exception. In *Salmonella* Typhimurium 14028, this phenomenon has been termed rdar (rough, dry and red) morphotype, because of the colony appearance on Congo red-containing plates; while smooth mutants were called “saw” (smooth and white) (202). It has been demonstrated that the production of a matrix composed of proteinaceous, thin, aggregative fimbriae (called curli in *E. coli* or tafi in *S. enterica* serovar Enteritidis) (199) and cellulose (279) is required for rugose colony morphology. Genes for curli production are coded by the *csg* operon (formerly *agf)*, while genes for cellulose production are

coded by the *bcs* operon. In addition, White *et al.* (262) showed the presence of a high MW polysaccharide that is distinct from cellulose or colanic acid that is also tightly associated with the curli protein.

The expression of rugose phenotype on rich solid media correlates with the formation of pellicles at the liquid-air interface in standing cultures grown in rich media with low osmolarity. Pellicle formation has been also shown in *S*. Enteritidis, *E. coli, P. fluorescens* and *V. cholerae* (189, 221, 224, 272). In addition, there is a close relationship between the rugose phenotype and formation of solid-surface associated (SSA) biofilms. Compared to biofilm formation, pellicle formation may be influenced more by atmospheric conditions. Mutations in some genes such as *csgD* and *ompR* can result in the loss of ability to form both biofilms and pellicles (81, 202). In *Salmonella* Enteriditis, the biofilm formation in minimal media, however, has distinct regulators including another novel GGDEF protein, GcpA (77). Whether the same components make up both pellicle and biofilm matrix is still unknown, since different growth conditions also affect the composition of biofilms. For example, in *Salmonella*, cellulose is the primary constituent of biofilms formed on glass, while those on gallstones lack cellulose (186). A *csgA*- strain, lacking the major subunit of curli, is unable to form either pellicles or biofilms, thus implying that curli may be another component of both forms of aggregates. However, while biofilms can be formed under different growth conditions, pellicles are usually formed only in liquid media under similar conditions and regulations as those for the rugose morphotype.

The conditional expression of the rugose morphotype reflects the regulation of the genes coding for two of the three currently known rugose matrix components, curli and

cellulose (Figure 1). A complex cascade of regulators centers at *csgD,* a LuxR-family of regulators, which is required for the production of both components. In turn, the transcription of *csgD* is positively controlled by a number of regulators including σ^S, the sigma factor required for transcription of a number of genes at stationary phase and under starvation conditions (199, 202). MlrA, a protein from the GGDEF-protein family, also positively regulates CsgD transcription (33). Cytoplasmic protein Crl is indirectly involved through positive regulation of σ^S activity. In addition, the response regulator OmpR functions in response to osmotic signals. Recently, it was shown that OmpR and Crl act in concert to modulate response to osmotic changes (118). The DNA binding proteins HNS and IHF (81) also play a role in negative regulation in response to microaerophilic conditions. This synchrony of regulation and expression eventually results in the production of a rugose matrix only in the stationary phase of growth at temperatures of 30°C or below, and at low oxygen tension.

The temperature dependence of the rugose phenotype in rich media, in part, may be explained by the temperature-regulation of curli expression, although some exceptions have been noted, where some *E. coli* and *Salmonella* strains can apparently express curli at 37°C (46, 202, 247, 279)), possibly because of sequence differences in the *csgD* promoter (82). The machinery for synthesis of curli is coded in two operons: *csgDEFG* and *csgBA*. The major and minor subunits of curli are encoded by *csgA* and *csgB*, respectively. Two chaperone proteins involved in curli production are coded by *csgE* and *csgF*, while *csgG* codes for a lipoprotein in the inner leaflet of the outer membrane that helps to serve as a platform for assembly (40). Once synthesized and transported to the cell surface, the major subunits CsgA are self-assembled upon the nucleated CsgB minor

subunits, a mechanism called nucleation-precipitation pathway. This mechanism was proposed after a study with intercellular complementation in *E. coli* K-12, in which an adjacently grown *csgB*$^-$ strain (the donor) and a *csgA*$^-$ strain (the recipient), each lacking Congo red (CR) binding, complemented each other to bind CR, thus revealing the presence of curli. However, a thorough explanation of the entire assembly process of curli remains elusive.

On the other hand, cellulose production in *S*. Typhimurium is only indirectly regulated by CsgD. CsgD is required for expression of AdrA, another protein of the GGDEF-family. The two *bcs* operons that code for the cellulose biosynthesis machinery are constitutively expressed; however, synthesis of cellulose occurs only when AdrA is produced. Therefore, AdrA is thought to regulate cellulose assembly at the post-transcriptional level, possibly by stabilizing cellulose subunits (279) (Figure 1).

For both curli and cellulose, synthesis occurs in the vicinity of the cell surface. Thus, the presence of an intact cell surface is necessary for the production of these matrix constituents and for adherence of the bacteria to each other. Notably, surface components may function in either a positive or negative fashion. One of these surface components is the lipopolysaccharide (LPS) in the outer membrane of gram-negative bacteria. For example, LPS is involved in the synthesis of another surface appendage, the Type I pilus. There is a lack of Type I pilus production in the absence of LPS in *E. coli*, possibly because of alteration in the production of outer membrane proteins (80). That LPS may also act in a negative fashion was revealed in a study of intercellular complementation of curli production in *Salmonella*, where results with *E. coli* K-12 could not be reproduced. It was further shown that the presence of O-antigen in *Salmonella*, which is lacking in *E.*

coli K-12, may block transfer of curli components between cells (262). The lack of LPS has been shown to affect, either positively or negatively, adherence of cells to abiotic surfaces during biofilm formation (80, 158, 186, 264). Thus, both types of multicellular forms, rugose colonies and biofilms, are affected by changes in the LPS, probably because of direct alteration in the cell surface. However, the involvement of LPS in the production of capsular polysaccharide, as well as surface appendage flagella, could also be indirect. This was shown in the activity of RcsC/B two-component system, which facilitates transcription of capsular synthesis genes and repressesion of the transcription of flagellar genes in response to alterations in the outer membrane, including LPS (179).

The overall direction of my research has been toward detection of factors, other than those described thus far, which are involved in rugose expression using random mutagenesis and screening the resulting mutants for altered rugose colony morphology. It was reasoned that, despite accumulating knowledge of some of the components and regulation of rugose expression, the mechanics of rugose matrix assembly and cellular influences on matrix production were still not completely understood. Herein, residual effects of transposon insertion in two genes that alter LPS formation, *ddhC* and *waaG*, are described. The changes in LPS independently retarded the appearance of the rugose phenotype primarily because of alterations in the synthesis of both curli and cellulose. Conversely, both mutations resulted in increased biofilm formation under certain conditions. The possible roles of LPS in rugose colony formation, and the possible pathways leading to biofilm formation in these LPS mutants, are further proposed.

3. MATERIALS AND METHODS

3.1. Strains

All strains used in this study were derived from either *S. enterica* serovar Typhimurium DT104 Rv (7), or *S. enterica* serovar Typhimurium LT2 (henceforth referred to as Rv and LT2, respectively). Stv, the stable, spontaneous, smooth mutant of *S*. Typhimurium Rv, was used as a negative control for rugose and pellicle formation (7). All of these strains and the plasmids are listed in Table 2. The high frequency generalized transducing bacteriophage P22 mutant HT*105/1 int-201* (213) was used for transduction in DT104 Rv by standard methods (147). All PCR reactions were performed using primers obtained from IDT DNA (Coralville, IA) (Table 3). Somatic serotyping was performed using Bacto-*Salmonella* O- polyclonal antiserum Group B factors 1, 4, 5, 12 (Difco, Detroit, MI).

3.2. Media and growth conditions

All strains were stored at –80˚C in LB media containing 25% glycerol. The strains were grown either in LB Miller (LB) base broth or LB agar (DIFCO), which contains only 0.5g NaCl/L, or M63 minimal media supplemented with 0.5% vitamin-free casamino acids (CAA) (Difco) and 0.2% glucose. To generate growth curves for Rv, Stv, LT2, the *ddhC* and *waaG* mutants, and the *waaG* complemented strains, overnight cultures grown at 37°C in LB with or without antibiotics were used to inoculate fresh media in tubes at a dilution of 1:100. The tubes were incubated with shaking at 210 rpm at either 28°C or 37°C, and the absorbance read at OD_{600} was measured periodically through 24 hours. Antibiotics were used at the following final concentrations: sodium

ampicillin, 100 μg/ml, and kanamycin sulfate, 50 μg/ml. To obtain isolated colonies and to observe progressive rugose colony formation, 100 μl of 10^{-6} to 10^{-8} dilutions of overnight cultures of *Salmonella* were spread plated onto LB plates and incubated at 22-25°C for 4 to 6 days. *Salmonella* were also streaked for individual colony isolation on LB agar where some colonies of the wt strain turned rugose in as few as 2-3 days, while some of the mutant colonies required 3-4 days to reveal rugosity. When streaked in straight lines on LB plates using a denser inoculum, the rugosity of the wt formed at 2 days while it took 3 days for the mutants streaked in the same fashion to reach their relatively maximum rugosity. For induction of pellicle formation, the strains were inoculated into 5 ml of LB broth in loosely capped 16 x 125 mm glass culture tubes and incubated without shaking at 22-25°C for 4 to 7 days. When the pellicle was formed it appeared on the surface of the LB broth as tenacious, tightly compacted growth. LB agar supplemented with Congo red (40μg/ml) and Coomassie brilliant blue (20 μg/ml) was also used to determine the Congo red-binding property of the colonies. Calcofluor (Fluorescent brightener 28, Sigma), used to detect cellulose, was dissolved in water at a concentration of 20 mg/ml and then added to agar media before autoclaving at a final concentration of 40 μg/ml.

3.3. Random mutagenesis and screening for Tn mutants with altered rugose phenotype

Random mutagenesis was performed by transforming the wild type strain *S.* Typhimurium DT 104 Rv with Tn5 in the transposon-tranposase (transposome) complex (EZ::TN Kan-2 , EPICENTRE, Madison, WI) by electroporation (Appendix A.1) (107). The transposase was activated by endogenous magnesium, resulting in the transposition

of Tn5 into the chromosome. Transformants were selected on LB-Kan plates. After observation at 25°C for 4 to 7 days, colonies that did not exhibit full rugosity compared to the wt Rv were selected. The stability of the altered rugose phenotype was confirmed by three passages on LB plates at 25°C for 4 days.

3.4. RATE analysis of the Tn mutants

Random Amplification of Transposon Ends (RATE) was employed to rapidly analyze EZ::TN transposon mutants (62). The method used a single primer (inv2), which is homologous to one end of the transposon but has minimum homology to the whole genome of *Salmonella* DT104, in a three-step PCR reaction. The reactions usually produced several bands because of some homology with some *Salmonella* sequences adjacent to the transposon end where the inv2 primer binds; however, only a few of the PCR fragments had a transposon end. The PCR products were sequenced using the transposon-specific sequencing primer (provided in the EZ::TN kit) in the DNA sequencing facility at the Center for Biosystems Research at the University of Maryland.

3.5. BLAST analysis

BLAST nucleotide analyses were performed in order to find homologous sequences in the *Salmonella* LT2 database (http://www.ncbi.nlm.nih.gov/BLAST/).

3.6. Deletion of *waaG, csgA,* and *bcsA* and complementation of *waaG*

Direct knock-out of *waaG, bcsA* and *agfA* in *S.* Typhimurium LT2 was performed using the method described by Datsenko and Wanner (55) (Appendix A.2). For deletion of *waaG*, primer pairs p*waaG*D11/12 were used in a PCR reaction with pKD4 plasmid as a template to amplify a Kan^R gene flanked by DNA regions flanking *waaG*. The PCR-

products were treated with DpnI and were electroporated (Appendix A.1) into LT2 carrying the Red helper plasmid pKD46 (Amp^R, strainYA104). Transformants were selected on LB plates containing Kanamycin. Primers p*waaG*11/p*waaG*12 corresponding to the sequence just outside of the deleted region were used in PCR reactions to verify the deletion of *waaG* and insertion of KanR gene in strain YA155. In addition, the primer pair pKanKD3/p*waaG*11 was used to confirm the presence of the junction region between the sequence just outside of the deleted region and the Kan^R gene. The same procedure was followed for *agfA* and *bcsA* deletions using primer pairs p*agfA*D11/12 and p*bcsA*D11/12, creating strains YA151 and YA159, respectively, and using primer pairs p*agfA*11/12 and p*bcsA*11/12 for PCR verification. For gene complementation, *waaG* was amplified from the LT2 strain using primers p*waaG*11/12. The PCR product was cloned into pCR4 (TOPO Cloning, Invitrogen, Carlsbad, CA), and the ligation mixture was transformed into *E. coli* TOP10. Plasmid pTOPO-*waaG* was isolated from the Amp^R transformants and the presence of an insert was verified by restriction analysis. The plasmid pTOPO-*waaG* was transformed into YA155 to create YA156 (Appendix A.3).

3.7. RT-PCR

Total RNA was isolated from 4 day-old colonies of LT2 and YA155 using the RNeasy kit (Qiagen, Valencia, CA). Approximately 1 μg of isolated RNA was treated with 1 unit of DNase (Invitrogen, Carlsbad, CA) for 30 min at 25°C. After inactivation of DNase by heating at 65°C for 10 min, the RNA was used as a template for reverse transcription using internal primers p*waaG*IN11/12 or p*waaP*IN11/12 and Superscript III Reverse Transcriptase (Invitrogen). The cDNA was amplified in separate PCR reactions using the same internal primers. The amount of total RNA was equalized by assessing the

RT-PCR products of the two strains using primers p16srRNA11/12 for 16s rRNA. No amplification product was obtained when the total RNA was used as a template in PCR reactions using these primers, showing lack of DNA contamination (data not shown).

3.8. LPS profiling

A 1:100 dilution of an overnight culture of *Salmonella* strains (Rv, Stv, LT2, the *ddhC* and *waaG* mutants, and the *waaG* complemented strain) in LB either with or without antibiotics was grown at 37°C to an OD_{600} of 0.6. Preparation of the cell lysate was done according to Hitchcock and Brown (105). LPS was separated by SDS-PAGE in tris-tricine gel (BioRad, Hercules, CA), and a silver-staining procedure was used to visualize the bands.

3.9. Novobiocin susceptibility

A series of two-fold dilutions of 10mg/ml novobiocin in 5 ml of LB broth (final concentrations of 200 to 0.8 μg/ml) was prepared in culture tubes. Fifty μL of an overnight culture of all strains (Rv, Stv, LT2, the *ddhC* and *waaG* mutants, and the *waaG* complemented strain) (OD_{600} adjusted to1.5) was added to 5.0 ml of LB broth. From this diluted culture, 50 μl was then added to each tube containing novobiocin, and followed by incubation at 37°C with shaking at 200 rpm. An OD_{600} of 0.2 or higher at 8h was considered as growth. The minimum inhibitory concentration (MIC) was determined from the lowest novobiocin concentration with no apparent growth (269).

3.10. Electron microscopy

Electron microscopy was performed on four day-old colonies (Rv, Stv, LT2, the *ddhC* and *waaG* mutants, and the *waaG* complemented strain) as described previously (7). The colonies were obtained after streaking the cells on LB plates, and selecting those that had produced maximum rugosity. Briefly, colonies, including a thin layer of agar underneath, were excised and fixed in 2% glutaraldehyde in PBS buffer pH 7.4 at RT for 1h and at 4°C overnight. They were then post-fixed with osmium tetroxide, followed by 2% aqueous uranyl acetate. The samples were then dehydrated with increasing concentrations of ethanol (75%, 90%, 95%, and 100%). They were critical point-dried, and coated with gold palladium alloy, and were observed with a Hitachi S-4700 SEM (Hitachi Scientific Inst., Gaithersburg, MD).

3.11. Isolation of curli protein

Diluted (10^{-6} to 10^{-7}) overnight broth cultures of each strain (Rv, Stv, LT2, the *ddhC* and *waaG* mutants, and the *waaG* complemented strain) were plated on LB and grown at 25°C to yield individual colonies. After either 2, 4, or 6 days, colonies were isolated and resuspended by vigorous vortexing in 10 mM Tris Buffer pH 6.8 in the presence of 2.0 mm size sterile glass beads. One milliliter of suspension (OD_{600} adjusted to 3.0) was centrifuged, and the cell pellet was re-suspended in 100 μL of SDS Sample Buffer (62.5 mM TrisCl pH 6.8, 10% glycerol, 2% SDS) and boiled for 10 min. The cell lysate was centrifuged and the pellet was washed once with sterile water, then dissolved in 100 μL of 97% formic acid (Sigma), frozen at –80°C, and lyophilized (46, 202).

3.12. SDS-PAGE and Western blotting

The lyophilized samples (formic-acid resistant proteins) were resuspended in 100 μL of SDS sample buffer and sonicated for 5 sec (Vibra cell, Sonics & Materials, Danbury, CT) before loading in a 16% polyacrylamide gel. Prestained Kaleidoscope standard proteins (Bio-Rad, Hercules, CA) were used as molecular weight markers. Equal loading was assessed visually by comparing the overall profile of formic acid-resistant proteins on the Coomassie-blue stained gel from each strain. Separated proteins were transferred onto polyvinylidene fluoride (PVDF) Immobilon-P membranes (Millipore, Bedford, MA). The membranes were then incubated overnight in 3% skim milk (wt/vol) in TTBS buffer (TBS buffer containing 0.1% Tween 20) at room temperature, and were probed with mouse monoclonal anti-SEF17 antibody (a kind gift from William Kay) (46) diluted 1:1000 in TTBS, followed with horseradish peroxidase-conjugated goat anti-mouse antibodies. The antibody-bound proteins were detected using ECL Detection reagents (Amersham Biosciences, Piscataway, NJ) and were exposed to Hyperfilm (Amersham Biosciences). The density of several bands on the film, visually similar in intensity, was measured using the Quantity One program. Curli isolation was repeated and tested several times with essentially the same pattern recovered by Western blotting (see Appendix A.4).

3.13. Biofilm assays and microscopic observations

To visualize the production of biofilms in all *Salmonella* strains in glass test tubes, cells were inoculated into 5 mL of either M63 media supplemented with 0.5% CAA and 0.2% glucose (M63), or LB Miller base broth [either alone (L) or supplemented with 0.2% glucose (LG) or 0.2% glucose and 0.4% NaCl (LGS)] (17) in loosely capped

16 x 125 mm borosilicate glass culture tubes. The tubes were incubated with shaking at 210 rpm at 37°C for 20h. Cells were observed under fluorescence microscopy (Olympus BX60, Olympus Optical Co. Hamburg, Germany) using a green filter after staining with 1% acridine orange (Sigma).

To measure early adherence of cells to a PVC surface, 100 μL of overnight cultures (OD_{600} adjusted to 1.5) grown in M63 media supplemented with 0.5% casamino acid and 0.2% glucose with (for the mutants) or without antibiotics were added to wells in a Falcon PVC microtiter plate (35-3912 and 35-3913) and incubated without shaking at 37°C for eight hours. To determine the amount of crystal violet binding to the attached cells, 100 μL of M63 media and 50 μL of 0.5% crystal violet solution were added to each well in the plate to stain the attached cells. After 15 min at room temperature the plate was rinsed gently by immersion in water several times until the rinse water ran clear. The plate was air-dried for 30 min, and 200 μL of 80:20 acetone:ethanol was added into each well for 10 min to release the crystal violet from the cells, after which the absorbance at 595 nm was read in a microtiter reader (Multiskan Ascent, Labsystems, Thermo Electron, Waltham, MA) (171) (see appendix A.5 for details). Values from replicate assays in 8 to 15 wells were averaged.

3.14. Motility assay

Three μl of an overnight culture of Rv, Stv, LT2, the *ddhC* and *waaG* mutants, and the *waaG* complemented strains, with a reading of 1.0 at OD600 was stabbed into swim agar plates [1% Tryptone, 0.5% NaCl, 0.25% Bacto-agar (Difco)]. Three strains

(either Rv, A18 and A1-9, or LT2, YA155 and YA156) were spot-inoculated per plate 4.0 cm apart followed by incubation at 30°C for 5h.

3.15. Cellulose Assay

Cells from each strain (Rv, Stv, LT2, the *ddhC* and *waaG* mutants, and the *waaG* complemented strain) were streaked in 5 cm-long straight lines spaced approximately 3 cm apart on 15 large (150 x 15 mm) LB plates (with antibiotics added as necessary), so that the wt cells turned rugose after 2 days of incubation at RT instead of the required 4 days when grown as individual colonies. At 4 days, all strains including the mutants had developed their relative maximum rugosity when streaked in this fashion, and cells were harvested by scraping the growth from the agar surface using loops. To prevent dehydration of the cell masses during collection, the cell masses obtained from each plate were left accumulated on the agar on one side of the plate, keeping the plate lid on, and the cell masses were removed just immediately before weighing. Approximately 2 g (wet weight) of cells were harvested. The cell masses were placed in 50 ml polystyrene conical tubes, which were subsequently covered with parafilm and lyophilized. From 2 g of wet weight, the yield was approximately 400 mg of dry weight in the wt strain and between 310-350 mg in the LPS mutants. The cells were mixed with 3 ml acetic-nitric reagent (8:2:1 acetic acid:nitric acid:dH_2O) in 25 ml polystyrene centrifuge bottles and were boiled for 30 min. The mixture was centrifuged and the pellet was transferred to 25 ml Corex centrifuge bottles, washed once with 3 ml dH_2O and once with 3 ml acetone. After drying with slow shaking at room temperature overnight, each pellet was dissolved in 125 µl of concentrated H_2SO_4 (Fisher) with slow shaking for 1 h at room temperature. Five µl of each sample was diluted by mixing with 400 µl dH_2O in a boil-proof

Eppendorf tube 1.7 ml size (Eppendorf, Brinkmann Instruments, Inc, NY). The amount of cellulose isolated was detected by adding 750 µl of chilled anthrone reagent (Sigma) (0.2 g in 100 ml H_2SO_4) to each tube, boiling the tubes for 5 min and reading the absorbance at 620 nm. The amount of cellulose in the samples was extrapolated from a standard curve derived from dilution of a known amount (10 mg) of Avicel cellulose (Fluka Biochemika, Buchs, Ireland) treated in the same manner as the samples (248).

4. RESULTS

4.1. Random mutagenesis

Transposon mutants were screened at four days, the period required for the wild type strain *S.* Typhimurium DT104 Rv to develop the full rugose phenotype at 25°C. Two mutants, A1-8 and A1-9, showed a reduced rugose morphology and were selected for further study. When plates were spread with serially diluted overnight cultures yielding approximately 10 colonies per plate, the colonies started growing from a single cell, and formed rugose more slowly. Thus, the development of rugose morphotype of these mutants could be observed more closely. Compared to the wild type rugose Rv colonies that exhibited the rdar phenotype on the Congo red plate at 4 days, the A1-8 and A1-9 mutant colonies were pink and smooth, with white peripheries (Figure 9A). A1-8 colonies had irregular edges while A1-9 colonies were slightly smaller with entire edges. At six days, both mutants had developed some corrugation and A1-8 showed a more pronounced Congo red binding similar to that in the wild type Rv. At six days, however, both mutants still had not developed full rugosity as compared to the wt. Only the center of the colonies were corrugated and interestingly, the corrugation lacked the complex

pattern exhibited by the wt strain. The *waaG* mutant developed more wild-type like rugose colonies than did the *ddhC* mutant when streaked with a high density inoculum on the plate (see materials and methods). The colonies of A1-9 were very elastic when pulled with a loop, and in some streak areas they became very adhesive, and stuck so strongly to the agar media that they could not be removed. Overall, the mutations in A1-8 and A1-9 appeared to result in retardation of the expression of the rugose phenotype, and in A1-9, there was also alteration in the property of the matrix.

When compared to the wild type Rv which produced thick pellicles, and Stv, which did not produce pellicles and exhibited dispersed growth in LB broth after four days at 25°C, both A1-8 and A1-9 produced pellicles similar to that seen in the wt. The main exception was that they had a slight reduction of the grooves seen in the wt pellicle (data not shown). No change in pellicle morphology was observed after four days (data not shown). There was a possibility that reduced rugosity may have resulted from the slower growth of the LPS mutants, whose colonies appeared to be smaller than those of the wt. However, this did not appear to be the case, since growth rates in LB broth at 28°C of A1-8 and A1-9 were comparable to that of the wt Rv (Figure 10). Only a very slight decrease in the rate of A1-9 was observed early in the exponential phase, and all three strains reached approximately the same OD_{600} value at 11 h.

Analysis of the site of transposon insertion in A1-8 and A1-9 revealed that the transposon had inserted into two genes that function in the production of LPS: *ddhC* (formerly *rfbH*) and *waaG* (formerly *rfaG*) after nt 553 and 612, respectively, with the Kan^R of the transposon transcribed in the same direction as each of the two genes (Figure 11).

4.2. Phenotypic characterization of *waaG* and *ddhC* mutants

To verify the alteration of LPS in the mutant strains, LPS profiles of the wild type as well as the mutant strains were analyzed. *ddhC* codes for CDP-4-keto-6-deoxy-D-glucose-3-dehydrase, which is involved in the synthesis of abequose, the last sugar component of the O-antigen in the LPS, and *waaG* codes for the enzyme UDP-glucose:lipopolysaccharide (LPS) α1,3-glucosyl transferase, which functions in the addition of a glucose molecule to the heptose II of the core polysaccharide of LPS (Figure 12A), making the latter mutant a "deep rough mutant." The term, deep rough mutants, refers to mutants with alterations in genes affecting the inner core of LPS, including *waaCDEF* (heptose transfer), *waaG* (glucose transfer), as well as *waaP* (phosphorylation of HepI). They are usually characterized by susceptibility to hydrophobic compounds, changes in sensitivity to LPS-specific bacteriophages, and reduced expressions of outer membrane proteins (OMPs), which in turn increase the amount of phospholipids in the outer membranes and redistribution of the phospholipids to fill in the gaps left by the loss of the OMPs (179).

S. Typhimurium DT104 wt Rv produced the typical "ladder" pattern on the SDS-PAGE gel, with different molecular weight bands separating LPS molecules containing lipid A and core polysaccharide with varying lengths of the O-antigen polysaccharide chain (Figure 12B). In comparison, the *ddhC* mutant expressed mostly a low molecular weight LPS corresponding to a band that was located slightly higher than the core polysaccharide with one repeat of O-antigen, possibly indicating a lack of complete O-antigen in the absence of abequose. The *waaG* mutant primarily produced incomplete core polysaccharide of the LPS. The alteration of the LPS O-antigen in both *ddhC* and

waaG mutants was further verified by somatic O-antigen analysis. While Rv cells agglutinated in the presence of group B *Salmonella* antiserum, no agglutination was observed when A1-8 and A1-9 cells were suspended in the antiserum. The absence of O-antigen was also confirmed by the inability of P22 phage, which requires complete O-antigen for attachment, to infect these two mutants (data not shown).

4.3. Matrix production

Scanning electron micrographs of the mutants and wild type cells of colonies at four days of growth, when the cells appeared to produce relatively maximum rugosity, showed differences in matrix production. The wild type Rv produced a fibrous matrix that was seen on high magnification as multiple fibers projecting from the perimeter of the cells, interconnecting them with adjacent cells, and forming tightly configured fibrillar mats (Figure 13A). Only a few loose cells were found occasionally throughout the colonies. On the bottom of colonies, longer, less organized fibrils were also seen emanating from the cells (Figure 13B). The *ddhC* mutant A1-8, however, produced reduced amounts of extracellular matrix with differential characteristics as compared with that of the wt. The matrix was fibrous, nodular, and the cells were more loosely associated with the matrix, showing an “eggs in the nest” profile (Figure 13C). Similar pictures were obtained from different areas (the shallow “grooves” and “hills”) of the colony. It was also noted that the cells were shorter than those in the wt. In contrast, mutant A1-9 produced a profuse and thicker matrix, which completely covered the cells such that individual cells could not be discerned (Figure 13D). The matrix appeared to be more fibrous and had a slime-like characteristic.

4.4. Curli production

Differences in Congo red binding were partly due to the change in curli production (45). Therefore, curli protein was isolated and Western blotting was performed to quantify CsgA, the major subunit of curli protein. Curli protein was produced by the wild type Rv starting at day two, when the cells still appeared to be smooth, with slightly increased production when the cells were obviously rugose at days four and six (Figure 14A). On the contrary, a reduced amount of curli was produced by A1-8 and A1-9 at day 2, 4, and 6 compared to that in the wt Rv. The amount of CsgA production by Rv and A1-8 at day 4 appeared to be similar, but further quantification of band density showed that A1-8 actually produced only 84% of that in Rv.

4.5. Calcofluor binding

In order to indirectly determine if cellulose production was affected by the mutations, the cells were then grown on LB plates containing calcofluor. Although the binding to calcofluor is not specific to cellulose only, correlation has been shown between the presence of cellulose and calcofluor binding (201, 221, 279) and has been used to identify mutants lacking exopolysaccharide, including cellulose, in bacteria such as *A. tumefaciens* (237). Visualized under UV light, calcofluor-bound A1-8 colonies seemed to have fluorescence intensity similar to the wt Rv, while A1-9 had relatively brighter fluorescence, compared to the parent strain (Figure 15), perhaps indicating that the individual mutations in *ddhC* and *waaG* may have had different effects on the production of calcofluor-binding polysaccharide (possibly cellulose).

4.6. Direct knock-out of *waaG* resulted in phenotypes similar to the transposon insertion mutants

To exclude the possibility of multiple transposon insertions, spontaneous mutations, and polar effects, and because of an inability to transduce the LPS mutations into a wild type Rv background, a single gene knock-out was performed. The *waaG* mutant was selected for deletion, since this mutant showed a more profound change in matrix production compared to the wild type Rv. Because of the multi-antibiotic resistant phenotype of *S*. Typhimurium DT104, transformation of the wt strain Rv with the λ Red helper plasmid (Amp^R) was not possible (55). Therefore the deletion was performed on the non-antibiotic resistant strain *Salmonella* Typhimurium LT2. The LT2 strain has either an *mviA* defect, (15, 233) or a rare UUG start codon in the *rpoS* gene (133), thus resulting in altered expression of *RpoS*. Nevertheless, the strain that we used exhibited a normal rugose phenotype as compared with the DT104 strain Rv (Figure 9A and Figure 9B).

The *waaG* gene is part of the *waaQGPBIJ* operon, which encodes the enzymes for synthesis and modification of the core polysaccharide of LPS (214). The selected procedure deletes only a single gene without affecting the adjacent gene in an operon because of the presence of rbs at the 3'end of the PCR product (55). Except for the last 25 bp, the mutation deleted the entire *waaG* gene, which was replaced by the Kan^R gene, later shown to be transcribed in the same direction as *waaG* (Figure 11). RT-PCR analysis confirmed that the mutation was not polar, since *waaP*, the gene downstream of *waaG* in the operon, was still transcribed in the knock-out strain YA155 (Figure 16)

As shown in Figure 9B, the *waaG* mutant of LT2, strain YA155, was smaller in colony size than the wt LT2. The growth rate of YA155 at 28˚C was somewhat reduced

as compared to the wt in the log phase (Figure 17A), however, just before reaching the stationary phase, there was a cross-over at about 30h in the growth curves and the *waaG* mutant reached an optical density (OD) even higher than that of the wt. A similar pattern of growth was observed at 37°C (Figure 17B), and the OD readings were confirmed by viable counts at periodic points during the growth curve (Figure 17C). Thus, at stationary phase, there were slightly more mutant than wt cells. While it might be surmised that a slower growth rate may be the reason for the smaller colony size in strain YA155, when one colony of each of the wt strain LT2 and YA155 grown at the same period (26h at 37°C), with colony sizes of 2.5 mm and 2 mm, respectively, were each serially diluted and viable cells were counted, approximately 50% more cells were present in the YA155 colony ($6.4x10^8$ cfu) than in the wt colony ($4.4x10^8$ cfu). These observations suggested that in this case, the colony size did not correspond to numbers of cells and rates of growth. The smaller colony size probably resulted from the smaller size of the cells. This further suggested that changes in the *waaG* mutants were probably not due to the slower growth and thus the presence of fewer numbers of cells, but were more likely the result of physiological changes exerted by the LPS core alteration.

Strain YA155 was similar phenotypically to the transposon mutant A1-9 in colony morphology and Congo red binding (Figure 9B). Strain YA155 produced a fragile pellicle, possibly due to the different wt background, since the wt strain of YA155, LT2, formed a thinner pellicle than the wt Rv (data not shown). The original phenotype could be restored when the gene was complemented into a plasmid in strain YA 156 (Figure 9B). The similarity of the LPS profiles between the transposon and deletion mutants was also further confirmed (Figure 12). The complemented strain produced an LPS chain

comparable to the wt, indicating that a single gene was likely responsible for the phenotypic changes in the *waaG* mutant (Figure 12B). Impaired curli production was also displayed by the knockout mutant YA155 at day 2. Although the amount of curli protein produced appeared to be similar to the wt visually at day four, further quantification of the band densities showed that the production in YA155 was only 70% of that in Rv. Eventual complementation increased curli production to a level similar to that exhibited by the wt strain (Figure 14B).

One characteristic of deep rough mutants is increased susceptibility to hydrophobic compounds such as novobiocin, as observed with both *waaG* mutants A1-9 and YA155 (Table 4). Compared to the more resistant wild type Rv, with (MIC 25 μg/ml), the *waaG* mutants were significantly more susceptible to novobiocin, revealing an MIC of less than 1.6 μg/ml. Both the wt LT2 and the *waaG* mutant YA155 showed the same change in susceptibility as those with Rv background. When the mutation in *waaG* was complemented with the *waaG* gene in a plasmid of strain YA156, the susceptibility was slightly diminished (MIC of 6.25 μg/ml). Interestingly, a transposon insertion mutation in *ddhC* (strain A1-8) resulted in an increase in the MIC (50μg/ml).

4.7. Both mutants are biofilm formers

When grown in rich media (LB) at 37˚C with shaking, neither the wt nor the mutants were able to form biofilms. However when grown in M63 minimal media supplemented with glucose and incubated with shaking at 37°C, the *ddhC* mutant (A1-8) and *waaG* mutants A1-9 and YA155 formed thick biofilms appearing as a ring at the liquid-air interface. *waaG* mutants also appeared as spots stuck to the walls of the tubes at

the liquid-solid interface (Table 5). When either 0.2% glucose alone (LG) or in combination with 0.4% NaCl was added to the LB media (LGS), both mutants again formed biofilms similar to those seen in minimal media (Figure 18). Thus, it seems that it was the presence of glucose and salt in the emended medium, and not the minimal medium per se, that promoted biofilm formation in the *waaG* mutant under these conditions. In contrast, the wild type strains Rv and LT2 formed no visible biofilms in any of the three different media at 37°C (data not shown).

At 28°C the wt strains formed biofilms only in L media, and *ddhC* showed a thick ring in all of the media except LB, while *waaG* produced biofilms in all four media (L, LG, LGS, and M63). Varying conditions thus induce biofilm formation differently in these strains. Neither *csgA* mutant YA 151 nor *bcsA* mutant YA159 formed any biofilms in any of the media under these growth conditions (Table 5).

Compared to growth in LB alone (L media), the addition of either glucose only (LG) or glucose and NaCl (LGS) enhanced the ability of the mutant cells to form visible clumps in the tubes. The cells also settled to the bottom of the tube causing the culture to appear clear (Figure 18). Microscopic observation of the *waaG* mutant YA155 grown in L media at 37°C showed that these cells were smaller in size than the wt or complemented strain YA156 (Figure 19A). In LG and LGS media, the YA155 cells formed clumps that were composed of aggregates of cells. Much smaller aggregates were seen in cells grown in LG compared to LGS (Figure 19B). Conversely, the wild type cells existed mostly as single cells, and formed turbid growth in L, LG or LGS (data not shown).

The formation of biofilms was also assessed quantitatively in the initial adherence stage on the PVC surface of microtiter wells at 37°C. A1-9 and 155 had approximately ten times as much crystal violet (CV) binding as that of the parent strains Rv and LT2, respectively, at 8h in the growth curve (Figure 20). The *ddhC* mutant also had an increase in adhesion, although not as much as that observed for the *waaG* mutant. The increase in CV binding correlates with the attached cell population size, which obviates any notion that the higher absorbance obtained from the microtiter assay was due primarily to an enhanced ability of the mutant strains, with altered LPS, to bind CV more capably than wt (see Appendix B). Because of the clumping of the mutant strains under the growth conditions used for the assay, and the smaller size of the mutant cells, the absorbance reading taken using the microtiter reader may not have been a precise comparison of the cell density between the different strains. Mixing of the microtiter plate, before the absorbance reading for the cells was taken, was essential. Nonetheless, even with these limitations, the assay allowed us to indirectly estimate relative cell density among strains based on OD values.

4.8. Motility and swarming

LPS mutations have been shown to be associated with unexplained reduction in motility (80), and motility is required in the early stage of biofilm formation by some bacteria such as *P. aeruginosa* (264). In the 5-hour motility assay, we showed that the wild type Rv had a diameter of 2.2 cm, while both mutants, A1-8 and A1-9, did not appear to swim out of the initial inoculation site (Figure 21). When wet mount preparations of the mutants and the wild type were observed microscopically, the mutant cells did not exhibit normal movement. There appeared to be more tumbling in a single

location as compared to the normal multi-directional swimming exhibited by the wild type. Compared to the wt strain LT2, which had a swarm diameter of 2.4 cm, the *waaG* deletion mutant YA155 did not appear to move out of the initial inoculation site after 6 h of incubation. The defect was partially restored in the complemented strain YA156, which had a swarm diameter of 1.9 cm. The inability of the mutants to swarm may be interepreted as either a loss of motility or chemotaxis. Despite this alteration, both strains nevertheless showed elevated amounts of biofilm production.

4.9. Cellulose production

The production of cellulose was further confirmed using the cellulose assay. Because cellulose is hygroscopic, wet weight comparisons between strains may not provide equivalent amounts of cell mass. Therefore, the same wet weight of cells would contain lesser amounts of cell mass of a cellulose overproducing strain than a wt strain. A better comparison is made when dried (lyophilized) cells are used in the experiments. Both LPS mutants produced more cellulose than the wt strain from the same amount of dry cell pellet. In fact, the *waaG* mutant YA 155 had the highest yield, almost three times the amount of cellulose as produced in the wt strain (Figure 22). Importantly, the increase in calcofluor binding might reflect the increase in cellulose production. Interestingly, the *csgA* mutant YA151, which did not produce curli, showed approximately the same amount of cellulose as the *waaG* mutant, indicating that the production of curli may actually impede cellulose production. As expected, the *bcsA* mutant YA159 showed an absence of cellulose production. We also discovered another similarity between YA155 and YA151, which was revealed through scanning electron microscopy (Figure 23). Both strains produced large globular structures up to approximately 100nm in diameter.

Similar structures, although slightly smaller, were also seen at a higher frequency in A1-8 than in the wt (data not shown). Although at present the significance of these structures is not known, they may possibly be related to the production of cellulose, because of the correlation between their occurrence and the increasing amounts of cellulose produced.

5. DISCUSSION

5.1. LPS alteration and its effect on the rugose phenotype

Rugose morphology in strains of *Salmonella* and *E. coli* has been associated with aggregative behavior and, because of its temperature sensitivity, it is a feature that is presumed to be associated with the ability of organisms to survive in environments outside of the host. In fact, it has been shown recently that curli-coding genes, the first components of the rugose matrix, are disrupted by either deletion or IS insertion in invasive bacteria such as *Shigella* and enteroinvasive *E. coli* (EIEE) (206), and those that code for cellulose, the second component, are also lacking in *Salmonella* isolates (present in other less invasive strains of *Salmonella*) that cause more invasive disease (198). Thus, adaptation to the environment inside the host at 37˚C, a temperature at which the rugose morphotype is not expressed, probably forces selective pressure against energy-consuming rugose formation once inside the host.

On further investigating the rugose phenomenon in *Salmonella*, the possibility of involvement of other cellular factors for rugose expression was considered. Two semi-rugose mutants A1-8 and A1-9 derived from random mutagenesis were selected because of aberrant rugose expression. Each had a transposon insertion in a gene involved in lipopolysaccharide (LPS) production: *ddhC* and *waaG.* In *Salmonella* Typhimurium, the

LPS is composed of lipid A, KDO, and the inner core composed of three phosphorylated heptose groups (HepI, HepII and HepIII), an outer core composed of three hexose groups, and repeating units of O antigen. *ddhC* is a member of the *rfb* operon encoding the locus for chromosomal O-antigen biosynthesis of the LPS. The enzyme coded by this gene, CDP-4-keto-6-deoxy-D-glucose 3 dehydrase, functions in catalyzing the formation of CDP-4-keto-3,6-deoxyglucose from CDP-4-keto-6 deoxyglucose. This reaction is an important step in the synthesis of abequose, one of the four hexoses in the polysaccharide repeat subunits of the O-antigen. The LPS profile for this mutant showed that the absence of *ddhC* prevented the cells from repeating the O-antigen chain. On the other hand, *waaG* codes for glucosyl-transferase, which functions in the transfer of glucose from UDP-glucose to heptose II in the inner core of the LPS structure (179). Disruption of this gene resulted in the production of a more severe truncation of LPS that lacked the outer core of LPS (Rd1 chemotype) (142). The fact that these two different levels of LPS mutations both retarded rugose morphology implied a positive role for LPS in rugose appearance. A similar phenomenon of rugose phenotype in *Vibrio cholerae* was also shown to be affected by mutations in two genes involved in LPS synthesis: *rfdB*, and *rfbE*, which blocked the switching of *Vibrio cholerae* from smooth to rugose (192). Although rugose morphology in *V. cholerae* is attributed to the presence of the exopolysaccharide VPS and its regulator VpsR (270), LPS was still shown to be involved, thus indicating that the synthesis and/or assembly of some of the components of the rugose matrix may depend on an intact cell surface in *V. cholerae*, as well.

5.2. Effect on curli production by *ddhC* and *waaG* mutations

The two different mutations of LPS appear to affect the production of matrix in opposing manners. While the *ddhC* inactivation reduced matrix production, the *waaG* deletion actually showed an increase in the amount of matrix production. To discern the reasons for this phenomenon, the effect of these mutations on two matrix components, curli and cellulose, were further investigated.

The *ddhC* mutation, which affects O antigen of the LPS, appeared to have minimal effect on Congo red binding. This corresponds to the findings of White *et al.* (262), that introduction of *galE* mutation in *S*. Enteritidis affected O antigen production, thus resulting in reduced aggregative morphology but with little alteration in Congo red binding. However, there was some retardation of curli production, which may have been enough to affect the rugose matrix.

The *waaG* mutant also showed a decrease in curli production compared to the wild type, and this production was restored when the mutant YA155 was complemented by plasmid-borne *waaG*, thus raising the question - how does the mutation in *waaG* possibly affect curli production?

One hypothesis is that it may be due to the effect of *waaG* mutation on the integrity of the outer membrane, as suggested by the major increase in susceptibility to the hydrophobic compound novobiocin in the *waaG* mutant compared to the wild type (an MIC of <1.6 μg/ml compared to 50). A recent study in *E. coli* showed that instead of reducing outer membrane proteins, *waaG* mutation eliminated phosphorylation in HepI and reduced (only 40%) phosphorylation of HepII in the core polysaccharide (269). The decrease in phosphorylation, similar to that seen in the *waaP* mutant lacking all

phosphorylation in the core polysaccharide would impair membrane integrity (179). The negatively charged phosphate groups in LPS have been implicated in maintaining membrane stability by allowing cross-linking of LPS molecules by divalent cations (179). The mutation in *ddhC*, on the other hand, which increased the MIC even higher than that in the wt, did not significantly affect curli production. Taken together, these results imply that the general outer membrane stability of the inner core LPS, normally phosphorylated, might have been compromised by *waaG* mutation, which, in turn, may impair normal curli production by affecting the transport and/or assembly of curli subunits. This hypothesis was supported by similar findings by Genevaux *et al.* with *E. coli* K-12 (80), in which transposon insertion in the genes for LPS-synthesis, *waaG* (*rfaG*), *waaP* and *galU*, resulted in reduced production of type I fimbriae. All three mutations affected phosphorylation of the inner core (*waaP* is required for phosphorylation of the two heptoses in the inner core of LPS and *galU* is required for production of UDP-glucose, thus having a similar role as *waaG* in LPS synthesis). The findings suggested that LPS mutation, which affected phosphorylation of the inner core, could affect curli production by decreasing the synthesis of usher proteins for the production machinery of those surface appendages, as has been shown in other gram negative bacteria.

It is possible that the effect of LPS alteration may actually send a more specific signal to certain genes, since recent evidence has shown that the loss in membrane integrity, due to the loss of phosphorylation in the inner core of LPS, might activate the RcsC/B phosphorelay system. The involvement of the RcsC/B in both the *ddhC* and the *waaG* mutants is strongly suggested by the lack of swimming ability in both mutants. Although further investigation is needed to confirm whether the mutant cells lack either

motility or chemotaxis, there seems to be a hint toward loss of motility, as has been shown in *E. coli* having mutations in the adjacent region, Δ*rfaQPBJ* (179). The RcsC/B two-component system is induced by general perturbation in the cell envelope, and in turn, it simultaneously regulates two different systems, i.e. the *wca* (formerly *cps*) locus for colanic acid capsule production is upregulated, resulting in mucoid colonies, and the *flhDC* operon, which codes for the master regulators for flagellar synthesis, motility and chemotaxis, is downregulated, resulting in loss of motility (71). In fact, it has recently been shown from a study using gene microarray that *csgD* is also downregulated during the activation of RcsC/B by overproduction of DjlA, another mutation that results in membrane perturbation (67). The results from the current study thus would indirectly support this conclusion, since repression of CsgD would result in downregulation of the *csgBA* operon, resulting in reduction of the amount of CsgA protein in the *waaG* mutant. Although tempting to accept, this proposition warrants further investigation of RcsC/B involvement in the *waaG* mutant phenotype, especially because mutation in different loci of *waaG* could result in different expressions of colanic acid (mucoidy), such as shown in the current study and by others in different host backgrounds (80, 179, 243). Colanic acid synthesis loci similar to those in *E. coli*, are present in *Salmonella* LT2 but have not yet been studied extensively (76, 226).

5.3. The effect of LPS alteration on cellulose overproduction

Although curli production was depressed in both A1-8 and A1-9, it was found that cellulose was overproduced in each of them. The increase was not as high in *ddhC* as for the *waaG* mutant and interestingly, cellulose overproduction was also shown by the curli mutant YA151 (*csgA*$^{-}$). These results seemed to signify that normal curli production

actually hinders cellulose production. Therefore, it is tempting to speculate that it was the decrease in curli production in the *waaG* mutant that was in large part responsible for the increase in the amount of measured cellulose. White *et al*. (262) have reported that both curli and cellulose are under similar regulation and are components of the same matrix, however, they may be produced at different times during the development of rugose morphology. Therefore, proper timing may be important in establishing the balance between the two matrix components, since a delay or reduction in curli production seems to affect cellulose synthesis. Results from my study of these two LPS mutants suggest that LPS may be significantly involved in maintaining this balance, thus causing us to consider that LPS may be yet another possible mechanism or mediator of regulation on cellulose synthesis.

It is worth mentioning that, in some instances, pathways for EPS and LPS synthesis are shared. For example, in *Salmonella*, the same precursor molecule, UDP-glucose, is used for LPS O-antigen and capsular polysaccharide (232). Thus, the *waaG* mutation, which disrupts the transfer of UDP-glucose to the LPS, may redirect the precursor to another polysaccharide pathway in which cellulose overproduction could occur. This switching has been shown in *algC* in *P. aeruginosa*, between the production of alginate and O-antigen (56). Interestingly, with *V. cholerae* and *Lactobacillus lactis*, mutants in *galU* and *galE*, coding for UDP-glucose phosphorylase and UDP-galactose epimerase for LPS synthesis, showed a lack of EPS production (23, 168).

5.4. Effect of LPS mutations on biofilm production

Biofilm formation in L media by the wt strains at 28˚C seemed to be dependent on curli and cellulose, as shown by the control strains YA151 (*cgsA*$^-$) and YA159 (*bcsA*$^-$),

both of which failed to form biofilms under these conditions. Thus, reduction in the amount of curli produced in the LPS mutants under these conditions suggests an explanation for the reduced grooves in pellicles in standing LB and reduced amounts of biofilms in shaken LB at 28˚C in the mutants A1-8 and A1-9 compared to the wt Rv. The decrease in biofilm formation in the LPS mutants at this temperature may also be the result of overproduction of cellulose. Excess production of EPS has been shown to impede fimbriae mediated adhesion (205).

However, in the presence of glucose, or glucose and NaCl, at 37°C or 28C, the amount of biofilm produced was reversed, with both mutants actually forming more biofilms than the wt. Thus, these observations reinforce those made with a *ddhC* mutant of *Salmonella* from a previous study (158), where there was an increase in adherence compared to the wt when grown in LB media with glucose at 30°C. These findings were in contrast to those found in a *waaG* mutant of *E. coli* K-12 (80), in which it was shown that the mutant exhibited reduced adherence to polystyrene surfaces compared to the wt strain, when the cells were grown in LB media at 37°C. In the present study, none of the strains, except Stv, produced biofilms in LB at 37°C. The decrease in adherence in the *E. coli* K-12 study was suggested to be due to the impeded production of type I fimbriae, since the level of adherence correlated with the amount of type I fimbriae produced. It is unknown if type I fimbriae have a role in adherence in our mutants. Since curli and cellulose are not optimally synthesized under conditions of high osmolarity, it is unlikely that these structures play a role in adherence. The difference in adherence property of the *waaG* mutants in the two studies may be due to the difference in genetic background, as revealed by the differences in colanic acid production by mutations in this gene.

Alternatively, it could be due to minor differences in assay conditions, which are not always clearly indicated. For example, while the growth media used in the current study is "LB", it is actually LB with a minimum amount of NaCl, thus differing from the regular LB media. The difference in NaCl concentration, albeit small, may affect adherence of the *waaG* mutant quite significantly. However, the inverse relationship between LPS and attachment has been shown previously (126, 238, 243), and the current study further confirmed that observation.

The observation that adherence of the LPS mutants increased at 28˚C and at 37˚C in the presence of glucose, or NaCl and glucose, in which synthesis of both curli and cellulose is probably repressed, prompted us to propose that these mutants may form biofilms under these conditions by activating another, distinct, biofilm-forming pathway. The use of an alternative pathway has been shown in several bacteria. In enteroaggregative *E. coli* (EAEC), biofilms formed when cells grown in media containing glucose and osmolarity required only aggregative adherence fimbriae (AAFII), but not the type I fimbriae, Ag43 and motility (217). In *V. cholerae*, where the formation of rugose matrix and biofilm formation requires the synthesis of the VPS polysaccharide, the VPS requirement was bypassed in the presence of Mg^{2+} in the growth media. The cells instead produced O-antigen polysaccharide for attachment (122). In addition, in *E. coli*, the requirement of colanic acid EPS can be circumvented by producing polysaccharide intercellular adhesion (PIA)-containing matrix when the carbon regulator *csrA* is mutated (257). This suggests that bacteria are versatile and can adapt to alteration in cell surfaces as well as growth environments to form biofilms. At the same time, this also shows the importance of biofilms to the cells, in that multiple pathways are

available for biofilm formation. Further identification of the matrix components of biofilms formed by the cells in the presence of glucose and NaCl would help to draw more definitive answers to the complexity of biofilm formation.

Initial bacterial affinity to surfaces can be affected by non-specific characteristics such as subtratum and cell surface properties. Cells with a more hydrophobic surface attach more easily to hydrophobic substances such as polystyrene, and less easily to hydrophilic surfaces such as glass and vice versa (145). This change in overall surface charge and hydrophobicity of the cell can be demonstrated through the loss of O antigen (178), or changes in charged EPS (264). Thus the LPS mutants, already lacking O-antigen (*ddhC*) or phosphorylation in the core LPS (*waaG*), became relatively more hydrophobic than the growth media LB, thus adhering less well to the hydrophilic glass surface compared to the wt strain. In contrast, the addition of NaCl might alter the ionic strength of the media, which could increase the ability of cells to attach to the glass. This correlation was demonstrated in strains with defined LPS core alterations expressing different combinations of the more hydrophilic B–band and the more hydrophobic A-band LPS in *P. aeruginosa* (145). The amount of cell retention to a hydrophobic surface corresponded to the level of hydrophobicity of the strains in the presence of NaCl concentrations greater than 1M, i.e.- those expressing the A-band showed the best retention. Adherence to hydrophilic glass surfaces by the strain having B–band LPS was shown to be greater than those having A–band LPS, suggesting that the presence of B-band LPS is the main mediator of adhesion to glass, (i.e. based on the hydrophilic status of the cell surface). The determination of the physicochemical surface properties including net surface charge, hydrophobicity *vs* hydrophilicity and electron-

donor/electron-acceptor characters, may help explain whether the mutations in *ddhC* and *waaG* affects these cell surface characteristics, ultimately contributing to the adherence properties of these cells (86).

The biofilm-forming ability of the *waaG* mutants in LG or LGS media was associated with the formation of large cell aggregates. Similar autoaggregation was shown in a deep-rough mutant containing a likely-polar transposon insertion in *waaQ* of *E. coli* MG1655 inside a mouse intestine (162), which was absent when the mutants were grown in LB media. The conditions inside the intestine, probably with increased osmolarity and/or ionic charges, might have contributed to aggregation in the mouse intestine assay. These findings endorse the hypothesis that alteration of cell surfaces by LPS affects not only adherence to abiotic surfaces, but also cell-to-cell adherence under certain growth conditions.

A great deal of attention has been given recently to the understanding of biofilm development and controls, and many researchers have employed diverse laboratory techniques and assay conditions to study the system. Although each of these techniques can complement limitations of the other, they also create differences in interpretation. The results of this study indicate that careful comparison of growth or assay conditions must be made when interpreting the effect of a single mutation on adherence since the same gene disruption may appear to either reduce or increase the biofilm forming ability of cells depending on the assay conditions.

5.5. Could cellulose overproduction involve the RcsC/B system?

With curli (a component of rugose matrix) production having been shown to be regulated by RcsC, one may then hypothesize that the change in cellulose production in

the *waaG* mutant may result from the activation of the RcsC/B system. In fact, activation of the RcsC/B has been shown to upregulate not only synthesis of colanic acid capsular polysaccharide in *E. coli,* but also synthesis of a number of capsular exopolysaccharides (EPS) in several capsule-producing enteric bacteria (259). Once activated, RcsC sends a signal to RcsA/B, which recognizes the conserved RcsA/B box (TaAGaatatTCctA), for example, in the promoter region of the *galF* promoter for the operon of K2 capsular antigen biosynthesis in *Klebsiella pneumoniae*; the *tviA* (*vipR*) promoter for the operon for Vi antigen in *S. typhi*; in addition to binding to the promoter for the *wca* operon for colanic acid synthesis in *E. coli* K-12. These three polysacharide synthesis proteins belong to the LuxR superfamily. Thus, it is possible that cellulose production may also be activated by this system. Interestingly, a very recent finding shows the involvement of RcsC/B in the repression of both *csg* operons (250). It is still unknown if the RcsA/B box is present in the promoter region of both promoters, because it does not have a very high degree of conservation in a number of RcsA/B-regulated promoters in *E. coli* (250).

However, this hypothesis may not go unchallenged. First of all, capsule production, although well studied in *E. coli*, is largely unknown in non-typhoid *Salmonella*. We have previously shown that the cells in pellicles of *S.* Typhimurium DT104 are encapsulated by anionic polysaccharide (7), and that capsular structure was present in the same strain grown in broth, however, knowledge about the nature of these capsular materials is not yet complete (146). However, cellulose has been implicated as one component of the pellicle in *S.* Enteritidis, *S.* Typhimurium and *P. fluorescens* SBW25 (212, 221, 224, 279) thus the possibility of a cellulose-comprising EPS, possibly as a capsule, may not be that remote. In the absence of colanic acid, biofilms were still

formed by *S*. Typhimurium on glass surface, indicating that this structure may not be a necessary biofilm component under these conditions (186). Nevertheless, RcsC activation may upregulate synthesis of a polysaccharide distinct from what is commonly produced by a strain. This was shown by the production of group I polysaccharide by an *E. coli* isolate which constitutively produced K54 capsule, as well (204). Thus, cellulose overproduction by RcsC/B could be possible whether or not cellulose makes up the predominant EPS materials. Secondly, since the activation of RcsC/B represses CsgD, it is more likely that the AdrA, the post-transcriptional factor required for assembly of cellulose and which requires CsgD for transcription, would also be downregulated, and thus cellulose would be underproduced instead of overproduced. However, recent findings showed that RcsB activation could trigger the transcription of *ugd*, a gene that is essential for the modification of LPS core polysaccharide by adding l-aminoarabinose to the 4'phosphate group (165). This gene is suspected to function in a manner similar to *ugd* in *S. pneumoniae* in capsular production. Thus, if the overproduction of cellulose involves the RcsC/B system, it is more likely to be induced by RcsC/B via another protein instead of through CsgD. This may indicate that the regulation of curli and cellulose production involves a number of systems that are interconnected, which is not surprising considering that they both contribute to the rugose matrix.

Nevertheless, overproduction of cellulose in *Salmonella* represents a new phenomenon, and the current study has shown that it may be related to the changes in cell surface. Cellulose production in enteric bacteria has only been recently discovered (279) (221), and its function other than forming biofilm matrix has not yet been exhaustively investigated. Additionally, further studies to elucidate the synthetic or alternative

pathways of production by *Salmonella* are essential, and may prove beneficial to the design of the eradication of cellulose-containing biofilms, thus, promoting interventions for better food safety. The implications of the benefit of the present findings in industrial settings should not be disregarded because the use of bacteria for cellulose biosynthesis for production of paper and medical devices has been recognized as an alternative to existing practices in plants. Also, the superior qualities of bacterial cellulose such as purity, greater strength and absorbancy, and biodegradability should be considered (203).

6. CONCLUSION

The physiology and genetics of *Salmonella* play a strong role in the complex regulation of its multicellular forms. In this respect, this study has aided in better understanding of rugose formation by showing the requirement for an intact cell surface, specifically the LPS, in normal matrix production. Additional knowledge of the effect of the cell surface on the formation of biofilms is needed. The findings in this study that LPS alteration can significantly increase cellulose production may shed new light on the involvement of LPS in the negative regulation of cellulose synthesis (Figure 24). Mechanisms of cellulose synthesis in enteric bacteria are still not well described. Analogies cannot be fully drawn to the well-defined system in *Gluconobacter* and *Agrobacterium*, two of only a few bacterial genera that were thought capable of producing this mainly plant-related polysaccharide. Differences, such as the involvement of AdrA in cellulose assembly observed only in *Salmonella,* make it difficult to conjure universal patterns of bacterial cellulose synthesis.

This study has hinted at the possibility of involvement of the RcsC/B system in regulating the production of curli in the presence of LPS mutations, although further confirmation of RcsC/B involvement is needed (Figure 24). It has recently been shown that growth on solid surfaces activates the RcsC/B system, however, the physiological stimuli of the RcsC/B system are still unknown (67). *E. coli* cells undergo envelope stress through membrane perturbation when growing on surfaces, which may activate the RcsC/B system. Other evidence seems to favor the activation of RcsC/B through the effect of alteration of the cell surface such as shown in DjlA overproduction and mutation in the core LPS, both of which resulted in an increase in EDTA and novobiocin susceptibilities. Findings such as these show that the intact cell surface plays an important role in adhesion and biofilm formation via signals sent by the RcsC/B. Since cellulose confers increased resistance to chlorine in enteric bacteria (221), knowledge of the mechanism of cellulose production could be essential to opening up avenues for control of the multicellular forms of *Salmonella*.

There is a rather large gap in the information base related to mutual effects of the surface molecules of the bacterial cell and its appendages. Knowledge thus far accumulated certainly suggests that there may be a greater interaction than thus far realized. This investigation has contributed in this regard by further describing circumstances related to the production and assembly of curli and cellulose to the mechanism of formation of multicellular types of *Salmonella* Typhimurium. In fact, the absence of intact LPS changes the production of curli and cellulose and the formation of rugose, pellicle, and biofilm formation. The use of non-polar gene deletion and its subsequent complementation further confirmed the role of LPS gene *waaG*. Furthermore,

the results appear to open additional possibilities of interaction between different systems such as RcsC/B, flagellar synthesis and the already complex rugose regulatory cascade or even changes in the physicochemical properties of the cell surface. With pursuant research, a better understanding of *Salmonella* survival in multicellular forms in its various niches is attainable.

Table 2. Strains and plasmids used in this study

Strains or Plasmid	Relevant description, or genotype	Relevant phenotype	Source or reference
S. Typhimurium DT104			(7)
Rv	wt	Rugose (rdar)	
Stv	Spontaneous smooth mutant of Rv	Smooth (saw)	(7)
A1-8	*ddhC*::Tn5	Altered rugose	This study
A1-9	*waaG*::Tn5	Altered rugose	This study
S. Typhimurium LT2	wt	Rugose	B. Bassler (231)
YA 104	LT2 (pKD46)		This study
YA 155	Δ*waaG*::*kan*	altered rugose	This study
YA 156	YA 155 (pTOPO *waaG*)	rugose	This study
YA 151	Δ*agfA*::*kan*	Semi rugose-pdar	This study
YA 159	Δ*bcsA*::*kan*	bdar	This study
S. Enteriditis 4b Δ*agfA*	Δ*agfA*	saw	W. Kay (45)
E. coli			
TOP10	F⁻ *mcr*A (*mrr-hsd*RMS-*mcr*BC) ϕ80*lac*Z.M15 .*lac*X74 *rec*A1 *ara*D139 *gal*U *gal*K (*ara-leu*) 7697 *rps*L (StrR) *end*A1		Invitrogen
Plasmids			
pTOPO	pCR 4 cloning vector, amp^R		Invitrogen
pTOPO *waaG*	pTOPO with *waaG* insert		This study
pKD46	λ Red helper plasmid, P*ara*, Ts ori, amp^R		B. Wanner (55) [*E. coli* genetic stock center (CGSC)]
pKD4	PCR template plasmid, FRT sites flanking Kan^R gene		B. Wanner (55) (CGSC)

Table 3. Primers used in this study

Primers	Sequence (5' to 3')	Source or reference[c]
p*waaG*11	CCC AAG CTT CGA CGA CAT CAT TCA GTT T[a]	5848-5830 [d]
p*waaG*12	CGG GGT ACC TAC CTT TAT GCC ACT TCA G[a]	4401-4419 [d]
p*waaG*D11	GAA AAA ATG CTG CCG CAT GAG GCA CGC ACC ATA GAT TTG GAC AGC CTG CTG TGT AGG CTG GAG CTG CTT C[b]	5681-5730 [d]
p*waaG*D12	TAG TGT GGT TAA CGG CGC TTT CAG CTC AAC CAT CTA AAT CAC CTG TAA TAC ATA TGA ATA TCC TCC TTA G[b]	4531-4580 [d]
p*waaG*IN11	GAG GGC ATC AGG TTC GTG T	5547-5566 [d]
p*waaG*IN12	AGG CGT TGC GTA AGG AAG G	4643-4662 [d]
p*waaP*IN11	TTC CTG AAG TGG CAT AAA G	4387-4405 [d]
p*waaP*IN12	AAA TAC TCA CGC ATA AAC C	3872-3890 [d]
p*csgA*D11	ATG GCT ATT CGC GTC ACC CAA CGC TAA TAC CGT TAC GAC TTT TAA ATC AAG TGT AGG CTG GAG CTG CTT C[b]	17701- 17750 [e]
p*csgA*D12	TTT GAA AGT GCG GCA AGG AGC AAT AAA GTA TGC ATA ATT TCC TCC CGA AAC ATA TGA ATA TCC TCC TTA G[b]	18271- 18320 [e]
p*csgA*11	TCA CCC AAC GCT AAT ACC G	17713-17732 [e]
p*csgA*12	CCT TGC TGA GTC GTG GTA A	18332-18350 [e]
p*bcsA*D11	ACG TCC GCC GGG AGC CTG CGA TGA GCG CCC TTT CCC GGT GGC TGC TTA TCG TGT AGG CTG GAG CTG CTT C[b]	11930-11881[f]
p*bcsA*D12	TAT CAT CAT TGT TGA GCC TGA GCC ATA ACC CGA TCC GAC GGC TGT ATC GCC ATA TGA ATA TCC TCC TTA G[b]	9281-9330 [f]
p*bcsA*11	ATG ATG CGG GCG ACA AAA C	4937-4955[f]
p*bcsA*12	CCT ATT ACC GCC GCA CAC A	14221-14239 [f]
p16s rRNA11	GAA GAG TTT GAT CAT GGC TC	21441-21460 [g]
p16s rRNA12	TAC GGT TAC CTT GTT ACG AC	19953-19972 [g]
pKanKD3	CAG TCA TAG CCG AAT AGC CT	Datsenko and Wanner (55)
inv2	GAA CTT TTG CTG AGT TGA AGG ATC A	Ducey and Dyer (62)

[a] Hind III and Kpn I sites are underlined
[b] Homologous sequence to the template plasmid pKD4 underlined
[c] Sequence number from *S.* Typhimurium LT2
[d] Sequence number from accession no. AF026386
[e] Sequence number from accession number AE008749
[f] Sequence number from accession number AJ315148
[g] Sequence number from accession number AE008820

Table 4. MICs for *S.* Typhimurium DT104 and LT2 and their derivatives when exposed to novobiocin

Strain	MIC (mg/mL)[a]
DT104 Rv	25
DT104 A1-8	50
DT104 A1-9	<1.6
LT2	25
LT2 YA 155	<1.6
LT2 YA 156	6.25

[a] MIC was determined from lowest concentration of novobiocin that inhibited growth of each strain. Inoculum was 50uL of 1:100 dilution of overnight cultures of the corresponding strain (OD_{600} values were initially adjusted to 1.5) in 5 ml of LB containing novobiocin (2 fold dilutions ranging from 200 to 0.8μg/ml). All tubes were incubated at 37˚C.

Table 5. Biofilm formation by *S*. Typhimurium

Strains	Biofilms[a] formed in media[b] at 37°C				Biofilms formed in media [b] at 28°C			
	L	LG	LGS	M63	L	LG	LGS	M63
Rv	-	-	-	-	+++	-	-	-
Stv	+	+	+	+	-	-	-	-
A1-8	-	+++	+++	+++	-	++	++	+++
A1-9	-	++	+	+++	+	++	+	+++
LT2	-	-	-	-	++	-	-	-
YA155	-	+++	++	++++[c]	++[d]	+	+	+++
YA151	-	-	-	-	-	-	-	-
YA159	-	-	-	-	-	-	-	-

[a] A (+++) indicates the presence of a thick ring on the tube wall at the liquid-air interface similar to that produced by the wt Rv in L media at 28˚C while a (-) indicates absence of a ring.

[b] Media used was LB only (L), LB supplemented with 0.2%glucose (LG), LB supplemented with 0.2% and 0.4% NaCl (LGS), and M63 minimal media supplemented with 0.5% casamino acids and 0.2% glucose (M63).

[c] Indicates the presence of an additional splotchy adherence on the tube wall below the surface of the broth

[d] No biofilm was formed when experiments were repeated using 250 mL flasks containing 30 ml of L media.

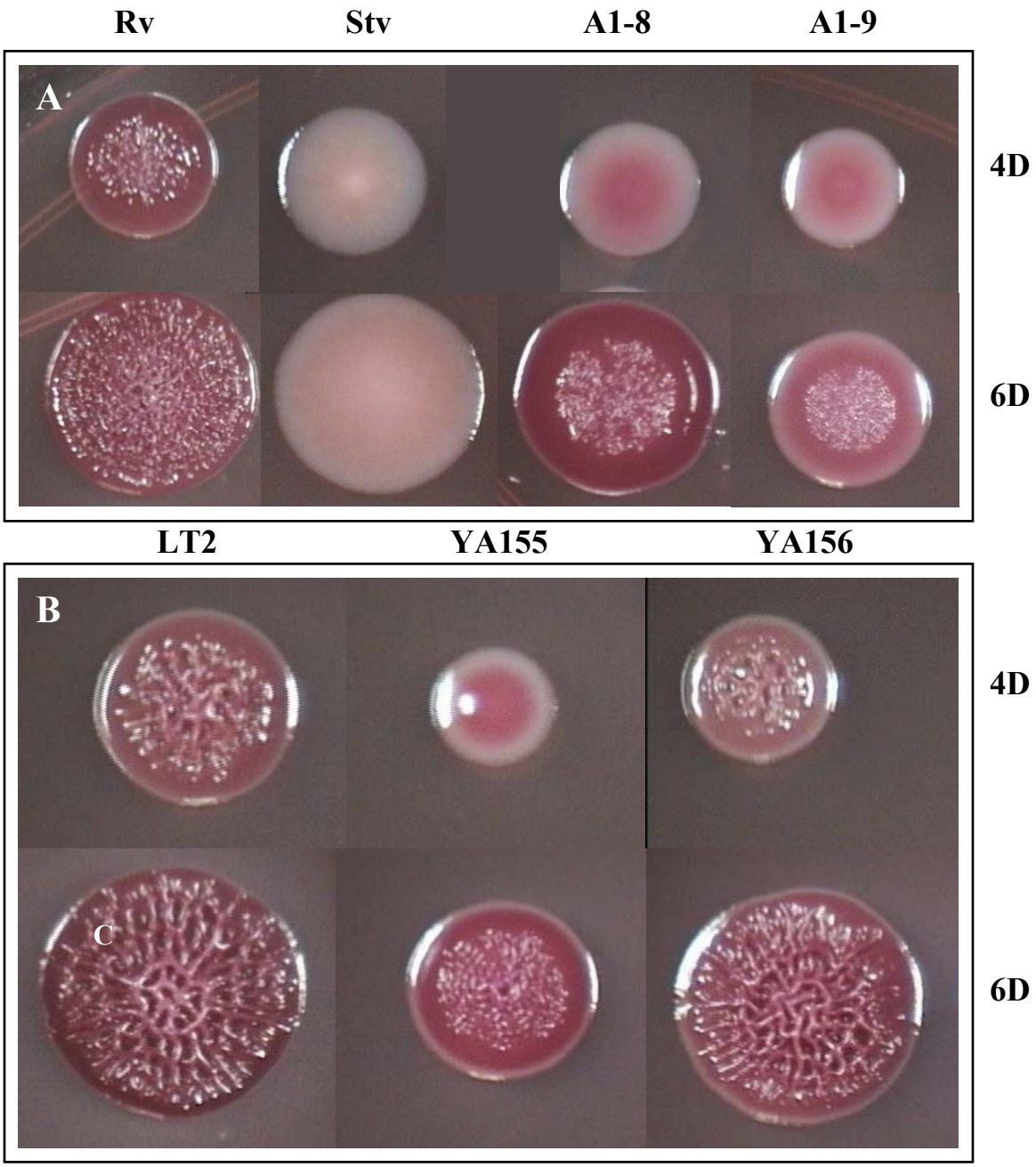

Figure 9. Growth of *S.* Typhimurium DT104 Rv and LT2 and their derivatives on LB CR plates at 4 days and 6 days at 25°C.

(A) Stv is a spontaneous mutant of Rv; A1-8 and A1-9 are *ddhC::Tn5* and *waaG::Tn5,* respectively; (B) YA 155 is a knock-out mutant of *waaG*(Δ*waaG::kan*), and YA156 is a complemented strain from YA155. Cells from overnight cultures grown at 37°C were serially diluted (10^{-6} to 10^{-8}) and were spread on LB plates to obtain individual colonies and grown at 25°C for 4 days (top) or 6 days (bottom).

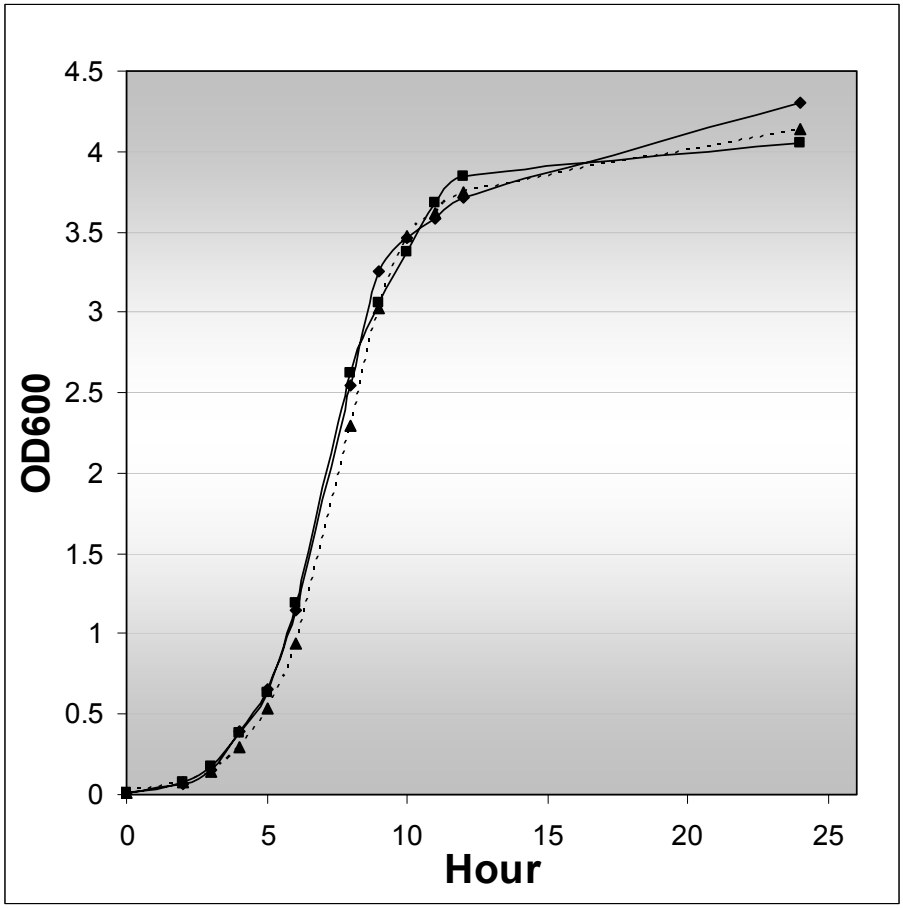

Figure 10. Growth curves of *S.* Typhimurium DT104 Rv, A1-8, and (A1-9) at 28˚C in LB broth.

OD_{600} was measured from subcultures containing LB broth inoculated with a 1/100 volume of overnight-grown cultures (OD_{600} values of the overnight cultures were adjusted to 1.0). Symbols: Rv (◆); *ddhC::Tn5* (A1-8) (--■--); and *waaG::Tn5* (A1-9) (▲).

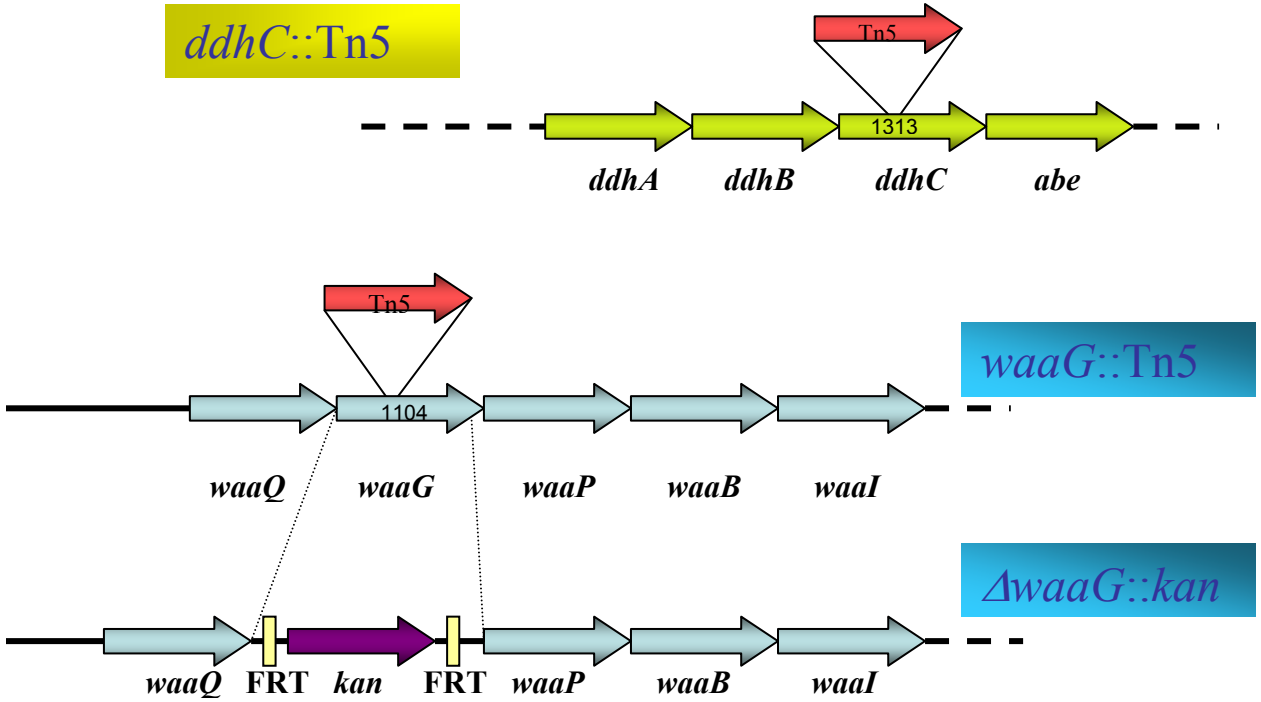

Figure 11. The sites of transposon insertion in strains A1-8 (*ddhC*::Tn5) and A1-9 (*waaG*::Tn5), and deletion in YA155 (Δ*waaG*::kan).

Number indicates the size of the respective genes in bp. Tn5 inserts at nt 553 in *ddhC* gene and at nt 612 in *waaG*. In strain YA155, the entire *waaG*, except for the last 25 bp, was deleted and replaced with a kan^R gene flanked by Flip Recombinase sites (FRT) that were created in the gene knock-out procedure. Dotted lines indicate the presence of additional genes in the operon.

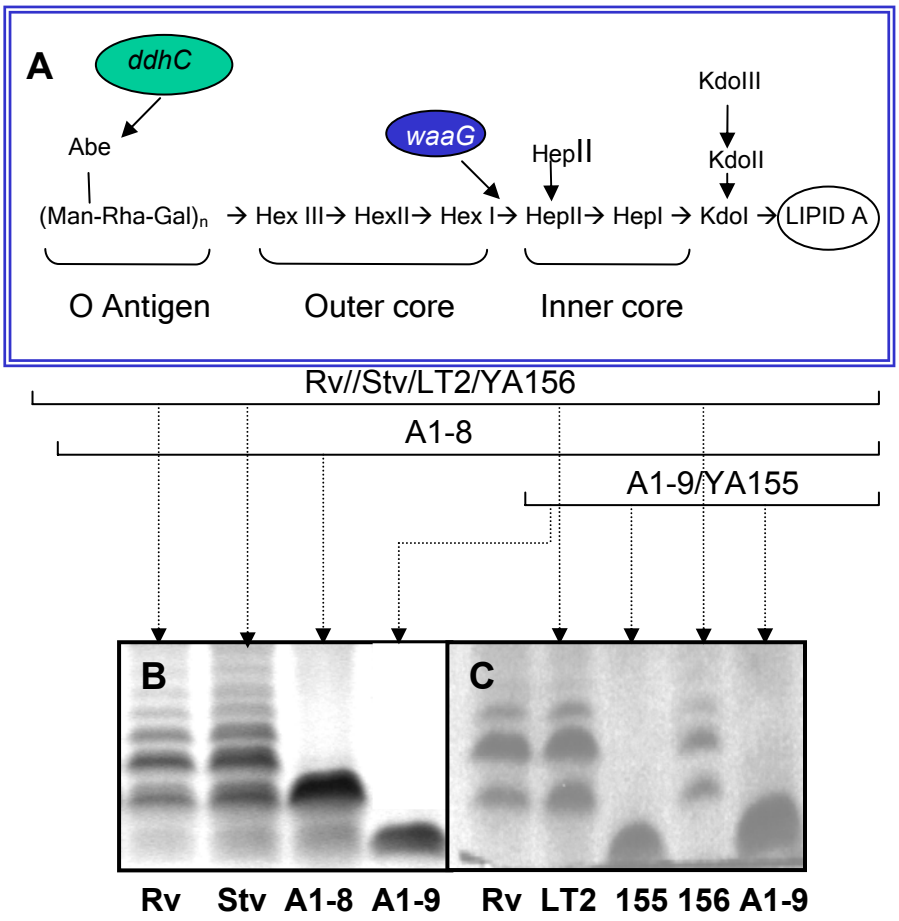

Figure 12. The general structure of lipopolysacharide (LPS) in *Salmonella* Typhimurium and the roles of both *ddhC* and *waaG* in LPS synthesis.

The structure of *Salmonella* LPS is shown in (A). (B) The LPS electrophoretic profiles of the *ddhC*::Tn5 (A1-8), and *waaG*::Tn5 (A1-9) of *S.* Typhimurium DT104 show the production of low molecular weight LPS as compared with the ladder pattern of the wt strain Rv. Profiles of LPS alteration similar to that in A1-9 was shown in the *waaG* knock-out strain YA155 (C). The production of low molecular weight LPS in mutants further confirmed the roles of both *ddhC* and *waaG* in determining the structure of LPS. Proteinase-K treated whole cell lysates were prepared from cells growing in early log phase at 37°C in LB, run on an SDS-PAGE gel, and silver-stained.

Figure 13. Scanning electron micrographs (SEM) of cells from intact colonies of *S.* Typhimurium DT104 Rv, and mutants A1-8 and A1-9 grown on LB agar for 4 days at 25°C.

Cells were streaked on LB agar for isolated colonies, and those reaching a relatively full rugosity after 4 days were prepared for SEM observation. A thick fibrous matrix covered most of the cells in Rv colonies as shown in (A), and was contrasted with some smooth cells occasionally seen lying on the cellular matrix. Some more loosely associated cells are present in the bottom of Rv colonies (B). *ddhC::Tn5* (A1-8) produced a thinner fibrous matrix (C). *waaG::Tn5* (A1-9), however, produced a much thicker, adhesive-like matrix (D) than that in the wt. Bar represents 1μm.

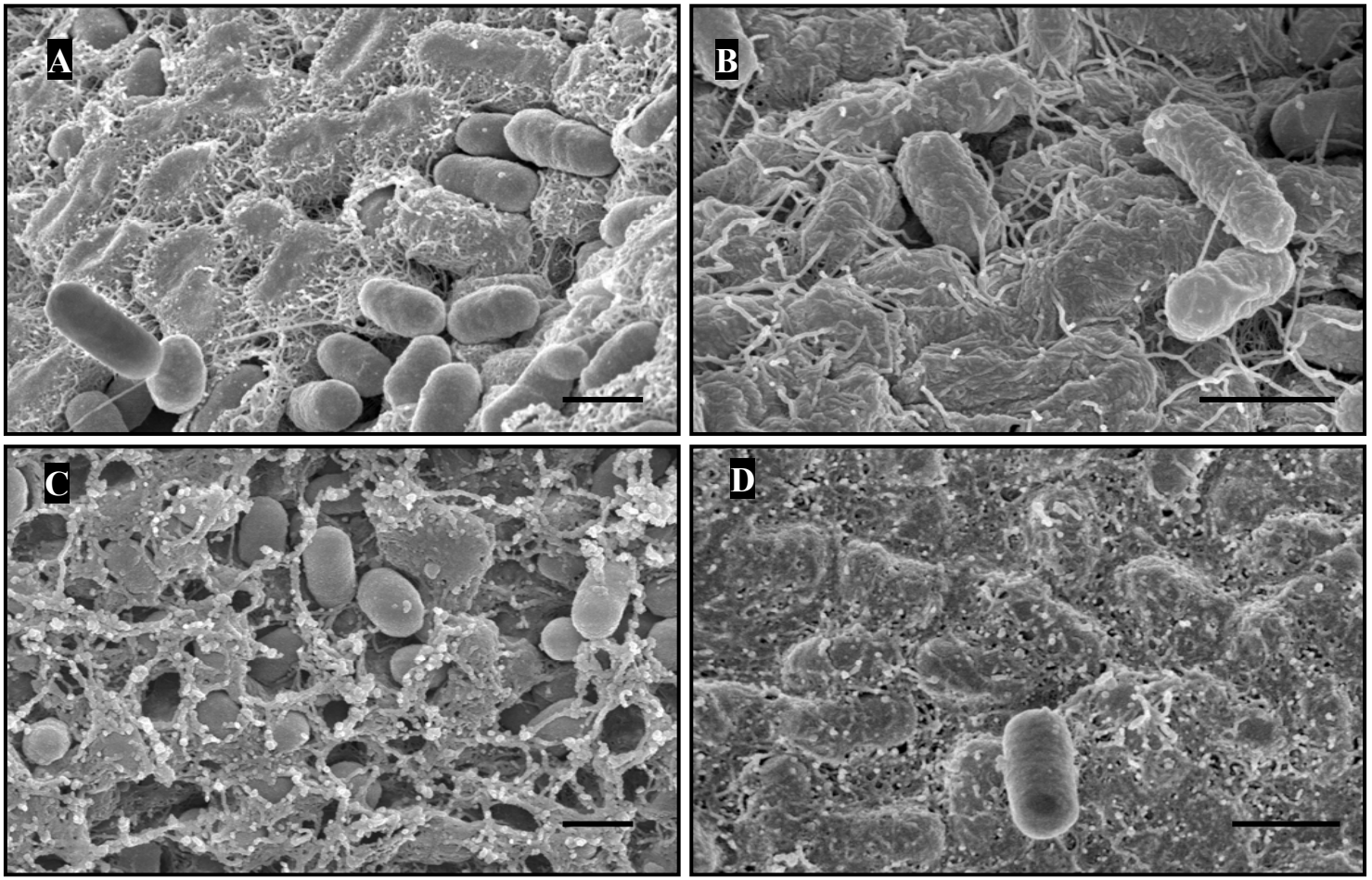
A
B
C
D

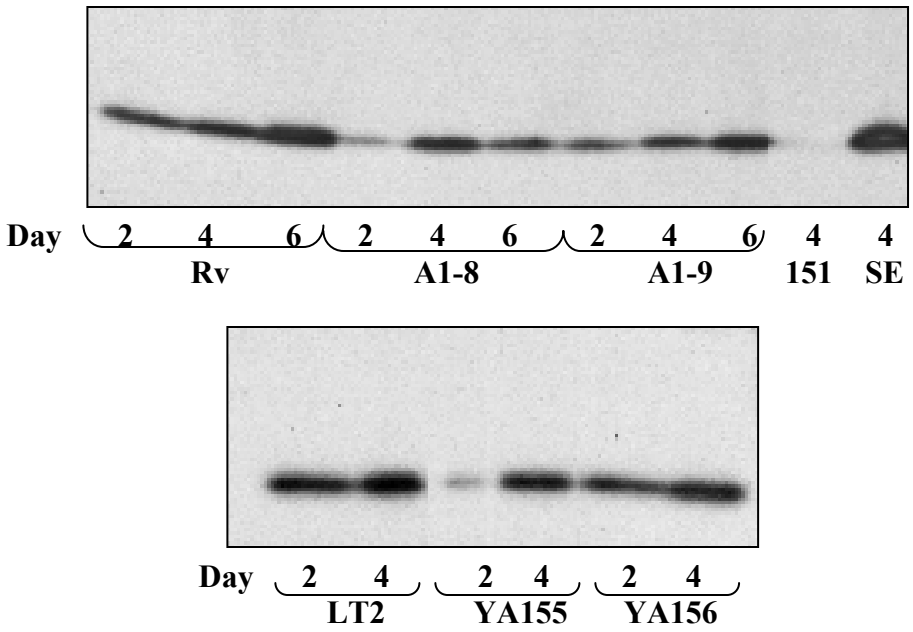

Figure 14. Curli production as judged from the major subunit CsgA production by the wt Rv and LT2 and their derivatives.

Curli production is shown for the wt Rv and its mutants *ddhC::Tn5* (A1-8) and *waaG::Tn5* (A1-9) mutants after 2, 4, and 6 days of growth (A), and the wt LT2 with its derivatives Δ*waaG*::*kan* (YA 155) and the *waaG* complemented strain of YA155 (YA156), after 2 and 4 days of growth on LB at 25˚C. Strains *S.* Typhimurium LT2 YA 151 (Δ *agfA*) and *S*. Enteritidis 4-b (SE) were included as negative and positive controls, respectively, in (A). Curli was isolated by formic acid treatment of whole cell lysates, separated by SDS-PAGE and probed with SE anti-AgfA monoclonal antibodies.

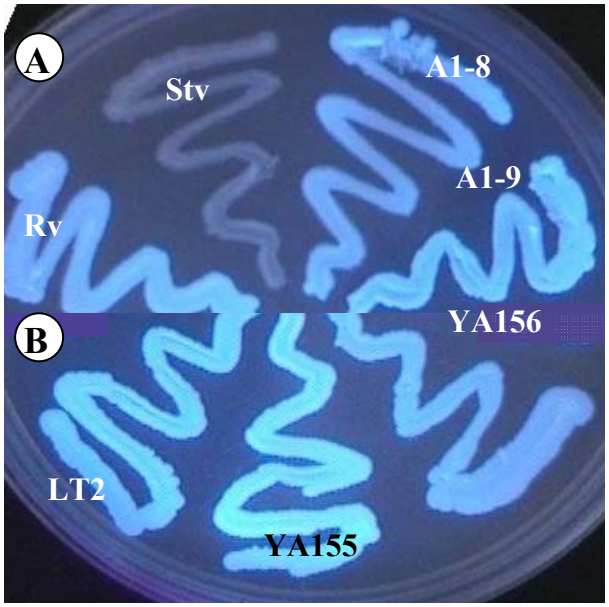

Figure 15. Growth of the wt *S.* Typhimurium DT104 Rv and LT2 and their derivatives on LB-calcofluor (CF) at 28˚C for 2 days.

Both *waaG* mutants *waaG*::*Tn5* (A1-9) and Δ*waaG*::*kan* (YA155) showed an increase in calcofluor (CF) binding compared to their respective wt strains Rv and LT2, respectively, while *ddhC*::*Tn5* (A1-8) did not show significant change in CF binding compared to the wt Rv. A high density inoculum was used followed by incubation for 48h at 25˚C. The CF binding of the colonies was evaluated visually under UV light.

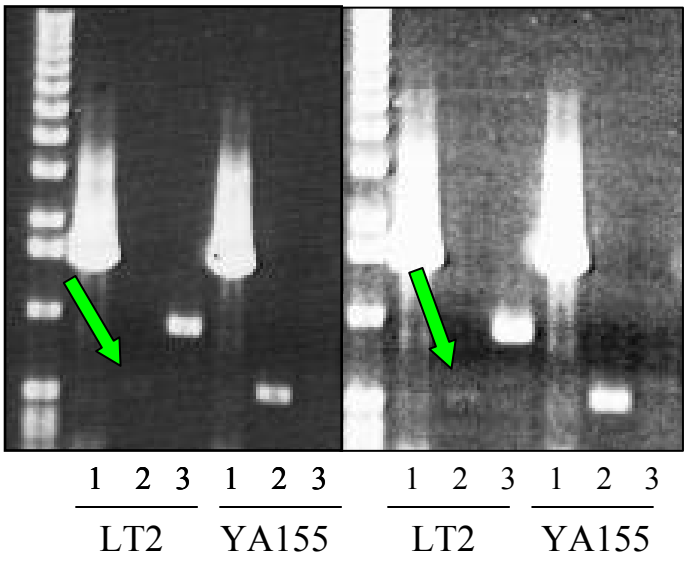

Figure 16. Expression of *waaG* and *waaP*, a gene adjacent to and immediately downstream of *waaG*, by the wt LT2 and Δ*waaG* mutant YA155 as shown by Reverse-Transcriptase (RT) PCR products.

RNA was isolated from colonies grown on LB agar for 4 days at 25˚C, and after treatment with DNAse, RT-PCR was performed on the isolated RNA using primers internal to the coding regions (see materials and methods). A 1 kb DNA ladder is included on the leftmost lane. The expression of 16s rRNA (1) by both strains was used to equalize the amount of loaded samples. *waaG* transcript was not expressed by the *waaG* knock out strain YA155 (lane 3), however, *waaP* was still expressed in both LT2 and YA155 (lane 2). Figure on the right was a copy of that on the left, brightened to enhance visualization of the *waaP* transcript (arrows).

Figure 17. Growth curves of the wt strain LT2, YA 155 (Δ *waaG*::*kan*) and the complemented strain YA 156 grown in LB at 25˚C or 37˚C.

The growth curves for LT2 (◆), Δ*waaG::kan* (YA155) (▲), and *waaG*-complemented strain (YA156) (■) in LB broth (supplemented with either kan for YA155 or kan amp for YA156) at 28˚C (A) and at 37˚C (B) are shown. The curves of YA155 showed cross-overs with those of the wt LT2 at both temperatures, and reached similar cell density as that observed in the wt at stationary phase. (C) The growth curves of LT2 (◆) and Δ*waaG::kan* (YA155) (▲) cells grown at 37˚C were compared by plotting the absorbance at 600 nm (solid lines) and viable cell counts (VC) (dotted lines) at 37˚C. The OD_{600} was measured from subcultures inoculated with 1:100 dilutions of overnight-grown cultures (OD_{600} values adjusted to 1.0).

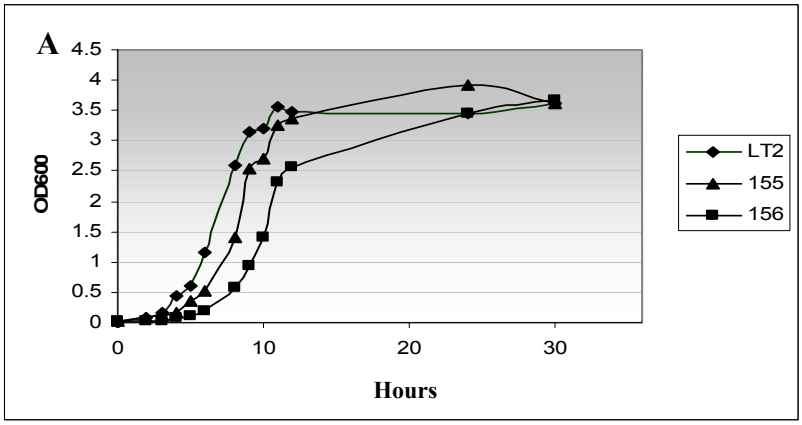
A
OD600
Hours
LT2
155
156

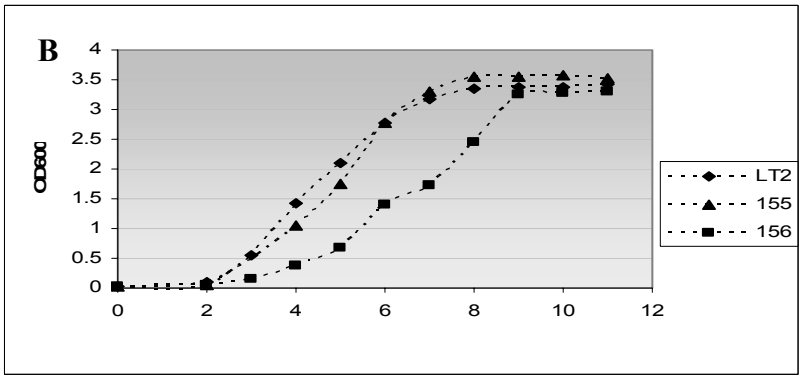
B
OD600
LT2
155
156

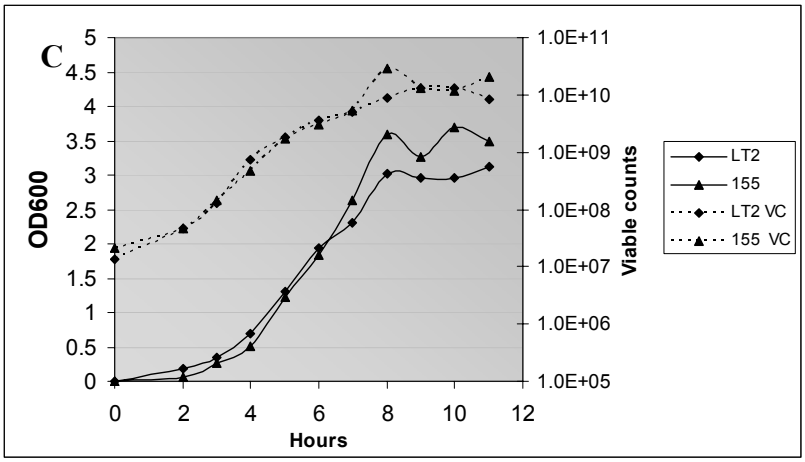
C
OD600
Viable counts
Hours
LT2
155
LT2 VC
155 VC

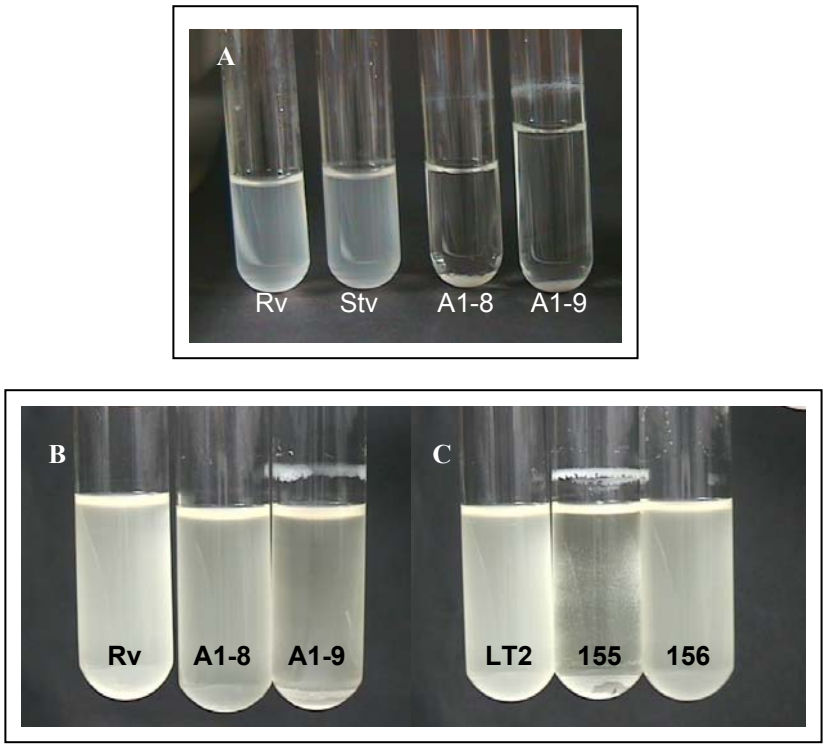

Figure 18. Production of biofilms by the *ddhC*::Tn5 (A1-8) and *waaG*::Tn5 (A1-9) mutants.

(A) Biofilm production by the LPS mutants *ddhC*::Tn5 (A1-8) and *waaG*::Tn5 (A1-9) was observed as rings on the tube walls at the liquid-air interface, while the wt Rv and spontaneous smooth mutant Stv did not adhere to the walls. Notice the clear media in both A1-8 and A-9, because of the formation of cell clumps that caused the cells to settle to the bottom of the tube. Bacteria were grown in M63 media supplemented with 0.2% glucose and 0.5% casamino acids at 37˚C with shaking at 250 rpm for 20h. Biofilms, lacking in the wt strains Rv and LT2, were also formed by the mutants A1-8 and A1-9 (B), and Δ*waaG*::*kan* (YA 155) (C), when cells were grown in LB broth supplemented with 0.2% glucose and 0.4% NaCl (LGS) under the same growth conditions. Complementation of *waaG* in strain YA156 eliminated the ability of cells to form biofilms. Strain A1-8 produced fragile biofilms, which detached easily, and cannot be visualized in figure (B).

Figure 19. Size comparison of the cells of wt LT2, the Δ*waaG*::*kan* YA155 and the *waaG*-complemented strain YA156 and the cell aggregation exhibited by YA155 in LG and LGS media

(A) The wt strain LT2, the Δ*waaG*::*kan* mutant YA155, and the complemented strain YA156 were grown side by side in LB broth at 37˚C with shaking at 250 rpm for 20h. The mutant YA155 appeared to be smaller in size when compared to the wt strain LT2 and to the complemented strain YA156. Figures in (A) were taken from microscopic observations of strains LT2 and YA156 grown in LG and LGS, respectively, but comparable cell size and arrangement of these two strains were seen in LB broth (data not shown). (B) Cell clumping by the *waaG* mutant *S.* Typhimurium YA155 grown in either LB broth (L), LB broth supplemented with either 0.2% glu (LG) or a combination of 0.2% glu and 0.4% NaCl (LGS). Cells were incubated with shaking at 37°C for 20h and stained with 1% acridine orange for observation under fluorescence microscopy. Magnification (A) 1000x, (B) 100x.

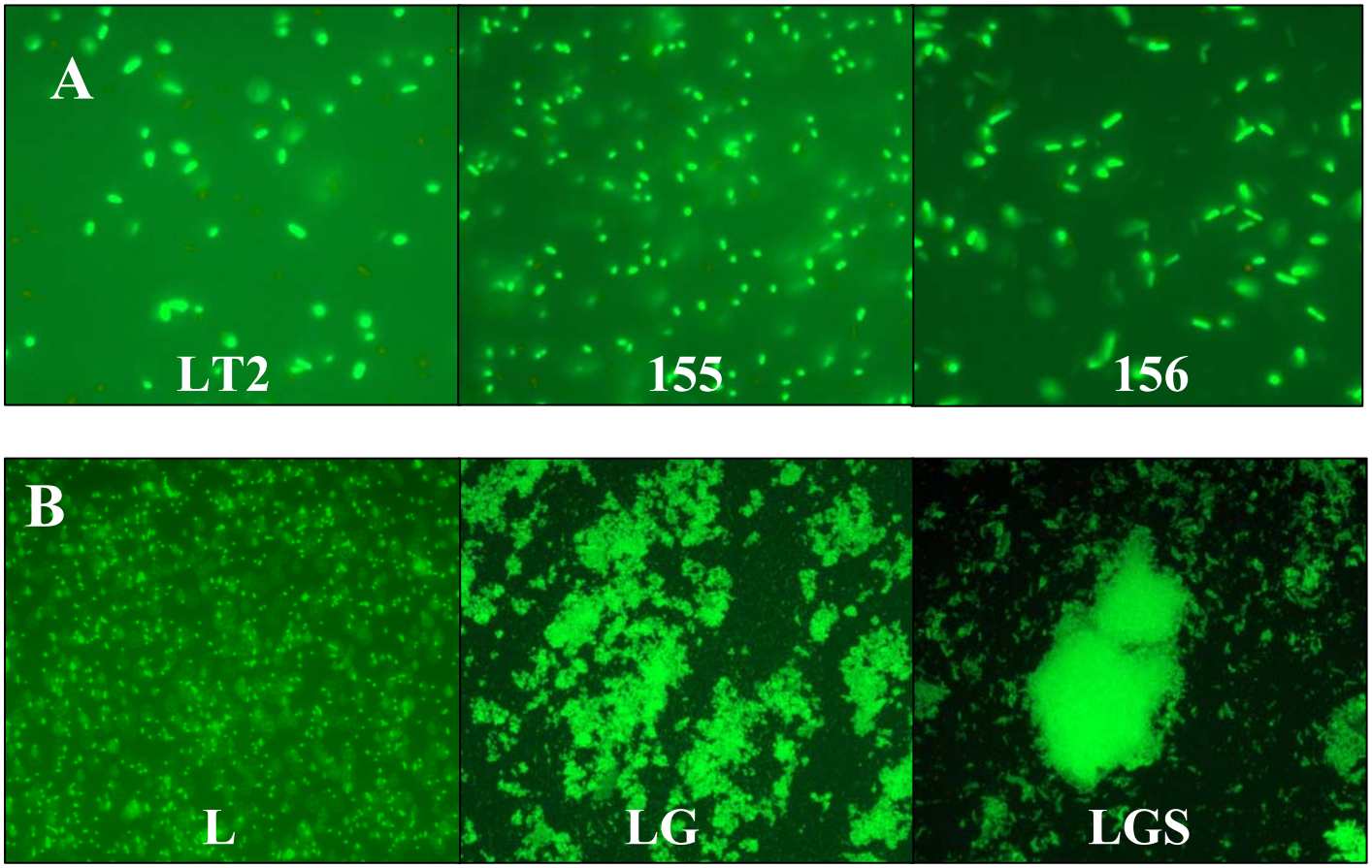
A
LT2
155
156
B
L
LG
LGS

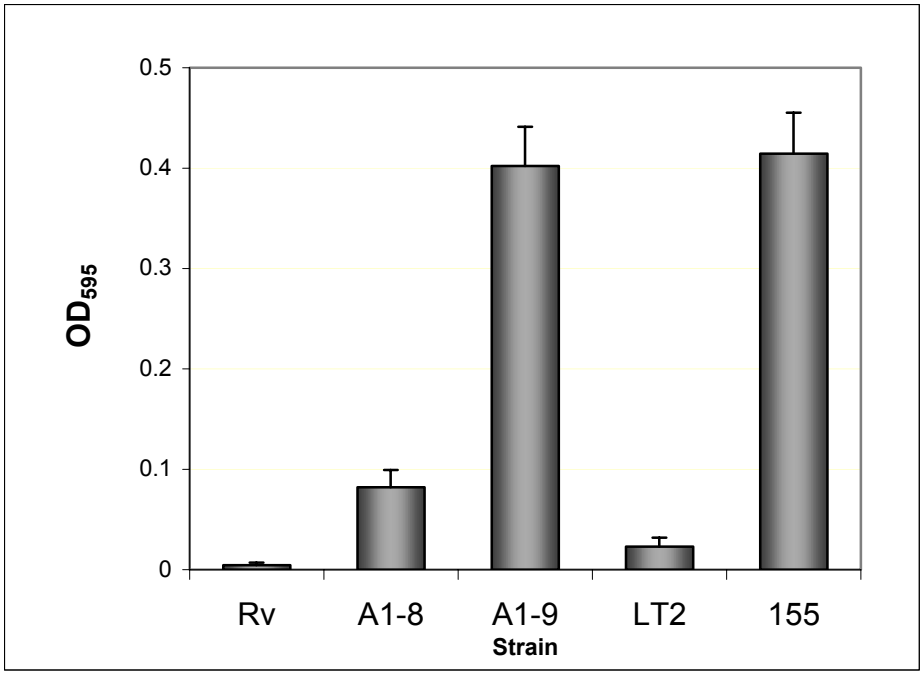

Figure 20. Assay for early adherence of the wt strains Rv and LT2 and their derivatives.

The mutants *ddhC::Tn5* (A1-8) and *waaG::Tn5* (A1-9) were shown to exhibit higher levels of adherence to PVC surfaces compared to the wt Rv, which was similarly shown in the Δ*waaG*::*kan* strain YA 155, when compared to the wt LT2 and the *waaG* complemented strain YA156. Cells were grown in M63 media supplemented with 0.2% glucose and 0.5 % CAA in microtiter wells for 8 h. The amount of attached cells was further quantified by staining the biofilms with crystal violet, and determining the absorbance at 595nm of the solubilized dye.

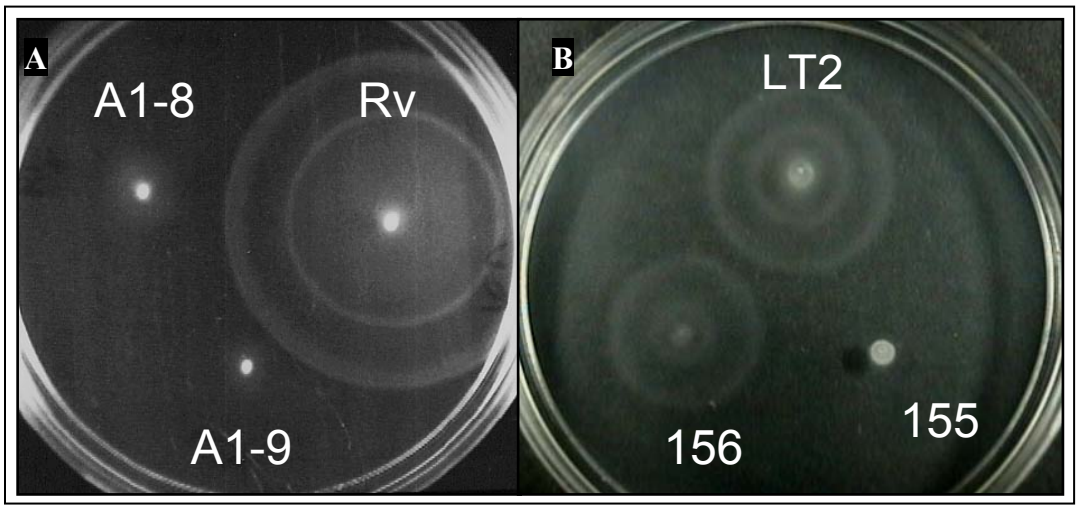

Figure 21. Motility assay for the wt Rv and LT2 and their derivatives.
The wt Rv displayed motility on the swim plates while in the mutants *ddhC::Tn5* (A1-8) and *waaG::Tn5* (A1-9), the motility is absent (A). The lack of motility was also shown in the *waaG* knock-out mutant YA 155, while, in comparison, it is present in the wt LT2 and in YA156, the complemented strain of YA155 (B). The same amount of O/N cultures with equal OD_{600} values from each strain were inoculated onto swim agar plates placed under incubation for 8h (A) or 5h (B) at 30˚C.

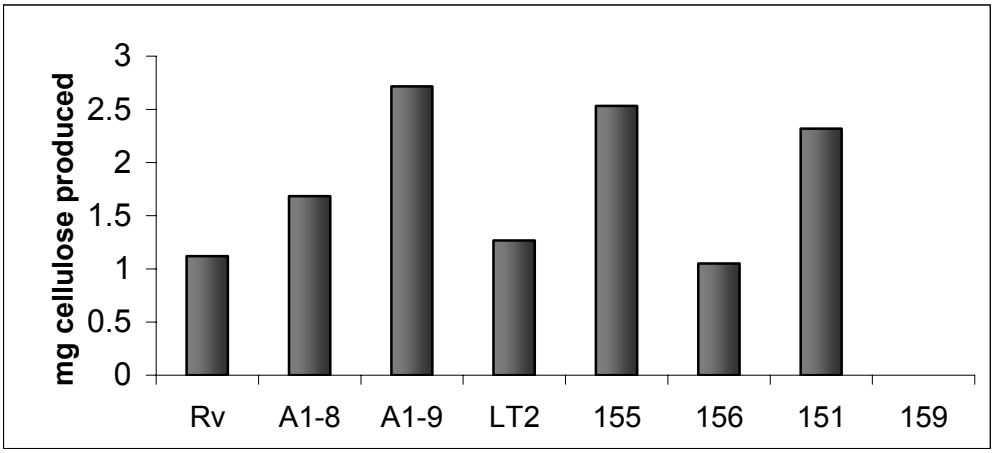

Figure 22. Cellulose production by the wt Rv and LT2 with their derivatives. Higher amounts of cellulose was produced by both *ddhC::Tn5* (A1-8) and *waaG::Tn5* (A1-9) mutants compared to the wt Rv. Higher cellulose production was also obtained from the *waaG* deletion mutant YA 155 compared to the wt LT2 and *waaG* complemented strain YA 156. Cellulose was isolated from 200 mg of lyophilized cell mass obtained from colonies of each strain streaked with a high density inoculum on LB plates, followed by 4-day incubation at 28˚C. Control strain Δ*csgA::kan* (YA151) and Δ*bcsA::kan* (YA159) were included as positive and negative controls, respectively.

Figure 23. Production of nodular structures and adhesive-like matrix in cellulose overproducing strains YA151 and YA155 as shown by SEM.

Figures A and B show the large nodular structures (arrows) in Δ*bcsA::kan* (curli ¯) strain YA151 (left) and Δ*waaG::kan* YA155 (right), while the adhesive-like material was seen in the matrix of both strains in (C) and (D). Cells were prepared from colonies as described in Figure 13. Bars 1μm.

YA151 YA155

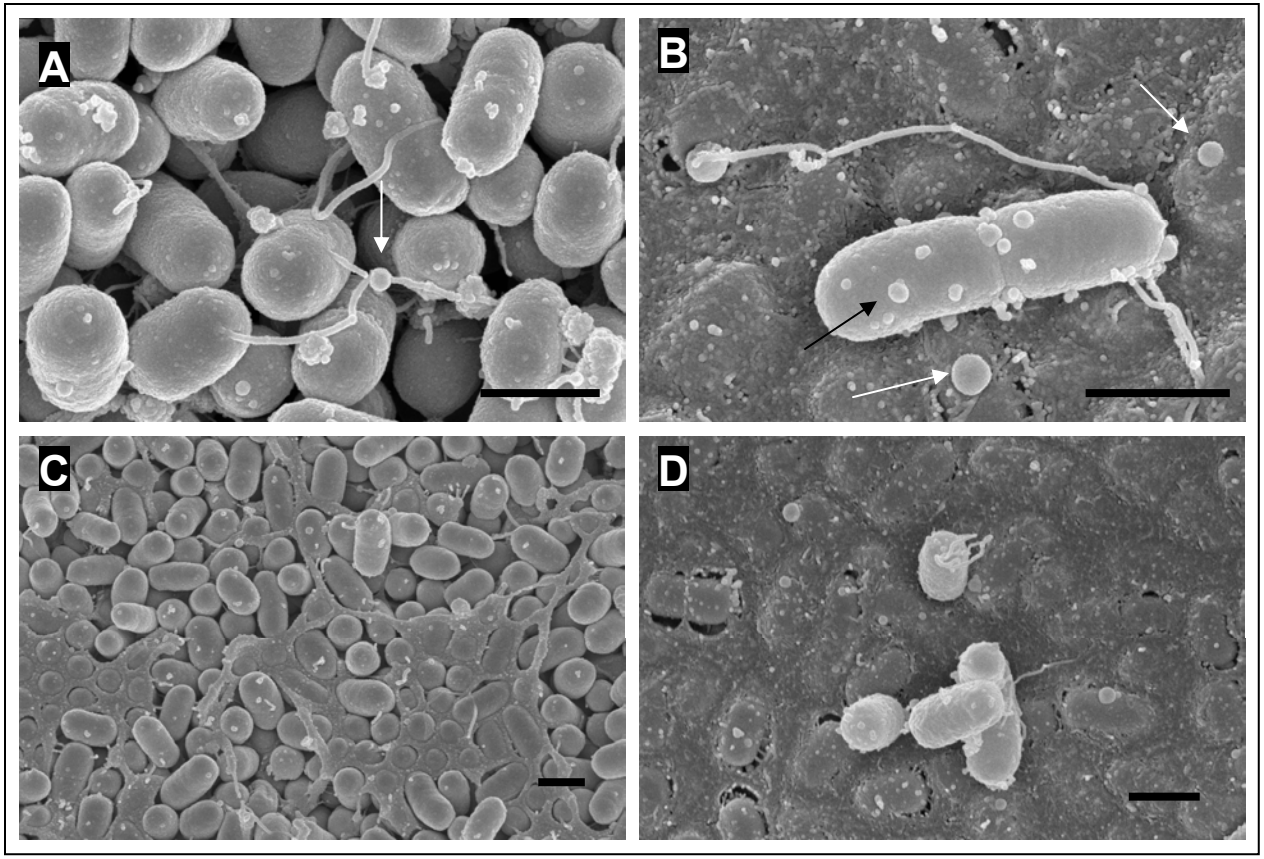

Figure 24. Resulting model of the effect of LPS truncation by *waaG* and *ddhC* mutations on rugose matrix formation.

Known regulatory mechanisms are shown in solid lines, hypothetical mechanisms are shown in dotted lines. Arrows show activation, oval arrows indicate repression. LPS truncation by *waaG* and *ddhC* mutations could directly activate the RcsC/B system, which may affect cellulose production in an unknown mechanism, or indirectly result in channelling the UDP-glucose precursor to cellulose, causing overproduction.

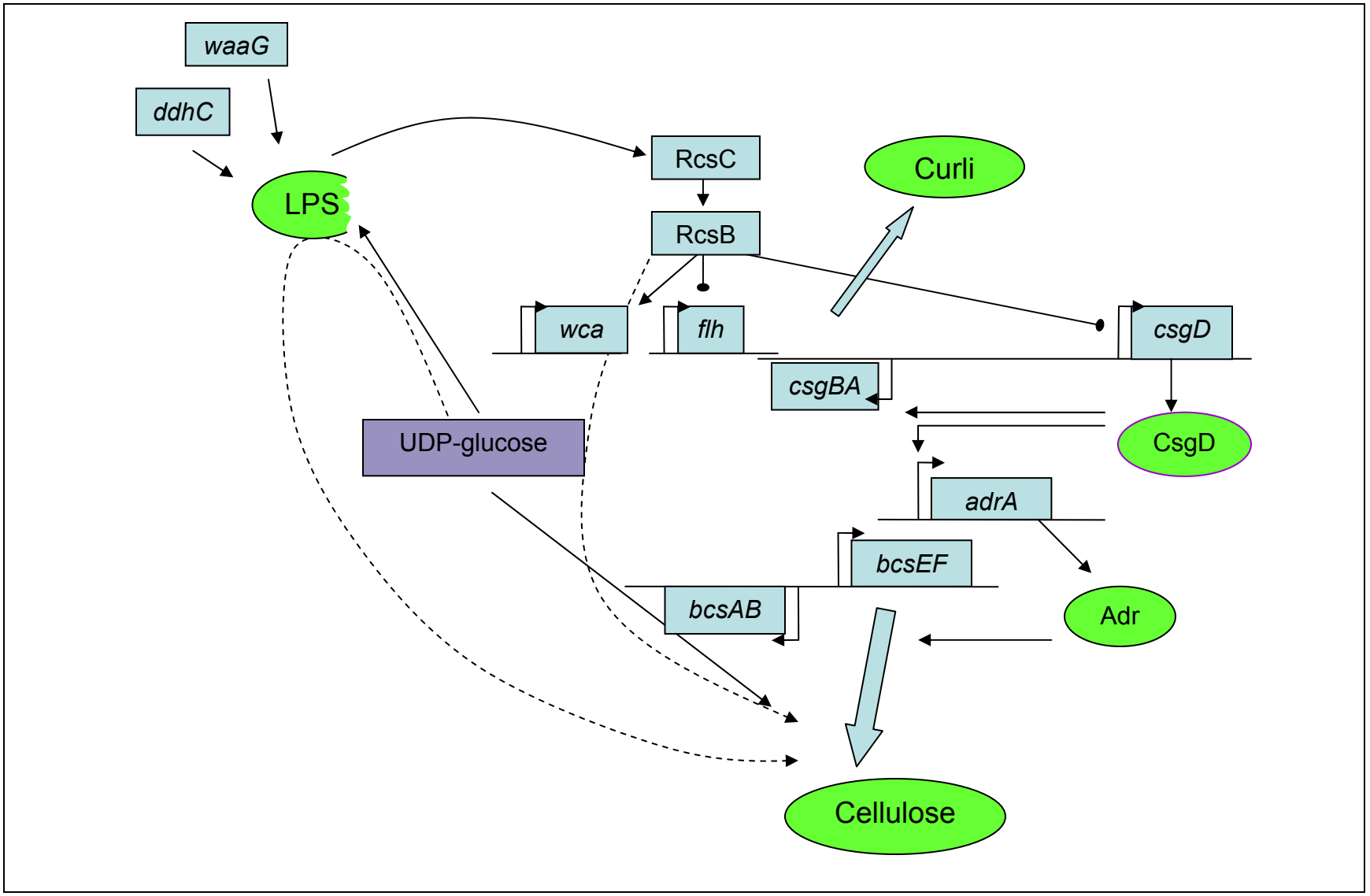
waaG
ddhC
LPS
RcsC
RcsB
Curli
wca
flh
csgD
csgBA
CsgD
UDP-glucose
adrA
bcsEF
bcsAB
Adr
Cellulose

CHAPTER 4 - Involvement of the RNA-Binding Protein Hfq in the Regulation of *csgDEF* and *csgBA* Operons for Rugose Expression in *Salmonella* Typhimurium

1. ABSTRACT

Rugose (rdar) colony morphology is a form of multicellular behavior exhibited by *Salmonella* Typhimurium through formation of cell aggregates under low temperature, low osmolarity, and at stationary growth phase. A number of transcriptional regulators, including RpoS, OmpR, CpxR, RcsB, IHF, and HNS, have been described for the expression of CsgD, the central regulator for synthesis of both curli and cellulose, the two components of matrix in rugose colonies. CsgD is required for transcription of the *csgBA* operon and of *adrA*, which code for curli and for AdrA protein required for post-transcriptional processing in cellulose synthesis, respectively. Here we report the involvement of Hfq, an RNA binding protein known to aid regulation by sRNA, in regulating both *csgB* and *csgD* promoters. Transposon mutation in *hfq* was found to eliminate the rugose phenotype and matrix production, biofilm and pellicle formation, and cell clumping. Interestingly, the results from promoter-*lacZ* fusion indicate that Hfq regulates both promoters at the transcriptional level. The reduction of curli was further confirmed by Western blotting of CsgA protein as well as direct observation by TEM after negative staining. It was therefore surmised that the effect of Hfq was a result of reduced level of RpoS, which required Hfq and DsrA for efficient translation at temperatures lower than 30˚C. However, when expression of the *csgB* promoter was uncoupled from RpoS in an *rpoS hns* double mutant, additional *hfq* mutation in this

double mutant background also diminished the *csgB* promoter activity. The lack of changes in the rugose phenotype and P*csgB* promoter activity in a *dsrA* mutant, compared to the wt, further suggests that Hfq may regulate both P*csgB* and P*csgA* independent of its role in promoting translation of RpoS. The finding of involvement of Hfq strongly suggests regulation at the post-transcriptional level. The possible mechanism of regulation of *csgB* and *csgD* promoters is further discussed.

2. INTRODUCTION

In environments external to the host, pathogenic bacteria encounter multiple stresses such as starvation, UV exposure, and many chemical insults. *Salmonella* has evolved ways to overcome these stresses, by upregulating specific stress-response genes (70). General responses, in part, include either entering the viable but non-culturable (VBNC) dormant state, or forming multicellular communities, where nutrient acquisition and protection are more feasible than in the single cell state. In the aquatic environment, multicellularity is manifested as biofilms, wherein *Salmonella* attach to surfaces and form structured communities enveloped in an exopolysaccharide matrix (48). Multicellular behavior renders survival advantages on solid media when cells aggregate in the form of rugose (wrinkled) colonies (7).

Conceivably, protection in the rugose or rdar [red, dry and rough, equal its properties on Congo Red (CR) agar] state is attributed to the production of a very strong matrix responsible for creating cell aggregates. The matrix contains at least two chemically inert polymers: curli proteins and cellulose molecules (202, 221, 279). A third component (a largely uncharacterized non-cellulose, non-colanic acid, polysaccharide) has also been reported (262). Curli and cellulose have also been shown to be necessary

for *Salmonella* aggregation in liquid media including biofilms, cell clumping, and pellicles. While curli constitute the bulk of the matrix, cellulose contributes to its flexibility and strength (201, 279). Expression of the rugose phenotype provides survival advantages to *Salmonella* against oxidative stress and low pH in the environment (7). The cellulose component protects cells from chlorine, although it appears to have no significant effect on virulence (221). Curli proteins have been described as promoting bacterial attachment to both abiotic (10, 185) and eukaryotic surfaces (174, 175); and playing a role in *E. coli* sepsis (20); as well as internalization by eukaryotic cells (88).

CsgD, a protein of the Lux-R superfamily, regulates the expression of two of the components of the extracellular matrix. It is required for the transcription of the *csgBA* and *csgDEFG* operons, which code for curli synthesis, and of *adrA*. The gene product of *adrA*, a GGDEF protein AdrA, is required for cellular production of cellulose, known to be encoded by constitutively-transcribed *bcs* operons (221, 279).

The expression of CsgD in *S.* Typhimurium is tightly regulated (Figure 1). It is expressed optimally only at low temperature, low osmolarity, and microaerophilic conditions, although at low iron conditions it is also expressed at 37°C. These regulations take place predominantly in the 521 bp intergenic region (IR) (81) between the two divergently transcribed *csgDEFG* and *csgBA* operons, in which binding has been described for several regulatory proteins. Sigma factor σ^S (encoded by *rpoS*) is required for the expression of CsgD, although the promoter sequence of *csgD* is suggestive of those recognized by sigma factor σ^{70} (202). OmpR responds to osmolarity by modulating its binding at 6 different sites in the IR. While binding at one of the sites (D1), centered at -50.5 from the transcriptional start of *csgD*, is required to activate the *csgD* promoter,

binding at the other sites (D2-D6) represses the activity, possibly under aerobic conditions (82). At high salt concentration, CpxR represses *csgD* transcription by binding to several different sites to either prevent binding of RNA polymerase (when binding at sites 1 and 2 in the region between –35 and the transcriptional start site), or to modulate *csgD* expression (when binding to sites overlapping with the activating site of OmpR) (82, 118). Several binding sites upstream of the transcriptional start site of *csgBA* operon have also been identified (118). In the presence of high salt concentrations, transcription, translation and phosphorylation of CpxR are increased (118).

A number of HNS binding sites have also been demonstrated, but depending on the host background, HNS could act as either an activator or a repressor (9, 82). HNS represses *csgD* expression under high sucrose conditions in *E. coli* (118). In the absence of HNS, the promoter activity is no longer dependent on σ^S, so in an *rpoS hns* double mutant, the transcription of *csgBA* operon continues, since it is directed by an RNA polymerase coupled with σ^{70} instead (9). IHF, another DNA binding protein, binds to one site in the IR overlapping the OmpR binding sites D3-D6 under microaerophilic conditions by activating the promoter for optimum activity and competing with the repressive OmpR sites, as well as introducing DNA bending. The effect of the binding of IHF to another binding site in the *csgD* ORF is still unknown (81). *csgD* promoter is also positively regulated by another regulator of the GGDEF family of proteins, MlrA, which requires sigma factor σ^S for its expression (33).

Binding of CsgD to the region overlapping the –35 box of the *csgBA* promoter positively regulates the transcription of the operon. The transcription is also dependent on σ^S. It has been shown that direct binding of Crl protein to σ^S increases binding specificity

of this sigma factor to the *csgB* promoter region, thus stimulating transcription by $E\sigma^S$. The accumulation of Crl is concomitant with that of σ^S: Crl is expressed more at stationary phase, and the stability of Crl is increased at 30˚C compared to 37˚C (24) (Figure 1).

The alternative sigma factor σ^S is involved in the regulation of both *csgD* and *csgB* operons. It is encoded by *rpoS*, which is expressed optimally during the stationary phase of growth and during osmotic stress. The expression of RpoS is regulated at both transcriptional and post-transcriptional levels. In *E. coli*, at low temperature, the translation *rpoS* transcript is promoted by the binding of a stable, small, 87 nt untranslated RNA (also called small RNA or sRNA) DsrA to the leader sequence of *rpoS* mRNA, thus releasing the ribosome binding site, which is normally occluded by the mRNA leader sequence, and increasing its stability (129, 143, 219). A similar mechanism of regulation is also employed by DsrA in *hns* translational regulation, however DsrA binds to both regions near the start and the stop codons of *hns* mRNA, thus preventing its translation and decreasing its stability (128). The consequence of DsrA negative regulation on HNS is to increase transcription of some HNS-repressed genes such as *rcsA*, which codes for the regulator of capsule production. Therefore, DsrA acts also as an antisilencer, although to observe this effect of HNS, a high level of DsrA is required (143). These functions of DsrA require the involvement of Hfq proteins, which enhance the stability and the activity of DsrA (128, 220).

Hfq (or HF-I) is an RNA binding protein that was first identified for its role in the replication of bacteriophage Qβ in *E. coli* (119). Cells devoid of Hfq are pleiotropic (246), partially because of the function of Hfq to promote efficient translation of RpoS.

However, Hfq also regulates other genes outside of the *rpoS* regulon (167), possibly because of its newly recognized role as an RNA chaperone in regulation by a number of sRNA (90, 228).

While attempting to identify other factors involved in the regulation of the rugose phenotype by random mutagenesis in this study, Hfq was shown to be also involved in the transcriptional regulation of both *csgD* and *csgB* promoters, and the effect on *csgB* promoter was observed both in the wt and in *rpoS hns* background. The possible mechanism of Hfq regulation, the involvement of DsrA, and the implication of the results of this study are further discussed.

3. MATERIALS AND METHODS

3.1 Strains and oligonucleotides

Wild type and derivatives of *S .enterica* serovar Typhimurium DT104 Rv, *S. enterica* serovar Typhimurium LT2, and mouse-virulent *S. enterica* serovar Typhimurium 14028 (henceforth referred to as Rv, LT2, and 14028, respectively) were used in this study (Table 6) (see Appendix C for a more complete list of strains). In some experiments, a spontaneous mutant strain of Rv lacking a matrix, Stv, was used as a negative control. *E. coli* TOP10 (Invitrogen) was used as a host during plasmid construction. All strains were stored as frozen stocks at -80˚C after an addition of sterile 50% glycerol (to a final concentration of 25%) to overnight cultures grown in LB broth. Alternatively, overnight colonies grown on LB agar were scraped and resuspended in a 1:1 mixture of double-strength LB: 50% glycerol. Frozen stock cultures were streaked on an LB plate and grown overnight at 37˚C before single colonies were used as an inoculum for any experiments. All plasmds used in this study are listed in Table7.

Transductional crosses using phage P22 HT 105/1 *int201* (213) were performed for strain constructions as described by Maloy (147). To obtain phage-free isolates, transductants were purified by streaking on green plates (39), and phage sensitivity was tested by cross-streaking with the clear-plaque mutant P22 H5 (a kind gift from T. Elliott). All primers used for PCR reactions were obtained from IDT DNA (Coralville, IA) (Table 8).

3.2. Media and growth conditions

All strains were grown in LB Miller base broth and agar (DIFCO), which contains only 0.5g NaCl/l (hereafter referred to as LB). Antibiotics were used at the following final concentrations (in μg/ml): sodium ampicillin, 100, chloramphenicol, 25, tetracycline, 25 and kanamycin sulfate, 50. Arabinose was used at a final concentration of 1mM, while X-gal was used at a final concentration of 60 μg/ml. The *Salmonella* strains were streaked for isolation of individual colonies on LB agar, or spread plated with 100μL of 10^{-6} to 10^{-8} dilutions of overnight cultures of each strain onto LB agar plates incubated at 22-25°C for 4 days to induce rugose colony formation. Inoculations of 5 ml of LB broth in 16x125 mm glass culture tubes capped with metal caps were intended to induce pellicle production, wherein the tubes were incubated without shaking at 22-25°C for four days. A thinner pellicle was also observed as cell aggregates floating on the surface of the culture, when cells were grown with very slow shaking under microaerophilic conditions (see the Miller assay below). To generate growth curves, strains were grown in either aerobic or microaerophilic conditions at 28˚C (see the Miller assay below), or at 37˚C under aerobic conditions, and cell densities at particular time points were determined by measuring turbidity at OD_{600}. Two independent cultures measured at the same time were used to generate the curves. Biofilms were observed as

rings attached to the walls of flasks or tubes. To determine the Congo red- and calcofluor-binding properties of the colonies, either Congo red (40μg/ml) and Coomassie brilliant blue (20μg/ml) or Calcofluor (40 μg/ml) (Fluorescent brightener 28, Sigma) was added to LB to make CR and CF plates, respectively (173, 202). The fluorescence of the colonies, as a measure of calcofluor binding property, was visually evaluated by comparing with the fluorescence obtained with the wt Rv or LT2 (matrix producing strains), or Stv (a non-matrix producing strain) using a handheld UV light.

3.3. Assay for catalase production

Cells from colonies grown on LB agar were transferred onto glass microscope slides and a drop of 30% H_2O_2 was placed on the cells. Immediate formation of bubbles indicated production of catalase.

3.4. Random mutagenesis and analysis of Tn insertion site

Tn5 in the transposon-tranposase (transposome) complex (EZ::TN Kan-2, EPICENTRE, Madison, WI) was electroporated into competent cells of wt Rv. Selection of transformants was performed on LB-Kan plates (89), and only those that exhibited impaired rugosity compared to the wt Rv after observation at 25°C for 4 to 7 days were selected. Stable changes in colony phenotype were assessed by three passages on LB plates at 25°C, each for 4 days.

The site of transposon insertion in A1-10 was determined by digesting the isolated genomic DNA with EcoRI, subsequently cloning the fragments (approximately 1-2 kb) into pUC19 (New England Biolabs) and then selecting for kanamycin-resistant clones after transformation into *E. coli* DH5-α. The recombinant plasmids were isolated from 10

clones and the presence of an insert from each clone was confirmed by restriction analysis. The site of transposon insertion from 5 clones was determined by sequencing at the Center for Biosystems Research (CBR) at the University of Maryland, College Park using the transposon-specific sequencing primer (provided in the EZ::TN kit, Epicentre, Madison, WI).

3.5. BLAST analysis

BLAST nucleotide analysis was performed in order to find homologous sequences in the *Salmonella* LT2 database (http://www.ncbi.nlm.nih.gov/BLAST/).

3.6. Deletion of *hfq*, *dsrA*, and *csgA*

Deletion of *hfq* in *S.* Typhimurium LT2 was performed using the direct knockout procedure described by Datsenko and Wanner (55) (Appendix A.2). First, PCR fragments were amplified using primer pairs p*hfq*D11/12, p*dsrA*D11/12 and pKD4 plasmid as the template to create PCR fragments containing the Kan^R gene flanked by FRT sequences plus 50 bp from both sides of the region to be deleted. After digestion with DpnI to remove residual template plasmid, the PCR fragments were separately transformed into the competent LT2 strain carrying the Red helper plasmid pKD46 (the λ Red system under P*ara* Ts ori,). Transformants were selected on LB Kan Amp plates in the presence of arabinose at 30°C. The transformants were passed several times on LB at 37°C to eliminate pKD46, after which Kan^R Amp^S colonies were selected by replica plating. This procedure deleted either the *hfq* or *dsrA* gene, replacing them with the Kan^R gene yielding strains YA153 and YA157, respectively. The gene deletion and the Kan^R insertion were confirmed by comparing the size of the PCR fragment in the wt and in the

mutants using the following PCR primer pairs: p*hfq*11/12 and p*dsrA*12/13, corresponding to the sequences just outside of the deleted region; pKanKD1/2, corresponding to the sequences on the Kan^R gene; and pKanKD3/p*hfq*11 and pKanKD3/p*dsrA*11, which amplify the junction region between *hfq* or *dsrA* and the Kan^R gene, respectively. This deletion procedure was not performed on Rv because of the Amp^R phenotype of this strain.

The Δ*hfq::Kan* and Δ*dsrA::Kan* deletion/insertion regions were separately transduced from LT2 into 14028 background by P22, using Kan^R as a selection marker, to create strains YA1153 and YA1157, respectively. The Kan^R gene in these strains was further eliminated by transforming them with FLP recombinase plasmid pCP20. FLP recombinase acted on the FRT sites flanking the Kan^R gene, resulting in the loss of the Kan^R and leaving a markerless Δ*hfq* (YA170) or Δ*dsrA* (YA171). The deletions were further confirmed by size comparison of PCR fragments amplified by p*hfq*11/12 or p*dsrA*12/13, followed by sequencing of the PCR fragments at the Center for Biosystems Research (CBR) at the University of Maryland, College Park using p*hfq*11 and p*dsrA*12 primers for *hfq* and *dsrA*, respectively.

3.7. Complementation

For gene complementation, *hfq* and *dsrA* genes were amplified from the wt strain 14028 using gene specific primer pairs p*hfq*11/12 and p*dsrA*11/12. The particular PCR fragment was cloned into pCR-4 (TOPO cloning, Invitrogen) to create pYA27 and pYA30 (Table7). Either the BamHI/HindIII fragment from pYA27, or the SmaI/KpnI fragment of pYA30 was separately subcloned into the corresponding sites in the low copy number plasmid pWSK29 (Amp^R) (33), resulting in pYA33 and pYA31 containing

the *hfq* and *dsrA* inserts, respectively. For complementation with pACYC184 (Tet^R Cm^R), the inserts from either pYA27 or pYA30 was isolated by digestion with EcoRI, whose sites flank the inserts in pCR4 plasmid, and are absent in either insert. The fragments were separately subcloned into EcoRI site of pACYC184 (thus disrupting the Cm^R gene, leaving Tet^R marker) to create pYA34 and pYA35 for *hfq* and *dsrA*, respectively. The plasmids were transformed into strains carrying either the *hfq* or *dsrA* mutation to complement the corresponding mutation.

3.8. Construction of the *hns rpoS* double mutant

The *hns::kan* mutation from TE7505 (*S.* Typhimurium LT2A background) was transduced into 14028 to create strain YA144. Although TE7505 showed mucoidy only at 25°C, all *hns* mutants in the 14028 background exhibited mucoidy at both 37 and 25°C. The *rpoS* mutation from strain TE5395 (*rpoS*:pRRT1, Amp^R) was transduced into YA144 to create YA147 (*hns rpoS* double mutant). The *hns::Kan* and *rpoS*:pRRT1 were transduced separately or in combination into either Δ*hfq* or Δ*dsrA* strains to create double and triple mutants (Table 6).

3.9. Construction of the *csgB* and *csgD*-promoter fusion plasmid

Primer pairs p*csgD*Z1/2 were used to amplify the intergenic region between the two divergently transcribed *csgDEFG* and *csgBA* operons, including parts of the *csgB* and *csgD* open reading frames (ORF) (see Appendix D for DNA sequences), in a PCR reaction using Pfx polymerase (Invitrogen). The PCR products were cloned into pCR-4 (pTOPO kit, Invitrogen). The plasmids were then digested with HindIII and SmaI, and the PCR fragment was subcloned into corresponding restriction sites in the operon fusion

plasmid pQF50Cm to create pYA26, in which the *csgD* Promoter (P*csgD*), including 210bp of the *csgD* ORF*,* was fused with the promoterless *lacZ* gene. The procedure was repeated using primers p*agfBZ*1/2, which amplified the same intergenic region, except that the restriction sites in the primers were switched, i.e., once cloned into pQF50Cm, the orientation of the insert was reversed and the promoter of *csgBA* operon, including 185 bp of *csgB*, was fused to the promoterless *lacZ*, to create pYA25. The presence and the orientation of the inserts were verified by digestion of the plasmids with EcoRV, which cuts the insert once at nt 127 of the *csgD* ORF. The plasmids were then separately transformed by electroporation into strains with different backgrounds.

For positive controls, the *lac* promoter was amplified from pCR-4 (Invitrogen) using primers p*lac*11 and p*lac*12 (Table 8) with SmaI and HindIII restriction sites as tails at the 5' and 3' ends of the fragment, respectively. The DNA fragment was ligated at the corresponding sites in pQF50Cm, resulting in pYA38 plasmid. The presence of an insert was verified with restriction digestion.

3.10. Miller assay

For preliminary analysis, wt 14028 carrying pYA26 was grown in 16x 150 mm glass tubes with varying amounts of LB broth (5, 10, 20, 25 ml) and in 125 ml flasks with either 25ml or 75 ml of LB with shaking at 150 rpm at 28˚C for 48h. Similar conditions, except for a faster shaking at 210 rpm, were used to grow wt strains carrying pYA25. In final experiments, cells were grown for up to 5 days (approximately 125 hr) at 28°C under optimum conditions for promoter activities: e.g.- aerobic conditions (15 ml LB media in 125ml flasks shaken at 210 rpm) for assaying P*csgB* activity, or microaerophilic conditions (75 ml of LB in 125ml flasks shaken at 150rpm) for assaying of P*csgD*

activity (81). Antibiotics were added into the media as needed. At particular time points, the biofilms from the walls of the flasks were scraped, and the flasks were shaken vigorously by hand to mix the planktonic cells, cell clumps, pellicles and biofilms in the flasks. Immediately, 750uL of the mixed culture was transferred into a microcentrifuge tube using a pipettor with wide pipet tips. The samples were then homogenized by vortexing, and subsequently with 10-15 second sonication bursts (Vibra cell sonicator, Sonics & Materials, Inc., Danbury, CT, set at 15 and minimum tune at 20-23). Only 5 sec sonication was applied to samples from strains that did not form any clumps or biofilms. At various times, either the broth culture only or the pellicle or biofilms, stuck to the walls of tubes or flasks, were used to assay activity. The activity of β-galactosidase was assayed on the sonicated samples following the Miller assay procedure described earlier(156). The activity of β-galactosidase, as a measure of promoter activity, was calculated against cell density (OD_{600}), where Miller units were obtained. With some strains, clumps, pellicles and/or biofilms precluded the use of density measurement, so the activity was calculated against mg protein where specific β-galactosidase activity was determined (see Appendix E). The amount of protein used in the assay was measured using the Bradford assay (Sigma) and quantitated using a standard curve with known amount of bovine serum albumin (BSA) (Sigma). The overall pattern and fold induction in all of the strains was very similar between those data using either Miller units or β-galactosidase specific activity (see Appendix E). Data presented was an average of two separate cultures for each strain, each in triplicate, and assayed simultaneously. Experiments were repeated at least twice. Although the absolute values of Miller units or specific β-galactosidase activity varied between assays, possibly because of some

variations in the BSA standard in the Bradford assay performed on different days, the same patterns of induction or repression of mutants compared to the wt were observed. Positive and negative controls [strains carrying the pQF50Cm vector with P*lac* insert (pYA38), or carrying the pQF50Cm vector only, respectively] were included in the assays.

3.11. Electron microscopy

To observe the presence of curli fimbriae by negative staining, cells from four-day old colonies grown on LB plates at 25°C were collected and resuspended in 750 μL of dH_2O. A 3μL sample was spotted onto formvar-carbon coated grids, fixed with 2% glutaraldehyde in PBS Buffer pH 7.4, rinsed with dH_2O and stained with 1% uranyl acetate. Samples were examined using Zeiss EM10 CA (Leo Electron Microscope, Thornwood, NY).

For scanning electron microscopy, 4-day old colonies grown on LB agar at 25°C were fixed with 2% glutaraldehyde in PBS buffer pH 7.4 at RT for 1h and at 4°C overnight. The colonies, including an approximately 1mm thickness of underlying agar was cut out and transferred to a well in a six-well tissue culture plate (Falcon). The samples were then postfixed with 1% osmium tetroxide, and subsequently with 2% aqueous uranyl acetate followed by dehydration with 75%, 90%, and 100% ethanol. Each sample was then critical point-dried, and coated with gold-palladium alloy. Samples were examined with a Hitachi S-4700 SEM (Hitachi Scientific Inst., Gaithersburg, MD).

3.12. Isolation of curli protein

Curli were isolated from four-day old colonies grown at 25°C on LB agar by first resuspending the colonies by vigorous vortexing in 10 mM Tris Buffer pH 6.8 in the presence of sterile glass beads (2.0 mm diameter). One milliliter of suspension (OD_{600} adjusted to 3.0) (202) was centrifuged for 5 min at 16,000 rpm, and the cell pellet was resuspended in 100 μL SDS Sample Buffer (62.5 mM TrisCl pH 6.8, 10% glycerol, 2% SDS) and was boiled for 10 min. The cell lysate was centrifuged as before, after which the pellet was washed once with sterile water, and subsequently dissolved in 100 μL 97% formic acid (Sigma), frozen, and lyophilized as formic-acid resistant protein preparation (46, 202).

3.13. SDS-PAGE and Western blotting

The lyophilized formic acid-resistant protein samples were resuspended in 100 μL of SDS sample buffer and sonicated for 5.0 sec before loading in a 16% polyacrylamide gel. Prestained Kaleidoscope standard proteins (Bio-Rad, Hercules, CA) were used as molecular weight markers. Loading was equalized by visual assessment of the overall profile of formic-acid resistant proteins on the Coomassie-blue stained gel. Separated proteins were transferred onto polyvinylidene fluoride (PVDF) Immobilon-P membranes (Millipore, Bedford, MA). The membranes were then incubated overnight in 3% skim milk (wt/vol) in TTBS buffer (TBS buffer containing 0.1% Tween 20) at room temperature, and probed with mouse monoclonal anti-SEF17 antibody (a kind gift from Dr. William Kay) diluted 1:1000 in TTBS, and then by horse-radish peroxidase-conjugated goat anti-mouse antibodies. The antibody-bound proteins were detected as

bands using ECL Detection reagents (Amersham Biosciences, Piscataway, NJ) and subsequent exposure to Hyperfilm (Amersham Biosciences).

4. RESULTS

4.1. The effect of mutation in *hfq* on the multicellular behavior of *S.* Typhimurium

The transposon mutant A1-10, which exhibited smooth colony morphology after 4 days of growth on LB agar at 25°C, was selected after the transposon mutagenesis procedure. This mutant had a minimum binding to Congo red, with colonies appearing white with a pinkish ring in the center (Figure 25A) and no aggregation of cells. This mutant also failed to form pellicles in static LB broth under the same growth conditions (Figure 25). When the cells were grown in liquid media with shaking, no biofilms were formed. Therefore, the multicellular behavior of A1-10 was abolished compared to that of the wild type Rv.

Congo red binding is an indirect measure of curli and cellulose production, since wt cells appear dark red, dry and rough (rdar). Those that lack curli appear as bright pink dry and rough colonies (pdar morphotype), while those that fail to produce cellulose appear brown dry and rough (bdar morphotype) (201). When grown on LB agar supplemented with calcofluor, strain A1-10 also showed minimum calcofluor binding (Figure 25C), indicating that the cells may have reduced production of polysaccharides with (1→3) and (1→4)-β-D-glucopyranosyl units, including cellulose, compared to the wt strain.

4.2. Analysis of Tn insertion

Sequencing of the region flanking the transposon insertion and the subsequent BLAST analysis showed that the transposon had inserted into nt 265 of the 309 bp *hfq* gene, with 10 bp (nt 255-264) repeated sequences before and after the transposon sequence. Hfq is an RNA-binding protein that was first discovered to aid in the replication of bacteriophage Qβ and has been previously shown to stabilize mRNA and aid recognition of target mRNA by sRNA (90). Similar to a previous description of an *hfq* mutant (246), A1-10 had somewhat reduced growth and yield compared to the wt Rv, as reflected by the smaller colony size of this mutant (Figure 25A). In addition, the A1-10 mutant also failed to produce catalase, as judged by its inability to form bubbles after exposure to 30% hydrogen peroxide (data not shown).

4.3. Electron microscopy (Analysis of bacterial morphology)

To directly examine cell surface changes brought about by the mutation, scanning electron microscopy (SEM) was performed. The results showed that the hfq-mutant A1-10 failed to produce the extracellular matrix seen in the colonies of the wt strain. The cells in the rugose colonies of wild type strain Rv are held together by an extensive fibrous matrix that are so thick, that compared to those cells not covered by the matrix they appeared to be approximately double the size (Figure 26). The cells are interconnected by short fibrillar materials that span the perimeter of the cells. In contrast, the thick matrix was absent in A1-10, and only some longer fibrillar materials were seen between the cells. Therefore, the changes in morphology, Congo red and calcofluor binding of A1-10 compared to the wt may have resulted from the apparent, impaired production of the extracellular matrix.

It was further observed that the cells, after negative staining and viewed with transmission electron microscopy, i.e.- not exposed to the dehydration process, appeared as blobs, and individual cell shapes could not be discerned, likely because of the presence of the thick matrix surrounding them (Figure 27) (262). This material was absent in the A1-10 cells, confirming results observed by SEM. More importantly, the curli fimbriae produced by the wild type seen as fibrous, tangled, appendages surrounding the cells (46), were lacking in A1-10 cells (Figure 27). There were some other appendages produced by A1-10, however, they did not resemble those produced in the wt. The mutant appendages were shorter, and more straight, which suggested that they may represent other types of fimbriae, or possibly shorter curli.

4.4. Similarity of the *hfq* knock-out mutant phenotypes to the transposon mutant

To confirm the role of *hfq* on the expression of the rugose phenotype, the *hfq* gene was further deleted using the one-step knockout procedure (55). We chose to perform the deletion in *S.* Typhimurium LT2 instead of using the wt strain *S.* Typhimurium DT104 Rv, characteristically resistant to multiple antibiotics, which prevented the use of common antibiotics for selection during transduction and transformation. The deleted region in the *hfq* gene was replaced with the Kan^R gene, which was transcribed in the same direction as *hfq*, to yield the Δ*hfq*::Kan^R strain (YA153). In this procedure, a ribosomal binding site is inserted at the end of the deleted region preventing a polar effect on genes downstream from the deletion site. To avoid further complications in the LT2 strain, which has defects in *rpoS* turnover (233), the mutation Δ*hfq*::KanR was then transduced into a 14028 background to yield strain YA1153 using Kan^R as a marker.

The phenotypes of the *hfq* mutant YA1153 were similar to those seen in DT104 Rv and LT2 backgrounds (strain A1-10 and YA153, respectively) (data not shown). Similar phenotypes were also observed when the Kan^R was further deleted to yield strain YA170 (Figure 25C). When the *hfq* gene in strain YA1153 was further complemented in a low copy plasmid pACYC184, the rate of growth, pellicle production, and biofilm formation were elevated, although not to the same levels as those shown in the wt (Figure 25B and data not shown). The cells were able to bind Congo red, but produced brownish colonies instead of red as observed in the parent strain 14028 (Figure 25C). Cells that are incapable of producing cellulose have been shown to produce the brown (bdar) morphotype (279), thus it was possible that the complemented strain still had impaired cellulose production. In fact, growth of the complemented strain in LB agar supplemented with calcofluor showed that the complemented mutant did not bind calcofluor to the same extent as the wild type cells (Figure 25D). These results suggested that the complementation of *hfq* only partially restored the production of polysaccharide in the *hfq* mutant, probably because of the instability of *hfq* mRNA expressed from a plasmid compared to that from the chromosome.

The growth curves of the wt, the Δ*hfq* mutant (YA 170) and pYA34-complemented strains (YA240) were shown in Figure 28. As expected, the *hfq* mutant grew more slowly than the wt at 37°C (Figure 28A) (doubling time of 162 min in A1-10 compared to 80 min in wt) and at 28°C (doubling time 185 min compared to 90 min in wt) (Figure 28B), and reached a lower cell density at stationary phase. At 37°C, while the stationary phase was reached by the wt strain and YA240 at 6 and 7 h, respectively, the mutant required 12 h. At 28°C under aerobic conditions, the mutant reached stationary

phase at 13h, while the wt and YA240 required 7 and 8h, respectively. On the other hand, at 28˚C under microaerophilic conditions, the wt and complemented strain YA240 reached stationary phase at 48 h, while the mutant did so at approximately 123h (5 days) (Figure 28C).

4.5. The role of Hfq in regulating *csgB* and *csgD* promoters in wild type background

4.5.1. LacZ fusion with csgD and csgB promoters

Hfq has been the subject of research in recent years, because of its function in aiding sRNAs in recognition of their targets. For example, Hfq is required for binding of sRNAs DsrA, RprA, or OxyS to RpoS mRNA for efficient translation, with growth conditions determining which sRNA participates in the translation process. To gain further knowledge of how Hfq regulates rugose expression, promoter-*lacZ* fusion was utilized as a marker for gene expression at the transcriptional level. *hfq* mutation resulted in the loss of extracellular matrix composed of curli and cellulose, both of which are regulated by *csgD*. Therefore, the effect of *hfq* mutation on both the *csgD* and the *csgB* promoters, which are divergently transcribed from the two operons *csgDEFG* and *csgBA*, was further studied. The DNA fragment that was fused to *lacZ* included the entire intergenic region between the two promoters, the site where most of the transcriptional regulation of both *csgB* and *csgD* promoters occurs. The fragments also included 184 bp of *csgB* and 197 bp of the *csgD* coding regions (Figure 29 and Appendix D). Thus, this construct resembles the pUGE1 construct for *csgD-lacZ* operon fusion by Gerstel and Romling (83), which includes 82 bp of *csgB* and 201 bp of *csgD*.

4.5.2. The activities of PagfB in biofilms and pellicles are higher than those in the planktonic cells.

Higher activities of both promoter constructs were obtained at late logarithmic phase compared to early log phase, confirming previous findings by Romling *et al.* (202) (data not shown). Preliminary results also showed that the activity of both P*csgB* and P*csgD* was higher when cells were grown under microaerophilic conditions. However, because reasonable levels of activity could be obtained for P*csgB* under aerobic conditions without having to compensate for slow growth, we chose to perform the Miller assay for P*csgB* under aerobic conditions, while P*csgD* activity, which was expressed in high amount only under microaerophilic conditions, was assayed under these growth conditions.

When grown in liquid media at 28˚C, the wild type cells of *S.* Typhimurium 14028 displayed multicellular behavior including formation of biofilms, cell clumps, and pellicles. We noticed that much thicker biofilms, seen as a ring approximately 1 cm wide on the tube walls, were formed by the wt cells under microaerophilic conditions, when compared to biofilms formed under aerobic conditions, (only approximately 3 mm wide) (Figure 30A). The expression of P*csgB* and P*csgD* in the fusion plasmid in wt strain 14028 was examined in planktonic cells, in biofilm cells, and in the mixture containing each type. The results showed that P*csgB* transcription was approximately nine times higher in the cells obtained from the biofilms than that observed in planktonic cells (Figure 30B). These higher activities confirmed previous findings of a direct correlation between the *csgA* transcription and biofilm formation, reinforcing the belief that curli are involved in biofilm formation (185). The mixture, with only approximately 30% of the activity of that in the biofilm cells, was probably an underestimate of promoter activity

under these conditions. However, since the mixture represented the average expression in the cellular community in the culture, it was then used in subsequent experiments to represent P*csgB* or P*csgD* activities in strains expressing multicellular behavior. A slightly higher expression of P*csgD* was also obtained from biofilms as well as the pellicle, the latter of which was also formed in low amount under microaerophilic conditions as a thin layer of cell aggregate floating on the surface of the broth (Figure 30C). Therefore, the subsequent Miller assays were performed using an aliquot of the mixture of all cells (planktonic, biofilms and clumps). The aggregates were dispersed by sonication before the assay. Further analysis showed some variability (10-20%) in the absolute promoter activity among the different samples forming aggregates, due to the heterogeneous nature of populations assayed, usually marked by large error bars. However, similar trends between the wt and the mutant strains were constantly obtained from independent cultures.

*4.5.3. Activities of P*csgB *and P*csgD *are eliminated in the hfq mutant*

When assayed under optimal conditions for *csgB* promoter expression at 48h (83), the activity of the *csgB* promoter was completely abolished in the Δ*hfq* background (YA170) compared to that in the wt strain, having a β-galactosidase activity of 49 compared to 4,016 nmole ONP/min/mg prot in the wild type strain (Figure 31). Similar results were obtained when Δ*hfq*::Kan background was used (data not shown). The growth of the *hfq* mutant in media containing chloramphenicol, albeit slightly slower and with lower yield compared to the wt, would argue against the inability of this mutant to allow replication of the fusion plasmid since the cells expressed the Cm^R phenotype. In addition, the Δ*hfq* mutant (strain YA282) exhibited even higher β-galactosidase activity

than the wt (YA 281) from a control plasmid pYA38, where the *lacZ* promoter was inserted in the cloning site of the same fusion plasmid used for the assay, pQF52Cm (2384 compared to 874 nmole of ONP/min/mg prot in YA282 and YA281, respectively). Thus, this indicates that the difference in P*csgB* activity is most likely due to *hfq* mutation, instead of defects in growth or plasmid multiplication. Subsequent complementation of the *hfq* in plasmid pACYC184 (15 copies per cell) (pYA34) increased the activity to about 1.75 fold times that seen in the wt strain, confirming the role of *hfq* in positive regulation of the *csgB* promoter. When complementation was performed in YA170 using pYA33 [pWSK29 vector, with a lower copy number of 8 per cell (256)], the activity was more similar to that seen in the wt (data not shown). This complementation also strongly supported the premise that the mutation of *hfq* in strains YA1153 and YA17 was probably non-polar.

The activity of P*csgD* was assessed at stationary growth phase under microaerophilic conditions, the optimal conditions for expression of this promoter (83). The wt showed a specific activity of approximately 4,580 nmol of ONP/mg prot/min. Compared to the wt strain 14028, the activity of *csgD* promoter in Δ*hfq* at 96h showed a decrease of about 38% (1,700 nmol ONP/mg prot/min) (Figure 32A). When the *hfq* mutation was complemented in a low copy plasmid pACYC184, the activity was increased to 5,680 nmol ONP/ min/ mg prot, slightly higher than the wt strain, although the activity was more similar to that in the wt. Comparison between control strains carrying pYA38 plasmids in the wt and Δ*hfq* background (strain YA281 and YA282, respectively) showed that the activity in YA 282 was even higher than that in the wt strain 14028, indicating that these mutant cells were capable of replicating the plasmids.

The decrease in P*csgD* activity in Δ*hfq* compared to that in the wt strain at 96h (38%) (Figure 32B), was essentially similar to the observation made at 48h of growth (29% of the wt) (data not shown). Because of the slow growth of the *hfq* mutant, the assay was repeated at 123h of growth (day 5), the stationary phase where the cell density level was similar to that of the wt cells (see growth curve in Figure 28C). While the P*csgD* activity of wt and complemented strains, which had entered stationary phase at 48h, stayed constant, the activity in the *hfq* mutant showed a slight increase, however, it only reached approximately 41% of the activity observed in the wt at day 5 (data not shown). These observations suggest that under these conditions, *hfq* is also required for the normal activity of P*csgD*; findings, which were similar to the results shown for P*csgB*. However, the reduction in activity was not as great as that seen for P*csgB*. Since the transcription of P*csgBA* is dependent on CsgD, reduction in the activity of P*csgB* may have been a result of reduced transcription of *csgD*.

4.6. The role of Hfq in regulating *csgBA* promoter activity in the *rpoS hns* background

4.6.1. hfq *mutation reduced P*csgB *activity in* rpoS hns *background*

Post-transcriptional regulation of RpoS (σ^S) is one of the known functions of Hfq. Thus, it is possible that reduced amounts of σ^S in the cells in the absence of Hfq may have been responsible for the effect of *hfq* mutation on the activity of both P*csgD* and P*csgB*, which are both dependent on Eσ^S RNA polymerase. In addition, the lack of catalase production in the *hfq* mutant indicates a lack of expression of *katE*, which is part of the σ^S regulon. In order to test the hypothesis that Hfq regulates the promoter activities of *csgD* and *csgBA* operons through σ^S expression, the regulation of P*csgB* promoter

from *rpoS* dependence was further uncoupled by deleting both *hns* and *rpoS*, thus allowing wt expression of the promoter even in the absence of *rpoS* (9). This double mutant strain was smooth, but still bound Congo red (see below).

The double mutations *rpoS hns* in wt 14028 background impaired growth. However, when the activity of *csgB* promoter was assayed in the *hns rpoS* background (strain YA209) under aerobic conditions at 72h, the activity was not much affected. In fact, it was higher than the wt strain YA130, reaching approximately 1.5x (6654 nmol/min/mg prot) (Figure 33) that in the wt (Figure 31). Deletion of *hfq* in this double mutant background (strain YA207) reduced the activity of P*csgB* more than 5 times (1211 nmol/min/mg prot). A repeat of the assay at 5 days did not show much increase for either the wt or Δ*hfq* strains (7908 vs 1764 nmol/min/mg prot, respectively). Complementation of Δ*hfq* in pYA34 plasmid (strain YA245) increased the activity to almost twice as much as that seen in the *rpoS hns* mutant. The *rpoS hns* and Δ*hfq rpoS hns* carrying the control plasmids pYA38 (strains YA and YA285, respectively) showed similar levels of activity, although they were lower than that seen in strain YA147 (*rpoS hns*) carrying P*csgB-lacZ* plasmid pYA26 (Figure 33, compared with Figure 31). These data indicate that Hfq is required for the activity of the promoter even in the absence of σ^S, highlighting yet another possible function of Hfq in regulating promoter activity independent of σ^S.

*4.6.2. The role of Hfq in regulating P***csgD** *in* **rpoS hns** *background*

It has been proposed that the *csgD* promoter, similar to the *csgB* promoter, is recognized by both σ^S and σ^{70} (185, 202). Therefore, an attempt was made to compare the activity of P*csgD* in *rpoS hns* double mutants (YA147), as well as Δ*hfq rpoS hns* (YA183), and the *hfq* complemented strain in *rpoS hns* background (YA243). Under

microaerophilic conditions, the growth of these strains was very much impaired. However, a high activity of P*csgD*, even higher than that shown by the wt strain 14028, was shown by strain YA147 (compare Figure 34 and Figure 32). These results thus confirmed that the P*csgD* was expressed in the absence of RpoS, similar to that shown in P*csgB*, possibly by recognition of the promoters by both σ^{70} and σ^{S}, as proposed earlier (184). The attempt to compare the activity of P*csgD* in *rpoS hns* background and Δ*hfq rpoS hns* (YA183) was inconclusive because an additional *hfq* mutation to *rpoS hns* background diminished the growth of the cells so much that, at best, only rarely was some poor growth obtained with this triple mutant under microaerophilic conditions. In addition, the control strain YA285, which is strain YA 183 carrying the control plasmid pYA38, showed reduced activity in these poorly grown cells (data not shown).

4.7. The effect of deletion of *dsrA* on expression of P*csgD* and P*csgB*

The above results strongly indicate that Hfq may regulate P*csgB* and P*csgD* independent of RpoS. To further test this hypothesis, strains with a deletion in *dsrA* were constructed, since the role of Hfq in regulating *rpoS* expression is to serve as a mediator for efficient binding between the regulatory small RNA *dsrA* and the *rpoS* mRNA during growth at low temperature (< 30˚C) (219). It was hypothesized that if Hfq regulates the expression of P*csgD* and/or P*csgB* at the RpoS level, deletion of *hfq* or *dsrA* would essentially have the same effect as reducing σ^{S} expression, which in turn would decrease the promoter activities of the *csgBA* and the *csgDEFG* operons.

The results, however, did not support this hypothesis. While deletion of *hfq* eliminated rugose morphology and Congo red binding, deletion of *dsrA* did not change any of the phenotypes exhibited by the wt strain 14028 (data not shown), except for a

very slight reduction of growth that was noticeable by the presence of slightly smaller colonies and by reduction in growth rate (data not shown and Figure 35). The growth reduction was not as great as that seen in the *hfq* mutant. The results from the Miller assay showed that while the activity of P*csgB* was eliminated in the *hfq* mutant, deletion of *dsrA* (YA171) only slightly reduced the activity to approximately 75% of that in the wt (Figure 31). Because of the heterogeneous nature of the assayed samples in the *dsrA* mutant (a biofilm former), we obtained activities ranging between 75% and 125% of that seen in the wild type. Generally speaking, there was not much change in P*csgB* activity in the *dsrA* mutant compared to the wt strain. Complementation of *dsrA* in pACYC184 increased the *csgB* promoter activity to about 1.5 times that seen in the wt.

A very similar trend was observed in P*csgD* activity at 48h (Figure 32B and data not shown) with insignificant reduction of activity in the *dsrA* background compared to that in the wt strain. Complementation with pYA35 (*dsrA* in pACYC184 vector) increased the activity to about twice as much as that seen in the wt.

P*csgB* activity of the *dsrA* mutants in *rpoS hns* background (YA185) also was not much affected compared to that in the *rpoS hns* mutant (YA147) (Figure 33). There were large variations in P*csgB* activities obtained in this triple mutant when data from several experiments were compared. The values ranged from 25% to 200% of the wt, overall seeming to indicate the lack of significant changes and indicating that *dsrA* is probably not required for P*csgB* activity in the absence of *rpoS* (see Appendix F). There were also no significant differences between the P*csgD* activities in *dsrA rpoS hns* and *rpoS hns* under microaerophilic conditions (Figure 34). Complementation with *dsrA* in pACYC184 plasmid allowed the activity of the *dsrA* and *dsrA rpoS hns* mutant to rise to levels

slightly higher than that of either the wt or the *rpoS hns* strains, respectively. Strains carrying the control plasmid pYA38 in Δ*dsrA* or Δ*dsrA rpoS hns* background confirmed that *dsrA* mutations did not affect plasmid replication (Figure 33 and Figure 34).

4.8. P*csgB* and P*csgD* were differently regulated at 37°C in *rpoS hns* background

At 37˚C, the activity of *csgD* and *csgB* promoters was lower in the wild type strains than those at the lower temperature 28˚C. It has been shown previously that, at this higher temperature, the promoter activity is not optimal (202). However, in the *rpoS hns* double mutant background, P*csgB* still exhibited a high amount of activity (Figure 36A), indicating that the *csgB* promoter is no longer temperature regulated in this double mutant background. Although the *csgD* promoter is exposed optimally under microaerophilic conditions, it was of interest to compare it with the *csgB* promoter aerobically at 37˚C. The *csgD* promoter, however, was only minimally expressed under this condition in both the wt and the *rpoS hns* background (Figure 36B), suggesting that although the deletion of *hfq* had a similar effect on both promoters at 28°C, the regulation of the two promoters may be different at higher temperatures.

4.9. Congo red and calcofluor binding characteristics of the mutants

Since the above results showed that *rpoS hns* mutation in wt background still allowed an even higher P*csgB* activity at 28˚C, the effect on P*csgB* activity of a single mutation in either *rpoS* or *hns* alone or in combination with *hfq* or *dsrA,* was tested. It was shown that the activity was eliminated in the *rpoS* mutant, confirming previous results. However, disruption of *hns* showed variable effects on the activity of P*csgB*, with some having higher activity, while other clones were slightly lower, than the wt (compare

Figure 33 and Figure 37). Mutants with *hns* background have been reported to have a tendency toward spontaneous secondary mutation (99, 134), including lesions in *rpoS* (13), which may have been the reason for some variability in the Miller assay on cells having *hns* mutations.

We also investigated the phenotypes and β-galactosidase activity of both fusion constructs in other *rpoS* and *hns* single and double mutant pairs. As shown in Figure 37, compared to the *rpoS* single mutation that resulted in white colonies on the Congo red plate, *hfq* mutation still allowed some binding of Congo red, yielding colonies with slightly pinkish coloration. Growth of *hfq* on calcofluor also showed slight fluorescence, while binding was eliminated in the *rpoS* mutant. The activity of both *csgD* and *csgB* promoters in *rpoS* background was either eliminated or was very low (Figure 37). Single mutations in either *dsrA* or *hns* changed neither Congo red nor calcofluor binding, although the *hns* mutant was mucoid. The activity of the *csgB* promoter in these single mutants reflects the phenotypes, since the activity was retained in *hns* and *dsrA* single mutants.

The mutation of *rpoS* seems to have a masking effect on the activity of both *csgB* and *csgD* promoters, since the activity is almost eliminated in double mutant strains *hfq rpoS* and *dsrA rpoS*. The effect could also be seen in the phenotypes of these strains grown on CR plates, since none of them bound Congo red or calcofluor. This indicates that the loss of CR or CF binding in these double mutants may be due to the loss of *rpoS* alone. In contrast, mutations in *hns* background retain the ability of cells to bind Congo red and calcofluor. The Δ*hfq hns* mutant, despite its poor growth under this condition,

also bound Congo red, therefore the low β-galactosidase activity of this strain was probably due to growth inhibition by the combination of these two deletions.

4.10. Production of curli protein by wt and *hfq* mutant in the wt and *rpoS hns* double mutant backgrounds

To correlate the activity of *csgB* promoter with the production of CsgA protein, assessment was performed by Western blotting using anti-AgfA (CsgA) monoclonal antibody (Figure 38). When similar amounts of samples from the wt, mutants and complemented strains were loaded (as judged from staining of total formic acid resistant - protein), the *hfq* mutants YA1153 (Δ*hfq*::Kan) and YA 170 (Δ*hfq*) produced much smaller amounts of CsgA protein compared to the wt strain 14028. Production of even larger amounts of CsgA in the complemented strains YA1153(pYA34) and YA170(pYA34) was restored, as shown by the appearance of the upper band that corresponded to the presence of multimers of CsgA (45), thus confirming results of the activity of P*csgB* in the Miller assay. The double mutant *rpoS hns* background (strain 147) was shown to produce a small amount of CsgA, similar to that in strain 183 (Δ*hfq rpoS hns*). The low amount of CsgA in strain YA 147 was not expected, since it was shown that the activity of *csgB* and *csgD* promoter in this background was similar to, or even higher than, that shown in the wt strain. We suspect that other background mutation may have occurred in this clone during growth, which is known to happen with strains carrying the *hns* mutation (13). Complementation of *hfq* mutation in the *rpoS hns* double mutant background restored the production of CsgA to a wt level. Therefore, the positive effect of Hfq on rugose formation, by affecting *csgB,* was consistently shown by the loss or reduction of promoter activity or curli production in the *hfq* mutants, compared to the

wt strain, using four different approaches: Congo red binding, Electron microscopy, P*csgB-lacZ* promoter fusion, and Western blotting.

5. DISCUSSION

5.1. Rugose and its importance

Multicellular behavior is necessary in different stages of bacterial life in response to unfavorable conditions. For example, under starvation in aquatic environments, formation of biofilms enhances nutrient acquisition, which would probably prove to be impossible for planktonic cells in swiftly moving currents. Also the extracellular matrix in rugose colonies allows survival under oxidative conditions and chlorine and ethanol stress (7, 83, 221).

5.2. *hfq* mutation eliminates multicellular behaviors

In this report, an *hfq* mutation was identified and characterized in *Salmonella* Typhimurium, which resulted in loss of the rugose phenotype. The observed loss of the rugose phenotype by the *hfq* mutant was concomitant with the absence of rugose matrix as well as normal curli and polysaccharide production. The *hfq* mutant also failed to form pellicles, cell clumping, and biofilms under the conditions tested. The role of Hfq was confirmed by disruption of *hfq* in three different *Salmonella* Typhimurium backgrounds: DT104 Rv, LT2, and 14028, with the same phenotypic changes observed in each strain. Furthermore, subsequent complementation of *hfq* in a plasmid allowed restoration of these phenotypes similar to those present in the wt. These variations in phenotype suggest the involvement of the RNA-binding protein Hfq in rugose expression.

The involvement of Hfq thus adds yet another component to the already-complicated regulation of multicellular behavior in *Salmonella*. Hfq is homologous to the eukaryotic Sm proteins that function in mRNA splicing and RNA processing. In bacteria, Hfq is required for regulation by small non-coding RNAs in response to specific environmental signals. It has been proposed that sRNA is looped around the Hfq protein, suggesting the direct interaction of this protein with the sRNA. Hfq may also act independently of sRNA to regulate the stability of mRNA. Thus, it was the purpose of this investigation to confirm if and how Hfq affects the expression of rugose morphotype.

5.3. The role of Hfq in the regulation of *csgDEFG* and *csgBA* operons and the use of *rpoS hns* double mutants

The results from the *lacZ* operon fusion suggested that *Hfq* is required for the normal regulation of both the *csgDEFG* and *csgBA* operons in wt background at the transcriptional level. The results were unexpected because of our present knowledge of *Hfq* as an RNA binding protein, which regulates post-transcriptionally (90, 228). Thus the effect of Hfq on these promoters may not be direct, instead, its regulation may lie in its role in the translation of *rpoS* (167), which is the alternative sigma factor required during the stationary phase of growth for the transcription of both P*csgD* and P*csgB* in *E. coli* and *S.* Typhimurium (46, 199).

Yet when RpoS dependence in the transcription of the two promoters was released in the *rpoS hns* double mutant background, the activity of both *csgD* and *csgB* promoters was still reduced in the absence of Hfq. This indicated that the effect of Hfq mutation on the two promoters was most probably independent of its function to promote efficient translation of *rpoS* in this double mutant background. However, the possibility

cannot be excluded that Hfq may regulate the P*csg*B and P*csgD* differently in either the presence of RpoS or in its absence in the *rpoS hns* background. Interestingly, the deletion of *dsrA* failed to show the same repressive effect as shown by Hfq on the two promoters, further suggesting that either DsrA acts differently in regulating *rpoS* translation at low temperature in *Salmonella* than it does in *E. coli*, or perhaps Hfq may not act together with this small RNA in the regulation of rugose colony formation.

The *csgD* promoter is also regulated by HNS (81), and has been proposed to be recognized also by both σ^S and σ^{70} (184). Here we show that the promoter was also expressed when both *rpoS* and *hns* were deleted, although the level was reduced to only about half of that in the wt background, thus adding to the list of genes expressed by the release of HNS repression of σ^{70}-directed transcription other than P*csgBA* and P*hdeBA* (9). Mutation of *hfq* in this double mutant background also seemed to decrease the activity of *csgD* promoter in the *csgD*-lacZ fusion construct, although the slow growth of this mutant prevented the formulation of further conclusions.

5.4. Limitations of the current approach and alternative methods

One constraint in the use of an *hfq* mutant in comparing promoter expression from a fusion plasmid with the wt strain is the pleiotropic nature of the *hfq* mutants, which includes slow growth and changes in plasmid supercoiling (246). Growth was even more reduced by *hns* mutation. However, we were able to show that the *hfq* mutant was actually physiologically active and capable of expressing normal β-galactosidase activity at the stationary phase of growth with the use of a positive control plasmid, in which the *lacZ* gene is fused to its own promoter. These results confirmed that the mutants were capable of plasmid multiplication. In addition, the lack of curli expression was shown not

only at the transcriptional level with a fusion plasmid, but also with direct evidence of the lack of normal curli production by the use of negative staining and EM, e.g.- lack of matrix production as shown by SEM, and a reduction of CsgA protein by Western blotting.

Assay for P*csgD* activity from a fusion plasmid has been performed using a *csgD* mutant background, which no longer exhibited multicellular behavior (83), after it was shown that CsgD did not negatively regulate its own promoter. However, we preferred to use wt background in assaying the activity because it is more physiologically relevant, and is more representative of the activity shown in the cellular community. Furthermore, mutation in *csgD* would not permit assaying the activity of P*csgB*, whose expression is dependent on CsgD.

Another alternative to using the *rpoS hns* double mutant to release *rpoS* dependence of the promoter without affecting growth would be to use L43R OmpR mutant (251). In this mutant, the promoter is no longer σ^S dependent, probably because the mutated OmpR binds effectively to the intergenic region thus freeing *rpoS* dependence (184). Another alternative would be the use of a strain carrying the *rpoS* gene with a deletion in the leader sequence, i.e. no longer DsrA-dependent. Nevertheless, we showed that the activity of *csgB* promoter was expressed at an even higher level than that in the wt in *hns rpoS* background.

5.5. Possible roles of Hfq on rugose matrix production

Because of the known function of *Hfq* as an RNA binding protein in bacteria, it is very likely that it positively regulates *csgD* and *csgB* operons post-transcriptionally. At this level, the role of Hfq in the expression of both promoters may be either direct or

indirect. Indirectly, Hfq may positively regulate one or more regulators of P*csgB* and P*csgD*. Since an *hfq* mutation affects curli as well as cellulose production (as judged from calcofluor binding), the effect of *hfq* may be upstream in the rugose regulatory pathway before it branches to curli and AdrA. Therefore, possible candidates include CsgD, MlrA, OmpR, and RcsC, based on current knowledge. It is very likely that Hfq interacts with a sRNA to exert this effect.

Directly, Hfq may interact with the mRNA transcript of either *csgD* or *csgB*. At this level, there are two possible roles of *Hfq*: (1) to stimulate the translation of the *csgB* and *csgD* transcript, most likely together with an sRNA, or (2) to increase the stability of the mRNA of *csgBA* and *csgDEF*. The first possibility can be excluded because the difference in β-galactosidase activity between the wt and the *hfq* strain was detected using an operon fusion construct, in which the *lacZ* gene has its own start codon and ribosome binding site; therefore, the translation of *lacZ* is independent of translational factors in the *csgB* and *csgD* operons. The second explanation is more feasible in that *Hfq* may act to stabilize both *csgB* and *csgD* transcript, which may affect the *lacZ* transcript downstream of the two genes in the fusion plasmid. In this scenario, there could possibly be an RNA stabilizing sequence in the region downstream of the transcriptional start site (between 5' untranslated region (UTR) and either the first 186 bp of *csgB* ORF or 210 bp of *csgD* ORF) included in the promoter fusion construct, wherein Hfq alone or in combination with another factor could bind and stabilize the transcript. Binding of Hfq may protect the transcript from degradation from RnaseIII, such as shown for the regulation of *rnc* operon of *E. coli* (180). Further analysis of the region downstream of the transcription start site may elucidate a specific RNA stabilizing region, and *Hfq*

binding to this region would provide evidence of this proposed role for *Hfq*. Hfq has been found to bind not only to sRNA, but also to mRNA, including that of *hdeA* and *hdeB* from the *hdeAB* operon (274). It is interesting to note that this operon is regulated by the σ^S-dependent promoter, and is under similar regulation as the *csgBA* operon, being transcribed at the wt level in the *rpoS hns* background (9). Furthermore, an additional binding site in Hfq distinct from that for sRNA, and proposed for mRNA and polyA stretch RNA, has also been demonstrated (155). Further evidence showing the presence of a specific binding site for Hfq in the mRNA transcript of both *csgDEFG* and *csgBA* would provide information necessary to determine the possible mechanism of action by Hfq.

Because the expression of the *csgBA* operon is dependent on CsgD, the effect of Hfq seen on the *csgB* promoter may result from a low level of CsgD, which was also downregulated by *hfq* mutation. Thus, we cannot exclude the possibility that Hfq may not directly regulate *csgBA* expression.

5.6. The involvement of DsrA on *csgB* Promoter

It is known that both DsrA and Hfq regulate *rpoS* together at the translational level and at the same location, since mutations in *rpoS* that release the dependence of *rpoS* translation on *Hfq* also release the dependence of *rpoS* from DsrA (143). Therefore, it was expected that the effects of an *hfq* mutation and a dsrA mutation on *csgB* and *csgD* promoters would be similar, if they both affect the level of σ^S. The absence of morphological change in the *dsrA* mutant thus was unexpected. Because both Hfq and DsrA have multiple targets, it may be reasonable to suggest that the expression of another factor may be altered under the conditions tested, which may counteract the effect of

reduced levels of σ^S. Alternatively, the regulation of *rpoS* by DsrA in *Salmonella* may be different from that shown in *E. coli*. Nevertheless, the different effects of *hfq* and *dsrA* mutations on rugose morphology and on the expression of both *csgB* and *csgD* promoters under the conditions tested pose the possibility that Hfq may not affect the regulation of rugose formation at the level of *rpoS* translation.

In an *hfq* mutant of *E. coli*, DsrA is unstable with a half-life reduced from 30 min in the wt to 1 min in the *hfq* mutant, and the sRNA in the *hfq* mutant was also truncated at the 3' end. Hfq may act by changing the structure of DsrA RNA or forming an active RNA-RNA complex. However the results from the present study indicated that the effects of mutations in *hfq* on the rugose formation pathway might not be due to its effect on DsrA. In fact, deletion of *dsrA* did not affect rugose colony phenotype, pellicle and biofilm formations, nor did it affect the activity of both *csgDEF* and *csgBA* operons, indicating that DsrA does not seem to play a major role in rugose formation in *Salmonella*. However, based on its role drawn from studies in *E. coli*, DsrA was expected to be positively regulating RpoS mRNA at temperatures below 30˚C (219), thus having a positive effect on the *csgD* and *csgB* promoters. Our results demonstrated that DsrA may not be the temperature regulator for either promoter in *S*. Typhimurium. Crl, a protein that binds to RpoS to recruit it to the *csgB* promoter, may be the major temperature regulator for rugose expression (Bogdour, 2004). It is unknown why strains having a *dsrA* background seem to show very large variations in P*csgD* and P*csgB* activities, similar to that shown in strains carrying *hns* mutation. It is possible that *dsrA* mutation, similar to *hns* mutation, may induce other unknown mutations.

5.7. Temperature regulation of *csgBA* is eliminated in *rpoS hns* background

The constitutive expression of the *csgBA* promoter in this study even at 37°C in *rpoS hns* background may indicate the lack of temperature regulation in the absence of *rpoS*. The constitutive expression of P*csgB* in the absence of RpoS both at 28˚C and 37˚C shown in the present study suggests that the temperature regulator which activates the *csgBA* promoter may involve RpoS. The results are in contrast to the report of Olsen *et al.* (173) in *E. coli* TP2600-1, in which fibronectin binding, which is an indirect measure of curli production, was lacking in a *hns rpoS* double mutant grown at 37°C compared to that grown at 26°C. The reason for this variance is still unknown, although we speculate that the Crl protein might regulate differently in the strain of *Salmonella* used in this study. For instance, in *E. coli*, only some strains that are curli deficient, such as HB101, can produce curli when Crl is overexpressed from a plasmid, but a few others (such as MC1029 and 1061) were not affected by overproduction of this protein (173).

6. CONCLUSIONS

Previous studies to characterize regulators at the *csgB* and *csgD* promoters have been carried out by identifying consensus DNA sequences (81, 82, 184). Although most transcriptional regulators are discovered using this method, regulators that function at post-transcriptional levels may not be revealed, because some lack consensus sequences for recognition or depend on the secondary structure of mRNA for regulation. The use of random mutagenesis allowed us to uncover regulation by the RNA-binding protein Hfq, thus adding another level to the complex, transcriptional, regulatory modes of multicellular behavior for *Salmonella* (Figure 39). While the results of this study provide a basis for possible regulation at the post-transcriptional level, further studies are needed

to elucidate the exact mechanism of Hfq regulation on the expression of both *csgD* and *csgB* operons. Hfq may act together with an sRNA, many of which have only recently been discovered using genome wide searches as well as co-precipitation with Hfq. Many sRNA(s) still have unknown targets. We have shown that the sRNA, DsrA, may not play a role in regulating the *csgB* and *csgD* promoters in the absence of RpoS. Knowing the role of Hfq in post-transcriptional regulation, it is reasonable to expect that either other sRNA(s) may contribute to the regulation, probably aided by Hfq for specific target recognition, or that Hfq may affect the stability of mRNA of both *csgDEF* and *csgBA* transcripts. Hfq has been shown to be present in *E. coli, Salmonella* Typhimurium, *Vibrio cholerae* and *V. harveyi, Brucella abortus*, *Listeria monocytogenes*, *Legionella pneumophila*, and *Pseudomonas aeruginosa* (32, 59, 135, 152, 166, 222) thus appearing to be common in bacteria, in general. Hfq has also been shown to have a role in virulence and survival strategies, and iron and galactose metabolism. This study shows that Hfq is also involved in positive regulation of multicellular behavior and biofilm formation in *S.* Typhimurium. Because of the high expression of Hfq (between 30,000-60,000 copies per cell) and the large number of sRNA(s) it regulates (274), Hfq may provide an alternative intervention site by which signals for the multicellular pathway can be blocked to diminish the survival capacity of *Salmonella*, and probably other bacteria, thus reducing their load in particular environment niches.

Table 6. Strains used in this study and their relevant characteristics

Strain	Genotype	Source or Ref
E. coli TOP10		Invitrogen
S. Typhimurium DT104		
11601		
Rv	rdar	Swaminathan[a]
Stv	spontaneous mutant, saw	SWJ
A1-10	*hfq:Tn5* (saw)	This study
S. Typhimurium LT2	wt	B. Bassler (231)
TE5395	*rpoS*::pRRT1 (Amp^R)	T. Elliott
TE7505	*hns1::kan*	T. Elliott
YA151	Δ*csgA*	See chapter 3
YA153	Δ*hfq::kan*	This study
YA157	Δ*dsrA::kan*	This study
S. Typhimurium 14028	Rugose, wt	BD Scientific
YA1153	Δ*hfq::kan*	This study
YA1157	Δ*dsrA::kan*	This study
YA1158	YA1157(pYA31)	This study
YA144	*hns*	TE7505x14028
YA147	*rpoS hns*	TE5395xYA144
YA170	Δ*hfq*	This study
YA171	Δ*dsrA*	This study
YA172	Δ*hfq rpoS*	This study
YA173	Δ*hfq hns*	TE7505xYA170
YA174	Δ*dsrA rpoS*	TE5395xYA171
YA175	Δ*dsrA hns*	YA144xYA170
YA183	Δ*hfq rpoS hns*	TE5395xYA173
YA185	Δ*dsrA rpoS hns*	TE5395xYA175
YA226	YA170(pYA33)	This study
YA227	YA171(pYA31)	This study
YA239	YA1153(pYA34)	This study
YA240	YA170(pYA34)	This study
YA243	YA183(pYA34)	This study
YA256	YA171(pYA35)	This study
YA259	YA185(pYA35)	This study

Table 7. Plasmids used in this study and their relevant characteristics

Plasmid	Relevant Characteristics	Source or Reference
pUC19	Amp^R, *lacZ*	New England Biolabs
pCR-4TOPO	Amp^R, Kan^R	Invitrogen
pWSK29	Cloning vector, Amp^R	R. Curtiss, Jr.. 3rd
pACYC184	Cloning vector, Tet^R Cm^R	New England Biolabs
pQF50 Cm	Operon fusion plasmid Cm^R	F. Norel
pKD4	PCR template plasmid, FRT sites flanking Kan^R gene	*E. coli* Genetic Stock Center (CGSC)
pKD46	Amp^R, λ Red system helper plasmid, P*ara*, Ts ori	CGSC
pCP20	FLP recombinase system, Amp^R	CGSC
pYA25	*PcsgB-lacZ* operon fusion in pQF50Cm	This study
pYA26	P*csgD-lacZ* operon fusion in pQF50Cm	This study
pYA27	p*hfq*11/12PCR fragment in the cloning site of pCR-4	This study
pYA30	p*dsrA*12/13 PCR fragment in the cloning site of pCR-4	This study
pYA31	*dsrA* insert from pYA30 at SmaI/KpnI sites of pWSK29, AmpR	This study
pYA33	*hfq* insert from pYA27 at BamHI/HindIII sites of pWSK29, AmpR	This study
pYA34	*hfq* insert from pYA27 at EcoRI site of pACYC184 Tet^R	This study
pYA35	*dsrA* insert from pYA30 at EcoRI site of pACYC184 TetR	This study
pYA38	P*lac-lacZ* operon fusion in pQF50Cm	This study

Table 8. Primers used in this study

Primer	Sequences	Reference or sequence number
p*csgB*Z1	5'- CCC AAG CTT TTC TTA TCC GCT TCC ATC AT –3' [a]	1632-16330 [f]
p*csgB*Z2	5'- TCC CCC GGG TCC GTG CCG ACT TGA CCA –3' [b]	17435-17428 [f]
p*csgDZ*3	5'- TCC CCC GGG AAG AAT AGG CGA AGG TAG TA – 3'[b]	17435-17428 [f]
p*csgDZ*4	5'- CCC AAG CTT AGG CAC GGC TGA ACT GGT -3'[a]	1632-16330 [f]
p*dsrA*12	5'-CGG GGT ACC TGA GCG GGT GAG CGT AGA C –3' [c]	1320-1338 [g]
p*dsrA*13	5'- TCC CCC GGG TGA GCG GGC TTA TTT CCA G -3' [b]	1712-1694 [g]
p*dsrA*D11	5 '- AAT CAT TCA TGT AAA AAA TAT TTA CTT GTC ATG CAA AAA AGT GTA GGC TGG AGC TGC TTC –3'[e]	1541-1580 [g]
p*dsrA*D12	5'- TTC ATG ATT TTA GTG TAA CAG AAG TAA ACC GTT AAA AAT GCA TAT GAA TAT CCT CCT TAG –3' [e]	1391-1430 [g]
p*hfq*D11	5'- GTA TCG TGC GCA ATT TTT CAG AAT CGA AAG CTT GTT CAA AGT ACA AAT AAG CAG TGT AGG CTG GAG CTG CTT C –3' [e]	18562-18611 [h]
p*hfq*D12	5'- ATA ACC AGC GGG GGC GAT TAT CCG ACG CCC CCG ACA TGG ATA AAC AGC GCC ATA TGA ATA TCC TCC TTA G –3' [e]	18942-18991 [h]
p*hfq*11	5'- CGC GGA TCC ACG AGA CAG TTG GCG AAG C –3' [d]	18416-18434 [h]
p*hfq*12	5'- CCC AAG CTT ACT CGC ACA AAC GCT CCA G –3' [a]	19280-19298 [h]
pKanKD3	5'- CAG TCA TAG CCG AAT AGC CT 3'	Datsenko and Wanner (55)
p*lac*11	5'- TCC CCC GGG GTA TTA CCG CT TTG AGT G -3'[b]	3873-3891 [i]
p*lac*12	5'- CCC AAG CTT GTC ATA GCT GTT TCC TGT G -3'[a]	203-221 [i]

[a] HindIII site underlined
[b] SmaI site underlined
[c] KpnI site underlined
[d] BamHI site underlined
[e] Sequences homologous to that in pKD4 template are underlined
[f] Sequence from *Salmonella* Typhimurium LT2 accession number AE008749
[g] Sequence from *Salmonella* Typhimurium LT2 accession number AE008788
[h] Sequence from *Salmonella* Typhimurium LT2 accession number AE008904
[i] Sequence from pCR-4 (Invitrogen)

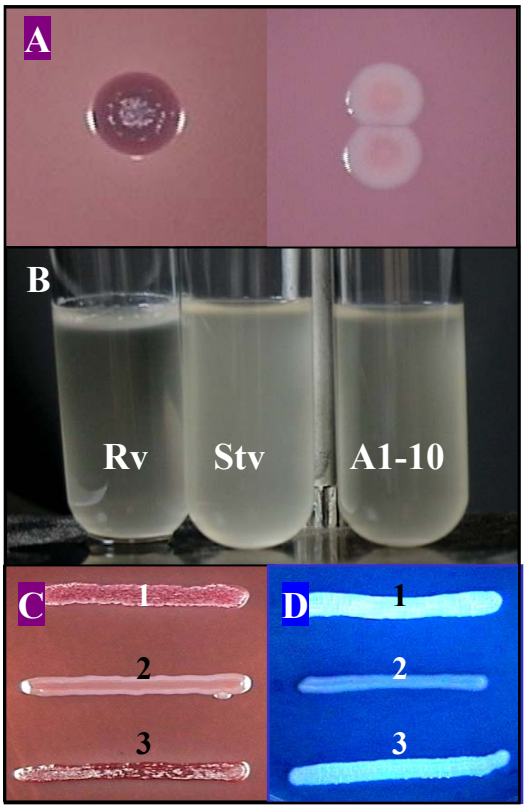

Figure 25. Multicellular phenotypes of *S.* Typhimurium are eliminated in the *hfq* mutant compared to the wt strain.

Single colonies of DT104 Rv (left) formed rugose, while the *hfq*::Tn mutant A1-10 (right) formed only the smooth phenotype on LB-CR media at 25°C for 4 days (A). Pellicles, seen as a thick layer on the surface of the broth in Rv (left), were not formed in the *hfq* mutant A1-10 (right), similar to that in the non-matrix forming mutant Stv (center) (B). Smooth colony morphology similar to A1-10 (C) and impaired calcofluor binding (D) were also observed in the *hfq* knock-out mutant YA170 (2), and pYA-complemented strain of YA170 (YA240) (3) restored the strains to a phenotype similar to that seen in the wt 14028 (1). Cells were grown for 2 days at 25°C on LB-CR and LB-CF for observation of Congo red- or calcofluor binding, respectively, in (C) and (D).

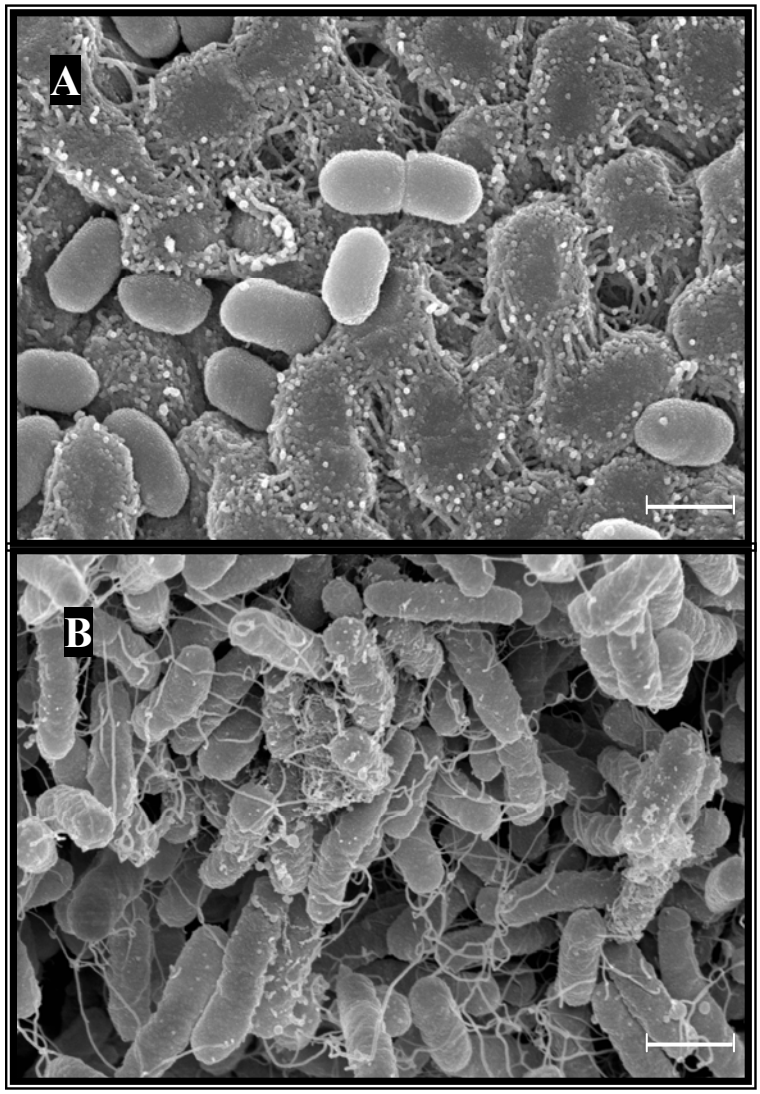

Figure 26. Scanning electron micrographs of the Rv and *hfq*::Tn5 mutant A1-10. Cells were grown on LB agar for 4 days at 25˚C. Most of the wt strain Rv (A) cells are covered with extracellular matrix, which was absent in the *hfq* mutant (B). Only fibrillar materials are seen surrounding A1-10 cells. Notice the elongated A1-10 cells compared to the wt. Bar 1 μm.

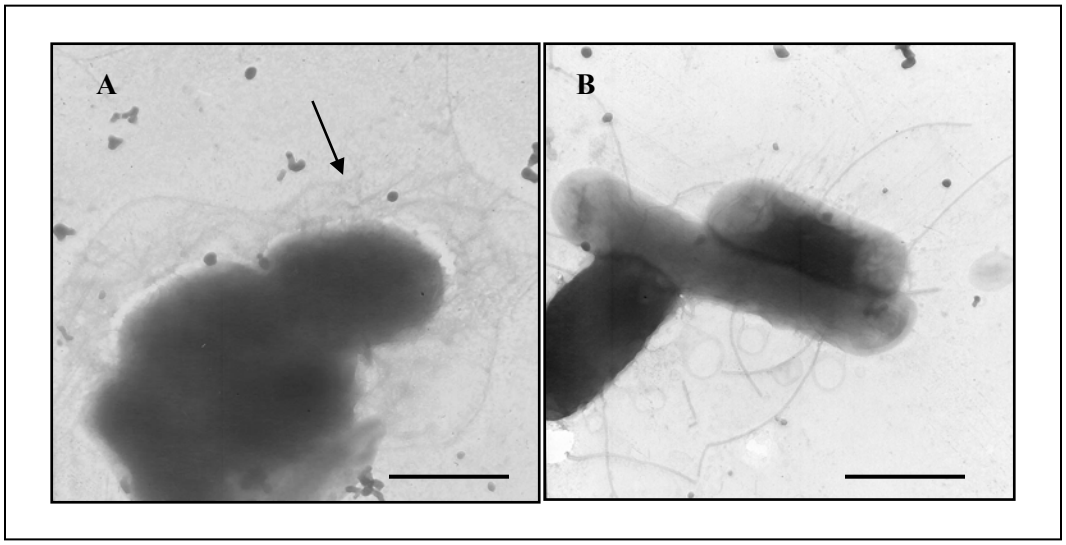

Figure 27. Matrix and curli production by the wt Rv and their absence in *hfq*::Tn mutant A1-10 as shown by transmission electron microscopy.

The wt strain *S*. Typhimurium DT104 Rv (A) produced amorphous matrix attaching cells together and curli fimbriae seen as the aggregative fibrous materials surrounding the cells (arrow). Both structures were missing in the *hfq* mutant A1-10 (B). Bars 1μm.

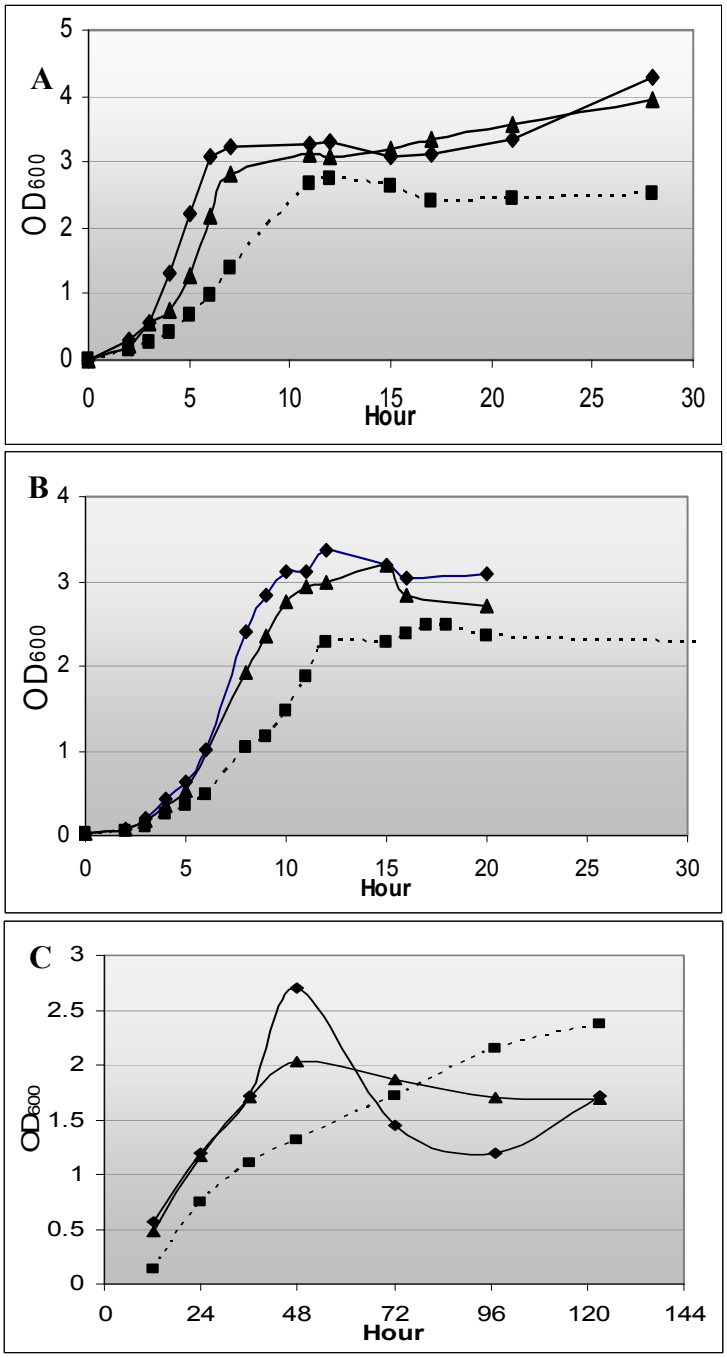

Figure 28. Growth curves of wt 14028, Δ*hfq* and *hfq* complemented strains.

Growth curves of 14028(◆), Δ*hfq* strain YA170 (---■---), and the complemented strain YA240 (▲) were plotted when all strains were grown under aerobic conditions at 37˚C (A) and 28˚C (B) and under microaerophilic condition at 28˚C (C). Two independent cultures were measured at the same time, and only representative data are presented. Experiments were repeated at least twice. The wt and complemented strains formed pellicles, biofilms, and clumps at stationary phase at 28˚C, and the OD_{600} measurements at this phase were only approximate.

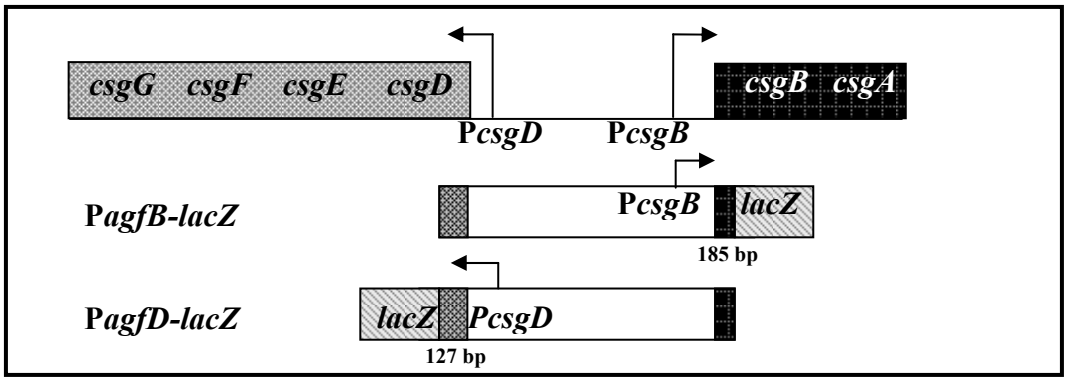

Figure 29. Fusion construct of promoters for *csgD and csgB* and *lacZ* to assay the expression of *csgB* and *csgD* operons.

The organization of the divergently transcribed *csgBA* and *csgDEFG* operons in *S.* Typhimurium, including the promoters and the direction of transcription (arrows) is shown on top. Promoter fusion in pQF50Cm plasmid between the *csgB* promoter (P*csgB*) and *lacZ* in pYA25, or between csgD promoter (P*csgD*) and *lacZ* in pYA26 (each include the intergenic region between the two operons) are also shown. Numbers indicate the size of either *csgB* or *csgD* ORF that were included in the fusion.

Figure 30. Biofilm production by thw wt strain 14028 and its derivatives and the expression of P*csgB* and P*csgD* in planktonic, biofilm and pellicle cells of the wt 14028.

(A) Thicker biofilms, as shown by a ring of growth on the walls of the flasks, were produced by the wt strain 14028 (pYA26) grown at 28˚C under microaerophilic conditions (marked as 14028M) than by 14028 (pYA25) grown under aerobic conditions (marked as 14028A). The *rpoS hns* strain (209M) did not produce a noticeable amount of biofilm under microaerophilic conditions. The expression in wt 14028 of both P*csgB* under aerobic conditions (B) and P*csg*D under microaerophilic conditions (C) were upregulated in the biofilms compared to the activity of the planktonic (free swimming) cells. P*csg*D was also upregulated in pellicle cells (C). The mixture of planktonic and biofilm cells under aerobic conditions, or planktonic, pellicle and biofilm cells under microaerophilic conditions, yielded an activity approximately halfway between that of planktonic only or biofilm only.

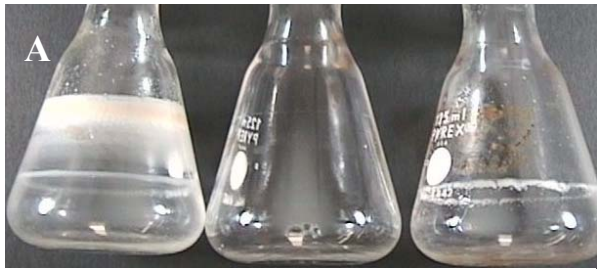

14028M 209M 14028A

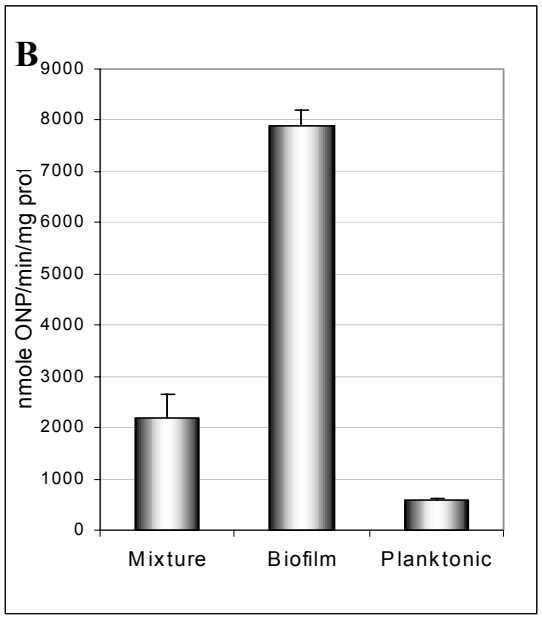

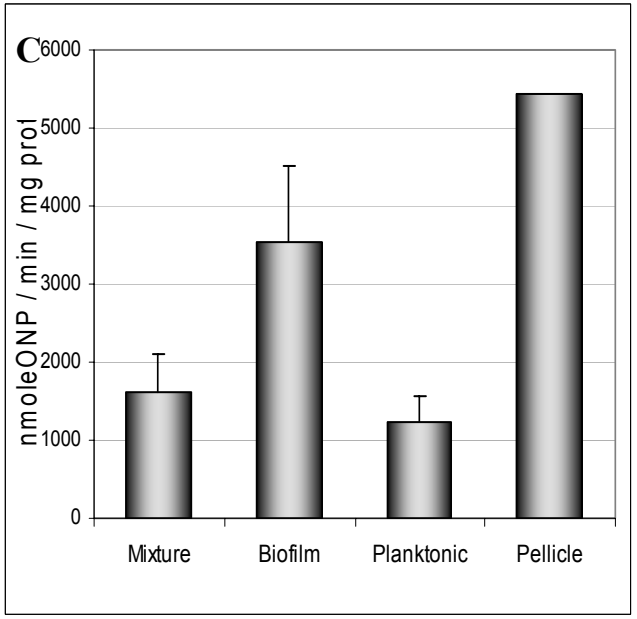

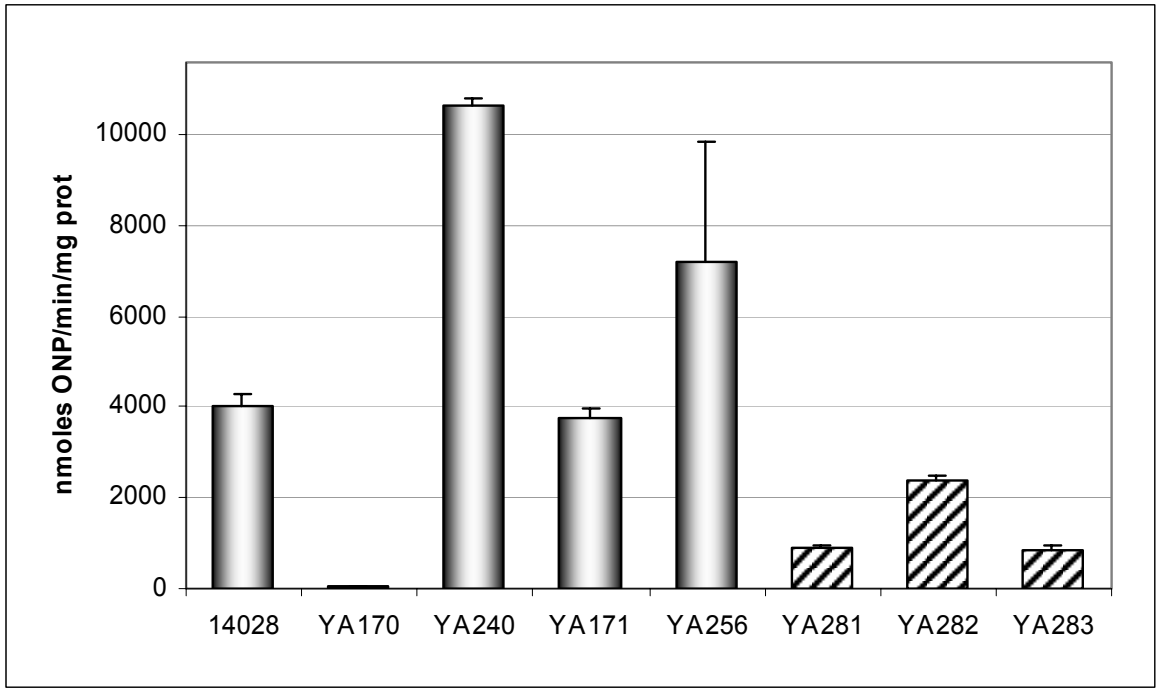

Figure 31. P*csgB* activity in wt 14028, Δ*hfq*, Δ*dsrA*, and complemented strains grown under aerobic conditions at 48h using the Miller assay.

Activities of the promoter for the *csgB* operon (P*csgB*) were measured from P*csgB-lacZ* fusion in the pYA25 plasmid. Strains assayed from left to right: the wt strain 14028, Δ*hfq* (YA170), *hfq* complemented strain (YA240), Δ*dsrA* (YA171) and *dsrA* complemented strain (YA256). Control strains carrying the same fusion plasmid pQF50Cm under the *lac* promoter (pYA38) in the wt, Δ*hfq* and Δ*dsrA* strains (YA281, YA282, and YA283, respectively) (hatched bars) are shown on the right. Results shown are averaged from two independent cultures, each from triplicate samples, assayed simultaneously. Error bars are shown on the top of each of the bars. The activities are expressed as specific β-galactosidase activity, with units in nmole of ONP released from ONPG/min/mg protein.

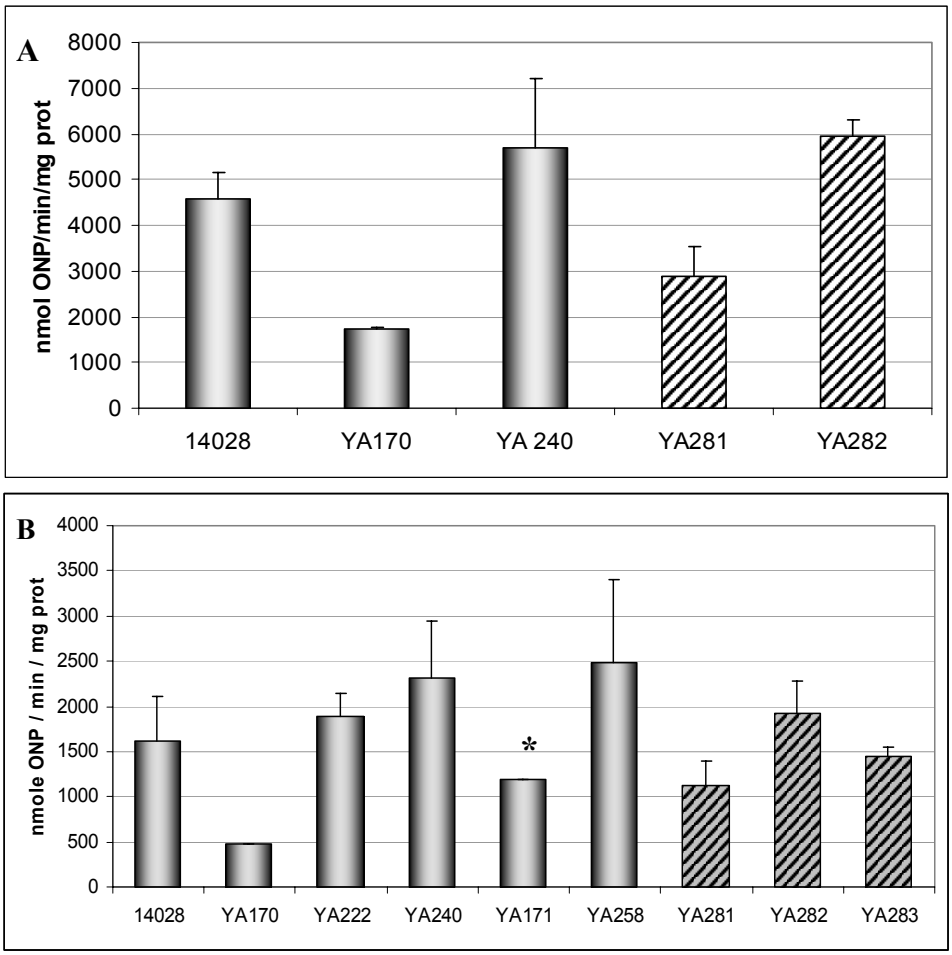

Figure 32. P*csgD* activity in wt 14028, Δ*hfq*, Δ*dsrA*, and complemented strains grown under microaerophilic conditions using the Miller assay.

(A) Activities of the promoter for the *csgD* operon (P*csgD*) were measured from P*csgD-lacZ* fusion in the pYA26 plasmid from cells grown at 96h, when YA170 reached stationary phase. Strains assayed from left to right: the wt strain 14028, Δ*hfq* (YA170), YA 170 complemented with *hfq* in the pACYC184 plasmid (strain YA240). Control strains carrying the pQF50Cm under Pl*ac* (pYA38) in wt and Δ*hfq* background, YA281 and YA282, respectively, are included (hatched bars). (B) The Miller assay was repeated in a separate experiment at 48 h for the wt, YA170 and YA 170 complemented with *hfq* in pWSK29 plasmid (strain YA222) or in pACYC184 (YA240), Δ*dsrA* (YA171) and *dsrA* complemented strain (YA258). Control strains carrying pYA38 in the wt, Δ*hfq* and Δ*dsrA* strains (YA281, YA282, and YA283, respectively) (hatched bars) are shown on the right. Note that absolute values for specific activities for each strain in (A) and (B) are different, due to differences in the Bradford protein assay standard curve generated on different days, although the pattern of activities compared to the wt were similar. (*) indicates that the reduction is insignificant when results from several different experiments were compared. Assay replicates, error bars, and units are as explained in Figure 31.

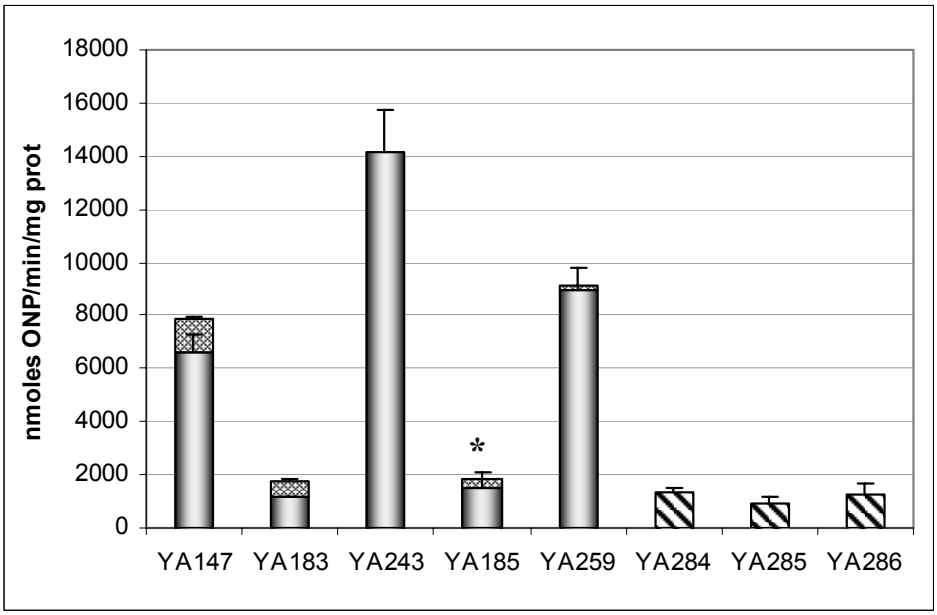

Figure 33. P*csgB* activity in *rpoS hns* background at 72h (day 3).
Promoter activity was measured from P*csgB-lacZ* fusion in pYA25. From left to right: *rpoS hns* (YA147), *hfq rpoS hns* (YA183), YA183 complemented with pYA34 (strain YA245), *dsrA rpoS hns* (YA208), and YA 185 complemented with pYA35 (strain 259). Control strains carrying pYA38 plasmids aer shown on the right (hatched bars): *rpoS hns* (YA284), *hfq rpoS hns* (YA285), and *dsrA rpoS hns* (YA286). Activities were essentially constant when assayed at 123 h (5 days) except for a slight increase in strain YA207 (from 18% at day 3 to 22% at day 5) (the difference between activities at day 3 and day5 are shown in cross-hatched bars on top of the main bars). (*) indicates insignificant reduction of activity compared to the wt when results from different experiments were combined. Assay replicates, error bars, and units are as explained in Figure 32.

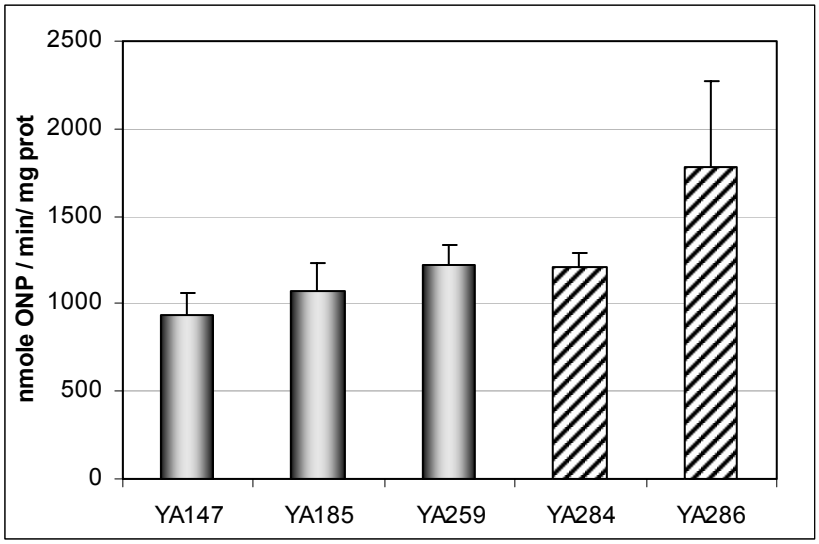

Figure 34. P*csgD* activity in wt, Δ*dsrA*, and *dsrA* complemented strains in *rpoS hns* background under microaerophilic conditions at 48h.

Promoter activity was measured from P*csgD-lacZ* fusion in pYA26. From left to right: *rpoS hns* (YA147), *dsrA rpoS hns* (YA185), *dsrA* complemented strain of YA185 (strain YA259), and strains carrying pYA38 control plasmids (hatched bars): *rpoS hns* (YA284) and *dsrA rpoS hns* (YA286).

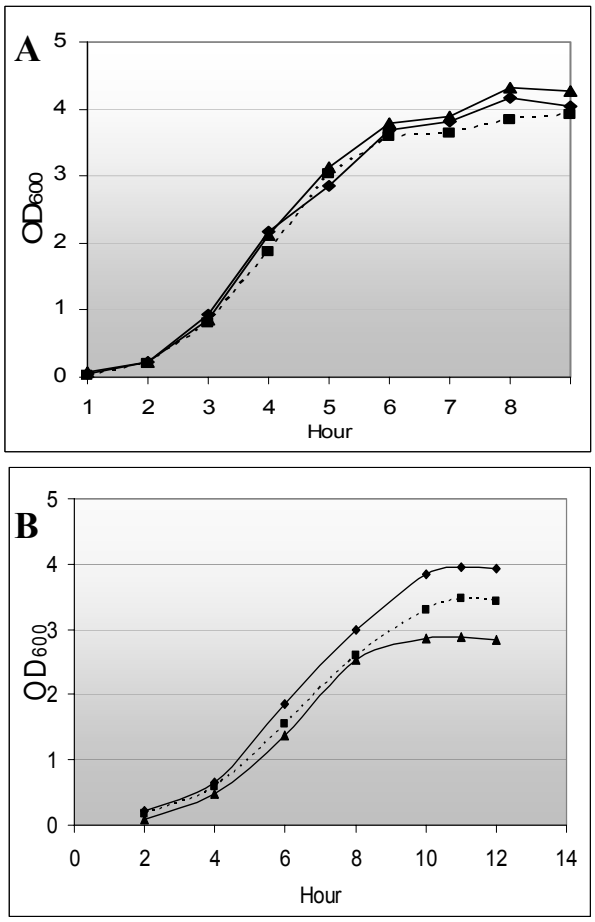

Figure 35. Growth curves of wt, Δ*dsrA* and *dsrA* complemented strains under aerobic conditions.

The wt strain 14028 (◆), YA1157 (Δ*dsrA*::*kan*) (--■--), and pYA34-complemented strain of YA1157 (strain YA 1158) (▲) were grown in LB broth under aerobic conditions at 37˚C (A) and 26˚C (B). All strains in (B) also carried the pYA26 plasmid

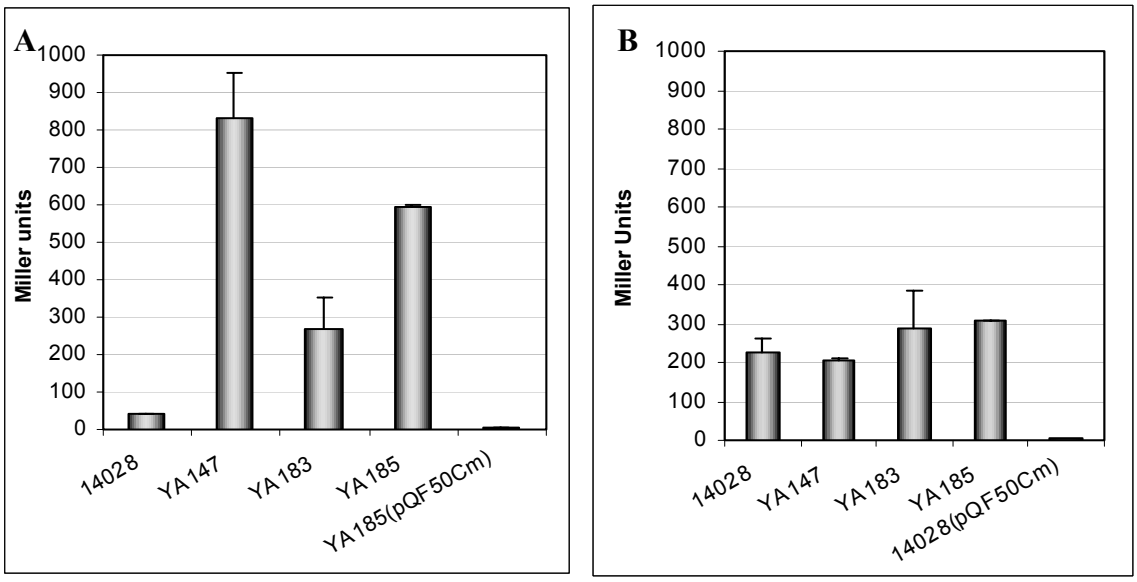

Figure 36. Activities of P*csgB* and P*csgD* in the wt and *rpoS hns* background at 37˚C.

Promoter activities were measured from *PcsgB-lacZ* in pYA25 (A) or P*csgD-lacZ* in pYA26 (B) in 14028, *rpoS hns* (YA147), as well as Δ*hfq rpoS hns* (YA183) and Δ*dsrA rpoS hns* (YA185). As a negative control, either YA185 or 14028 carrying the fusion vector pQF50Cm was included. Cells were grown under aerobic conditions for 24h at the less optimal temperature 37˚C in the wt background. Activities are expressed as Miller units.

Figure 37. Activities of P*csgD* and P*csgB* in the wt, and *hfq, dsrA, rpoS*, and *hns* single mutants and in multiple background combinations.

The promoter activities of both *csgB* (top) and *csgD*(bottom) operons were compared between wt and either *hfq* or *dsrA* mutants in either wt background, or in *rpoS* or *hns* background, or in *rpoS hns* backgrounds. The activities were further compared with Congo red binding phenotype on CR plates, and calcofluor binding phenotype on CF plates incubated at 25°C for 48h. From left to right: the wt strain 14028, Δ*hfq* (YA170), Δ*dsrA* (YA171), *hns* (YA144), Δ*hfq hns* (YA173), Δ*dsrA hns* (YA175), *rpoS* (TE5395), Δ*hfq rpoS* (YA172), Δ*dsrA rpoS* (YA174), *rpoS hns* (YA147), Δ*hfq rpoS hns* (YA183), and Δ*dsrA rpoS hns* (YA185).

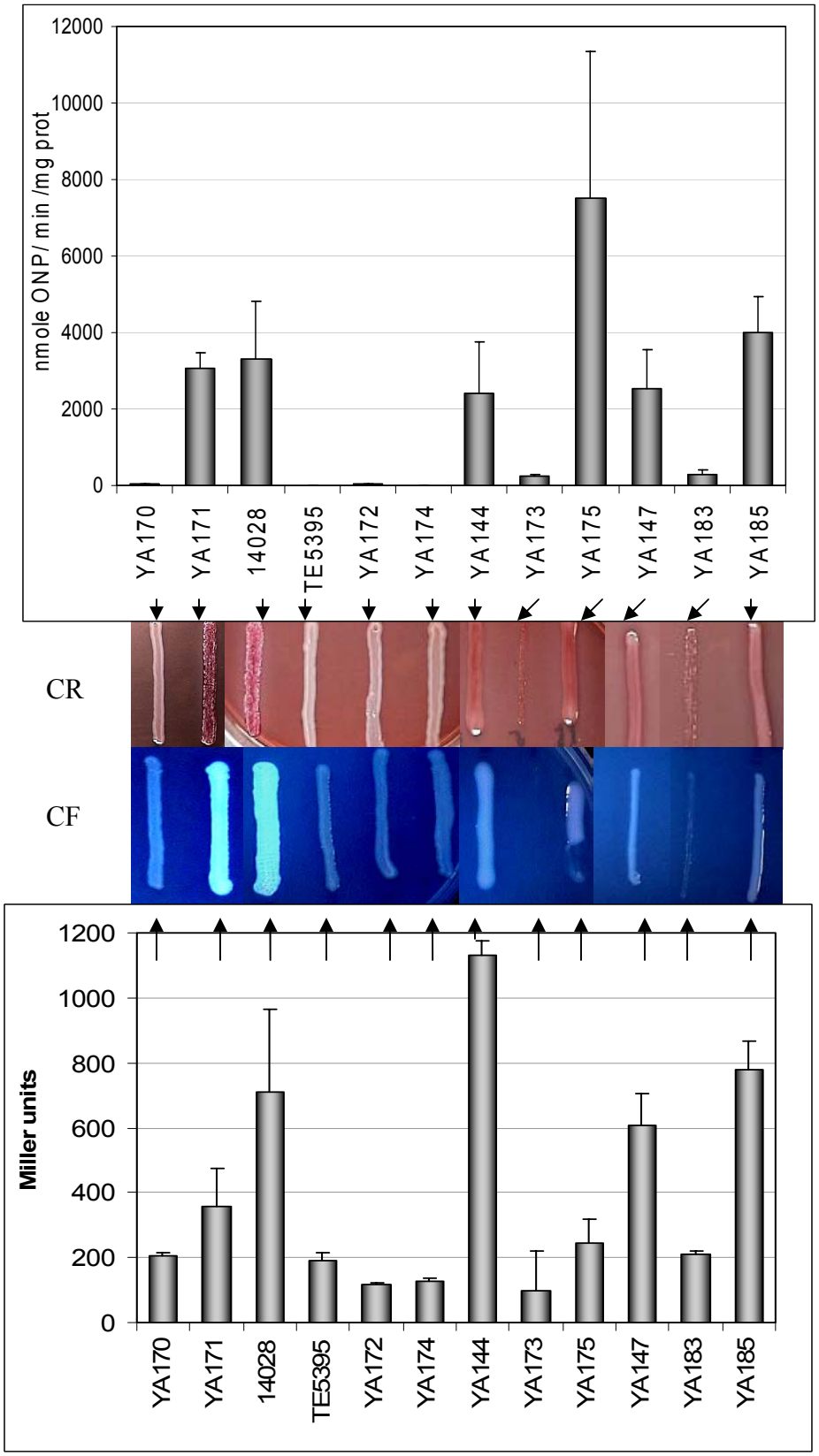
12000
10000
8000
6000
4000
2000
0
nmole ONP/ min /mg prot
YA170
YA171
14028
TE5395
YA172
YA174
YA144
YA173
YA175
YA147
YA183
YA185
CR
CF
1200
1000
800
600
400
200
0
Miller units
YA170
YA171
14028
TE5395
YA172
YA174
YA144
YA173
YA175
YA147
YA183
YA185

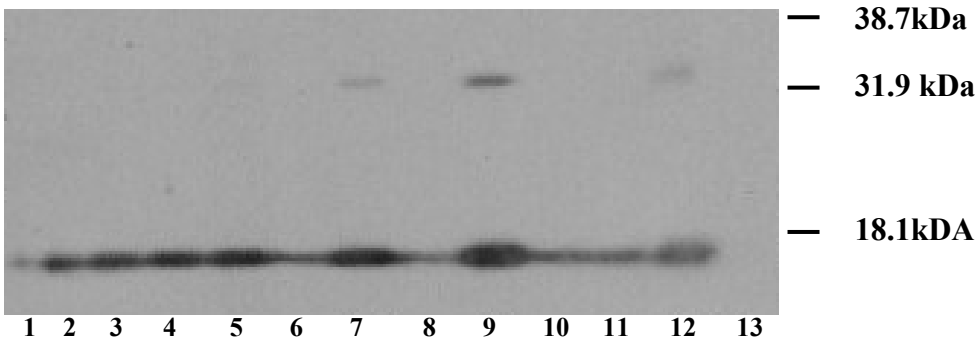

Figure 38. Western blot showing the production of curli protein (CsgA) by the wt, *hfq* mutants, and *hfq* complemented strains in wt or *rpoS hns* backgrounds.

Curli proteins were isolated by formic acid treatment from cells streaked with high inoculum on LB and grown at 28C for 48 h. The proteins were probed with anti-AgfA (CsgA) monoclonal antibodies. CsgA monomers are shown by the presence of bands approximately 17 kDa in size. Dimers of CsgA sometimes appear as the upper bands approximately 33 kDa in size. From left to right: Lane 1-5 wt 14028 (1.0, 2.5, 5.0,7.5, 10.0 uL of samples), Lane 6: Δ*hfq::kan* (YA1153), Lane7: YA 1153 complemented with pYA34 (strain YA239), Lane 8: YA 170, Lane 9: YA170 complemented with pYA34 (YA240), Lane 10: *rpoS hns* (YA147), Lane 11: Δ*hfq rpoS hns* (YA183), Lane 12: YA183 complemented with pYA34 (YA 243), Lane 13: LT2 Δ*csgA* (YA151).

Figure 39. Resulting model of Hfq and DsrA involvements in rugose matrix formation.

Known regulatory mechanisms are shown in solid lines, hypothetical mechanisms are shown in dotted lines. Arrows show activation, oval arrows indicate repression, while lines without arrowheads show no involvement. Hfq may affect transcription of both *csgB* and *csgD* promoters directly or indirectly through promoter activator intermediates, while DsrA seems to have less influence on the transcription of the two promoters.

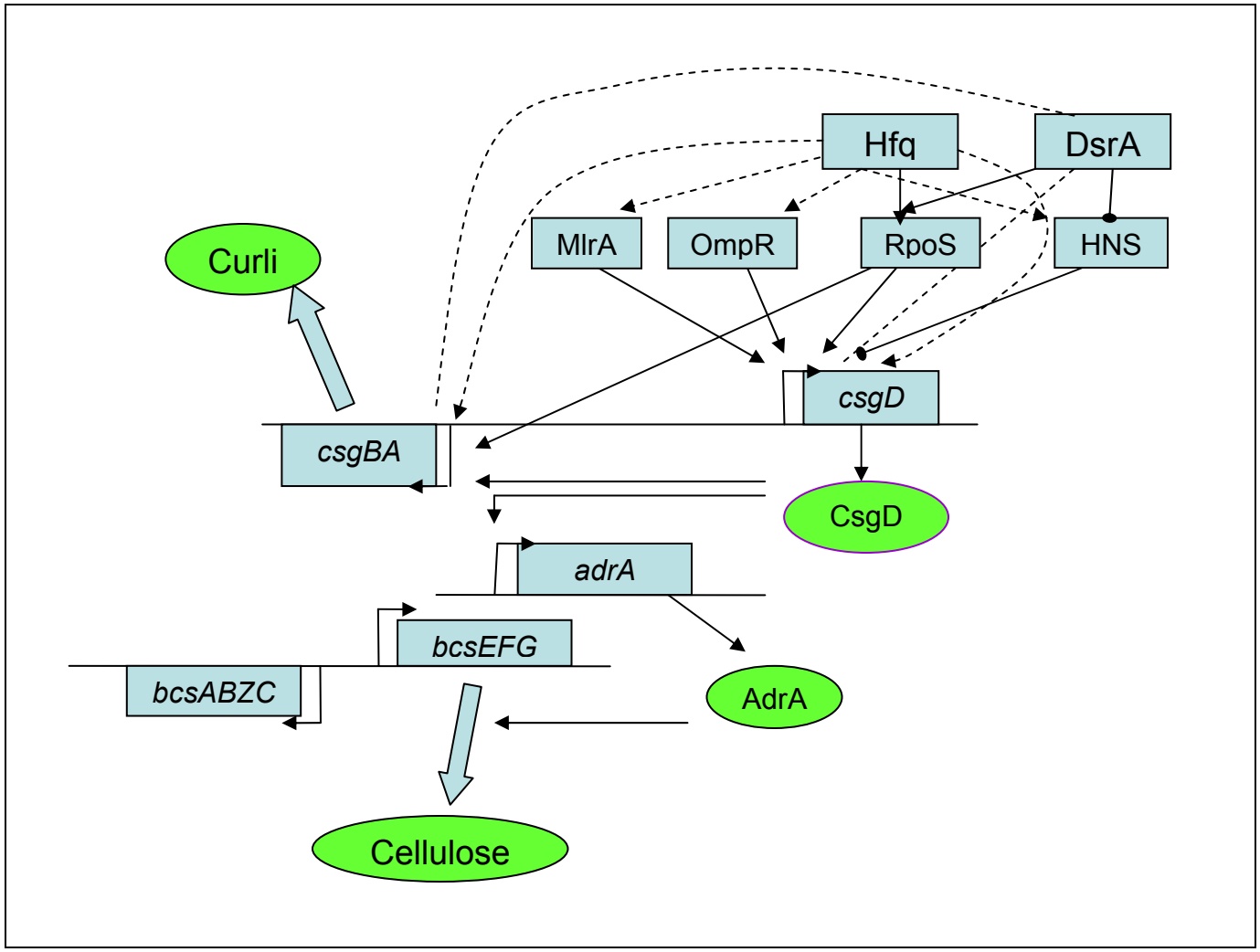
Hfq
DsrA
MlrA
OmpR
RpoS
HNS
Curli
csgD
csgBA
CsgD
adrA
bcsEFG
bcsABZC
AdrA
Cellulose

CHAPTER 5 - Concluding Remarks and Future Directions

1. RUGOSE COLONY PHENOTYPE AND ITS SIGNIFICANCE

Although our past view of bacteria has been focused on individual cells that are free-swimming and growing logarithmically (64), the recent focus on biofilms as a multicellular form of bacteria forming at the stationary phase of growth has caused us to shift our attention in another direction (47). In much the same way, rugose colonies, cellular aggregates forming at late stationary phase, have now received more consideration. While studies in clinical bacteriology and molecular biology have required use of pure cultures of freshly grown cells with smooth colony types, other colony types were considered as "contaminants", as shown by Bruce White's study (263). However at present, there is more evidence suggesting that rugose or wrinkled colony types, exhibited mostly at stationary phase, are probably an easily visible screen for matrix and biofilm formers.

This study was initiated with screening for alteration of the rugose phenotype. Actually, some of the transposon mutants used had slight alterations of the rugose phenotype. However, subsequent analysis actually showed that, in the case of *waaG* mutants, these slight alterations, in fact, resulted from changes in the matrix. A similar observation was shown in *Pseudomonas*, where a slight alteration of growth media by addition of increasing amounts of glucose, actually changed the colony phenotype, probably due to changes in the matrix constituents (29, 30). While this phenotype appeared to be trivial at first, it has now served as a good indication of matrix production.

The present study, using initial colony morphotype for screening, has resulted in a very interesting and important finding regarding the requirement of intact cell surfaces on rugose phenotype (Figure 24). We showed that changes in LPS brought about changes in cell surface properties, and resulted in a dramatic change in the ability of cells to produce cellular appendages under certain conditions, which may promote their dispersion or adhesiveness to surfaces and with each other.

How can the results of this study be possibly implemented in the control of biofilms? Knowing the importance of both substratum and cellular surfaces in affecting initial attachment for cells, there is a potential to alter the properties of the *substratum*. For example, application of some substance that can alter the "conditioning film", a thin layer of substance that forms immediately after a solid object is submerged in growth media, may either reduce or eliminate attachment at the first stage of biofilm formation by altering the physicochemical property of the substratum (178). In addition, changes in *bacterial* surface can facilitate either dispersion or adhesion to a surface, as well as cell-to-cell aggregation. Therefore, the results from the present study could be considered in two different ways. Firstly, control of biofilm formations may be exerted by a modification of the substratum that could lead to alteration of surface molecules on the cell, which in turn may bring about changes in expression of genes participating in matrix production. It has been shown that bacteria growing on a surface upregulate expression of a large number of genes, including those encoding the biosynthetic machinery for LPS (255). Thus, any modification that could interfere with such gene expression may be considered. The results of this study suggest a defensive response from the organism, however, i.e.- alteration of cell surface properties may lead to activation of alternative

pathways for biofilm formation. Therefore, we must consider that the organisms can follow multiple pathways, a perspective that should receive high priority in research endeavors.

2. FURTHER STUDIES ON BIOFILMS

Research on biofilms has intensified in the past few decades. The stages of biofilm formation have been established, although variations among different bacterial species exist. Formation of biofilms is a significant feature in the list of cellular characteristics that make cells resistant to antibiotics. We know that environmental conditions affect matrices and shapes of biofilms. However, the question now becomes, how are the different pathways of matrix formation regulated within a single species of bacteria? Could it be that they are phase shifted? Or instead of on-or-off switches, could matrix production be regulated for gradual expression? We have seen in some examples how tightly biofilms are regulated. For example, in *Salmonella*, three different two-component systems are actively sensing osmolarity changes and send the message inside the cells whether or not to produce biofilms (118). Both OmpR and CpxR respond to changes in osmolarity, although they act in opposite ways to ensure that biofilms or the multicellular form is produced under the right conditions. When growth conditions change to low osmolarity, for example, OmpR binds to its binding region, while some CpxR molecules are still bound to their binding sites. Hence, rather than redundant, the involvement of the two systems allows the cells to fine tune the response, such that a gradual change results.

It is evident that, although initial studies on biofilms were possible because of the finding of biofilms generated from a single species, such as *Pseudomonas,* in the lungs of a cystic fibrosis patient, biofilms in nature contain mostly mixed species, such as those in river streams and dental plaques. Although the study of a mixed species now seems to be very complicated, it may well be necessary to further our understanding of bacteria in nature. The term multicellular behavior in bacteria may be better comprehended by viewing it as a symbiotic relationship among cells in their natural habitat, each of which contributes to the overall differentiated and distributed functions of the biofilms.

Multicellularity has been implicated not only in a differentiated structure such as biofilms, but also in the formation of structured multicellular systems in a monotype bacterial colony, presumably originating from clones of a single bacterium. These observations were exemplified in the formation of highly structured two dimensional fractal colony patterns in *Bacillus subtilis*, forming lattice and snow-flake-like structures (150) that was formed only under the highest concentration of agar and lowest concentration of nutrient. Changing the concentrations of either agar or nutrients resulted in different patterns, indicating that both nutrient availability and agar wetness may dictate the morphology. Another example was observed in *E. coli* colonies exhibiting different expressions of β-galactosidase when grown in media containing X-gal (216). Newly growing cells on the periphery of colonies showed patterns of blue colors alternating with white, or there were differential expressions within wedges of a single colony. Thus, these observations suggested (i) that cells in a colony are not merely aggregates of the same type, and (ii) they are not passively present in the colony as a result of multiplication.

The ability of bacteria to develop patterned bacterial colony morphology is quite fascinating. The process is dictated by both environmental and genetic factors. It was thought that the *dcw* (division cell wall) locus, which includes *ftsZ*, plays a role in determining the direction of cell separation after septation at the boundary of the colonies. Secretion of metabolic byproducts at the site where nutrients become limiting may act as a signal for cells to continue dividing or to be immobilized, and restraint of bacterial motility is an important factor that determines colony morphology (154). Some bacteria, such as *Bacillus subtilis*, release sufactants to modify surface wetness, a process called self-chemotaxis, where bacteria react to their own secretion, to influence the colony pattern (150). In addition, cells use both spatial and temporal regulation for colony expansion. For example, in *Bacillus* the pattern is governed by alternating mound and jet movement of the cells. The concentration gradient of nutrients, as influenced by growth in the neighboring cells, may also be an important factor (207).

Electron microscopic observations in *S.* Typhimurium, in the present study, revealed differences between cells in different parts of a rugose colony. Considering the wrinkles formed on the colony surface, cells on the "hill" seem to be covered more by the matrix, while those in the "valley" consisted mainly of actively replicating cells lacking matrix (data not shown). Cells on the bottom of a rugose colony produced different amounts of matrix than those on the cell surface (see Figure 13A and Figure 13B). Apparently, division of labor does occur in a colony, possibly for survival advantages of the bacterial community. What mechanisms do *Salmonella* use to communicate the message to other members of the community?

Although much has been accomplished in biofilm research, many of the studies were done on submerged biofilms or those attached to surfaces at liquid-air interface. Compared with our knowledge of biofilms, very little is known about pellicles. Pellicles were originally thought to be formed only by fungi. Now, additional studies have shown that they are formed by many bacterial genera such as *Pseudomonas, Staphylococcus, Vibrio,* and *Aeromonas*. Pellicles represent multicellular behavior in static media, a behavior pertinent to environments such as swamps and marshes. Pellicles presumably have a major potential for disease spreading because of its location at the water surface and because of the presence of a large number of cells in very strong aggregates. In addition, pellicles represent another example of division of labor among cells in an aggregate with oxidative capabilities on the surface versus those with fermentative capabilities on the bottom side (265). Biofilms are very much dependent on environmental conditions, and sometimes multiple alternative pathways seem to be utilized by the cells. My findings have shown that although rugose colony formation and biofilm formation are both expressed by a strain, their correlations are not always linear. In contrast, formation of pellicles in rich liquid media seems to be very much correlated with the expression of rugose phenotypes on rich solid media. Because of the correlation, it is tempting to suggest that the components of the matrix in pellicles may be the same as those in the rugose colonies. However little has been done to analyze these components biochemically, although mutation analysis seems to suggest that both cellulose and curli do affect the pellicle texture. We have shown that cells in pellicles are covered with capsular-like materials. What makes up the capsular material? Comparison between a wt strain and colanic-acid deficient mutants showed no significant differences in biofilm

structure (186). Under what conditions is colanic acid expressed? It is still unknown why different strains of *Salmonella* having the same mutation, e.g.- *waaG*, either produce or do not produce colanic acid. Does *Salmonella* Typhimurium produce colanic acid capsule under conditions where pellicles are formed? Are bacteria capable of producing both colanic acid and cellulose and expressing them both? If they do, is there a "phase" regulation modulating the expression of either or both?

Almost certainly in nature, pellicles would be formed by mixed species. To date, only a few studies have been performed on pellicle development. In one, it was shown that motility is required for the movement of bacteria to the surface to form pellicles, however, flagella are not required for matrix production (200). The cells lacking flagella formed clumps instead of pellicles. In another study it was interestingly shown that, although cellulose non-producing bacteria cannot form pellicle by themselves, they are similarly incorporated into the pellicle with the wt cells when the two types of cells were mixed together (212). Pellicle formation was not much affected in this mixture. It was further shown that pellicles are not buoyant. Although they form aggregates on the surface of broth media, they require attachment to a support such as the wall of the tubes. Extended incubation of tubes containing pellicles showed that undisturbed pellicles eventually would sink in broth media after self-detachment. Thus pellicles possibly serve a function similar to that of a consortium for cellular communities to disperse cells. However, many questions are still unanswered. How do cells form pellicles? How do they sense the oxygen tension in the growth media? How do cells come together to the surface and form aggregates? What promotes recruitment of cells to the pellicle? Are

there dynamics in the pellicles similar to those seen in biofilms? Further studies may aid in filling the gaps between the present findings.

3. THE NEW PLAYERS: CELLULOSE AND c-di-GMP

Investigations of rdar (rugose) colonies first revealed the involvement of curli, and then the study with the curli regulator CsgD further led to discovery of cellulose (221, 279). Cellulose was originally considered to be a product exclusive to plants, but that premise changed after cellulose production was also demonstrated in a few bacteria, e.g. the plant pathogen *Agrobacterium,* during pathogenesis, and acetic acid bacteria, *Gluconobacter xylinus*, which are found in fruits. More recent findings by Romling's group (279) as well as Lassa's (221) have expanded further the number of microorganisms capable of cellulose production. The use of bacterial cellulose (biocellulose) in industry has been practiced for a number of years, mostly from *Gluconobacter xylinus* (203). These most recent findings could provide new opportunities to engineer biocellulose synthesis in *E. coli* or *Salmonella*, two of the well-studied enteric bacteria. Many biotechnology applications have used *E. coli* because of ease of growth and the abundantly available information about this organism. The opportunity to increase yield would be desirable, and the use of a curli deficient mutant or a *waaG* mutant might be a possible approach for improving cellulose production.

Early studies in biocellulose synthesis in *Agrobacterium* and *Gluconobacter* also revealed the utilization of GGDEF proteins as c-di-GMP cyclases in the synthesis of c-di-GMP, and proteins with EAL domains, which putatively function as phosphodiesterases, to degrade the c-di-GMP to maintain the normal level of this molecule. The recent

findings of cellulose production in enteric bacteria have caused investigators to reconsider the roles of c-di-GMP. Several studies have shown that this molecule may play an even greater role in bacterial communication for biofilm formation, causing a switch to a sessile mode of growth (1). This type of regulation has been demonstrated in a number of bacteria expressing rugose (wrinkled) phenotypes, such as *Pseudomonas fluorescens and P. aeruginosa, Gluconobacter xylinus, Salmonella Typhimurium, Escherichia coli, Vibrio cholerae and V. parahaemolyticus,* and *Yersinia pestis* (1, 52, 197, 242). Further genetic studies have demonstrated c-di-GMP to be a novel secondary messenger for a number of systems, including positive regulation of cellulose and curli production, as well as repressor for motility (52, 197). However, biochemical studies are still required to confirm these largely genetic-based hypotheses, rooted in DNA and amino acid sequence homologies. Since intercellular signaling, in either liquid or solid media, must occur for the coordination of multicellular behaviors, it would be of interest to elucidate how the signaling takes place. The molecule responsible for this communication in *Salmonella* has not been discovered, and the involvement of AI-2 autoinducer has been excluded (83, 260). The involvement of c-di-GMP seems to suggest that this molecule may be a candidate for cell-to-cell signaling.

4. IS sRNA THE NEXT REGULATOR?

Complex regulation of rugose morphology has mainly been studied at the transcriptional level, with the findings showing that a number of DNA binding proteins are involved (Figure 1). However, the regulatory picture is yet to be completed. For instance, the temperature regulator and sensor for rugose morphology is still unknown. In

E. coli, Crl protein presently controls temperature regulation at the *csgB* promoter by direct binding to regulate its activity, while DsrA acts as a temperature control to regulate the amount of σ^S in the cell (24); however, the temperature control of the central regulator CsgD is still unknown. It has been postulated that in addition to Crl, there may be another mechanism of temperature regulation because the transcription of *csgBA* is still temperature-dependent in *rpoS hns* double mutant background (9, 24). Our finding in *Salmonella* Typhimurium showed a discrepancy in these results, since we showed that the temperature regulation of PcsgB was eliminated in the *rpoS hns* background, further suggesting that Crl may be regulating temperature dependence of P*csgB*.

In addition, we showed that the RNA binding protein Hfq is involved in positive regulation of both *csgB* and *csgD* promoters (Figure 39). The involvement of Hfq has provided a strong indication that RNA, and possibly sRNA, might be involved. Hence, the intricate regulation of rugose morphotype may include yet another level, i.e.-post transcriptional. Would a known or newly discovered sRNA, act together with Hfq to regulate temperature sensitivity of rugose expression? The present study seems to rule out the sRNA, DsrA, a temperature regulator for RpoS expression, as a temperature regulator for the rugose morphotype expression . Much has been learned about the sRNA regulatory mechanism in *E. coli,* but whether the same mechanisms apply to either *Salmonella* or other bacteria remains to be explored.

Other evidence has also indirectly hinted at the involvement of sRNA in the rugose morphotype. For example, the activation of the RcsC two-component system induces sRNA RprA, which in turn activates RpoS. Thus changes in the cell surface, such as in the LPS, as sensed by RcsC, can be manifested as an increase in RpoS regulated

genes through the activity of RprA, which also requires Hfq for its activity (144). Thus higher activity can possibly be produced, even in the absence of RpoS stimuli such as glucose starvation or oxidative stress. Therefore the findings from the present study can potentially catalyze commencement of new studies on RNA regulation in RpoS-dependent multicellular forms of *Salmonella.* Further, and most interestingly, such studies may shed new light into the mechanism by which the different regulatory systems of LPS, flagella, curli, and cellulose synthesis, are interrelated and synchronized.

5. WHAT ARE THE IMPLICATIONS OF IMPROVED KNOWLEDGE OF C-DI-GMP, HFQ AND/OR SRNA INVOLVEMENT?

The involvement of c-di-GMP in multicellular and sessile modes of growth of a number of bacteria has implicated a requirement for nucleotides. There has been evidence showing that impaired regulation of nucleosides affected the synthesis of c-diGMP, which in turn altered rugose phenotype and Congo red binding (52). For example, mutation in *cytR* in *V. cholerae*, whose gene products function in scavenging of nucleosides, switch the cells to rugose morphology (102). Furthermore, mutation of *pnp*, coding for polynucleotide phosphorylase, an enzyme that regulates mRNA degradation, impaired Congo red binding and *csgA* expression (43). Thus, regulation of nucleotides is indirectly involved in multicellular behavior. It would be interesting to see whether *pnp* mutation exclusively affects mRNA stability or if it also affects sRNA, and hence its interaction with its target mRNA. In fact, alteration of transcript stability has been used as a method by bacteria to adapt to their many environments. Therefore, potentially, control of multicellular phenotypes may be exerted to some extent at this level, as has been

proposed for virulence of *Salmonella* (43), or by affecting Hfq expression or activity, rather than downstream at the synthesis level for matrix components. Finally, many of these questions provide a basis for further research into the exciting field of gene regulation of rugose phenotypes and multicellular behavior in *Salmonella* as well as other bacteria.

APPENDICES

Appendix A- Experimental Protocols

Appendix A.1-Preparation of Electrocompetent Cells and Electroporation

Purpose:

To prepare cells that are ready to be transformed by electroporation.

Protocol:

1. Grow cells O/N in LB with shaking at 37˚C.
2. Subculture 2.5 ml of O/N culture into 250 ml fresh media (1:100), grow at 37˚C shaking 200 rpm until OD_{600} reaches 0.6. For wild type cells this takes 3-4 h.
3. Transfer culture into ice-cold 250 ml-size centrifuge bottles. Keep in ice
4. Refrigerate the centrifuge to 4C by running the centrifuge at 5Krpm for 5 min at 4C.
5. Pellet the cells, 6K 10 min 4˚C.
6. Wash the pellet by re-suspending in 250 ml of **ice-cold** sterile distilled water (1 vol).
7. Centrifuge, 6K 10 min 4˚C.
8. Wash in 125 ml of **ice-cold** water (½ vol). Centrifuge as above.
9. Wash in 10 ml vol of **ice-cold 10% glycerol** (1/15vol). Transfer into 50 ml centrifuge bottles. Centrifuge, 10K 5 min 4˚C.

10. Draw off the supernatant. Resuspend in 10 % glycerol to give a total of 1 ml of suspension. Usually the liquid that remains after you draw off the supernatant is sufficient to resuspend the cells.
11. Aliquot into ice-cold microcentrifuge tubes, 45 µl each.
12. Instant-freeze in ethanol-dry ice bath (recommended, if available), and then freeze at –80˚C.

Notes: refrigerate all tubes and solution at least O/N at 4˚C before use. All the tubes and the cells must be kept in ice during the whole procedure, otherwise the cells can lose their competence.

Transformation by Electroporation

Protocol:

1. Thaw out the electrocompetent cells **in ice**.
2. Chill down the electroporation cuvettes (BIORAD, 2 mm gap) in ice.
3. Turn on the electroporator (Micropulser-BIORAD) and use the EC-2 settting.
4. Have the SOC media ready at RT, and a set of pipettors closeby and set at 1 ml, 40µl, and 2 µl, and disposable 10 ml sterile plastic tubes all labeled with each transformation.
5. Add 2ul of plasmid or DNA to be transformed into one tube of electrocompetent cells, incubate in ice for exactly min.
6. During the 1 min period, pipet out 1 ml of SOC media, set aside. Then dry the chilled cuvette with kimwipes until it's really dry but still cold.

7. After the 1 min period, transfer the cells+plasmid mixture (40 ul) into the dry, chilled cuvette.
8. Pulse by pushing the pulse button down until the machine beeps. (If it doesn't beef or it sparks, the machine will read "arc," the electroporation did not work, redo step5 with a fresh tube of competent cells.)
9. Immediately, add the 1 ml Room temp SOC media into the cuvette, and then transfer the mixture into a sterile 10 ml plastic tube.
10. Shake at 37C for 1-2 hrs.
11. Plate 100 ul onto a selective plate. Incubate plates O/N at 37˚C.

Note: if transforming a temperature sensitive plasmid, do all incubations at 30˚C.

SOC media (1L):

1. Measure ~900ml of distilled H_2O
2. Add 20g Bacto Tryptone.
3. Add 5g Bacto Yeast Extract.
4. Add 2ml of 5M NaCl.
5. Add 2.5ml of 1M KCl.
6. Add 10ml of 1M $MgCl_2$
7. Add 10ml of 1M $MgSO_4$
8. Add 20ml of 1M glucose
9. Adjust to 1L with distilled H_2O.
10. Sterilize by autoclaving.

Appendix A.2-One-Step Gene Knock-out

Purpose:

To delete a single gene from a strain.

Strains, plasmid and media:

- Plasmid pKD46 (Lambda Red) (**Ts**, 6kb, ampR, Lambda under P*ara*) from strain MG1655/pKD 4. To isolate: grow host at **30˚C**.
- Plasmid pKD4 (KanR template) from strain YA103.
- Plasmid pCP20 (to remove kan^R from the deletion mutant)
- Strain ST LT2 (to be deleted)
- LB plates containing kanamycin 50μg/ml or ampicillin 100μg/ml

Protocol:

Preparation of LT2:

1. Make electro-competent LT2 grown at 37˚C. See protocol on electrocompetent cells (Appendix A.1).
2. Transform LT2 with pKD46. Check for the presence of plasmids in the transformants by doing plasmid miniprep.
3. Prepare electrocompetent LT2/pKD46 (Grow LT2/pKD46 at **30˚C)** in LB with amp100 and arabinose 1mM O/N, subculture 1:100 the next day in 5 ml media/amp/ara until OD600= 0.6 (see Appendix A.1).

PCR of Kan R with flanking region:

1. PCR mix:

10x Rxn mix	5μL (already contains 1mM Mg and dNTPs)
Template pKD4	1μl (isolated 6/22, A prep)
Deletion primers	1μl each of 10uM stock (see note below)
dH_2O	41.5 μL
Pfx polymerase	0.5 μl (added last)

   Perform PCR reactions for 30 cycles
2. Run 5μL on gel, if product is there in large quantity, re-run the whole PCR product on Crystal violet gel. Gel extract. Dissolve in 30 μl dH_2O

   Run 3ul on gel. If not much product there, redo PCR.
3. Digest the gel extracted PCR product (total) with DpnI (1 hr to O/N) to digest template, if any, which remains.
4. Clean up the digestion mixture from enzyme and buffer using the columns from Qiaquick gel extraction kit (without running the samples on gel). Elute the DNA in 20ul elution buffer (10 mM Tris pH8.0)
5. Run the gel to check the presence of PCR product.

Electroporation:

1. Transform electrocompetent LT2/pKD46 (40ul) with 2-5μλ of the DpnI-digested PCR product. BIORAD Micropulser setting EC2, 2 mm-gap cuvettes. A negative control was also done (cells pulsed without any DNA).

2. Add 1 ml Room Temperature-SOC media, incubate 1h 37˚C, spread 500 μL onto LB Kan, incubate O/N at 37˚C.

The remaining transformation mix is kept O/N at RT. If there are no colonies from the first spreading, replate the rest of transformation mix. Usually there are between 10-50 transformants.

3. Pick 5 KanR colonies of each transformation, restreak for isolation on an LB plate without antibiotics O/N at 37˚C (to colony purify).
4. Streak each of the 5 on LB and also on LB+ amp100, grow at **37˚C**. Select the **ampS** colonies.
5. If all are still amp^R, restreak on LB and incubate at **43˚C**. Restreak on LB and LB amp to look for amp^S colonies that have lost the plasmid.
6. Repurify those that are amp^S on LB Kan.
7. Prepare glycerol stock from the LB Kan plate.

Notes :

Deletion primers are designed : 50bp tail homologous to the flanking region of the chromosomal region to be deleted plus 20bp homologous region to the drug resistance cassette in pKD3, pKD4 or pKD13.

Appendix A.3-Preparation of Chemically Competent Cells and Transformation by Heat Shock

Purpose:

To prepare cells that are ready to be transformed by heat shock.

Protocol:

1. Grow cells O/N in LB with shaking at 37˚C.
2. Subculture 1 ml of O/N culture into 100 ml fresh media (1:100), grow at 37˚C shaking 200 rpm until OD_{600} reaches 0.6 (could be between 0.5-1.0). For wild type cells to reach OD_{600} 0.6 it usually takes 3-4 hrs.
3. Transfer culture into ice-cold 250 ml-size centrifuge bottles. Keep in ice for 15-30 min.
4. Refrigerate the centrifuge to 4C by running the centrifuge at 5Krpm for 5 min at 4C. Label and chill microcentrifuge tubes for the last step.
5. Pellet the cells 6K 7 min 4˚C.
6. Wash pellet by resuspending completely in 50 ml of **ice-cold** magic solution (1/2 vol).
7. Keep cell suspension in ice for 45 min.
8. Centrifuge 6K 7 min 4˚C.
9. Resuspend pellet in 7 ml of **ice-cold magic solution** (1/15vol).
10. Aliquot into ice-cold microcentrifuge tubes, 100 µl each.

11. Instant-freeze in ethanol-dry ice bath (recommended, if available), and then freeze, or just freeze immediately at –80˚C.

Magic Solution:	$CaCl_2$	60 mM (Stock of 1M, Autoclaved)
	Glycerol	15% (Stock of 50%, autoclaved)
	MOPS (or PIPES)	pH710mM (Stock of 1M, filtered)

Mix with sterile dH2O to the correct concentration, store 100 ml/bottle, covered with aluminum foil at 4˚C

Notes: refrigerate all tubes and solution at least O/N at 4˚C before use. All the tubes and the cells must be kept in ice during the whole procedure, otherwise the cells can lose their competence.

Transformation by Heat Shock

Protocol:

1. Thaw out the chemically competent cells **in ice**.
2. Chill down some microcentrifuge tubes (corresponds to the number of transformations to be done) by placing in ice. Transfer 40 µl of chemically competent cells into each tube.
3. Set the Temperature of the waterbath to 42°C. Prepare the SOC media at RT and disposable 10 ml sterile plastic tubes all labeled with each transformation to be done.

4. Add 2µl-5µl of the plasmid to be transformed into one tube of chemically competent cells, incubate in ice for 30 min (Always include a negative control, where only cells, but no DNA, is added).
5. Transfer the tubes to 42°C waterbath for exactly 1 min.
6. Incubate the tubes by placing in ice for 2 min.
7. Add 250µl SOC media into each tube, and then transfer the mixture into sterile 10 ml plastic tubes.
8. Shake at 37˚C for 1-2 hrs.
9. Plate 100 µl onto a selective plate. Dry the plates, and incubate O/N at 37°C.

Note: if transforming a temperature sensitive plasmid, do all incubations at 30°C.

Appendix A.4-Western blotting of the curli proteins

Curli preparation

Cells were collected from 4-day old plates. Approximately 10 colonies with an estimated diameter of 5 mm were resuspended in 500µl 10mM Tris pH8.0. 100 µl glycine pH2 was added to solubilize non-curli proteins, then the supernatant and the pellet was separated. 200µl of 98% formic acid was added to the pellet to solubilize the curli proteins to subunits, and the formic acid was then removed by lyophilization. The lyophilized samples were resuspended in 1x SDS sample buffer (62.5mM TrisCl pH6.8, 2% SDS, 10%glycerol, 5% mercaptoethanol) before loading. The supernatant was mixed at 1:1 ratio with 2X SDS sample buffer. Five µl of the pellet or 15 µl of the supernatant was loaded in the gel.

Since the pellet contained only a portion of the total protein from the cells, there was a problem of equalizing the amount of protein loaded in the gel. Using the alternative method, this problem was avoided. The cells from the 4-day old colonies were suspended in 10mM Tris pH 8.0 to an OD600 of 3.0, or an OD600 of 2.5 for the rugose cells, which form aggregates. The cells were then pelleted, and the pellet was resuspended in 200 µl of 98% formic acid to extract the curli proteins. The acid was removed by lyophilization, and the dried sample was resuspended in the SDS sample buffer. five µl of each sample was then loaded on the gel.

STEP-BY-STEP PROTOCOL for WESTERN BLOTTING

1. **SDS-PAGE**

Purpose: To separate proteins based on size)

Protocol:

To make 2 minigels:

A. Resolving gel (12% acrylamide): In a disposable 50 mL conical tube

Add:	40% acrylamide (37.5:1 acrylamide: Bis acrylamide) :	3.00 ml
	4x(1.5M) Tris/Cl pH8.8	2.50 ml
	10% SDS	0.20 ml
	ddH_2O	4.30 ml
Total 10 mL		

Mix, degas for 10 min

Then add	10% ammonium persulfate (freshly made)	100µL
	TEMED	10µL

Mix slowly, pour into the gel apparatus in a continuous stream to prevent bubbles. Stop when the top is approximately 1 cm below the teeth of the combs. Usually, one minigel takes about 8 ml.

Layer the acrylamide gel with water saturated butanol (take top layer of the butanol and water mixture) to level the top of the gel.

Polymerization takes about 1 hr. Prepare stacking gel 10 min before the end of the 1 hr period.

B. Stacking gel (4% acrylamide) (for 2 gels) total 5 mL

Add:	40% acrylamide (37.5:1 acrylamide: Bis acrylamide) :	0.50 ml
	4x (0.5M) Tris/Cl pH6.8	1.25 ml
	10% SDS	0.05 ml
	ddH_2O	3.15 ml
		Mix, degas for 10 min
Then add	10% ammonium persulfate (freshly made)	50μL
	TEMED	5μL

Rinse the surface of resolving gel from butanol with 1x SDS PAGE running buffer, use a kimwipe to remove remaining liquid. Then pour the acrylamide mix on top to make the stacking gel. Put the comb last. Polymerization takes 30 min.

2. **PROTEIN STAINING**

Purpose: To view proteins in an SDS gel which will be blotted

Protocol:

1. Soak the gel in **Coomassie Blue Stain** for 30 min with gentle agitation.

(50% methanol, 0.05% Coomassie Brilliant BlueR-250 Sigma, % acetic acid, 40% H_2O) (Dissolve 0.5 g Coomassie blue in 500 ml methanol, then add 100 ml acetic acid and 400 ml dH_2O).

2. Discard the staining solution. Destain by soaking the gel with gentle agitation in **Destaining solution** (5% Methanol, 7% acetic Acid, 8% dH_2O) 2h-O/N, until white background is obtained.
3. Take a picture with the Gel-doc program (Kodak Molecular Imaging Systems), if using UV light, place the gel in the white box-(usually in the drawer under the gel box).

3. **REMOVAL OF THE COOMASSIE BLUE FROM FROM AN SDS GEL**

Purpose: To remove the stain from a gel that will be blotted

Protocol:

1. Soak the gel in d H2O for 15 min
2. Equilibrate by soaking the gel in 25mMTris base/192 mM glycine/1%SDS for 1 h with gentle agitation. (2 parts of 5x Running buffer, 0.9-1 part of 10% SDS, 7 parts dH_2O).
3. Equilibrate in 25mMTris base/192 mM glycine (1X Running buffer) for 30 min.
4. Perform the Western Blot (see below)
5. After the transfer, soak the membrane 10-30 min in 100% methanol (if using nylon or PVDF membrane) to remove bound Commassie blue.

4. PROTEIN BLOTTING (WESTERN BLOT)

Purpose: To transfer proteins from an SDS Gel to a PVDF Membrane.

Note: Always wear **gloves** to handle the gel and the membrane.

Protocol:

1. Remove the stacking gel from the resolving gel.
2. Equilibrate gel 30 min in transfer buffer

   Transfer buffer: 15% methanol in 1X Running Buffer (keep cold at 4˚C).
3. Cut the PVDF membrane (Immobilon, Millipore, IPVM20200, 0.45um pore size) and 4 pieces of filter papers (VWR 28298-022) about the size of the gel +1-2 mm on each edge. Cut top left corner of the membrane to mark the orientation, (**important**).
4. Place transfer buffer in the electrophoresis tank. Assemble transfer sandwich **in order** as below. **All parts** of the sandwich should be wetted with the transfer buffer. To wet the sponge: place inside the tank with the transfer buffer, and then press the sponge to remove bubbles. For the PVDF membrane, just before placing it in the sandwich, immerse the membrane briefly in 100 % methanol (place it at an angle to prevent bubbles).

   Transfer sandwich from the bottom (black side of the sandwich holder) to the top (white side):

   - Fiber pad sponge pre-wetted with the transfer buffer
   - 2 layers of filter paper pre-wetted with the transfer buffer. Remove bubbles from under the filter papers by rolling with a 5 ml pipet
   - The SDS-PAGE gel, cut in the top left corner
   - The PVDF membrane pre-wetted with 100% methanol
   - 2 layers of filter papers pre-wetted with the transfer buffer.
   - Fiber pad sponge prewetted with the transfer buffer

5. Lock the sandwich into place, then place it in the tank. The **BLACK SIDE** of the sandwich should be on the **BLACK SIDE** of the blotting apparatus.
6. Place the cooling pack (kept in –80 freeezer) beside the blotting apparatus.
7. Electroporate 100V for 1 h, (power supply must be able to supply current of about 1Amp).
8. Mark the standard proteins in the ladder with a pencil. (**Important**!)

6. IMMUNOPROBING

Purpose: To probe the protein of interest with an antibody

Protocol:

1. Make sure the standard proteins are marked with a pencil (See 4.8 above)
2. If the blotted gel was stained with Coomassie blue before transfer, place the membrane in 100% methanol for 10 min to remove the bound stain (See 3. 5 above).
3. Place the membrane in TTBS Blocking buffer for 15 min.

   TTBS Blocking buffer: 0.1% Tween-20 in 1x TBS

   (1mL Tween-20 in 1L of 1x TBS)

   10x TBS (Tris-buffered saline pH8.0): 1.5M NaCl, 100mM TrisCl pH8.0 (To make 500 ml: add 50 ml of 1M Tris-Cl pH 8.0 and 43.8g NaCl to dH2O)
4. Block the membrane in 3% milk in TTBS 1h to O/N. (3g skim milk in 100ml TTBS).
5. Rinse the membrane 2x 15 min in TTBS.

6. Dilute the primary antibody in TTBS. (For Rabbit Anti SEF-17 dilute 1:200-1:1000 (5uL in 5mL TTBS)
7. Place the membrane in a sealable plastic bag (3 sides are already sealed the size of the membrane width + 0.5 cm on each side). Place 5 mL of the primary antibody, seal. Rock for 1h in a 360°C rocker. The primary antibody can be reused up to 3 times, keep at 4°C.
8. Wash the membrane in TTBS 3 x 10 min.
9. Dilute secondary antibody (Goat anti rabbit-Horse Radish Peroxidase [HRPO] conjugate) 1:5000 in TTBS (4uL of 1:1 reconstituted Ab:glycerol into 10 mL TTBS), and place it in a plastic tray. Place the membrane in the tray and agitate for 1 h.
10. Wash in TTBS 3x10 min.

7. ECL DEVELOPING

Pupose: To view the probed proteins

Protocol :

1. Drain the TTBS wash from the membrane by holding one corner of the membrane with a forceps and touching the other end across the membrane to a piece of kimwipe.
2. Mix 1 ml of reagent 1 and 1 ml of reagent 2 (Amersham ECL kit). Make sure the pipette tips are changed between the two bottles.
3. Spot the reagent mixture throughout the membrane
4. Incubate for 1 min

5. Expose the membrane to a piece of hyperfilm (Amersham) for 1 min or as long as needed to obtain sufficient band density.

Appendix A.5-Biofilm Assay

Purpose:

To measure the number of attached cells, therefore indicating the level of cell adherence.

Reagents:

1. M63 media (see below) supplemented with 0.5% casamino acids (CAA, vitamin-free)
1. 0.5% crystal violet solution, filtered.
2. 80:20 Ethanol:acetone solution.

Protocol:

Day1.

1. From the glycerol stock, streak for isolation the strain to be tested. Grow O/N at 37˚C with shaking at 250 rpm.

Day 2:

1. Inoculate 1ml M63+ 0.5% CAA media O/N with a single colony from the plate. Include an uninoculated tube as a negative control.

Day 3:

1. Dilute the O/N culture 1:100 (2 ml of CAA media + 20 µl of O/N culture). Place the diluted culture in a sterile trough. Transfer 100 µl of the diluted culture into

each of two columns of wells in the microtiter plate (PVC, Falcon 35-3912, lid 35-3913) using a multichannel pipettor.

Repeat for M63+ 0.5% CAA media only (for a negative control) in two columns of the plate.

2. At particular time points, take the absorbance at 595nm of the plate (Ascent Multiskan reader)
3. Then add 50 µl of 0.5 % crystal violet (let the solution sit for at least a week before use to prevent having clumps). Leave the microtiter plate at RT for **15 min**.
4. Wash the plate by first pouring the stained culture into a beaker, and then immersing the microtiter plate several times into a kill pan filled with tap water until it runs clear. **Disinfect** both wash containers with concentrated bleach.
5. Air-dry the plate in the hood for **30 min**.
6. Add 200 ul 80:20 Ethanol:acetone solution into each well. Leave for **exactly 10 min** at RT.
7. During the 10 min period, transfer 112.5ul of 80:20 Ethanol:acetone solution into each well of a new sterile Costar microtiter plate.
8. Transfer 12.5 ul of the CV-stained solution from step 5 above into corresponding wells in the Costar plate (total now is 125ul/well, 1:10 dilution).
9. Read OD at 595 nm using the microtiter reader

M63 Media (5X): with 0.2% glu and 0.5% CAA (Per L):

KH2PO4	68.0 g	Add dH_2O to 1L, Autoclave
$(NH4)_2$ SO4	10.0 g	
$FeSO4.7H_2O$	2.5 mg	

Carbohydrate solution	10.0 ml	Filter sterilize separately
$MgSO4.7H_2O$	1.0 ml	
Casamino acids	50.0 ml	

pH 7.0 $\pm$ 0.2 at 25˚C

Carbohydrate solution (20%) : 20g of glucose, add dH_2O so that the total volume 100 mL dH_2O. Filter sterilize

$MgSO_4.7H_2O$ (1M) : add 24.65g MgSO4.7H2O to 100 mL dH_2O. Mix & filter sterilize

Casamino acids (10%) : add 20g to dH2O so that the final volume is 200 mL. Mix and filter sterilize.

To make 1L of a 1x media:

Cool media after autoclaving to 40C, aseptically transfer:

200 ml of 5x stock solution

779 mL of sterile dH2O,

10mL 20% glucose solution,

1 mL of 1M MgSO4.7H2O solution

50mL 10% casamino acids solution. Mix thoroughly.

Appendix B - Determination of total cell density and the number of attached cells to complement the crystal violet assay to measure early adherence

Purpose

This experiment was performed to complement the microtiter crystal violet assay (see section 3.13 in chapter 3) to measure the number of cells adhering to the PVC surface, which correlates with the amount of biofilm formed early by the wt and the LPS mutants. Since the mutants had alterations in their cell walls, it was necessary to show that the increase in the amount of crystal violet reflected an increase in the number of attached cells, and not an increase in crystal violet binding by the same number of mutant cells as observed in the wt.

Method

100 μL of overnight cultures from the wt and the mutant strains (OD_{600} adjusted to 1.5) grown in M63 media supplemented with 0.5% casamino acid and 0.2% glucose with (for the mutants) or without antibiotics were added to wells in a Falcon PVC microtiter plate (35-3912 and 35-3913) and incubated without shaking at 37°C for eight h. Absorbance at 595 nm was determined in a microtiter plate reader (Multiskan Ascent, Labsystems, Thermo Electron, Waltham, MA) to determine the total cell density, i.e. attached and planktonic cells. Because some cells settled to the bottom of the wells, the plates were mixed well before absorbance was read. The cell suspension was transferred to a new Corning microtiter plate, and the absorbance at 595 nm was read to quantify the

number of unattached (planktonic) cells. The population size of attached cells was determined by subtracting the OD595 of the planktonic cells from that of the total cell density from corresponding wells. Values from replicate assays in 8 to 15 wells were averaged.

Results

The results are shown in Figure 40.

Conclusions

The results from this experiment (Figure 40) seemed to correlate with those in the crystal violet assay (see Figure 20), showing that the increase in crystal violet binding in the *waaG* and *ddhC* mutants was concomitant with an increase in the percentage of attached cells, indicating that both mutations resulted in increased cell adherence.

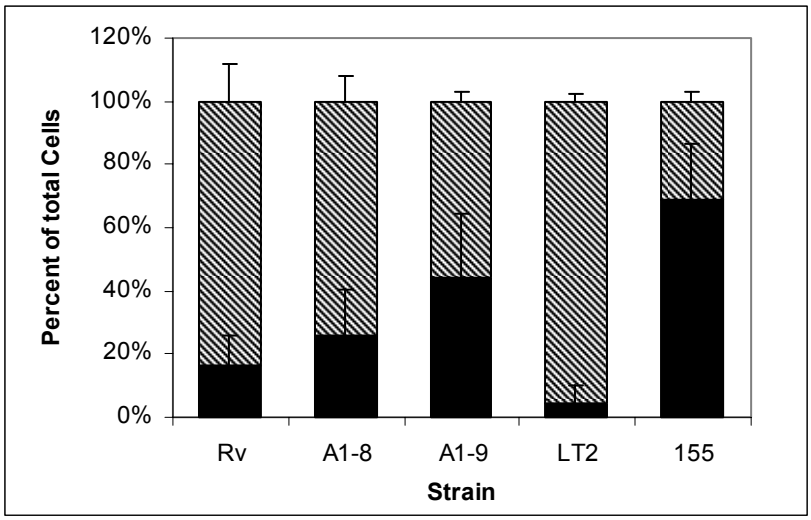

Figure 40. Initial adherence of *S*. Typhimurium DT104 Rv and LT2 and their mutants to PVC surface.

Cells were grown in M63 media supplemented with 0.2% glucose and 0.5 % CAA in microtiter wells for 8 hours, and the density of swimming (planktonic) cells (hatched area) and the attached cells (solid area) were determined as described in methods. Rv: wt; A1-8, *ddhC*::Tn5, A1-9, *waaG*::Tn5; LT2, wt; YA155, Δ*waaG*::Kan, YA156, complemented strain of YA155.

Appendix C - List of Strains Used in This Study

The following table includes all the strains used in this study as listed by strain number. Although in the text (chapter 4) all the strains were listed as either the wt, mutant and complemented strains, e. g. 14028, Δ*hfq* (YA171), and Δ*hfq*(pYA34) or (YA 240), all strains carrying additional plasmids were numbered differently (hence, 14028 carrying pQF50Cm or pYA26 would have two different numbers). The mutation in *rpoS* was *rpoS*::pRRT1, originated from strain TE5395, and for simplicity, will be referred to as *rpoS*, while that in *hns* was *hns*1::Kan from strain TE7505, and will be referred to as *hns*.

Table 9. Strains used in this study as listed by strain numbers

Strain	Relevant Characteristics	Source, Reference or Description
E .coli		
YA103	*E. coli* λpir (pKD4)	Invitrogen
YA237	TOP10 *E. coli* (pYA 34)	*hfq* in EcoRI site of pACYC 184
YA238	TOP10 *E. coli* (pYA 35)	*dsrA* in EcoRI site of pACYC 184
S. typhimurium LT2		
YA150	wt LT2	B. Bassler
TE5395	*rpoS*::pRRT1	T. Elliott
TE7505	*hns1*::Kan	
YA104	LT2 (pKD46)	Wt LT2 carrying the λ-red helper plasmid

YA105	14028 (pKD46)	Wt 14028 carrying the λ-red helper plasmid
YA 151	LT2 Δ*csgA*	LT2 with *csgA* deletion
YA 153	LT2 Δ*hfq*	LT2 with *hfq* deletion
YA 157	LT2 Δ*dsrA*	LT2 with *dsrA* deletion
YA 158	YA157 (pYA31)	*dsrA* deletion complemented
S. typhimurium 14028	$rugose_{28C}$, $smooth_{37C}$	BD Scientific
YA1153	Δ*hfq*::*kan*	153x14028
YA1157	Δ*dsrA*::*kan*	157x14028
YA1158, (also see YA255)	YA1157 (pYA31)	Δ*dsr::kan* complemented
YA130	14028 (pYA25)	14028 (P*csgB-lacZ*)
YA131	14028 (pYA26)	14028 (P*csgD-lacZ*)
YA136	YA1157 (pYA25)	Δ*dsrA*::*kan* (P*csgB-lacZ*)
YA137	YA1157 (pYA26)	Δ*dsrA*::*kan* (P*csgD-lacZ*)
YA138	YA1158 (pYA25)	Δ*dsrA*::*kan* complemented (P*csgB-lacZ*)
YA139	YA1158 (pYA26)	Δ*dsrA* complemented (P*csgD-lacZ*)
YA141	14028 (pQF50Cm)	Wt carrying the promoter-fusion vector
YA143	LT2 Δ*csgD*	*csgD* deletion mutant
YA144	14028 *hns*1::*Kan*	TE7505x14028
YA145	*rpoS hns*	TE7505xTE5395
YA146	*rpoS hns*	TE5395xTE7505
YA147	*rpoS hns*	TE5395xYA144
YA162	1153 (pYA25)	Δ*hfq*::*kan* (P*csgB-lacZ*)
YA163	1153 (pYA26)	Δ*hfq*::*kan* (P*csgD-lacZ*)

YA165	1153 (pQF50Cm)	Δ*hfq* carrying the promoter-fusion vector
YA166	1157 (pQF50Cm)	Δ*dsrA* carrying the promoter-fusion vector
YA167	1158 (pQF50Cm)	Δ*dsrA* complemented carrying the promoter-fusion vector
YA168	131(pWSK29)	Wt 14028 (P*csgD-lacZ*) carrying complementation vector
YA170	Δ*hfq*	*hfq* deletion mutant without kan^R marker
YA171	Δ*dsrA*	*dsrA* deletion mutant without kan^R marker
YA172	Δ*hfq rpoS*	TE5395xYA170
YA173	Δ*hfq hns1::kan*	TE7505xYA170
YA174	Δ*dsrA rpoS*	TE5395xYA171
YA175	Δ*dsrA hns1::kan*	TE7505xYA171
YA176	Δ*hfq*::*kan rpoS*	TE5395xYA1153
YA177	Δ*hfq*::*kan rpoS*	YA153xTE5395
YA183	Δ*hfq rpoS hns1::kan*	YA173xTE5395
YA185	Δ*dsrA rpoS hns1::kan*	YA175xTE5395
YA186	144 (pYA25)	*hns* (P*csgB-lacZ*)
YA187	144 (pYA26)	*hns* (P*csgD-lacZ*)
YA188	144 (pQF50Cm)	*hns* carrying the promoter-fusion vector
YA189	147 (pQF50Cm)	*hns rpoS* carrying the promoter-fusion vector
YA190	170 (pYA26)	Δ*hfq* (P*csgD-lacZ*)
YA191	171 (pYA26)	Δ*dsrA* (P*csgD-lacZ*)

YA192	172 (pYA26)	Δ*hfq rpoS*(P*csgD-lacZ*)
YA193	173 (pYA26)	Δ*hfq hns*(P*csgD-lacZ*)
YA194	174 (pYA26)	Δ*dsrA rpoS*(P*csgD-lacZ*)
YA195	175 (pYA26)	Δ*dsrA hns* (P*csgD-lacZ*)
YA197	183 (pYA26)	Δ*hfq rpoS hns*(P*csgD-lacZ*)
YA198	185 (pYA26)	Δ*dsrArpoShns*(P*csgD-lacZ*)
YA199	147 (pYA26)	*rpoS hns* (P*csgD-lacZ*)
YA200	170(pYA25)	Δ*hfq* (P*csgB-lacZ*)
YA201	171 (pYA25)	Δ*dsrA* (P*csgB-lacZ*)
YA202	172 (pYA25)	Δ*hfq rpoS*(P*csgB-lacZ*)
YA203	173 (pYA25)	Δ*hfq hns* (P*csgB-lacZ*)
YA204	174 (pYA25)	Δ*dsrA rpoS*(P*csgB-lacZ*)
YA205	175 (pYA25)	Δ*dsrA hns* (P*csgB-lacZ*)
YA206	182 (pYA25)	Δ*hfq rpoS hns* (P*csgB-lacZ*)
YA207	183 (pYA25)	Δ*hfq rpoS hns* (P*csgB-lacZ*)
YA208	185 (pYA25)	Δ*dsrA rpoS hns* (P*csgB-lacZ*)
YA209	147 (pYA25)	*rpoS hns* (P*csgB-lacZ*)
YA210	170(pQF50Cm)	Δ*hfq* carrying the promoter-fusion vector
YA211	171 (pQF50Cm)	Δ*dsrA*carrying the promoter-fusion vector
YA212	172 (pQF50Cm)	Δ*hfq rpoS*carrying the promoter-fusion vector
YA213	173 (pQF50Cm)	Δ*hfq hns*carrying the promoter-fusion vector
YA214	174 (pQF50Cm)	Δ*dsrA rpoS*carrying the promoter-fusion vector
YA215	175 (pQF50Cm)	Δ*dsrA hns* carrying the promoter-fusion vector

YA216	182 (pQF50Cm)	Δ*hfq rpoS hns* carrying fusion vector
YA217	183 (pQF50Cm)	Δ*hfq rpoS hns* carrying the promoter-fusion vector
YA218	185(pQF50Cm)	Δ*dsrA rpoS hns* carrying the promoter-fusion vector
YA219	5395(pQF50Cm)	*rpoS* carrying the promoter-fusion vector
YA220	5395(pYA25)	*rpoS* (P*csgB-lacZ*)
YA221	5395 (pYA26)	*rpoS* (P*csgD-lacZ*)
YA222 (also see 241)	190 (pYA33)	Δ*hfq* complemented (P*csgD-lacZ*)
YA223 (also see 242)	200(pYA33)	D*hfq* complemented (P*csgB-lacZ*)
YA226 (also see 240)	170 (pYA33)	Δ*hfq* complemented
YA227	171 (pYA31)	Δ*dsrA* complemented
YA229	162 (pYA33)	Δ*hfq*::*kan* complemented (P*csgB-lacZ*)
YA230	163 (pYA33)	Δ*hfq*::*kan* complemented (P*csgD-lacZ*)
YA235	5395 (pYA33)	*rpoS*::pRRT1 (*hfq*)
YA239 (also see 233)	1153 (pYA34)	Δ*hfq*::*kan* complemented
YA240 (also see 226)	170 (pYA34)	Δ*hfq* complemented
YA241 (also see 222)	190 (pYA34)	Δ*hfq* complemented (P*csgD-lacZ*)
YA242 (also see 223)	200 (pYA34)	Δ*hfq* complemented (P*csgB-lacZ*)
YA243	183 (pYA34)	Δ*hfq rpoS hns* (*hfq*)

YA244	197 (pYA34)	Δ*hfq rpoS hns* (*hfq*) (P*csgD-lacZ*)
YA245	207(pYA34)	Δ*hfq rpoS hns* (*hfq*) (P*csgB-lacZ*)
YA246	1153 (pACYC184)	Δ*hfq*::*kan* (vector)
YA247	170 (pACYC184)	Δ*hfq* (vector)
YA249	200 (pACYC184)	Δ*hfq* (vector) (P*csgB-lacZ*)
YA250	183 (pACYC184)	Δ*hfq rpoS hns* (vector)
YA251	197 (pACYC184)	Δ*hfq rpoS hns* (vector) (P*csgD-lacZ*)
YA252	207(pACYC184)	Δ*hfq rpoS hns* (vector) (P*csgB-lacZ*)
YA253	14028 (pYA35)	Wt with *dsrA* overexpressed
YA254	131 (pYA35)	Wt with *dsrA* overexpressed (P*csgD-lacZ*)
YA255	1157 (pYA35)	Δ*dsrA*::*kan* complemented
YA256	171 (pYA35)	Δ*dsrA* complemented
YA257	191 (pYA35)	Δ*dsrA* complemented (P*csgD-lacZ*)
YA258	201 (pYA35)	Δ*dsrA* complemented (P*csgB-lacZ*)
YA259	185 (pYA35)	Δ*dsrA rpoS hns* (*dsrA*)
YA260	198 (pYA35)	Δ*dsrA rpoS hns* (*dsrA*) (P*csgD-lacZ*)
YA261	208 (pYA35)	Δ*dsrA rpoS hns* (*dsrA*) (P*csgB-lacZ*)
YA262	1157 (pACYC184)	Δ*dsrA*::*kan* (vector)
YA263	171 (pACYC184)	Δ*dsrA* (vector)
YA264	191(pACYC184)	Δ*dsrA* (vector)(P*csgD-lacZ*)
YA265	201 (pACYC184)	Δ*dsrA* (vector)(P*csgB-lacZ*)
YA266	185 (pACYC184)	Δ*dsrA rpoS hns* (vector)
YA267	198 (pACYC184)	Δ*dsrA rpoS hns* (vector) (P*csgD-lacZ*)
YA268	208(pACYC184)	Δ*dsrA rpoS hns* (vector) (P*csgB-lacZ*)

Appendix D - Sequence of the DNA Regions used for promoter–*lacZ* fusion in pQF50Cm

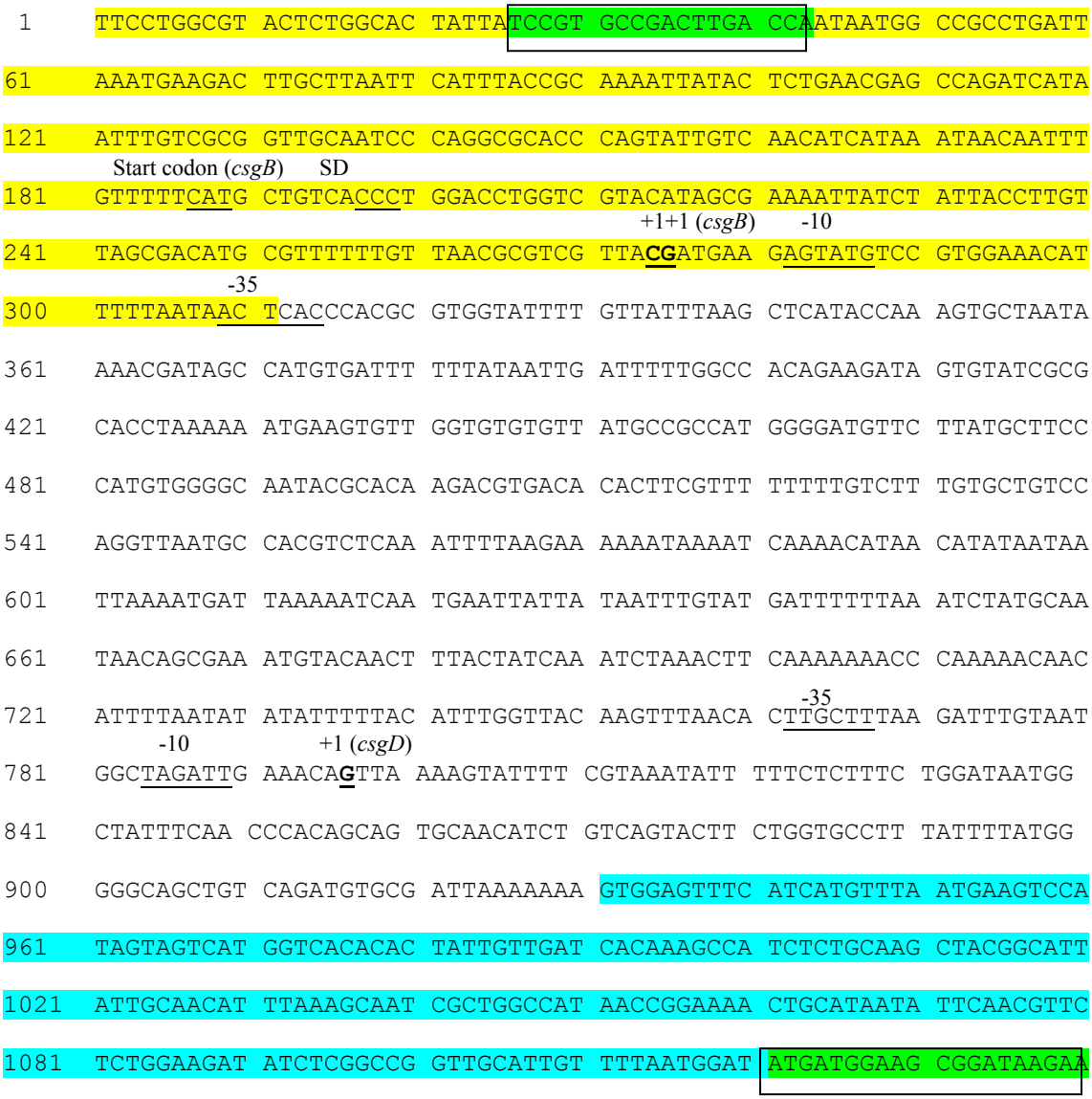

Figure 41. The DNA sequence of the intergenic region between *csgB* and *csgD* Boxed regions indicate the primer sequences used to amplify the DNA region for the *lacZ* fusions. Sequence shown is the complementary sequence from sequence 17460-16321(from accession number AE008749). Highlighted sequences indicate the genes *csgB* (top) and *csgD* (bottom). Promoter sequences are obtained from Gerstel and Romling, 2003 (80) and Collinson *et al*., 1996 (44) for *csgD* and *csgB*, respectively.

Appendix E - Miller Assay Procedure and Calculations

Purpose

To indirectly quantify the activity of the *csgD* or *csgB* promoters that are fused to a promoter-less *lacZ* gene in pQF50Cm.

Reagents

1. Z buffer:

   0.06M $Na_2HPO_4.7H_2O$, 0.04M $NaH_2PO_4.H_2O$, 0.01M KCl 0.001M $MgSO_4$, pH 7.0, and 0.05M β-merchaptoethanol (Sigma) was added just before use.

2. 0.1M Phosphate buffer:

   0.06M $Na_2HPO_4.7H_2O$, 0.04M $NaH_2PO_4.H_2O$, pH 7.0.

3. ONPG solution:

   4mg *o*-nitrophenyl-β-D-galactoside (ONPG) (Sigma) per ml of 0.1M phosphate buffer

4. 1M Na_2CO_3 solution.

Method

Cells were grown under aerobic or microaerophilic conditions (see section 3.10 in chapter 4), and at designated time points, the biofilm attached to the flask's walls, pellicles, and clumps were all mixed with the planktonic cells, and approximately 750µl

samples were transferred into an Eppendorf tube. The OD_{600} of the culture was also measured, when needed.

The samples were sonicated for about 10 sec to disperse aggregated cells, after which between 50 and 200 µl of the sonicated cultures were added into a microcentrifuge tube containing Z buffer to a total volume of 1 ml. Next, 100 µl of chloroform and 50µL of 0.1% SDS were added into each tube, and the tubes were vortexed. After temperature equilibration in a heating block at 28˚C for 5 min, 200 µl of ONPG solution was added to start the reaction (total assay volume was 1.75 ml). Once a yellow color developed, indicating the release of *o*-nitrophenol (ONP), the reaction was stopped by adding 500µl of 1M Na_2CO_3 solution, and the length of time between the start and end of the reaction was recorded. All tubes were vortexed after the addition of each solution. The tubes were centrifuged for 2 min to separate the chloroform residue from the assay mix. The supernatant was transferred into disposable cuvettes and the OD_{420} (wavelength at which light is absorbed by ONP) and OD_{550} (the wavelength at which light is absorbed by media interference) were measured.

To assay the amounts of protein in the samples, 50 µl of the sonicated sample used for the Miller assay was added into 1.5 ml of Bradford reagent (Sigma) at room temperature in 1.7 ml disposable cuvettes. The sample was mixed by pipetting. After 20 min at RT, the absorbance at 595 nm was measured. A standard curve was generated from the absorbance reading of BSA (0.25 to 1.0 mg of BSA per ml of LB media) assayed with Bradford reagent. The concentration of protein in each sample was expressed in mg/ml, and this amount was multiplied by the volume used in the Miller assay (in ml) to obtain total mg protein.

The activity of β-galactosidase was adjusted against cell density (OD_{600}), for which the Miller units were obtained (per min) using this calculation: (1000) (OD_{420}-1.75xOD_{550})/ (t)(V)(OD_{600}) where t is time of the assay in min, and V is volume of culture assayed.

When the presence of clumps and biofilms in some strains prevented us from measuring cell density, activities of β-galactosidase in all strains were also calculated against mg protein, for which the specific β-galactosidase activity was determined as the total micromoles of ONP released per min per mg protein using the following calculations: [(OD_{420}-1.75xOD_{550}) x tot volume in tube] /[ε x tot min x tot mg protein x ml culture assayed], where total volume in tube was 1.75 ml, and the molar extinction coefficient (ε) for ONP was 4.5 (using 1 cm path cuvettes).

Results and conclusions

An example of how the calculations between β-galactosidase activity and the Miller units compare is shown in Figure 42.

The activities shown in nmoleONP/min/mg protein shown in the figure was approximately twice as much as that for the Miller units. However, results from different experiments showed a range between 2-4 times (data not shown). The same patterns of promoter induction or repression were always obtained with both calculation methods.

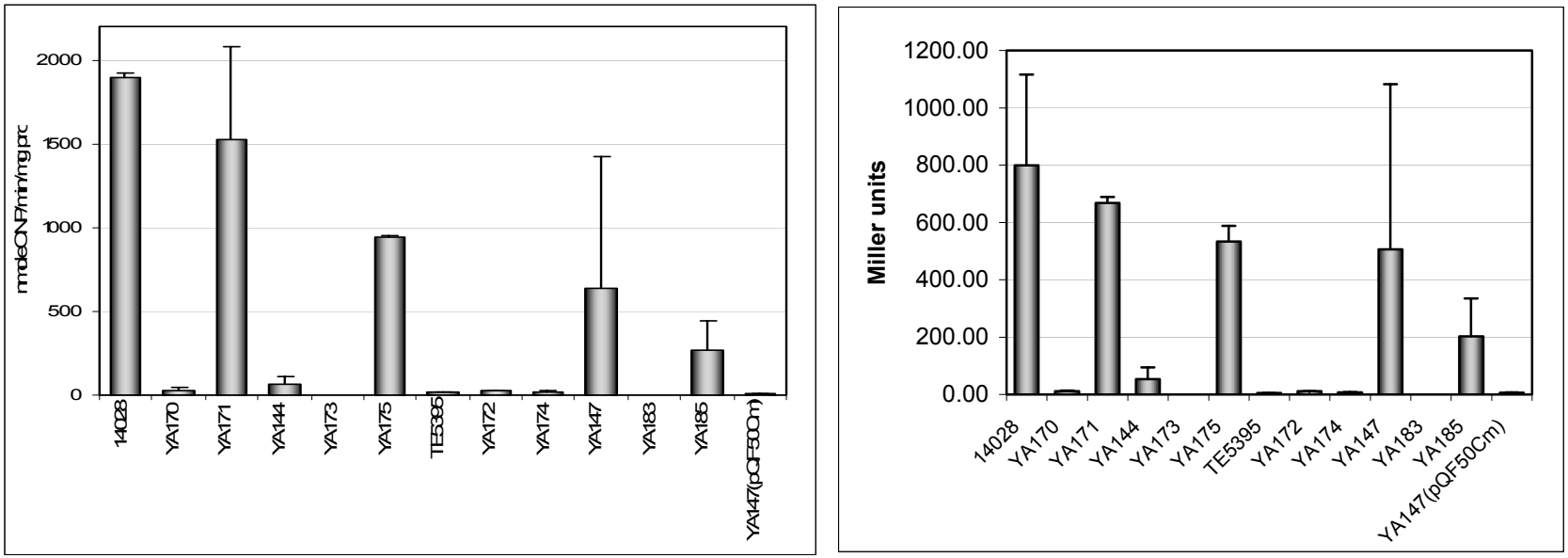

Figure 42. Comparison between Miller units and β-galactosidase specific activities.

The Miller assay was performed on strains grown under aerobic conditions for 24h at 28˚C, and either β-galactosidase activity (in nmole ONP/min/mg prot) (left) or Miller units (right) was calculated. All strains carried the P*csgB-lacZ* operon fusion plasmid (pYA25). From left to right: the wt strain 14028, Δ*hfq* (YA170), Δ*dsrA* (YA171), *hns* (YA144), Δ*hfq hns* (YA173), Δ*dsrA hns* (YA175), *rpoS* (TE5395), Δ*hfq rpoS* (YA172), Δ*dsrA rpoS* (YA174), *rpoS hns* (YA147), Δ*hfq rpoS hns* (YA183), Δ*dsrA rpoS hns* (YA185), and YA147 carrying the fusion vector pQF50Cm.

Appendix F - More data on the Miller assay on P*csgB* activity of *dsrA* mutant in wt and *rpoS hns* background

As discussed in chapter 4, strains carrying *dsrA* mutation, either in wt or *rpoS hns* background showed variations in promoter activities. illustrates these variations when compared to the figures in Chapter 4. For example, while the P*csgB* activity in Δ*dsrA* strain (YA171) seemed to be reduced to approximately half of the wt in the figure below, it was not reduced much in Figure 31 (chapter 4). In addition, the P*csgB* activity in *dsrA* mutant in *rpoS hns* double mutant background (YA185) appeared to be reduced to approximately 66%, while that in Figure 33 (chapter 4) was reduced to approximately 25%, and in Figure 37 it was increased slightly compared to that in the *rpoS hns* background (YA147). Considering these variations, I concluded that the reduction in activity in these mutants was probably not significant (indicated by the * mark in Figure 33 in chapter 4).

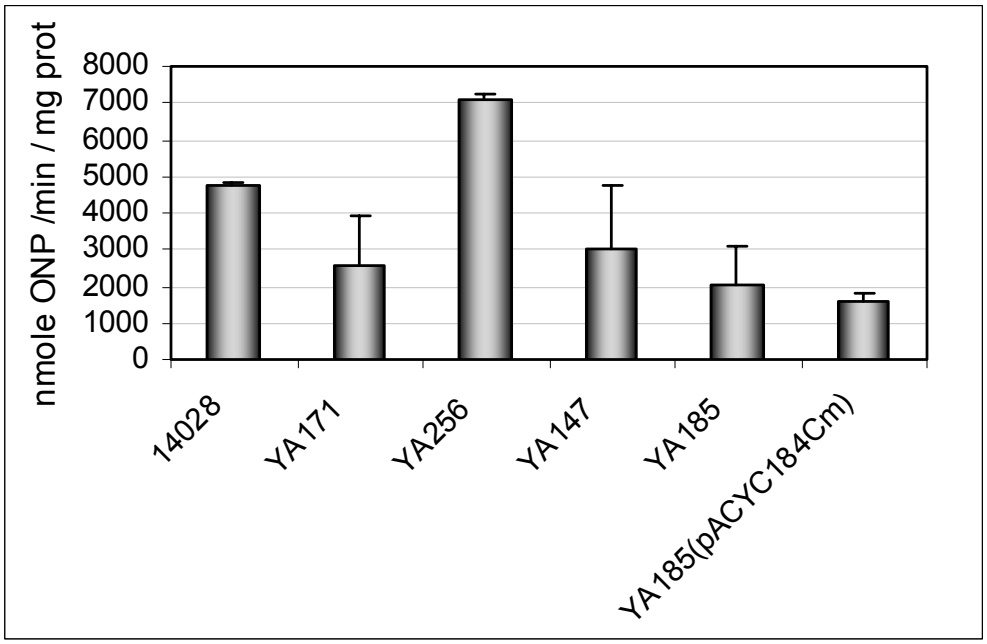

Figure 43. P*csgB* activities from *dsrA* mutant in wt and *rpoS hns* background. The Miller assay was performed on strains grown under aerobic conditions for 48h at 28˚C, and promoter activity was expressed as β-galactosidase activity (in nmole ONP/min/mg prot). All strains carried P*csgB-lacZ* operon fusion plasmid (pYA25). From left to right: the wt strain 14028, Δ*dsrA* (YA171) and *dsrA* complemented strain (YA256), *rpoS hns* (YA147), Δ*dsrA rpoS hns* (YA185) and strain YA185 carrying complementation vector pYACYC184.

REFERENCES

1. **Aldridge, P., R. Paul, P. Goymer, P. Rainey, and U. Jenal.** 2003. Role of the GGDEF regulator PleD in polar development of *Caulobacter crescentus*. Mol. Microbiol. **47:**1695–1708.

2. **Ali, A., J. A. Johnson, A. A. Franco, D. J. Metzger, T. D. Connell, J. G. Morris, Jr., and S. Sozhamannan.** 2000. Mutations in the extracellular protein secretion pathway genes (eps) interfere with rugose polysaccharide production in and motility of Vibrio cholerae. Infect. Immun. **68:**1967-1974.

3. **Altier, C.** 2005. Genetic and environmental control of *Salmonella* invasion. J. Microbiol. **43:**85-92.

4. **Altier, C., M. Suyemoto, and S. D. Lawhon.** 2000. Regulation of *Salmonella enterica* serovar typhimurium invasion genes by *csrA*. Infect. Immun. **68:**6790-6797.

5. **Altuvia, S., A. Zhang, L. Argaman, A. Tiwari, and G. Storz.** 1998. The *Escherichia coli* OxyS regulatory RNA represses *fhlA* translation by blocking ribosome binding. EMBO J. **17:**6069-6075.

6. **Anderson, K. E., S. W. Joseph, R. Nasution, Sunoto, T. Butler, P. F. Van Peenen, G. S. Irving, J. S. Saroso, and R. H. Watten.** 1976. Febrile illnesses resulting in hospital admission: a bacteriological and serological study in Jakarta, Indonesia. Am J Trop Med Hyg **25:**116-121.

7. **Anriany, Y. A., R. M. Weiner, J. A. Johnson, C. E. deRezende, and S. W. Joseph.** 2001. *Salmonella enterica* serovar Typhimurium DT104 displays a rugose phenotype. Appl. Environ. Microbiol. **67:**4048-4056.

8. **Arnold, C. N., J. McElhanon, A. Lee, R. Leonhart, and D. A. Siegele.** 2001. Global analysis of *Escherichia coli* gene expression during the acetate-induced acid tolerance response. J. Bacteriol. **183:**2178-2186.

9. **Arnqvist, A., A. Olsen, and S. Normark.** 1994. σ-dependent growth phase induction of the *csgBA* promoter in *Esherichia coli* can be achieved in vivo by σ 70 in the absence of the nucleoid-associated protein H-NS. Mol. Microbiol. **13:**1021-1032.

10. **Austin, J. W., G. Sanders, W. W. Kay, and S. K. Collinson.** 1998. Thin aggregative fimbriae enhance *Salmonella enteritidis* biofilm formation. FEMS Microbiol. Lett. **162:**295-301.

11. **Baggesen, D. L., D. Sandvang, and F. M. Aarestrup.** 2000. Characterization of *Salmonella enterica* serovar typhimurium DT104 isolated from Denmark and comparison with isolates from Europe and the United States. J. Clin. Microbiol. **38:**1581-1586.

12. **Barker, J., and S. F. Bloomfield.** 2000. Survival of *Salmonella* in bathrooms and toilets in domestic homes following salmonellosis. J. Appl. Microbiol. **89:**137-144.

13. **Barth, M., C. Marschall, A. Muffler, D. Fiscer, and R. Hengge-Aronis.** 1995. Role for the histone-like protein H-NS in growth phase-dependent and osmostic regulation of σ^S and many σ^S-dependent genes in *Escherichia coli*. J. Bacteriol. **177:**3455-3464.

14. **Baudart, J., K. Lemarchand, A. Brisabois, and P. Lebaron.** 2000. Diversity of *Salmonella* strains isolated from the aquatic environment as determined by serotyping and amplification of the ribosomal DNA spacer regions. Appl. Environ. Microbiol. **66:**1544-1552.

15. **Bearson, S., J. Benjamin, W. Swords, and J. Foster.** 1996. Acid shock induction of RpoS is mediated by the mouse virulence gene *mviA* of *Salmonella typhimurium*. J. Bacteriol. **178:**2572-2579.

16. **Beasley, W. J., S. W. Joseph, and E. Weiss.** 1981. Improved serodiagnosis of *Salmonella* enteric fevers by an enzyme-linked immunosorbent assay. J. Clin. Microbiol. **13:**106-114.

17. **Beenken, K. E., J. S. Blevins, and M. S. Smeltzer.** 2003. Mutation of *sarA* in *Staphylococcus aureus* limits biofilm formation. Infect. Immun. **71:**4206-4211.

18. **Besser, T. E., C. C. Gay, J. M. Gay, D. D. Hancock, D. Rice, L. C. Pritchett, and E. D. Erickson.** 1997. Salmonellosis associated with *S. typhimurium* DT104 in the USA. Vet. Rec. **140:**75.

19. **Beuchat, L. R.** 1995. Pathogenic microorganisms associated with fresh produce. J. Food Protect. **59:**204-216.

20. **Bian, Z., A. Brauner, Y. Li, and S. Normark.** 2000. Expression of and cytokine activation by *Escherichia coli* curli fibers in human sepsis. J. Infect. Dis. **181:**602-612.

21. **Blum, P. H., S. B. Jovanovich, M. P. McCann, J. E. Schultz, S. A. Lesley, R. R. Burgess, and A. Matin.** 1990. Cloning and in vivo and in vitro regulation of cyclic AMP-dependent carbon starvation genes from *Escherichia coli*. J. Bacteriol. **172:**3813-3820.

22. **Boaretti, M., M. Lleo, B. Bonato, C. Signoretto, and P. Canepari.** 2003. Involvement of *rpoS* in the survival of *Escherichia coli* in the viable but non-culturable state. Environ. Microbiol. **5:**986-996.

23. **Boels, I. C., A. Ramos, M. Kleerebezem, and W. M. de Vos.** 2001. Functional analysis of the *Lactococcus lactis galU* and *galE* genes and their impact on sugar nucleotide and exopolysaccharide biosynthesis. Appl. Environ. Microbiol. **67:**3033-3040.

24. **Bougdour, A., C. Lelong, and J. Geiselmann.** 2004. Crl, a low temperature-induced protein in *Escherichia coli* that binds directly to the stationary phase sigma subunit of RNA polymerase. J. Biol. Chem. **279:**19540-19550.

25. **Boyd, A., and A. M. Chakrabarty.** 1995. *Pseudomonas aeruginosa* biofilms: role of the alginate exopolysaccharide. J. Ind. Microbiol. **15:**162-1688.

26. **Boyd, D., A. Cloeckaert, E. Chaslus-Dancla, and M. R. Mulvey.** 2002. Characterization of variant *Salmonella* genomic island 1 multidrug resistance regions from serovars Typhimurium DT104 and Agona. Antimicrob. Agents. Chemother. **46:**1714-1722.

27. **Boyd, D., G. A. Peters, A. Cloeckaert, K. S. Boumedine, E. Chaslus-Dancla, H. Imberechts, and M. R. Mulvey.** 2001. Complete nucleotide sequence of a 43-kilobase genomic island associated with the multidrug resistance region of *Salmonella enterica* serovar Typhimurium DT104 and its identification in phage type DT120 and serovar Agona. J. Bacteriol. **183:**5725-5732.

28. **Boyd, D. A., G. A. Peters, L. Ng, and M. R. Mulvey.** 2000. Partial characterization of a genomic island associated with the multidrug resistance region of *Salmonella enterica* Typhymurium DT104. FEMS Microbiol. Lett. **189:**285-291.

29. **Branda, S. S., and R. Kolter.** 2004. Multicellularity and biofilms. *In* M. Ghannoum and G. O'Toole (ed.), Microbial biofilms. ASM Press, Washington, D. C.

30. **Branda, S. S., S. Vik, L. Friedman, and R. Kolter.** 2005. Biofilms: the matrix revisited. Trends Microbiol. **13:**20-26.

31. **Briggs, C. E., and P. M. Fratamico.** 1999. Molecular characterization of an antibiotic resistance gene cluster of *Salmonella typhimurium* DT104. Antimicrob. Agents Chemother. **43:**846-849.

32. **Brown, L., and T. Elliott.** 1996. Efficient ranslation of the Rpos sigma factor in *Salmonella typhimurium* requires host factor I, an RNA-binding protein encoded by the *hfq* gene. J. Bacteriol. **178:**3763-3770.

33. **Brown, P. K., C. M. Dozois, C. A. Nickerson, A. Zuppardo, J. Terlonge, and R. Curtiss, 3rd.** 2001. MlrA, a novel regulator of curli (Agf) and extracellular matrix synthesis by *Escherichia coli* and *Salmonella enterica* serovar Typhimurium. Mol. Microbiol. **41:**349-363.

34. **Carlson, S. A., M. Browning, K. E. Ferris, and B. D. Jones.** 2000. Identification of diminished tissue culture invasiveness among multiple antibiotic resistant *Salmonella typhimurium* DT104. Microb. Pathogen **28:**37-44.

35. **Carlson, S. A., R. M. Willson, A. J. Crane, and K. E. Ferris.** 2000. Evaluation of invasion-conferring genotypes and antibiotic-induced hyperinvansive phenotypes in multiple antibiotic resistant *Salmonella typhimurium* DT104. Microb. Pathogen **28:**373-378.

36. **Caroff, M., and D. Karibian.** 2003. Structure of bacterial lipopolysaccharides. Carbohydr Res. **338:**2431-2447.

37. **Catalao, L. P., M. Joao, V. S. Ferreiro, M. L. Fidalgo, M. E. Garcia Rosado, and J. J. Borrego.** 2000. Occurrence of *Salmonella* spp in estuarine and coastal waters of Portugal. Antonie Van Leeuwenhoek **78:**99-106.

38. **CDC.** 1999. *Salmonella* surveillance: annual tabulation summary, 1998. U. S. Department of Health and Human Services, CDC.

39. **Chan, R. K., and D. Botstein.** 1972. Genetics of bacteriophage P22. I. Isolation of prophage deletions which affect immunity to superinfection. Virol. **49:**257-267.

40. **Chapman, M. R., L. S. Robinson, J. S. Pinkner, R. Roth, J. Heuser, M. Hammar, S. Normark, and S. J. Hultgren.** 2002. Role of *Escherichia coli* curli operons in directing amyloid fiber formation. Science **295:**851-855.

41. **Chopra, A. K., J. H. Huang, X. Xu, K. Burden, D. W. Niesel, M. W. Rosenbaum, V. L. Popov, and J. W. Peterson.** 1999. Role of *Salmonella* enterotoxin in overall virulence of the organism. Microb. Pathog. **27:**155-171.

42. **Clarke, D. J., S. A. Joyce, C. M. Toutain, A. Jacq, and I. B. Holland.** 2002. Genetic analysis of the RcsC sensor kinase from *Escherichia coli* K-12. J. Bacteriol. **184:**1204-1208.

43. **Clements, M. O., S. Eriksson, A. Thompson, S. Lucchini, J. C. Hinton, S. Normark, and M. Rhen.** 2002. Polynucleotide phosphorylase is a global regulator of virulence and persistency in *Salmonella enterica*. Proc. Natl. Acad. Sci. U S A. **99:**8784-8789.

44. **Cole, G. T.** 1986. Preparation of microfungi for scanning electron microscopy., p. 1-38. *In* H. C. Aldrich and W. J. Todd (ed.), Ultrastructure techniques for microorganisms. Plenum Press, New York, NY.

45. **Collinson, S. K., S. C. Clouthier, J. L. Doran, P. A. Banser, and W. W. Kay.** 1996. *Salmonella enteritidis agfBAC* operon encoding thin, aggregative fimbriae. J. Bacteriol. **178:**662-667.

46. **Collinson, S. K., L. Emody, K. H. Muller, T. J. Trust, and W. W. Kay.** 1991. Purification and characterization of thin, aggregative fimbriae from *Salmonella enteritidis*. J. Bacteriol. **173:**4773-4781.

47. **Costerton, J. W.** 2004. A short history of the development of biofilm concept, p. 4-19. *In* M. Ghannoum and G. O'Toole (ed.), Microbial biofilms. ASM Press, Washington, DC.

48. **Costerton, J. W., K. J. Cheng, G. G. Geesey, T. I. Ladd, J. C. Nickel, M. Dasgupta, and T. J. Marrie.** 1987. Bacterial biofilms in nature and disease. Annu. Rev. Microbiol. **41:**435-464.

49. **Costerton, J. W., P. S. Stewart, and E. P. Greenberg.** 1999. Bacterial biofilms: a common cause of persistent infections. Science **284:**1318-1322.

50. **Coutard, F., M. Pommepuy, S. Loaec, and D. Hervio-Heath.** 2005. mRNA detection by reverse transcription-PCR for monitoring viability and potential virulence in a pathogenic strain of *Vibrio parahaemolyticus* in viable but nonculturable state. J. Appl. Microbiol. **98:**951-961.

51. **Crerar, S. K., T. J. Nicholas, and M. D. Barton.** 1999. Multi-resistant *Salmonella typhimurium* DT104 - implications for animal industries and the veterinary profession. Aust. Vet. J. **77:**170-171.

52. **D'Argenio, D. A., and S. I. Miller.** 2004. Cyclic di-GMP as a bacterial second messenger. Microbiol. **150:**2497-2502.

53. **Daily, O. P., R. M. Debell, and S. W. Joseph.** 1978. Superoxide dismutase and catalase levels in halophilic vibrios. J. Bacteriol. **134:**375-380.

54. **Dannon, D., L. Goldstein, Y. Marikovsky, and E. Skutelsky.** 1972. Use of cationized ferritin as a label of negative charges on cell surfaces. J. Ultrastruct. Res. **38:**500-501.

55. **Datsenko, K. A., and B. L. Wanner.** 2000. One-step inactivation of chromosomal genes in *Escherichia coli* K-12 using PCR products. Proc. Natl. Acad. Sci. U. S. A. **97:**6640-6645.

56. **Davies, D.** 2000. Physiological events in biofilm formation., p. 37-52. *In* P. G. D. G. Allison, H. M. Lapin-Scott and M. Wilson (ed.), Community structures and cooperation in biofilms. Cambridge University Press, New York, NY.

57. **Davies, D. G., M. R. Parsek, J. P. Pearson, B. H. Iglewski, J. W. Costerton, and E. P. Greenberg.** 1998. The involvement of cell-to-cell signals in the development of a bacterial biofilm. Science **280:**295-298.

58. **Deziel, E., Y. Comeau, and R. Villemur.** 2001. Initiation of biofilm formation by *Pseudomonas aeruginosa* 57RP correlates with emergence of hyperpiliated and highly adherent phenotypic variants deficient in swimming, swarming, and twitching motilities. J. Bacteriol. **183:**1195-1204.

59. **Ding, Y., B. M. Davis, and M. K. Waldor.** 2004. Hfq is essential for *Vibrio cholerae* virulence and downregulates sigma expression. Mol. Microbiol. **53:**345-354.

60. **Dorel, C., O. Vidal, C. Prigent-Combaret, I. Vallet, and P. Lejeune.** 1999. Involvement of the Cpx signal transduction pathway of *E. coli* in biofilm formation. FEMS Microbiol. Lett. **178:**169-175.

61. **Doublet, B., D. Boyd, M. R. Mulvey, and A. Cloeckaert.** 2005. The *Salmonella* genomic island 1 is an integrative mobilizable element. Mol. Microbiol. **55:**1911-1924.

62. **Ducey, T., and D. Dyer.** 2002. Rapid identification of EZ::TN TM transposon insertion sites in the genome of *Neisseria gonorrhea*. Epicentre Forum **9:**6-7.

63. **Dworkin, M.** 1999. Fibrils as extracellular appendages of bacteria: their role in contact-mediated cell-cell interactions in *Myxococcus xanthus.* Bioessays **21:**590-595.

64. **Dworkin, M.** 1997. Multicellularism versus the single microbe, p. 3-13. *In* J. A. Shapiro and M. Dworkin (ed.), Bacteria as multicellular organism. Oxford University Press, New York, NY.

65. **Elsinghorst, E. A.** 1994. Measurement of invasion by gentamicin resistance. Methods Enzymol. **236:**405-420.

66. **Fassel, T. A., and C. E. Edminston, Jr.** 2000. Ruthenium red and the bacterial glycocalyx. Biotech. Histochem. **74:**194-212.

67. **Ferrieres, L., and D. J. Clarke.** 2003. The RcsC sensor kinase is required for normal biofilm formation in *Escherichia coli* K-12 and controls the expression of a regulon in response to growth on a solid surface. Mol. Microbiol. **50:**1665-1682.

68. **Finlay, B. B., S. Ruschkowski, and S. Dedhar.** 1991. Cytoskeletal rearrangements accompanying *Salmonella* entry into epithelial cells. J. Cell Sci. **99:**283-296.

69. **Foster, J. W., and H. K. Hall.** 1990. Adaptive acidification tolerance response of *Salmonella typhimurium*. J. Bacteriol. **172:**771-778.

70. **Foster, J. W., and M. P. Spector.** 1995. How *Salmonella* survive against the odds. Annu. Rev. Microbiol. **49:**145-174.

71. **Francez-Charlot, A., B. Laugel, A. Van Gemert, N. Dubarry, F. Wiorowski, M. P. Castanie-Cornet, C. Gutierrez, and K. Cam.** 2003. RcsCDB His-Asp phosphorelay system negatively regulates the *flhDC* operon in *Escherichia coli*. Mol. Microbiol. **49:**823-832.

72. **Friedman, L., and K. R.** 2004. Genes involved in matrix formation in *Pseudomonas aeruginosa* PA14 biofilms. Mol. Microbiol. **51:**675-690.

73. **Fux, C. A., J. W. Costerton, P. S. Stewart, and P. Stoodley.** 2005. Survival strategies of infectious biofilms. Trends Microbiol. **13:**34-40.

74. **Galan, J. E.** 1996. Molecular genetic bases of *Salmonella* entry into host cells. Mol. Microbiol. **20:**263-271.

75. **Galan, J. E., and R. r. Curtiss.** 1989. Cloning and molecular characterization of genes whose products allow *Salmonella typhimurium* to penetrate tissue culture cells. Proc. Natl. Acad. Sci. U. S. A. **86:**6383-6387.

76. **Garcia-Calderon, C. B., M. Garcia-Quintanilla, J. Casadesus, and F. Ramos-Morales.** 2005. Virulence attenuation in *Salmonella enterica rcsC* mutants with constitutive activation of the Rcs system. Microbiol. **151:**579-588.

77. **Garcia, B., C. Latasa, C. Solano, F. G. Portillo, C. Gamazo, and I. Lasa.** 2004. Role of he GGDEF protein family in *Salmonella* cellulose biosynthesis and biofilm formation. Mol. Microbiol. **54:**264-277.

78. **Gauthier, M. J., B. Labedan, and V. A. Breittmayer.** 1992. Influence of DNA supercoiling on the loss of culturability of *Escherichia coli* cells incubated in seawater. Mol. Ecol. **1:**183-190.

79. **Geissmann, T. A., and D. Touati.** 2004. Hfq, a new chaperoning role: binding to messenger RNA determines access for small RNA regulator. EMBO J. **23:**396-405.

80. **Genevaux, P., P. Bauda, M. S. DuBow, and B. Oudega.** 1999. Indentification of Tn10 in the *rfaG, rfaP*, and *gaIU* genes involved in lipopolysaccharide core biosynthesis that affect *Escherichia coli* adhesion. Arch. Microbiol. **172:**1-8.

81. **Gerstel, U., C. Park, and U. Romling.** 2003. Complex regulation of *csgD* promoter activity by global regulatory proteins. Mol. Microbiol. **49:**639-654.

82. **Gerstel, U., and U. Romling.** 2003. The csgD promoter, a control unit for biofilm formation in Salmonella typhimurium. Res. Microbiol. **154:**659-667.

83. **Gerstel, U., and U. Romling.** 2001. Oxygen tension and nutrient starvation are major signals that regulate *agfD* promoter activity and expression of the multicellular morphotype in *Salmonella typhimurium*. Environ. Microbiol. **3:**638-648.

84. **Ghigo, J. M.** 2001. Natural conjugative plasmids induce bacterial biofilm development. Nature **412:**442-445.

85. **Ginocchio, C. C., S. B. Olmsted, C. L. Wells, and J. E. Galan.** 1994. Contact with epithelial cells induces the formation of surface appendages on *Salmonella* Typhimurium. Cell **76:**717-724.

86. **Giovannacci, I., G. Ermel, G. Salvat, J. L. Vendeuvre, and M. N. Bellon-Fontaine.** 2000. Physicochemical surface properties of five *Listeria monocytogenes* strains from a pork-processing environment in relation to serotypes, genotypes and growth temperature. J. Appl. Microbiol. **88:**992-1000.

87. **Gonzalez-Flecha, B., and B. Demple.** 2000. Genetic responses to free radicals. Homeostasis and gene control. Annu. N Y Acad. Sci. **899:**69-87.

88. **Gophna, U., M. Barlev, R. Seijffers, T. A. Oelschlager, J. Hacker, and E. Z. Ron.** 2001. Curli fibers mediate internalization of *Escherichia coli* by eukaryotic cells. Infect. Immun. **69:**2659-2665.

89. **Goryshin, I. Y., J. Jendrisak, L. M. Hoffman, R. Meis, and W. S. Reznikoff.** 2000. Insertional transposon mutagenesis by electroporation of released Tn5 transposition complex. Nat. Biotechnol. **18:**97-100.

90. **Gottesman, S.** 2004. The small RNA regulators of *Escherichia coli*: roles and mechanisms*. Annu. Rev. Microbiol. **58:**303-328.

91. **Gottesman, S., and V. Stout.** 1991. Regulation of capsular polysaccharide synthesis in *Escherichia coli* K12. Mol. Microbiol. **5:**1599-1606.

92. **Guard-Petter, J., L. H. Keller, M. M. Rahman, R. W. Carlson, and S. Silvers.** 1996. A novel relationship between O-antigen variation, matrix formation, and invasiveness of *Salmonella enteritidis.* Epidemiol. Infect. **117:**219-231.

93. **Gupte, A.** 2001. Determination of viable non-culturability in some *Salmonella* species with evidence of their resuscitation. M. S. Thesis. University of Maryland College Park, College Park, MD.

94. **Gupte, A., C. DeRezende, and S. Joseph.** 2003. Induction and resuscitation of viable but nonculturable *Salmonella enterica* serovar Typhimurium DT104. Appl. Environ. Microbiol. **11:**6669-6675.

95. **Hall-Stoodley, L., J. W. Costerton, and P. Stoodley.** 2004. Bacterial biofilms: from the natural environment to infectious disease. Nature Rev. Microbiol. **2:**95-108.

96. **Hall-Stoodley, L., and P. Stoodley.** 2005. Biofilm fomation and dispersal and the transmission of human pathogens. Trends Microbiol. **13:**7-10.

97. **Halsey, T. A., A. Vazquez-Torres, D. J. Gravdahl, F. C. Fang, and S. J. Libby.** 2004. The ferritin-like Dps protein is required for *Salmonella enterica* serovar Typhimurium oxidative stress resistance and virulence. Infect. Immun. **72:**1155-1158.

98. **Hammar, M., A. Arnqvist, Z. Bian, A. Olsen, and S. Normark.** 1995. Expression of two *csg* operons is required for production of fibronectin- and congo red-binding curli polymers in *Escherichia coli* K-12. Mol. Microbiol. **18:**661-670.

99. **Harrison, J. A., D. Pickard, C. F. Higgins, A. Khan, S. N. Chatfield, T. Ali, D. C. J., C. E. Hormaeche, and G. Dougan.** 1994. Role of HNS in the virulence phenotype of pathogenic salmonellae. Mol. Microbiol. **3:**133-140.

100. **Hasman, H., M. A. Schembri, and P. Klemm.** 2000. Antigen 43 and type 1 fimbriae determine colony morphology of *Escherichia coli* K-12. J. Bacteriol. **182:**1089-1095.

101. **Hassen, A., N. Jedidi, N. Saidi, H. Kallali, A. Boudabous, and M. Ennabli.** 1996. Isolation of *Salmonella* in wastewaters and study of indicator bacteria survival in soils. Arch. Inst. Pasteur Tunis **73:**173-177.

102. **Haugo, A. J., and P. I. Watnick.** 2002. *Vibrio cholerae* CytR is a repressor of biofilm development. Mol. Microbiol. **45:**471-483.

103. **Heinrichs, D. E., J. A. Yethon, and C. Whitfield.** 1998. Molecular basis for structural diversity in the core regions of the lipopolysaccharides of *Escherichia coli* and *Salmonella enterica*. Mol. Microbiol. **30:**221-232.

104. **Helms, M., P. Vastrup, P.-S. Gerner, and K. Molbak.** 2003. Short and long term mortality associated with foodborne bacterial gastrointestinal infection:registry-based study. BMJ **326:**357-361.

105. **Hitchcock, P. J., and T. M. Brown.** 1983. Morphological heterogeneity among *Salmonella* lipopolysaccharide chemotypes in silver-stained polyacrylamide gels. J. Bacteriol. **154:**269-277.

106. **Hochhut, B., U. Dobrindt, and J. Hacker.** 2005. Pathogenicity islands and their role in bacterial virulence and survival, p. 234-254. *In* W. Russel and H. Herwald (ed.), Concepts in Bacterial Virulence. Karger, New York, NY.

107. **Hoffman, L., and J. Jendrisak.** 1999. Use of EZ::TNTM TransposomesTM for genetic analysis and direct sequencing of bacterial genomic DNA. Epicentre Forum **6:**1-7.

108. **Holt.** Bergey's Manual of Determinative Bacteriology., 9th ed, vol. Williams Wilkins, Baltimore, MD.

109. **Hosek, G., D. Leschinsky, S. Irons, and T. J. Safranek.** 1997. Multidrug resistant *Salmonella* serotype Typhimurium-United States, 1996. Morbid. Mortal. Weekly Rep.**:**46.

110. **Humphrey, T.** 2004. *Salmonella*, stress response and food safety. Nature Rev. Microbiol. **2:**504-509.

111. **Humphrey, T. J.** 2001. *Salmonella* Typhimurium definitive type 104. A multi-resistant *Salmonella*. Int. J. Food Microbiol. **67:**173-186.

112. **Hurley, B. P., and B. A. McCormick.** 2003. Translating tissue culture results into animal models: the case of *Salmonella typhimurium*. Trends Microbiol. **11:**562-569.

113. **Ingham , S. C., Y. C. Su, and D. S. Spangenberg.** 2000. Survival of S*almonella typhimurium* and *Escherichia coli* O157:H7 in cheese brines. Int. J. Food Microbiol. **61:**73-79.

114. **Jackson, K. D., M. Starkey, S. Kremer, M. R. Parsek, and D. J. Wozniak.** 2004. Identification of *psl*, a locus encoding a potential exopolysaccharide that is essential for *Pseudomonas aeruginosa* PAO1 biofilm formation. J. Bacteriol. **186:**4466-4475.

115. **Johnson, J. A., P. Panigrahi, and J. G. J. Morris.** 1992. Non-O1 *Vibrio cholerae* NRT36S produces a polysaccharide capsule that determines colony morphology, serum resistance, and virulence in mice. Infect. Immun. **60:**864-869.

116. **Jonson, A., S. Normark, and M. Rhen.** 2005. Fimbriae, pili, flagella, and bacterial virulence., p. 67-89. *In* W. Russel and H. Herwald (ed.), Concepts in bacterial virulence., vol. 12. Karger, New York, NY.

117. **Jorgensen, F., S. Leach, S. J. Wilden, A. Davies, G. S. A. B. Stewart, and T. Humprey.** 2000. Invasiveness in chickens, stress resistance and *rpoS* status of wild-type *Salmonella enterica subsp. enterica* serovar Typhimurium definitive type 104 and serovar Enteritidis phage type 4 strain. Microbiol. **146:**3227-3235.

118. **Jubelin, G., A. Vianney, C. Beloin, J. M. Ghigo, J. C. Lazzaroni, P. Lejeune, and C. Dorel.** 2005. CpxR/OmpR interplay regulates curli gene expression in response to osmolarity in *Escherichia coli*. J. Bacteriol. **187:**2038-2049.

119. **Kajitani, M., A. Kato, A. Wada, Y. Inokuchi, and A. Ishihama.** 1994. Regulation of the *Escherichia coli hfq* gene encoding the host factor for phage Q beta. J. Bacteriol. **176:**531-534.

120. **Kelley, W. L., and C. Georgopoulus.** 1997. Positive control of the two-component RcsBC/B signal treansduction network by DjlA: a member of the DnaJ family of molecular chaperones in *Escherichia coli*. Mol. Microbiol. **25:**913-931.

121. **Kennedy, M., R. Villar, D. Vugia, T. Rabatsky-Ehr, M. M. Farley, M. Pass, K. Smith, P. Smith, P. R. Cieslak, B. Imhoff, P. M. Griffin, and E. I. P. F. W. Group.** 2004. Hospitalizations and deaths due to *Salmonella* infections, FoodNet, 1996-1999. Clin. Infect. Dis. **38 Suppl 3:**S142-S148.

122. **Kierek, K., and P. I. Watnick.** 2003. Environmental determinants of *Vibrio cholerae* biofilm development. Appl. Environ. Microbiol. **69:**5079-5088.

123. **Kirov, S., L. A. Donovan, and K. Sanderson.** 1999. Functional characterization of type IV pili expressed on diarrhea-associated isolates of *Aeromonas* species. Infect. Immun. **67:**5447-5454.

124. **Kjaergaard, K., M. A. Schembri, H. Hasman, and P. Klemm.** 2000. Antigen 43 from *Escherichia coli* induces inter- and intraspecies cell aggregation and changes in colony morphology of *Pseudomonas fluorescens*. J. Bacteriol. **182:**4789-4796.

125. **Kudo, H., K. J. Cheng, and J. W. Costerton.** 1987. Interactions between *Treponema bryantii* and cellulolytic bacteria in the in vitro degradation of straw cellulose. Can. J. Microbiol. **33:**244-248.

126. **Landini, P., and A. J. Zehnder.** 2002. The global regulatory *hns* gene negatively affects adhesion to solid surfaces by anaerobically grown *Escherichia coli* by modulating the expression of lipopolysaccharide and flagellar genes. J. Bacteriol. **184:**1522-1529.

127. **Le Derout, J., M. Folichon, F. Briani, G. Deho, P. Regnier, and E. Hajnsdorf.** 2003. Hfq affects the length and the frequency of short oligo(A) tails at the 3' end of *Escherichia coli rpsO* mRNAs. Nucleic Acids Res. **31:**4017-4023.

128. **Lease, R. A., and M. Belfort.** 2000. Riboregulation by DsrA RNA: trans-actions for global economy. Mol. Microbiol. **38:**667-672.

129. **Lease, R. A., and M. Belfort.** 2000. A trans-acting RNA as a control switch in *Escherichia coli*: DsrA modulates function by forming alternative structures. Proc. Natl. Acad. Sci. U. S. A. **97:**9919-9924.

130. **Lease, R. A., M. E. Cusick, and M. Belfort.** 1998. Riboregulation in *Escherichia coli:* DsrA RNA acts by RNA:RNA interactions at multiple loci. Proc. Natl. Acad. Sci. U. S. A. **95:**12456-12461.

131. **Lee, C. A., and S. Falkow.** 1990. The ability of *Salmonella* to enter mammalian cells is affected by bacterial growth state. Proc. Natl. Acad. Sci. U. S. A. **87:**4304-4308.

132. **Lee, C. A., B. D. Jones, and S. Falkow.** 1992. Identification of a *Salmonella typhimurium* invasion locus by selection for hyperinvasive mutants. Proc. Natl. Acad. Sci. U. S. A **89:**1847-1851.

133. **Lee, I. S., J. Lin, H. K. Hall, B. Bearson, and J. W. Foster.** 1995. The stationary phase sigma factor sS (RpoS) is required for a sustained acid tolerance response in virulent Salmonella typhimurium. Mol. Microbiol. **17:**155-167.

134. **Lejeune, P., and A. Danchin.** 1990. Mutations in the *bglY* gene increase the frequency of spontaneous deletions in *Escherichia coli* K-12. Proc. Natl. Acad. Sci. U. S. A. **87:**360-363.

135. **Lenz, D. H., K. C. Mok, B. N. Lilley, R. V. Kulkarni, N. S. Wingreen, and B. L. Bassler.** 2004. The small RNA chaperone Hfq and multiple small RNAs control quorum sensing in *Vibrio harveyi* and *Vibrio cholerae*. Cell **118:**69-82.

136. **Lesn, J., S. Berthet, S. Binard, A. Rouxel, and F. Humbert.** 2000. Changes in culturability and virulence of *Salmonella typhimurium* during long-term starvation under desiccating conditions. Int. J. Food Microbiol. **60:**195-203.

137. **Lim, S., M. Joe, S. Song, M. Lee, J. W. Foster, and Y. Park.** 2002. *cuiD* Is a crucial gene for survival at high copper environment in *Salmonella enterica* serovar Typhimurium. Mol. Cells **14:**177-184.

138. **Loewen, P. C., and R. Hengge-Aronis.** 1994. The role of the sigma factor σ^S (KatF) in bacterial global regulation. Annu. Rev. Microbiol. **48:**53-80.

139. **Loewen, P. C., B. Hu, J. Strutinsky, and R. Sparling.** 1998. Regulation in the *rpoS* regulon of *Escherichia coli*. Can. J. Microbiol. **44:**707-717.

140. **Loferer, H., M. Hammar, and S. Normark.** 1997. Availability of the fibre subunit CsgA and the nucleator protein CsgB during assembly of fibronectin-binding curli is limited by the intracellular concentration of the novel lipoprotein CsgG. Mol. Microbiol. **26:**11-23.

141. **Looney, W. J.** 2000. Small-colony variants of *Staphylococcus aureus*. Br. J. Biomed. Sci. **57:**317-322.

142. **MacLachlan, P. R., and K. E. Sanderson.** 1985. Transformation of *Salmonella typhimurium* with plasmid DNA: differences between rough and smooth strains. J. Bacteriol. **161:**442-445.

143. **Majdalani, N., C. Cunning, D. Sledjeski, T. Elliott, and S. Gottesman.** 1998. DsrA RNA regulates translation of RpoS message by an anti-antisense mechanism, independent of its action as an antisilencer transcription. Proc. Natl. Acad. Sci. U. S. A. **95:**12462-12467.

144. **Majdalani, N., D. Hernandez, and S. Gottesman.** 2002. Regulation and mode of action of the second small RNA activator of RpoS translation, RprA. Mol. Microbiol. **46:**813-826.

145. **Makin, S. A., and T. J. Beveridge.** 1996. The influence of A-band and B-band lipopolysaccharide on the surface characteristics and adhesion of *Pseudomonas aeruginosa* to surfaces. Microbiol. **142:**299-307.

146. **Mallinson, E. T., R. G. Miller, C. E. de Rezende, K. E. Ferris, J. deGraft-Hanson, and S. W. Joseph.** 2000. Improved plating media for the detection of *Salmonella* species with typical and atypical hydrogen sulfide production. J. Vet. Diagn. Invest. **12:**83-87.

147. **Maloy, S. R., V. J. Stewart, and R. K. Taylor.** 1996. Genetic analysis of pathogenic bacteria., vol. Cold Spring Harbor Laboratory Press., Cold Spring Harbor, NY.

148. **Masse, E., and S. Gottesman.** 2002. A small RNA regulates the expression of genes involved in iron metabolism in *Escherichia coli*. Proc. Natl. Acad. Sci. U. S. A. **99:**4620-4625.

149. **Matin, A.** 1991. The molecular basis of carbon-starvation-induced general resistance in *Escherichia coli*. Mol. Microbiol. **5:**3-10.

150. **Matsushita, M.** 1997. Formation of colony patterns by a bacterial cell population, p. 366-393. *In* J. A. Shapiro and M. Dworkin (ed.), Bacteria as multicellular organism. Oxford University Press., New York, NY.

151. **Matthysse, A. G., D. L. Thomas, and A. R. White.** 1995. Mechanism of cellulose synthesis in *Agrobacterium tumefaciens*. J. Bacteriol. **177:**1076-1081.

152. **McNealy, T. L., V. Forsbach-Birk, C. Shi, and R. Marre.** 2005. The Hfq homolog in *Legionella pneumophila* demonstrates regulation by LetA and RpoS and interacts with the global regulator CsrA. J. Bacteriol. **187:**1527-1532.

153. **Mead, P. S., L. Slutsker, V. Dietz, L. F. McCaig, J. S. Bresee, C. Shapiro, P. M. Griffin, and R. V. Tauxe.** 1999. Food-related illness and death in the United States. Emerg. Infect. Dis. **5:**607-625.

154. **Mendelson, N. H., and B. Salhi.** 1996. Patterns of reporter gene expression in the phase diagram of Bacillus subtilis colony forms. J Bacteriol **178:**1980-1989.

155. **Mikulecky, P. J., M. K. Kaw, C. C. Brescia, J. C. Takach, D. D. Sledjeski, and A. L. Feig.** 2004. *Escherichia coli* Hfq has distinct interaction surfaces for DsrA, *rpoS* and poly(A) RNAs. Nat. Struct. Mol. Biol. **11:**1206-1214.

156. **Miller, J. H.** 1992. A short course in bacterial genetics, vol. Cold Spring Harbor Laboratory Press, Plainview, NY.

157. **Mills, D. M., V. Bajaj, and C. A. Lee.** 1995. A 40 kb chromosomal fragment encoding *Salmonella typhimurium* invasion genes is absent from the corresponding region of the *Escherichia coli* K-12 chromosome. Mol. Microbiol. **15:**749-759.

158. **Mireles, J. R., 2nd, T. A., and R. M. Harshey.** 2001. *Salmonella enterica* serovar typhimurium swarming mutants with altered biofilm-forming abilities: surfactin inhibits biofilm formation. J. Bacteriol. **183:**5848-5854.

159. **Mizunoe, Y., S. N. Wai, A. Takade, and S. Yoshida.** 1999. Isolation and characterization of rugose form of *Vibrio cholerae* O139 strain MO10. Infect. Immun. **67:**958-963.

160. **Mohanty, B. K., V. F. Maples, and S. R. Kushner.** 2004. The Sm-like protein Hfq regulates polyadenylation dependent mRNA decay in *Escherichia coli*. Mol. Microbiol. **54:**905-920.

161. **Molbak, K., D. L. Baggesen, F. M. Aaerestrup, J. M. Ebbesen, J. Engberg, K. Frydendahl, P. Gerner-Smidt, A. M. Petersen, and H. C. Wegener.** 1999. An outbreak of multidrug-resistant, quinolone-resistant *Salmonella enterica* serotype typhimurium DT104. New England J. Med. **341:**1420-1425.

162. **Moller, A. K., M. P. Leatham, T. Conway, P. J. M. Nuijten, L. A. M. de Haan, K. A. Krogfelt, and P. S. Cohen.** 2003. An *Escherichia coli* MG1655 lipopolysaccharide deep-rough core mutant grows and survives in mouse cecal mucus but fails to colonize the mouse large intestine. Infect. Immun. **71:**2142-2152.

163. **Morris, J. G., Jr., M. B. Sztein, E. W. Rice, J. P. Nataro, G. A. Losonsky, P. Panigrahi, C. O. Tacket, and J. A. Johnson.** 1996. *Vibrio cholerae* O1 can assume a chlorine-resistant rugose survival form that is virulent for humans. J. Infect. Dis. **174:**1364-1368.

164. **Mouslim, C., and E. A. Groisman.** 2003. Control of the *Salmonella ugd* gene by three two-component regulatory systems. Mol. Microbiol. **47:**335-344.

165. **Mouslim, C., T. Latifi, and E. A. Groisman.** 2003. Signal-dependent requirement for the co-activator protein RcsA in transcription of the RcsB-regulated *ugd* gene. J. Biol. Chem. **278:**50588-50595.

166. **Muffler, A., D. Fischer, and R. Hengge-Aronis.** 1996. The RNA-binding protein HF-I, known as a host factor for phage Qß RNA replication, is essential for *rpoS* translation in *Escherichia coli*. Genes Dev. **10:**1143-1151.

167. **Muffler, A., D. D. Traulsen, D. Fischer, R. Lange, and R. Hengge-Aronis.** 1997. The RNA-binding protein HF-I plays a global regulatory role which is largely, but not exclusively, due to its role in expression of the sigmaS subunit of RNA polymerase in *Escherichia coli*. J. Bacteriol. **179:**297-300.

168. **Nesper, J., C. M. Lauriano, K. E. Klose, D. Kapfhammer, A. Kraiss, and J. Reidl.** 2001. Characterization of *Vibrio cholerae* O1 El tor *galU* and *galE* mutants: influence on lipopolysaccharide structure, colonization, and biofilm formation. Infect. Immun. **69:**435-445.

169. **Nickel, J. C., J. B. Wright, I. Ruseska, T. J. Marrie, C. Whitfield, and J. W. Costerton.** 1985. Antibiotic resistance of *Pseudomonas aeruginosa* colonizing a urinary catheter in vitro. Eur. J. Clin. Microbiol. **4:**213-218.

170. **O'Toole, G., H. B. Kaplan, and R. Kolter.** 2000. Biofilm formation as microbial development. Annu. Rev. Microbiol. **54:**49-79.

171. **O'Toole, G. A., and R. Kolter.** 1998. Initiation of biofilm formation in *Pseudomonas fluorescens* WCS365 proceeds via multiple, convergent, signaling pathways: a genetic analysis. Mol. Microbiol. **28:**449-461.

172. **O'Toole, G. A., L. A. Pratt, P. I. Watnick, D. K. Newman, V. B. Weaver, and R. Kolter.** 1999. Genetic approaches to study of biofilms. Methods Enzymol. **310:**91-109.

173. **Olsen, A., A. Arnqvist, M. Hammar, S. Sukupolvi, and S. Normark.** 1993. The RpoS sigma factor relieves H-NS -mediated transcriptional repression of *csgA*, the subunit gene of fibronectin - binding curli in *Escherichia coli*. Mol. Microbiol. **7:**523-536.

174. **Olsen, A., A. Jonsson, and S. Normark.** 1989. Fibronectin binding mediated by a novel class of surface organelles on *Escherichia coli*. Nature **338:**652-625.

175. **Olsen, A., M. J. Wick, M. Morgelin, and L. Bjorck.** 1998. Curli, fibrous surface proteins of *Escherichia coli*, interact with major histocompatibility complex class I molecules. Infect. Immun. **66:**944-949.

176. **Opara, O.** 1992. An evaluation of environmental factors leading to the development of methodologies to reduce *Salmonella* contamination on poultry farms. Master's thesis. University of Maryland College Park, College Park, MD.

177. **Palmer, R. J., Jr., and D. C. White.** 1997. Developmental biology of biofilms: implications for treatment and control. Trends Microbiol. **5:**435-440.

178. **Palomar, J., A. M. Leranoz, and M. Vinas.** 1995. *Serratia marcescens adherence*: the effect of O-antigen presence. Microbios **81:**107-113.

179. **Parker, C. T., A. W. Kloser, C. A. Schnaitman, M. A. Stein, S. Gottesman, and B. W. Gibson.** 1992. Role of the *rfaG* and *rfaP* genes in determining the lipopolysaccharide core structure and cell surface properties of *Escherichia coli* K-12. J. Bacteriol. **174:**2525-2538.

180. **Pessi, G., C. Blumer, and D. Haas.** 2001. *lacZ* fusions report gene expression, don't they? Microbiol. **147:**1993-1995.

181. **Pickard, D., J. Wain, S. Baker, A. Line, S. Chohan, M. Fookes, A. Barron, P. O. Gaora, J. A. Chabalgoity, T. N., C. Scholes, N. Thomson, M. Quail, J. Parkhill, and G. Dougan.** 2003. Composition, acquisition, and distribution of the Vi exopolysaccharide-encoding *Salmonella enterica* pathogenicity island SPI-7. J. Bacteriol. **185:**5055-5065.

182. **Popoff, M. R.** 2005. Bacterial exotoxins, p. 28-54. *In* W. Russel and H. Herwald (ed.), Concepts of bacterial virulence. Karger, New York, NY.

183. **Pratt, L. A., W. Hsing, K. E. Gibson, and T. J. Silhavy.** 1996. From acids to *osmZ*: multiple factors influence synthesis of the OmpF and OmpC porins in *Escherichia coli*. Mol. Microbiol. **20:**911-917.

184. **Prigent-Combaret, C., E. Brombacher, O. Vidal, A. Ambert, P. Lejeune, P. Landini, and C. Dorel.** 2001. Complex regulatory network controls initial adhesion and biofilm formation in *Escherichia coli* via regulation of the *csgD* gene. J. Bacteriol. **183:**7213-7223.

185. **Prigent-Combaret, C., G. Prensier, T. T. Le Thi, O. Vidal, P. Lejeune, and C. Dorel.** 2000. Developmental pathway for biofilm formation in curli-producing *Escherichia coli* strains: role of flagella, curli and colanic acid. Environ. Microbiol. **2:**450-464.

186. **Prouty, M., and J. Gunn.** 2003. Comparative analysis of *Salmonella enterica* serovar Typhimurium biofilm formation on gallstones and on glass. Infect. Immun. **71:**7154-7158.

187. **Quintero, E. J., and R. M. Weiner.** 1995. Evidence for the adhesive function of the exopolysaccharide of *Hyphomonas* strain MHS-3 in its attachment to surfaces. Appl. Environ. Microbiol. **61:**1897-1903.

188. **Raetz, C. R., and C. Whitfield.** 2002. Lipopolysaccharide endotoxins. Annu. Rev. Biochem. **71:**635-700.

189. **Rainey, P. B., and T. M.** 1998. Adaptive radiation in a heterogeneous environment. Nature **394:**69-72.

190. **Raivio, and T. Silhavy.** 1997. Transduction of envelope stress in *Escherichia coli* by the Cpx two-component system. J. Bacteriol. **179:**7724-7733.

191. **Ramesh, N., S. W. Joseph, L. E. Carr, L. W. Douglass, and F. W. Wheaton.** 2002. Evaluation of chemical disinfectants for the elimination of *Salmonella* biofilms from poultry transport containers. Poult. Sci. **81:**904-910.

192. **Rashid, M. H., C. Rajanna, A. Ali, and D. K. Karaolis.** 2003. Identification of genes involved in the switch between the smooth and rugose phenotypes of *Vibrio cholerae*. FEMS Microbiol. Lett. **227:**113-119.

193. **Rathman, M., L. P. Barker, and S. Falkow.** 1997. The unique trafficking pattern of *Salmonella typhimurium*-containing phagosomes in murine macrophages is independent of the mechanism of bacterial entry. Infect. Immun. **65:**1475-1485.

194. **Reynolds, T. B., and G. R. Fink.** 2001. Baker's yeast, a model for fungal biofilm formation. Science **291:**878-881.

195. **Rice, E. W., C. J. Johnson, R. M. Clark, K. R. Fox, D. J. Reasoner, M. E. Dunnigan, P. Panigrahi, J. A. Johnson, and J. G. Morris, Jr.** 1992. Chlorine and survival of "rugose" *Vibrio cholerae*. Lancet **340:**740.

196. **Robleto, E. A., I. Lopez-Hernandez, M. W. Silby, and S. B. Levy.** 2003. Genetic analysis of the AdnA regulon in *Pseudomonas fluorescens*: nonessential role of flagella in adhesion to sand and biofilm formation. J. Bacteriol. **185:**453-460.

197. **Romling, U.** 2005. Characterization of the rdar morphotype, a multicellular behaviour in Enterobacteriaceae. Cell. Mol. Life Sci. **62:**1234-1246.

198. **Romling, U.** 2002. Molecular biology of cellulose production in bacteria. Res. Microbiol. **153:**205-212.

199. **Romling, U., Z. Bian, M. Hammar, W. D. Sierralta, and S. Normark.** 1998. Curli fibers are highly conserved between *Salmonella typhimurium* and *Escherichia coli* with respect to operon structure and regulation. J. Bacteriol. **180:**722-731.

200. **Romling, U., and M. Rohde.** 1999. Flagella modulate the multicellular behavior of *Salmonella typhimurium* on the community level. FEMS Microbiol. Lett. **180:**91-102.

201. **Romling, U., M. Rohde, A. Olsen, S. Normark, and J. Reinkoster.** 2000. AgfD, the checkpoint of multicellular and aggregative behaviour in *Salmonella*

typhimurium regulates at least two independent pathways. Mol. Microbiol. **36:**10-23.

202. **Romling, U., W. D. Sierralta, K. Eriksson, and S. Normark.** 1998. Multicellular and aggregative behaviour of *Salmonella typhimurium* strains is controlled by mutations in the *agfD* promoter. Mol. Microbiol. **28:**249-264.

203. **Ross, P., R. Mayer, and M. Benziman.** 1991. Cellulose biosynthesis and function in bacteria. Microbiol. Rev. **55:**35–58.

204. **Russo, T. A., and G. Singh.** 1993. An extraintestinal, pathogenic isolate of *Escherichia coli* (O4/K54/H5) can produce a group 1 capsule which is divergently regulated from its constitutively produced group 2, K54 capsular polysaccharide. J. Bacteriol. **175:**7617-7623.

205. **Ryu, J. H., and L. R. Beuchat.** 2005. Biofilm formation by *Escherichia coli* O157:H7 on stainless steel: effect of exopolysaccharide and curli production on its resistance to chlorine. Appl. Environ. Microbiol. **71:**247-254.

206. **Sakellaris, H., N. K. Hannink, K. Rajakumar, D. Bulach, M. Hunt, C. Sasakawa, and B. Adler.** 2000. Curli loci of *Shigella* spp. Infect. Immun. **68:**3780-3783.

207. **Salhi, B., and N. H. Mendelson.** 1993. Patterns of gene expression in Bacillus subtilis colonies. J Bacteriol **175:**5000-5008.

208. **Sameshima, T., M. Akiba, H. Izumiya, J. Terajima, K. Tamura, H. Watanabe, and M. Nakazawa.** 2000. *Salmonella typhimurium* DT104 from livestock in Japan. Jpn. J. Infect. Dis. **53:**15-16.

209. **Sandvang, D., L. B. Jensen, D. L. Baggesen, and S. B. Baloda.** 2000. Persistence of a *Salmonella enterica* serotype Typhimurium clone in Danish pig production units and farmhouse environment studied by pulsed field gel electrophoresis (PFGE). FEMS Microbiol. Lett. **187:**21-25.

210. **Santo Domingo, J. W., S. Harmon, and J. Bennett.** 2000. Survival of *Salmonella* species in river water. Curr. Microbiol. **40:**409-417.

211. **Santos, R. L., S. Zhang, R. M. Tsolis, A. J. Baumler, and L. G. Adams.** 2002. Morphologic and molecular characterization of *Salmonella typhimurium* infection in neonatal calves. Vet. Pathol. **39:**200-215.

212. **Scher, K., U. Romling, and S. Yaron.** 2005. Effect of heat, acidification, and chlorination on *Salmonella enterica* serovar typhimurium cells in a biofilm formed at the air-liquid interface. Appl. Environ. Microbiol. **71:**1163-1168.

213. **Schmieger, H.** 1972. Phage P22 mutants with increased or decreased transductional abilities. Mol. Gen. Genet. **119:**75-88.

214. **Schnaitman, C. A., and J. D. Klena.** 1993. Genetics of lypopolisaccharide biosynthesis in enteric bacteria. Microbiol. Rev. **57:**655-682.

215. **Schuppli, D., G. Miranda, H. C. Tsui, M. E. Winkler, J. M. Sogo, and H. Weber.** 1997. Altered 3'-terminal RNA structure in phage Qbeta adapted to host factor-less *Escherichia coli*. Proc. Natl. Acad. Sci. U. S. A. **94:**10239-10242.

216. **Shapiro, J. A.** 1997. Multicellularity, the rule, not the exception. Lessons from *Escherichia coli* colonies., p. 14-49. *In* J. A. Shapiro and M. Dworkin (ed.), Bacteria as multicellular organisms. Oxford University Press., New York, NY.

217. **Sheikh, J., S. Hicks, M. Dall'Agnol, A. D. Phillips, and J. P. Nataro.** 2001. Roles for Fis and YafK in biofilm formation by enteroaggregative *Escherichia coli*. Mol. Microbiol. **41:**983-997.

218. **Sippel, J. E., H. K. Mamay, E. Weiss, S. W. Joseph, and W. J. Beasley.** 1978. Outer membrane protein antigens in an enzyme-linked immunosorbent assay for *Salmonella* enteric fever and meningococcal meningitis. J. Clin. Microbiol. **7:**372-378.

219. **Sledjeski, D. D., A. Gupta, and S. Gottesman.** 1996. The small RNA, DsrA, is essential for the low temperature expression of RpoS during exponential growth in *Escherichia coli*. EMBO J. **15:**3993-4000.

220. **Sledjeski, D. D., C. Whitman, and A. Zhang.** 2001. Hfq is necessary for regulation by the untranslated RNA DsrA. J. Bacteriol. **183:**1997-2005.

221. **Solano, C., B. Garcia, J. Valle, C. Berasain, J. M. Ghigo, C. Gamazo, and I. Lasa.** 2002. Genetic analysis of *Salmonella enteritidis* biofilm formation: critical role of cellulose. Mol. Microbiol. **43:**793-808.

222. **Sonnleitner, E., S. Hagens, F. Rosenau, S. Wilhelm, A. Habel, K. E. Jager, and U. Blasi.** 2003. Reduced virulence of a *hfq* mutant of *Pseudomonas aeruginosa* O1. Microb. Pathog. **35:**217-228.

223. **Spector, M. P.** 1998. The starvation-stress response (SSR) of *Salmonella*. Adv. Microb. Physiol. **40:**233-279.

224. **Spiers, A. J., J. Bohannon, S. M. Gehrig, and P. B. Rainey.** 2003. Biofilm formation at the air-liquid interface by the *Pseudomonas fluorescens* SBW25 wrinkly spreader requires an acetylated form of cellulose. Mol. Microbiol. **50:**15-27.

225. **St Geme, J. W., 3rd, and D. Cutter.** 1996. Influence of pili, fibrils, and capsule on in vitro adherence by *Haemophilus influenzae* type b. Mol. Microbiol. **21:**21-31.

226. **Stevenson, G., S. J. Lee, L. K. Romana, and P. R. Reeves.** 1991. The *cps* gene cluster of *Salmonella* strain LT2 includes a second mannose pathway: sequence of two genes and relationship to genes in the *rfb* gene cluster. Mol. Gen. Genet. **227:**173-180.

227. **Stoodley, P., K. Sauer, D. G. Davies, and J. W. Costerton.** 2002. Biofilms as complex differentiated communities. Annu. Rev. Microbiol. **56:**187-209.

228. **Storz, G., J. A. Opdyke, and A. Zhang.** 2004. Controlling mRNA stability and translation with small, noncoding RNAs. Curr. Opin. Microbiol. **7:**140-144.

229. **Suci, P. A., M. W. Mittelman, F. P. Yu, and G. G. Geesey.** 1994. Investigation of ciprofloxacin penetration into *Pseudomonas aeruginosa* biofilms. Antimicrob. Agents Chemother. **38:**2125-2133.

230. **Sukupolvi, S., R. G. Lorenz, J. I. Gordon, Z. Bian, J. D. Pfeifer, S. J. Normark, and M. Rhen.** 1997. Expression of thin aggregative fimbriae promotes interaction of *Salmonella typhimurium* SR-11 with mouse small intestinal epithelial cells. Infect. Immun. **65:**5320-5325.

231. **Surette, M. G., and B. L. Bassler.** 1998. Quorum sensing in *Escherichia coli* and *Salmonella typhimurium*. Proc. Natl. Acad. Sci. U. S. A. **95:**7046-7050.

232. **Sutherland, I.** 1990. Biotechnology of microbial exopolysaccharides, vol. Cambridge University Press, New York, NY.

233. **Sword, W., B. Cannon, and W. Benjamin, Jr.** 1997. Avirulence of LT2 strains of *Salmonella typhimurium* results from a defective *rpoS* gene. Infect. Immun. **65:**2451-2453.

234. **Takeda, S., Y. Fujisawa, M. Matsubara, H. Aiba, and T. Mizuno.** 2001. A novel feature of the multistep phosphorelay in *Escherichia coli*: a revised model of the RcsC --> YojN --> RcsB signalling pathway implicated in capsular synthesis and swarming behaviour. Mol. Microbiol. **40:**440-450.

235. **Takeuchi, A.** 1967. Electron microscope studies of experimental *Salmonella* infection. I. Penetration into the intestinal epithelium by *Salmonella typhimurium.* Am. J. Pathol. **50:**109-136.

236. **Tauxe, R. V.** 1991. *Salmonella*: A postmodern pathogen. J. Food Protect. **54:**563-568.

237. **Thomashow, M. F., J. E. Karlinsey, J. R. Marks, and R. E. Hurlbert.** 1987. Identification of a new virulence locus in *Agrobacterium tumefaciens* that affects polysaccharide composition and plant cell attachment. J. Bacteriol. **169:**3209-3216.

238. **Thomsen, L. E., M. S. Chadfield, J. Bispham, T. S. Wallis, J. E. Olsen, and H. Ingmer.** 2003. Reduced amounts of LPS affect both stress tolerance and virulence of *Salmonella enterica* serovar Dublin. FEMS Microbiol. Lett. **228:**225-231.

239. **Threlfall, E. J., F. J. A., L. R. Ward, and B. Rowe.** 1996. Increasing spectrum of resistance in multiresistant *Salmonella typhimurium*. Lancet **347:**1053-1054.

240. **Threlfall, E. J., J. A. Frost, L. R. Ward, and B. Rowe.** 1994. Epidemic in cattle and humans of *Salmonella typhimurium* DT 104 with chromosomally integrated multiple drug resistance. Vet. Rec. **134:**577.

241. **Threlfall, E. J., M. L. Hall, and B. Rowe.** 1992. *Salmonella* bacteraemia in England and Wales, 1981-1990. J. Clin. Pathol. **45:**34-36.

242. **Tischler AD, C. A.** 2004. Cyclic diguanylate (c-di-GMP) regulates *Vibrio cholerae* biofilm formation. Mol Microbiol. **53:**857-869.

243. **Toguchi, A., M. Siano, M. Burkart, and R. M. Harshey.** 2000. Genetics of swarming motility in *Salmonella enterica* serovar typhimurium: critical role for lipopolysaccharide. J. Bacteriol. **182:**6308-6321.

244. **Toutain, C. M., N. C. Caiazza, and G. O'Toole.** 2004. Molecular basis of biofilm evelopment in pseudomonads., p. 43-63. *In* M. Ghannoum and G. O'Toole (ed.), Microbial biofilms. ASM Press., Washington, D. C.

245. **Tsui, H. C., G. Feng, and M. E. Winkler.** 1997. Negative regulation of *mutS* and *mutH* repair gene expression by the Hfq and RpoS global regulators of *Escherichia coli* K-12. J. Bacteriol. **179:**7476-7487.

246. **Tsui, H. C., H. C. Leung, and M. E. Winkler.** 1994. Characterization of broadly pleiotropic phenotypes caused by an *hfq* insertion mutation in *Escherichia coli* K-12. Mol. Microbiol. **13:**35-49.

247. **Uhlich, G. A., J. E. Keen, and R. O. Elder.** 2001. Mutations in the *csgD* promoter associated with variations in curli expression in certain strains of *Escherichia coli* O157:H7. Appl. Environ. Microbiol. **67:**2367-2370.

248. **Updegraff, D. M.** 1969. Semimicro determination of cellulose in biological materials. Anal. Biochem. **32:**420-424.

249. **Vaara, M.** 1993. Antibiotic-supersusceptible mutants of *Escherichia coli* and *Salmonella typhimurium*. Antimicrob. Agents Chemother. **37:**2255-2260.

250. **Vianney, A., G. Jubelin, S. Renault, C. Dorel, P. Lejeune, and J. C. Lazzaroni.** 2005. Escherichia coli tol and rcs genes participate in the complex network affecting curli synthesis. Microbiology **151:**2487-2497.

251. **Vidal, O., R. Longin, C. Prigent-Combaret, C. Dorel, M. Hooreman, and P. Lejeune.** 1998. Isolation of an *Escherichia coli* K-12 mutant strain able to form biofilms on inert surfaces: involvement of a new *ompR* allele that increases curli expression. J. Bacteriol. **180:**2442-2449.

252. **Vytvytska, O., I. Moll, V. R. Kaberdin, A. von Gabain, and U. Blasi.** 2000. Hfq (HF1) stimulates *ompA* mRNA decay by interfering with ribosome binding. Genes Dev. **14:**1109-1118.

253. **Wai, S. N., M. Y., T. A., S. I. Kawabata, and S. I. Yoshida.** 1998. *Vibrio cholerae* O1 strain TSI-4 produces the exopolysaccharide materials that determine colony morphology, stress resistance, and biofilm formation. Appl. Environ. Microbiol. **64:**3648-3655.

254. **Wall, P. G., D. Morgan, K. Lamden, M. Ryan, M. Griffin, E. J. Threlfall, L. R. Ward, and B. Rowe.** 1994. A case control study of infection with an epidemic strain of multiresistant *Salmonella typhimurium* DT104 in England and Wales. Commun. Dis. Rep. CDR. Rev. **4:**R130-R135.

255. **Wang, Q., J. G. Frye, M. McClelland, and R. M. Harshey.** 2004. Gene expression patterns during swarming in *Salmonella typhimurium*: genes specific to surface growth and putative new motility and pathogenicity genes. Mol. Microbiol. **52:**169-187.

256. **Wang, R. F., and S. R. Kushner.** 1991. Construction of versatile low-copy-number vectors for cloning, sequencing and gene expression in *Escherichia coli*. Gene **100:**195-199.

257. **Wang, X., J. F. Preston, 3rd, and T. Romeo.** 2004. The *pgaABCD* locus of *Escherichia coli* promotes the synthesis of a polysaccharide adhesin required for biofilm formation. J. Bacteriol. **186:**2724-2734.

258. **Watnick, P. I., and R. Kolter.** 2000. Biofilm: city of microbes. J. Bacteriol. **182:**2675-2679.

259. **Wehland, M., and F. Bernhard.** 2000. The RcsAB box. Characterization of a new operator essential for the regulation of exopolysaccharide biosynthesis in enteric bacteria. J. Biol. Chem. **275:**7013-7020.

260. **Wessells, K.** 2003. The effect of autoinducer-2 activity and lipopolysaccharide production on the formation of the rugose colony morphology in *Salmonella* Typhimurium DT104. Undergraduate honors thesis. University of Maryland College Park, College Park, MD.

261. **Whitchurch, C. B., T. Tolker-Nielsen, P. C. Ragas, and J. S. Mattick.** 2002. Extracellular DNA required for bacterial biofilm formation. Science **295:**1487.

262. **White, A. P., D. L. Gibson, S. K. Collinson, P. A. Banser, and W. W. Kay.** 2003. Extracellular polysaccharides associated with thin aggregative fimbriae of *Salmonella enterica* serovar Enteritidis. J. Bacteriol. **185:**5398-5407.

263. **White, P. B.** 1938. The rugose variant of vibrios. J. Pathol. Bacteriol. **46:**1-6.

264. **Williams, V., and M. Fletcher.** 1996. *Pseudomonas fluorescens* adhesion and transport through porous media are affected by lipopolysaccharide composition. Appl. Environ. Microbiol. **62:**100-104.

265. **Wingender, J., T. R. Neu, and H. Flemming.** 1999. What are bacterial extracellular polymeric substances? *In* J. Wingender, T. R. Neu, and H. Flemming (ed.), Microbial extracellular polymeric substances: characterization, structure and function. Springer, New York, NY.

266. **Wood, J. M., E. Bremer, L. N. Csonka, R. Kraemer, B. Poolman, T. van der Heide, and L. T. Smith.** 2001. Osmosensing and osmoregulatory compatible solute accumulation by bacteria. Comp. Biochem. Physiol. A Mol. Integr. Physiol. **130:**437-460.

267. **Wu, M. T., S. A. Carlson, and D. K. Meyerholz.** 2002. Cytopathic effects observed upon expression of a repressed collagenase gene present in *Salmonella* and related pathogens: mimicry of a cytotoxin from multiple antibiotic-resistant *Salmonella enterica* serotype Typhimurium phagetype DT104. Microb. Pathog. **33:**279-287.

268. **Wyckoff, T. J., B. Thomas, D. J. Hassett, and D. J. Wozniak.** 2002. Static growth of mucoid *Pseudomonas aeruginosa* selects for non-mucoid variants that have acquired flagellum-dependent motility. Microbiol. **148:**3423-3430.

269. **Yethon, J. A., E. Vinogradov, M. B. Perry, and C. Whitfield.** 2000. Mutation of the lipopolysaccharide core glycosyltransferase encoded by *waaG* destabilizes outer membrane of *Escherichia coli* by interfering with core phosphorylation. J. Bacteriol. **182:**5620-5623.

270. **Yildiz, F. H., N. A. Dolganov, and G. K. Schoolnik.** 2001. VpsR, a member of the response regulators of the two-component regulatory systems, is required for expression of *vps* biosynthesis genes and EPS(ETr)-associated phenotypes in *Vibrio cholerae* O1 El Tor. J. Bacteriol. **183:**1716-1726.

271. **Yildiz, F. H., X. S. Liu, A. Heydorn, and G. K. Schoolnik.** 2004. Molecular analysis of rugosity in a *Vibrio cholerae* O1 El Tor phase variant. Mol. Microbiol. **53:**497-515.

272. **Yildiz, F. H., and G. K. Schoolnik.** 1999. *Vibrio cholerae* El Tor: Identification of a gene cluster required for the rugose colony type, exopolysaccharide production, chlorine resistance, and biofilm formation. Proc. Natl. Acad. Sci. U. S. A. **96:**4028-4033.

273. **Zhang, A., S. Altuvia, A. Tiwari, L. Argaman, R. Hengge-Aronis, and G. Storz.** 1998. The OxyS regulatory RNA represses *rpoS* translation and binds the Hfq (HF-I) protein. EMBO J. **17:**6061-6068.

274. **Zhang, A., K. M. Wassarman, C. Rosenow, B. C. Tjaden, G. Storz, and S. Gottesman.** 2003. Global analysis of small RNA and mRNA targets of Hfq. Mol. Microbiol. **50:**1111-1124.

275. **Zhang, S., R. A. Kingsley, R. L. Santos, H. Andrews-Polymenis, M. Raffatellu, J. Figueiredo, J. Nunes, R. M. Tsolis, L. G. Adams, and A. J. Baumler.** 2003. Molecular pathogenesis of *Salmonella enterica* serotype typhimurium-induced diarrhea. Infect. Immun. **71:**1-12.

276. **Zhou, D., M. S. Mooseker, and J. E. Galan.** 1999. Role of the *S. typhimurium* actin-binding protein SipA in bacterial internalization. Science **283:**2092-2095.

277. **Zhu, J., and J. J. Mekalanos.** 2003. Quorum sensing-dependent biofilms enhance colonization in *Vibrio cholerae*. Dev. Cell. **5:**647-656.

278. **Zogaj, X., W. Bokranz, M. Nimtz, and U. Römling.** 2003. Production of cellulose and curli fimbriae by members of the family *Enterobacteriaceae* isolated from the human gastrointestinal tract. Infect. Immun. **71:**4151-4158.

279. **Zogaj, X., M. Nimtz, M. Rohde, W. Bokranz, and U. Romling.** 2001. The multicellular morphotypes of *Salmonella typhimurium* and *Escherichia coli* produce cellulose as the second component of the extracellular matrix. Mol. Microbiol. **39:**1452-1463.

CURRICULUM VITAE

Yuda Adha Anriany

Dept. of Cell Biology and Molecular Genetics
Rm. 2117 Bldg. 231 Microbiology
Univ. of Maryland, College Park, MD 20742
(301) 405-5451

3422 Tulane Drive Apt #23
Hyattsville, MD, 20783
(301) 422-2544
anriany@umd.edu

EDUCATION

Ph. D in Microbiology August 2005
University of Maryland, College Park, Maryland

M.S. in Biology December 1996
Virginia Polytechnic Institute and State University, Blacksburg, Virginia

B. S. in Biology, *Magna cum Laude* graduate December 1995
Virginia Polytechnic Institute and State University, Blacksburg, Virginia

DISSERTATION

"Toward a Better Understanding of the Cellular, Molecular, and Genetic Bases of Rugose Morphology in *Salmonella* Typhimurium"

This work involved characterization and analysis of transposon mutants of *S*. Typhimurium that had an altered rugose (wrinkled) colony phenotype and biofilm formation. My studies resulted in identification of a cellular factor, LPS, required for normal production of both curli and cellulose components of the extracellular matrix as well as an additional regulatory mechanism by Hfq protein in the transcription of *csgD*, coding for the central regulator of curli and cellulose production CsgD, and the *csgBA* operon, coding for the curli subunits CsgB and CsgA, independent of RpoS.

(Dissertation directed by Dr. Sam W. Joseph, readers include: Dr. Douglas Julin, Dr. Suman Mukhophadhyay, Dr. Wenxia Song, Dr. Richard Stewart, Dr. Gisela Storz, and Dr. Ronald Weiner).

OTHER RESEARCH EXPERIENCE

Graduate Research, University of Maryland January 2003- May 2003
(with advisor Dr. Sam W. Joseph)
Assisting with the investigation of the effect of rugose phenotype as a survival strategy in biofilms. Funded by the Joint Institute of Food Safety and Nutrition (JIFSAN)

Graduate research, Veterinary Medicine May 2002 - July 2002
(with advisor Dr. Sam W. Joseph and with Dr. Suman Mukhophadhay)

Assisting in the research on differential display, comparing gene expression between rugose-and non-rugose expressing strains

Graduate research August 1995-December 1996
Virginia Polytechnic Institute and State University (with advisor Dr. G. William Claus)
Research for a master's thesis on the activity of sorbitol- and sorbose-dehydrogenases of *Gluconobacter* species

SUPERVISORY EXPERIENCE

Supervised 10 undergraduate researchers, and 2 graduate students during laboratory rotation; managed laboratory safety compliance in the laboratory

Moderator for "International GTA Question and Answer Session" August 2004
Presentation given at the Graduate Teaching Assistant Orientation, University of Maryland, College Park, Maryland

TEACHING EXPERIENCE

University of Maryland, College Park

Teaching assistant for General Microbiology Laboratory (BSCI223) Summer, 2005 and 2001, Spring 2000 and 1999, Fall 1999 and 1998

Teaching assistant for Epidemiology and Public Health (BSCI425) Spring 2005, 2004, and 2002

Teaching assistant for Pathogenic Microbiology Laboratory (BSCI424) Fall 2004, 2003, 2001, and 2000

Laboratory Preparatory Coordinator for Pathogenic Microbiology Laboratory (BSCI424) Fall 2004

Laboratory Preparatory Coordinator for General Microbiology Laboratory (BSCI223) Summer 1999

Virginia Polytechnic Institute and State University

Teaching Assistant for General Microbiology Laboratory (BIOL2614) Spring 1996

Teaching Assistant for General Biology Laboratory (BIOL1015 and 1016) Fall and Spring 1995

TRAINING

A Field Guide to GenBank and NCBI December 2002

Molecular Biology Resources
Univ. of Maryland, College Park, Maryland

Radiation protection training May 2002
Univ. of Maryland, College Park, Maryland

AWARDS & RECOGNITION

Distinguished Teaching Assistant May 2004 and May 2000
Dept. of Cell Biology and Molecular Genetics,
University of Maryland, College Park, Maryland
Award given annually to the top 10% of Graduate Teaching Assistants in each Department by the Center for Teaching Excellence

Andrew J. Moyer Award May 2003 and May 2000
Dept. of Cell Biology and Molecular Genetics
Univ. of Maryland, College Park, Maryland
Award given annually to graduate students in the Department who show excellent progress in their research

Goldhaber Travel Award May 2001
Dept. of Cell Biology and Molecular Genetics
Univ. of Maryland, College Park, Maryland

Who's Who among Students in American Colleges January1995
Virginia Polytechnic Institute and State University

PROFESSIONAL ORGANIZATIONS

American Society for Microbiology (ASM) Since 1993
Golden Key Honor Society, Virginia Tech chapter 1993
Gamma Beta Phi, Virginia Tech chapter 1994
Phi Beta Kappa, Virginia Tech chapter 1995

PRESENTATIONS

"Mutations in the LPS of *Salmonella enterica* September 2003
serovar Typhimurium DT104 disrupt formation of the rugose phenotype"
Poster presented at ASM Conference on *Salmonella*: Pathogenesis, Epidemiology, and Vaccine Development, Sardinia, Italy

"Rugose phenotype in *Salmonella* Typhimurium DT104" September 2001
Presented at the ASM Washington DC-chapter meeting, Arlington, Virginia

"*Salmonella enterica* serovar Typhimurium DT104 displays May 2000
a rugose phenotype"
Poster presented at the ASM General Meeting, Orlando, Florida

"Biphasic growth of *Gluconobacter oxydans* in media containing sorbitol" May 1997
Poster presented at the ASM General Meeting, Miami, Florida

PUBLICATIONS

deRezende, C. E., **Y. A. Anriany**, S. W. Joseph and R. M. Weiner. 2005. A capsular polysaccharide surrounds smooth and rugose types of *Salmonella enterica* serovar Typhimurium DT104. Appl. Environ. Microbiol. In Press.

Anriany, Y. A., R. M. Weiner, J. A. Johnson, C. E. deRezende, and S. W. Joseph. 2001. *Salmonella enterica* serovar Typhimurium DT104 displays a rugose phenotype. Appl. Environ. Microbiol. 67:4048-4056.

MANUSCRIPTS IN PREPARATION

Anriany Y. A., S. N. Sahu, K. R. Wessells, L. M. McCann, and S. W. Joseph. Mutations in *ddhC* and *waaG* of *Salmonella* Typhimurium affect the rugose phenotype, curli and cellulose production, and biofilm formation.

Anriany, Y. A. and S. W. Joseph. The positive role of Hfq in curli production and biofilm formation in *S.* Typhimurium.

SPECIAL RECOGNITION

A photograph from AEM 67:4048 (2001) was used for the March 2002 cover of Microbiology and Molecular Biology Reviews.